

Final Report

for

Gravity Gradient Boom and Antenna Material Study

Contract No. : NAS5-9597

18 August 1967

Approved:

H. R. Wiant

**H. R. Wiant
Project Leader**

Prepared by

**Convair division of General Dynamics
San Diego, California**

for

**Goddard Space Flight Center
Greenbelt, Maryland**

SUMMARY

This is the final report of Contract NAS5-9597, Gravity Gradient Boom and Antenna Material Study, conducted by Convair division of General Dynamics, H. R. Wiant, Project Leader. The object of the study was to produce a rigidized, woven screen material having sufficient spring action to immediately and repeatedly form a tubular shape when freed of all restraint. The study was conducted in three phases consisting of: 1) the development of woven screen rigidizing procedures, 2) the generation of a mathematical model to predict thermal deflection of uncoated screen materials, and 3) a limited testing and evaluation program to verify the mechanical properties of rigidized screens.

Three Elgiloy-Copper Beryllium screens having different percent open-areas were rigidized by brazing and formed into 45-foot booms. Continuous processes were developed to permit these fabrications. A theoretical thermodynamic analysis of the screen-type boom was conducted and used as a basis for the practical application. An engineering prototype deployment mechanism was designed, fabricated, and tested to prove the feasibility of deployment and reroll of the rigidized screen boom. A limited testing and evaluation phase was conducted to determine the overall general characteristics of the low-distortion screen boom concept.

The wire screen boom concept proved to be a highly practical approach to the development of a low thermal distortion boom for space application. The complex nature of a rigidized, woven, dual material screen boom precluded analytical stress analysis, but selected physical parameters produced booms well within the envelope of usability. The thermal analysis of uncoated wire screen booms was used as a basis for final fabrications and proved highly adequate. The entire analysis and computer program is presented in full detail. The testing phase, although limited in extent, showed the wire screen boom to be uniform and reliable. The engineering prototype deployer was simple, direct, and reliable. The basic design was developed as potential space hardware.

This study proved the basic concept of a wire screen boom. The significant reduction in thermal distortion over solid tape-type booms could be further improved by absorptivity control coatings. Limitations in boom length are those concerned with weaving and not with rigidizing processing, although both could be improved. Joining development of wire screen splices could result in unlimited lengths of uniform, highly efficient booms for gravity gradient and antenna applications. Minor modifications in the deployment mechanism would permit unlimited space applications.

The Convair division of General Dynamics identification number for this report is GDC-ZZL67-010.

ACKNOWLEDGMENTS

The Gravity Gradient Boom and Antenna Material Study, Contract NAS5-9597, was conducted only through the combined efforts of many people in many disciplines. Mr. H. R. Wiant was Project Leader and responsible for the rigidization and boom forming process development, and testing. Mr. G. Sawyer was the key technician throughout the program. Mr. C. Maikish was instrumental in the successful equipment and deployer fabrication. Deployer design was conducted by M. E. Wrench, who also acted as consultant to the program. Mr. G. Howell conducted all of the thermal analysis presented in Appendix II. Mr. R. Hager conducted the thermal deflection testing, and Mr. M. Herbert consulted on stress and combined mechanical testing.

TABLE OF CONTENTS

<u>Section</u>		<u>Page</u>
1	INTRODUCTION	1
2	DISCUSSION	3
2.1	WIRE SCREEN BOOM PROCESS DEVELOPMENT	3
2.1.1	Material Selection	4
2.1.2	Wire Screen Mesh Selection	5
2.1.3	Woven Screen Rigidizing Process Development	7
2.1.4	Boom Forming	22
2.1.5	Delivered Booms	34
2.2	THERMAL ANALYSIS	39
2.3	TESTING AND EVALUATION	39
2.3.1	Screen Boom Handling Characteristics	39
2.3.2	Bending Strength	41
2.3.3	Boom Straightness Testing	49
2.3.4	Storage and Flexure Testing	67
2.3.5	Thermal Cycling	67
2.3.6	Thermal Deflection Testing	69
2.4	DEPLOYMENT MECHANISM FOR WIRE SCREEN BOOMS.	81
3	CONCLUSIONS AND RECOMMENDATIONS	93
3.1	WIRE CLOTH BOOM AND PROCESSING	93
3.2	TESTING AND EVALUATION	95
3.3	DEPLOYMENT MECHANISM	96
3.4	RECOMMENDATIONS FOR FUTURE WORK	96
4	NEW TECHNOLOGY	97
4.1	IMPROVED DEPLOYABLE BOOM	97
4.2	FORMING OF WIRE CLOTH BOOMS.	98
 <u>Appendix</u>		
I	CONTRACT NAS5-9597 — WORK STATEMENT	I-1
II	WIRE SCREEN RIGIDIZING PROCESS AND CONTINUOUS BOOM FORMING	II-1
III	MATHEMATICAL MODEL AND DIGITAL COMPUTER PROGRAM FOR SOLUTION OF TEMPERATURE DISTRIBUTION AROUND SCREEN TYPE TUBULAR GRAVITY GRADIENT ELEMENTS	III-1

LIST OF ILLUSTRATIONS

<u>Number</u>		<u>Page</u>
1	Basic Wire Screen Brazing Cycle	11
2	MOD I Continuous Screen Processing Equipment Shown In Flux/ Braze Alloy Slurry Dipping Mode	15
3	MOD I Continuous Screen Processing Equipment Shown In Brazing Mode	16
4	MOD II Continuous Screen Processing Equipment Shown In Flux/ Braze Alloy Slurry Dipping Mode	18
5	MOD II Continuous Screen Processing Equipment Shown In Brazing Mode	19
6	MOD I Continuous Tube Forming Furnace, End View, Showing Screen Cold Forming Nozzle	25
7	MOD I Continuous Tube Forming Equipment, Overall View	26
8	MOD II Continuous Tube Forming Equipment, Overall View	28
9	Transport Mechanism, Deforming Mandrel, and Take-Up Reel of Rewind Modification of Tube Forming Equipment	29
10	Biaxial Beraloy A Screen Joint As Brazed, Magnification 200X, Etch: See Text	31
11	Biaxial Beraloy A Screen Joint As Brazed and Heat-Treated, Magnification 200X, Etch: See Text	31
12	Biaxial Beraloy A (0.009 to 0.008 inch) Screen Joint As Brazed. Longitudinal Section Showing Circumferential Boom Wire In Cross-Section, Magnification 200X, Etch: See Text	32
13	Biaxial Beraloy A (0.009 to 0.008 inch) Screen Joint As Brazed. Transverse Section Showing Longitudinal Boom Wire In Cross-Section, Magnification 200X, Etch: See Text	32
14	Elgiloy - Beraloy A Screen Boom Joint As Heat-Treated. Elgiloy In Circular Cross Section, Magnification 200X, Etch: See Text	33
15	Elgiloy - Beraloy A Screen Boom Joint As Heat-Treated. Beraloy In Circular Cross-Section, Magnification 200X, Etch: See Text.	33
16	Alloy Certification, March 24, 1966 Shipment of Beraloy A	35
17	Alloy Certification, March 25, 1966 Shipment of Beraloy A	36

LIST OF ILLUSTRATIONS, Contd

<u>Number</u>		<u>Page</u>
18	Alloy Certification, March 31, 1966 Shipment of Beraloy A	37
19	Alloy Certification, Elgiloy	38
20	Temperature Difference vs. Circumferential Wire Mesh Size and Absorptivity for Elgiloy/Beryllium Copper Booms	40
21	Constant Bending Moment Test With Simultaneously Applied Torsional Moment	42
22	Component Parts of Test Sample	43
23	MOD I Combined Bending and Torsional Moment Test Apparatus . .	44
24	MOD II Combined Bending and Torsional Moment Test Apparatus . .	45
25	Bending Moment vs. Boom Diameter, 12 × 20 × 0.009 Beraloy A . .	48
26	Bending Moment vs. Circumferential Mesh Count, Beraloy A, 12-Mesh Warp, 0.009-Inch Wire Size	48
27	Bending Moment vs. Deflection for Three Seam Positions, Run 318 .	50
28	Bending Moment vs. Deflection for Three Seam Positions, Run 319 .	51
29	Bending Moment vs. Deflection for Three Seam Positions, Run 320 .	52
30	Boom Straightness Testing Via Water Flotation Method	53
31	Boom Straightness, Biaxial Beryllium Copper, 12 × 14 Mesh, E-68 .	55
32	Boom Straightness, Biaxial Beryllium Copper, 12 × 14 Mesh . . .	56
33	Boom Straightness, Biaxial Beryllium Copper, 12 × 20 Mesh, E-2 .	57
34	Boom Straightness, Elgiloy/Beryllium Copper, 12 × 11.5 Mesh, Run 318	58
35	Boom Straightness, Elgiloy/Beryllium Copper, 12 × 16.5 Mesh, Run 319	59
36	Boom Straightness, Elgiloy/Beryllium Copper, 12 × 17 Mesh . . .	60
37	Boom Straightness, Elgiloy/Beryllium Copper, 12 × 26 Mesh, Run 302	61
38	Boom Straightness, Elgiloy/Beryllium Copper, 12 × 26 Mesh, X-4 .	62
39	Boom Straightness, Elgiloy/Beryllium Copper, 12 × 26 Mesh, Run 320	63

LIST OF ILLUSTRATIONS, Contd

<u>Number</u>		<u>Page</u>
40	Boom Straightness, Elgiloy/Beryllium Copper, 12 × 26 Mesh, Run 320	64
41	Boom Straightness, Elgiloy/Beryllium Copper, 12 × 26 Mesh, 1-66 .	65
42	Boom Straightness, Elgiloy/Beryllium Copper, 12 × 26 Mesh, X-1 .	66
43	Thermal Cycling Test Apparatus	68
44	Deflection Recording Camera and Housing	71
45	Camera Assembly with Sample Boom Mounted	72
46	Boom Test Assembly in Thermal-Vacuum Chamber	73
47	Complete Thermal-Vacuum Test Setup	74
48	Thermal Deflection Test, Run 1	75
49	Thermal Deflection Test, Run 2	76
50	Thermal Deflection Test, Run 3	77
51	Thermal Deflection Test, Run 4	78
52	Thermal Deflection Test, Run 5	79
53	Thermal Deflection Test, Run 6	80
54	Temperature History, Run 5	82
55	Temperature History, Run 6	83
56	Temperature Difference and Deflection vs. Time, Run 6	84
57	Stabilized Temperature vs. Angular Displacement	85
58	Deployment Mechanism with Partially Extended Screen Boom on DC Power Supply for Demonstration Purposes	86
59	Deployment Mechanism with Screen Boom Fully Retracted to Show Details	87
60	Deployment Mechanism, Oblique View, Showing Powered Roller, Drive and Guide	88
61	Deployment Mechanism, Bottom View, Showing Powered Roller, Drive, and Guide	89
62	Deployment Mechanism, Boom End View, Showing Typical Screen Boom Ploy and Powered Contour Rollers	90

LIST OF TABLES

<u>Number</u>		<u>Page</u>
1	Elgiloy Data	5
2	Elgiloy Response to Processing Cycles	6
3	Brazing Alloy Data	12
4	Beraloy A Physical Properties as Function of Aging Cycle (Average of Two Specimens)	23
5	Physical Specifications of Delivered Booms, Elgiloy - Beraloy A Wire Mesh	34
6	Beraloy A Boom Strength, Average of Two Specimens	46
7	Elgiloy - Beraloy A Boom Bending Strength	47
8	Thermal Cycling Test Results	69
9	Deployment Mechanism Characteristics.	92

GLOSSARY OF WIRE CLOTH TERMS

COUNT:	Number of open spaces per lineal inch.
CRIMP:	Undulations in warp and fill wires which lock all wires in position. Sometimes called double crimp because both warp and fill wires are crimped.
FILL WIRE:	Wire running transversely through the cloth. Also called the shute wire.
MESH:	Number of openings per lineal inch, measured from the center of any wire. See rectangular mesh and square mesh.
OFF-COUNT MESH:	Rectangular mesh.
RECTANGULAR MESH:	Mesh count greater in one direction than in the other. Sometimes called Off-Count mesh.
ROLL:	The standard method of packing wire cloth. A standard roll contains 100 lineal feet.
SELVAGE:	The finished woven edge of wire cloth.
SHUTE WIRE:	Wire running transversely through the cloth. Also called fill wire.
SPACE:	Size of the clear opening between parallel adjacent wires.
SQUARE MESH:	Mesh count identical in both directions.
WARP WIRE:	Wire running parallel to the length of the cloth.
WEAVE:	The manner in which warp and fill wires are interwoven. Plain weave cloth has each warp wire passing alternately over and under the fill wires at right angles.

SECTION 1

INTRODUCTION

This report presents in detail the history and results of the Gravity Gradient Boom and Antenna Material Study, conducted under Contract NAS5-9597. The broad objective of the program was the production of rigidized, woven screen material having sufficient spring action to immediately and repeatedly form a tubular shape when freed of all restraint.

The program was conducted in four overlapping phases consisting of:

- a. The development of procedures for rigidizing the nodes of woven screen material.
- b. The generation and verification of a mathematical model to predict thermal deflection of uncoated screen materials.
- c. A limited testing and evaluation program to verify the mechanical properties of the particular rigidized screens selected for delivery.
- d. Development of a device capable of deploying a wire screen boom.

The work statement from Contract NAS5-9597 has been reprinted in this report as Appendix I for reference to scope, materials, constraints, and limitations.

This summary of work performed is presented in the order of the four phases listed above. The phase devoted to the development of procedures for rigidizing wire screen and subsequent boom forming was conducted throughout the entire program. Comprehensive processing details are presented in a chronological context. A complete processing procedure is included in Appendix II. The detailed thermal analysis of wire mesh booms is included in Appendix III.

Straightness and distortion problems have effected considerable limitations on the use of deployable booms in spacecraft operation. The use of rigidized woven screen has certain advantages over tape in this application. Broadly presented, the wire screen can be woven of dissimilar materials to independently optimize parameters in two directions. Thus, thermal conductivity in the circumferential direction and thermal expansion longitudinally can be optimized in a boom by judicious selection of materials. Uniformity of properties of long lengths of screen is not affected by processing as are the properties of tape or foil. Finally, the overall properties of wire screen can be predetermined for a particular application through the proper selection of wire and mesh sizes. In this manner, the mechanical properties can be varied, as can the percent-open-area for illumination of the normally shaded side of a boom.

SECTION 2

DISCUSSION

This section presents the development of processes required to rigidize woven screen material and to form the screen material into booms of specified physical characteristics. It describes the equipment developed and constructed to manufacture such booms on a continuous basis and presents testing methods and results of limited tests performed on finished boom lengths. The section also includes a detailed description of a mechanism developed to deploy and retract wire screen booms.

2.1 WIRE SCREEN BOOM PROCESS DEVELOPMENT

The development of continuous rolls of deployable boom material was accomplished in several phases of increasing complexity. Initial feasibility experiments using 1 by 12-inch strips of stainless steel screen were replaced by processing 4 by 36-inch strips to develop quasi-continuous parameters and techniques. The initial use of stainless steel (Type 304 SS) screen was based on the availability of such material. These process developments were conducted while biaxial beryllium copper alloy 25 (Beraloy A) screen in three different mesh sizes was ordered, woven, and delivered.

Screen processing development continued with 4 by 36-inch strips of the Beraloy A screen for some process modification prior to the construction and use of the continuous screen processing equipment capable of handling bulk material in rolls. Concurrently with the continuous screen rigidizing equipment development, work was progressing on continuous tube or boom forming devices. Techniques were also developed concurrently to utilize the selected longitudinal wire material, Elgiloy, in conjunction with Beraloy A. The two-metal wire screen was ordered from a vendor when processing details, procedures, and requirements were well enough established.

Techniques for processing screen lengths in excess of 50 feet were fully developed on the biaxial Beraloy screen by the time the delivery hardware screen was woven. Failure of the vendor to supply the Elgiloy wire part of the special screen in a cold-worked condition, as had been ordered, required rapid development of a secondary cold-working technique on the brazed Elgiloy screen. Cold work is necessary for the Elgiloy to respond to thermal treatment. All subsequent development work was then conducted on the two-material screen.

Forming of the brazed screen into tubular or boom shape was initially accomplished on mandrels using conventional furnaces and a batch technique for short lengths. The initial model of the continuous-tube former utilized a cable and winch device to form straight boom lengths, limited only by the available space (68 feet). A major modification was made to this equipment to enable continuous rewinding of the formed boom and thus be truly continuous.

Development of all processing techniques was complicated by the requirement for three different percent-open-area booms. Although the processing techniques were tolerant of many variables, the introduction of three widely varying wire mesh screens effectively required three different techniques or modifications. The introduction of a screen stretching operation for the Elgiloy again produced three different mesh sizes and subsequent changes in techniques.

2.1.1 MATERIAL SELECTION. Selection of a material for the longitudinal wire was based strongly on processing potentials. The material's physical and mechanical properties were taken into account, but were clearly secondary to the primary requirements of:

- a. Lower coefficient of thermal expansion than Beraloy A (contractual).
- b. Capability or potential of being woven into screen in conjunction with the Beraloy A.
- c. Compatibility with Beraloy A heat treatment.
- d. Capability of being brazed.

Naturally, the selected material required the properties for booms in gravity gradient applications, i.e.:

- a. It had to be nonmagnetic
- b. It required potential for having spring properties.

The thermal conductivity, electrical properties, and modulus were not initially considered in the primary material selection.

The only material with any potential for meeting all of the requirements was Elgiloy, a 40 percent cobalt-based alloy. The initial attractiveness of this alloy was its coefficient of thermal expansion (for contractual obligations), its nonmagnetic quality, and its characteristics as a corrosion-resistant spring material. This material has a high modulus, is capable of having exceedingly high strength, and is both brazable and weldable. It was, furthermore, available as a standard item, is readily drawn into wire, and it has properties which made it potentially weavable. A list of properties of Elgiloy is given in Table 1.

The only drawback to the alloy was the heat-treatment requirement. Compatibility with Beraloy was questionable at a first glance; it had a heat-treatment cycle of 5 hours at 980° F compared with 600 to 700° F for 1 to 2 hours for the copper beryllium alloy. Tests conducted on Elgiloy wire, however, revealed distinct potential for circumventing the apparent noncompatibility through proper processing procedures.

Table 1. Elgiloy Data

Nominal Composition:

Cobalt	-	40%	Manganese	-	2%
Chromium	-	20%	Carbon	-	0.15%
Nickel	-	15%	Beryllium	-	0.04%
Molybdenum	-	7%	Iron	-	Balance
Density	-	0.300 lb/in. ³			
Specific Gravity	-	8.3			
Linear Expansion	-	12.7×10^{-6} per ° C (0-50° C)			
Mean Thermal Coefficient of Expansion	-	15.17×10^{-6} per ° C (0-500° C)			
Thermal Conductivity	-	0.0298 Cal/sec/CC/° C			
Permeability	-	Varies from 1.00012 at -140° C to 1.00003 at +200° C			
Heat Treatment	-	980° F - 5 hr (Nominal)			
Maximum Properties (85% Cold Work)	-	Ultimate Strength	-	368,000 psi	
		Yield Strength	-	280,000 psi	
		Proportional Limit	-	233,000 psi	
		Modulus of Elasticity	-	29.5×10^6	
		Hardness (R _C)	-	56-59	

Final longitudinal material selection was not made until basic processing procedures had been established on biaxial copper beryllium wire mesh. As will be detailed in later sections, the brazing cycle consisted of a short excursion to approximately 1300° F. While the recommended heat treatment for Elgiloy was 980° F, it was known that response might be achieved at the higher temperatures for a much shorter but well controlled time. Elgiloy wire having varying amounts of cold work or percent cold reduction was subjected to simulated brazing cycles in a 1300° F furnace (using foil shields to inhibit the heating rate), and then the physical properties were determined. The results of these tests, presented in Table 2, were sufficient to make the selection of Elgiloy as the longitudinal wire material final.

2.1.2 WIRE SCREEN MESH SELECTION. A study was made to determine the magnitude of the problem of stress analysis of a wire mesh boom. As was expected, the analysis of slit tubular screen elements proved to be exceedingly complex. Analytic studies were discontinued when it was realized that a comprehensive analysis could not be conducted within the scope of the overall program. Therefore, a course of

Table 2. Elgiloy Response to Processing Cycles

CONDITION AND PROCESSING TREATMENT	F _{ty} (psi)		F _{tu} (psi)	ELONGATION (%)
	1% -10 IN.	0.1% OFFSET		
As Received - Soft Reduction	67,800	65,900	139,300	70.10
Soft Reduction + 1300° F 60 sec	68,800	66,200	137,600	60.33
Soft Reduction + 1300° F 60 sec + 700° F, 1 hr	69,100	66,500	137,200	60.50
As Received - 24% RA Cold	104,500	130,000	191,100	10.25
24% RA Cold + 1300° F 60 sec	133,800	183,400	204,200	2.50
24% RA Cold + 1300° F 60 sec + 700° F, 1 hr	135,700	173,200	200,300	2.55

action was followed wherein wire mesh was woven to give a wide variety of conditions for future empirical selection of final mesh sizes. Copper beryllium screen was ordered on the basis of a single warp count but with separate sections having different fill or shute counts. Specific terminology used in this report will refer to the wire mesh count as the second number. The third and fourth numbers are the diameters of the longitudinal (warp) and circumferential (shute) wires, respectively. If warp and shute are identical, only one diameter is given.

A roll of screen with a 12-count warp, 100 feet in length was woven by the Tyler Co., Cleveland, Ohio, having a 50-foot section with 12-mesh shute, 25 feet of 16 mesh, and 25 feet of 20 mesh. Wire size was 0.009-inch diameter. Screen width was 48 inches. Judicious cutting of this screen yielded the following:

12 x 12 x 0.009	50 feet - 80.0 percent open area
12 x 16 x 0.009	20 feet - 76.4 percent open area
12 x 20 x 0.009	20 feet - 73.1 percent open area
16 x 12 x 0.009	4 feet - 76.4 percent open area
20 x 12 x 0.009	4 feet - 73.1 percent open area

The basis for selection of these meshes was a combination of minimum wire diameter with minimum mesh count, (thus yielding a highest percent-open-area that could be commercially woven) and, progressively, the reduction in percent-open-area by increasing the shute. Since processing was being accomplished in quasi-continuous 36 to 40-inch lengths, crosscutting of the two off-count meshes provided a fourth and fifth mesh for evaluation of strength.

Selection of mesh sizes for the Elgiloy - Beraloy A screen was based on experimental bending strength tests on biaxial copper beryllium booms, general guidelines developed in the stress study, thermal analysis studies, and practical considerations concerning weavability of screen. It was found that a small-diameter boom composed of large-diameter wire with wide mesh spacing and maximum percent-open-area is required to minimize the thermal gradient. From mechanical strength considerations, however, a large-diameter boom composed of multitudes of small wires is needed for maximum strength (on an equal weight basis). The boom diameter is a direct function of the circumferential wire diameter (modified of course by nodal considerations) so as not to exceed the yield point of the wire when flattened from a circular shape. From processing and testing considerations, a single boom diameter in the specified percent-open-areas was desired and contractually required.

Many compromises were made in the overall selection of three mesh sizes in the required ranges. A nominal boom diameter of 0.75 inches was established for delivery items and a range of circumferential wire sizes was determined. Combinations of these wires with assumed warp wire diameters were examined for percent-open-area, potential thermal properties, potential bending strength, processability, and weavability. One other important factor was considered, i. e., the use of a single wire size and mesh size for the warp (Elgiloy) with variation of the percent-open-area solely by changing the shute count (Copper Beryllium). This consideration was important from a weaving time and cost aspect and, furthermore, was judged necessary from a practical processing viewpoint. In consideration of all factors, a 12-mesh warp of 0.009-inch Elgiloy was chosen for the constant warp. A 0.008-inch Beraloy A shute was chosen and shute mesh varied to obtain the various percent-open-areas. With these parameters, a 14-mesh shute yielded a 79 percent open area for the above 75-percent requirement, a 20-mesh shute yielded a 74 percent open area for the 60-to-75-percent requirement, and a 30-mesh shute yielded a 67.5 percent open area as being the smallest practical open area that could be formed into a usable boom.

2.1.3 WOVEN SCREEN RIGIDIZING PROCESS DEVELOPMENT

2.1.3.1 Process Requirements and Selection. Selection of a welding or brazing process for rigidizing the nodal points or nodes of woven screen was dictated by two major considerations. First, it was known that one of the materials to be joined would be Beraloy A, a material not noted for weldability, and that the second material would be a dissimilar material. Second, the number of joints to be made would preclude any method not applicable to multiplicity. Resistance and fusion welding were eliminated almost immediately from all consideration. Ultrasonic welding was the only welding process, per se, to receive even passing attention.

Brazing was selected as the node joining process since its inherent advantages far outweigh those of any other method. These are, in brief: applicability to dissimilar materials, adaptability to continuous processing, wide variety of processing conditions, and a highly advanced state-of-the-art.

It was recognized that the overall rigidizing process and subsequent boom forming would have to be continuous in nature. Node joining would have to have a very high level of integrity and repeatability. The process should not have any deleterious effects upon the screen structure components, and Beraloy A aging cycles could not have any effects upon the brazed joints.

Silver alloy brazing, covering the temperature range of the lowest commercially available alloy (1145° F) to the nominal annealing temperature of Beraloy (1475° F), was therefore selected as the basic process for rigidizing wire mesh screens for boom application.

2.1.3.2 Brazing Process Development. A statement of the problem confronting the investigators at the start of this material study might have been: How can one or two million joints be brazed in an hour? Development of a brazing process with that capability was initiated by proving that it could be done a few hundred joints at a time in a batch process under ideal conditions. From there, the same number processed under practical conditions, followed by short strips processed in a quasi-continuous manner, then, longer and wider lengths processed similarly to obtain parameters, and finally processing of continuous lengths.

The initial brazing studies were conducted on stock stainless steel screen, Type 304, woven from 0.009-inch diameter wire in a 16 mesh (i. e., $16 \times 16 \times 0.009$ Type 304 SS) to define problem areas and to resolve them as required. Feasibility studies were conducted on 2-in.² samples, using a wide variety of alloy and flux application methods. These samples were brazed for varying periods of time over a wide temperature range using inert, reactive, and air atmospheres. Significant observations of this initial series of tests were:

- a. The extremely smooth mirror finish of finely drawn wire inhibits flow but not wetting of braze alloy.
- b. Fluxless brazing in a reactive atmosphere gave excellent results but did not tolerate contaminants without impairing the overall effect.
- c. Powdered brazing alloy, dispersed in a flux, brazed the screen nodes equally as well as those joined in a protective atmosphere.
- d. The low mass of the screen afforded very short heating cycles.
- e. Uniformity of braze alloy application was the key to overall braze joint uniformity.

A second series of braze tests was processed in strip form. It became rapidly apparent that the application of flux and braze alloy to the screen, where they were needed and in the amounts that they were required was the major problem area. Flux and alloy slurries were applied in most conceivable ways such as doctor bars, brush, spray, roll transfer, and dipping. Of all means investigated, spray and dipping were the most feasible and promising. Flux dipping was soon proved to be a more effective

and versatile means of application and spray methods were eliminated. Flux dipping also had its drawbacks. When flux was applied in sufficient quantities to coat only the wires, it would ball at the nodes or in the middle of horizontal wires between nodes and leave the remainder of the wire unprotected. Likewise, when the flux was applied in a heavy enough body to bridge the entire span between wires, upon heating the viscosity dropped to low values leaving a similar condition to the case where flux was applied only to the wires. Proper viscosity control and progressive high temperature drying cycles for the flux resolved the flux application problem sufficiently to proceed with a larger sample size.

A small, but exceedingly important investigation was performed to determine the most suitable flux. Most commercially available silver brazing fluxes were evaluated to some degree. It was found that there was one outstanding flux for this application, i. e., Handy and Harman Flux Type B-1. It provided the best wire coverage, exhibited long life under brazing conditions, and was supplied in a conveniently heavier-than-required viscosity. Although all of the fluxes evaluated were effective as flux, H & H B-1 was the only flux that could be removed after brazing with only a simple warm-water wash. All others required shock treatment either with boiling water or with a mechanical method. This ease of B-1 removal was its most important characteristic.

Proper control of the flux was the most critical development aspect throughout the program, even while processing screen booms for delivery under the contract. Application of the flux and braze alloy in slurry form was, in the least, exasperating. Required uniform amounts of slurry could be applied at times without difficulty, at other times all went wrong and application ended with upwards of 5 percent "windows" (one square not filled). Although the occurrence of random windows did not affect the end brazing result, the four wires forming the window frame were left uncoated and subsequently would oxidize during brazing. A flux modification study was undertaken to improve the uniformity during application and to raise the molten-state viscosity. Wetting agents were not effective in promoting uniformity of application. There was strong evidence that their use was inhibiting brazing and therefore this approach was abandoned. Molten-state viscosity control was very effectively accomplished through the addition of 15 percent sodium fluoride to the H & H B-1 flux. It markedly reduced the occurrence of windows after brazing. Application uniformity was resolved by dipping in a very-heavy-viscosity slurry and passing the overly-heavy-coated screen immediately through infrared radiation from heat lamps. Changes in viscosity could be obtained wherein a very closely controlled amount of flux could be retained on the screen. Simple changes in infrared intensity through power control of the lamps allowed almost instantaneous changes in the amount of slurry retained on the screen. The greater uniformity in application was apparent both in the drying cycle and in the subsequent brazing operation.

A strip sample size of 3 and 4 inches by 36 inches was utilized for development of quasi-continuous processing parameters. During this series of process development tests, flash or strike copper-plating was introduced into the process as a wettable

surface to overcome the problems associated with the very smooth wires. Also during this series, the Beraloy A screen in three mesh sizes was introduced and rapid transfer of brazing technology from the stainless steel was accomplished. A flash silver plate was substituted for the copper because it was slightly more effective and could be applied from room temperature solutions instead of the elevated temperatures required for copper plating. The successful rigidizing of all copper beryllium screen provided screen material to other development areas for heat treatment into cylindrical boom sections up to 36 inches in length for physical and mechanical testing. It was rapidly learned that the specific high-temperature flux drying cycle, a fairly heavy braze alloy overlay on the wires, and heavy crimp in the screen contributed to failure of screen booms to perform as expected. Flux application and drying cycles were changed to eliminate premature Beraloy aging. The screen was given a calendaring operation (see Section 2.1.3.5) to reduce the crimp ratio, and the amount of braze alloy was changed slightly through actual reduction in amount in the slurry and by flux slurry application modifications. The brazing cycle was also modified to minimize the exposure time above 800° F. These changes not only improved the mechanical and physical properties of the screen, but were immensely effective in raising the percentage of brazed joints to well above 99 percent. Of these modifications, the most effective improvement was due to the calendaring of the screen. This had the effect of providing an enlarged, flat contact area at the node, eliminating the occasional loose point-to-point contact of round wires.

Brazing process development was conducted primarily on 4 by 36-inch strips of screen to determine continuous processing parameters. This work was done using a vertical slot-type furnace, consisting of two indirectly-heated sides of Inconel X spaced 2 inches apart. Height and width were 6-1/2 and 9 inches, respectively. A 1 by 6-inch slot at top and bottom permitted the screen to pass through. A small thyrotron-controlled, variable-speed DC motor and a series of pulleys provided quasi-continuous operation.

Heating and brazing studies on this equipment were valuable in the overall process development in that they provided a rapid means of processing short lengths for further work, used a minimum quantity of screen, and allowed quantitative process parameters to be obtained. The Elgiloy brazing and heat treating cycle developed on this equipment remained basically unchanged for the remainder of the program. This is shown in Figure 1 as a time-temperature plot from a screen test-run. Of primary interest with copper beryllium is the utilization of a short brazing cycle so as to minimize the time of exposure to temperatures above 800° F. Use of furnace temperatures well above the actual brazing temperature permitted control of the actual brazing temperature and exposure time by travel speed of the screen through the furnace. The combination of furnace temperature and screen speed therefore gave very accurate control of the entire set of variables.

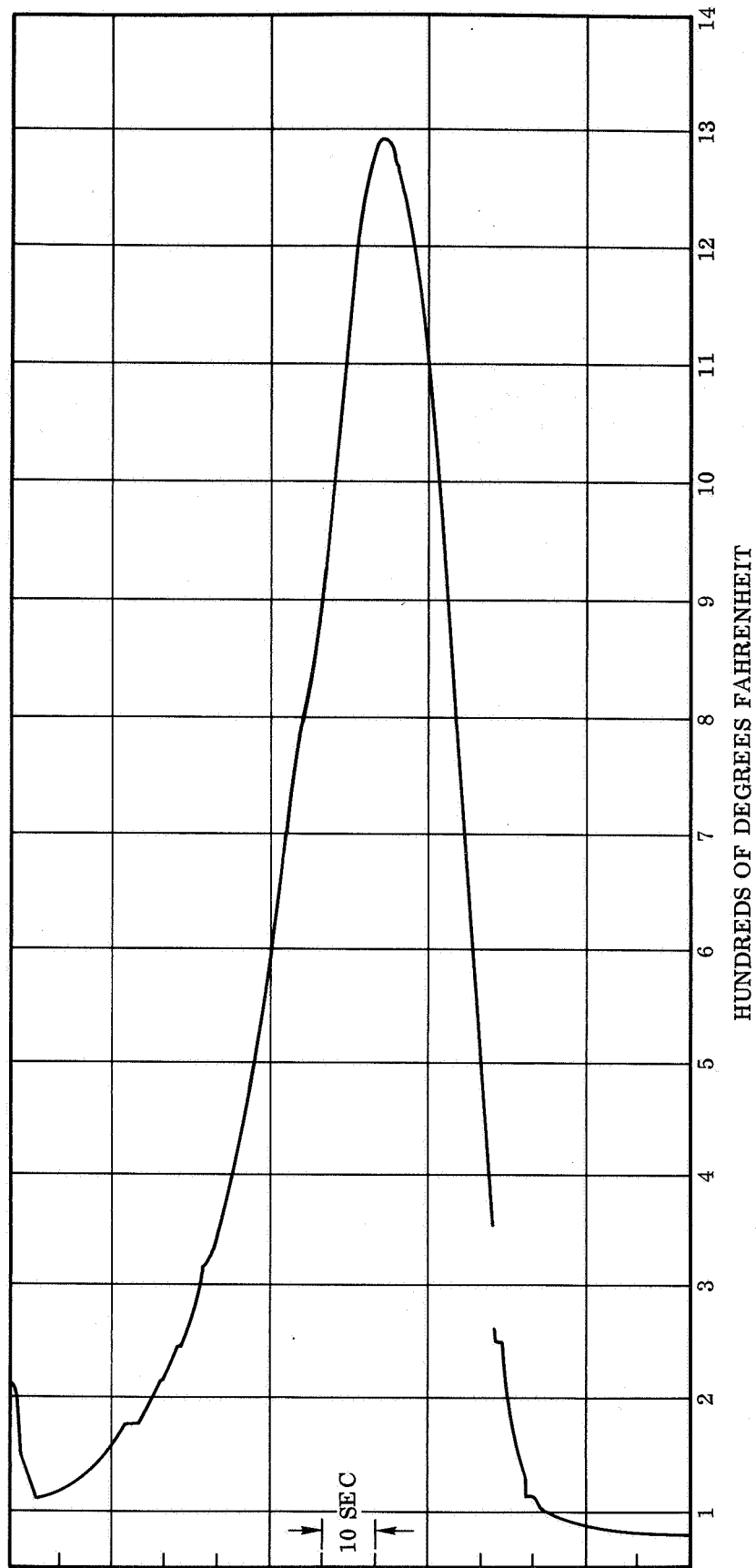


Figure 1. Basic Wire Screen Brazing Cycle

Selection of the brazing alloy was primarily influenced by the necessity for a short cycle, compatibility with the Beraloy and the reasonably narrow temperature range. The alloy compositions given in Table 3 were investigated for applicability and use. The BAg-1 and BAg-1a alloys were far superior in their ability to form smooth fillets rapidly and the final selection between these two was in favor of the 50 percent silver alloy with its lower cadmium content.

The required brazing temperature for screen was determined by equipment and coatings. Although the brazing process is very tolerant of changes in temperatures where almost 100 degrees of superheat is concerned, the uniformity of the end wire coating and fillet was much more demanding of the need for controlled temperatures and screen travel speeds. Necessity for a closely controlled flux coating was more and more evident as the brazing parameters were determined. The overall mass of the flux and its residual moisture content were strongly contributing factors toward the need for development of controllable process elements. Although the equipment developed for continuous roll processing had all necessary controls, visual monitoring for proper brazing became the most reliable control. Overall braze temperature under the conditions of high furnace temperature could be changed instantaneously through screen speed changes.

Table 3. Brazing Alloy Data

ALLOY	COMPOSITION (%)					MELTING POINT (° F)	FLOW POINT (° F)
	Ag	Cu	Zn	Cd	OTHER		
BAg 1a	50	15.5	16.5	18	3 Ni	1160	1175
BAg 3	50	15.5	15.5	16		1170	1270
BAg 1	45	15	16	24		1125	1145
BAg 2	35	26	21	18		1125	1295
BAg 8	72	28				1435	1435

2.1.3.3 Continuous-Brazing Process Development. The basic techniques developed in quasi-continuous processing of 3-foot lengths of screen were used in continuous processing of rolls of screen. The parameters of temperature, time, and travel speed were phased into the overall design of equipment. It was realized that, in many instances, screen could not be handled in the same manner that foil or strip could. It was also realized that many changes in the processes would be forthcoming as a result of these differences. Therefore, the continuous processing equipment was constructed on a modular basis using an adaptable framework of Unistrut.

Calendering operations were performed on a 6-inch, two-high rolling mill in the laboratory. Feed and take-up rolls and stands were constructed especially for the purposes of screen calendering. Feed roll tension was maintained manually as was take-up roll tension and drive. Problems associated with this calendering operation are discussed in detail in Section 2.1.3.5.

Degreasing and cleaning facilities that existed in the laboratory were utilized for the rolled screen. Cleaning was entirely conducted on the bulk roll using a Turco 1000 W ultrasonic cleaning tank and overflow-type rinse tanks. A forced-convection oven was used for drying operations.

The first major change in adaptation to continuous processing occurred in the plating operation. As mentioned above, silver-plating for wettability was selected over copper, which had been previously used, since plating could be conducted at room temperature. The plating line consisted of a feed roll with a sliding or rubbing current contact and a drag/tension device, a Plexiglas plating tank, a two-stage spray wash and rinse, a drying tower oven and a take-up roll. Plating was accomplished at 36 inches per minute.

While the initial concept for continuous processing contained some elements of truly continuous processing from raw screen to complete rigidization, early work showed that it was decidedly not the proper avenue of approach. The application of the flux/brazing alloy slurry to the screen is a good example. Until the process was completely debugged, the application was halted, slowed, speeded up, and otherwise changed. Had this been tied in with brazing, no screen would have ever been processed in other than short lengths.

The flux dipping and drying operation was changed when applied to the continuous process for a full roll. Control of flux viscosity via temperature and agitation could not be maintained over the extended periods of time required for long rolls of screen. The previously described use of infrared heating for the instantaneous viscosity control was developed during the initial continuous processing runs. The low-temperature flux drying cycles for prevention of premature aging of copper beryllium alloy were also instituted at this time along with necessary modifications to the ovens.

Problems that were anticipated with the tracking of the screen over idler and drive rolls never materialized. The basic problem was that of maintaining tension as required for each particular step. This was also the major problem in the application of the earlier developed brazing techniques to continuous processing. It was temporarily solved through the use of a pony-brake arrangement on the shaft of the feed roll.

Completely manual controls were used throughout for processing speed. Although the diameter of the take-up roll was constantly changing, manual changes through a variable-speed DC drive motor required only periodic adjustment for compensation.

Speed indications were obtained from timed reference marks on known-diameter idler drums or wheels and by reference to a calibration chart.

Flux removal was accomplished in bulk by immersion in warm water, followed by immersion and spray rinsing with clear water.

Figures 2 and 3 show the initially developed processing equipment in the two major processing arrangements for flux application and brazing. The power supply on the left hand side of Figure 2 was used during the plating operation. The plating tank (not shown) occupied the space directly beneath the supply roll on the left. Drying tower oven temperatures and brazing furnace temperature were continuously recorded by the strip chart recorder. Brazing temperature was maintained at the required point with the Thermac controller and power supply, shown above the strip chart recorder.

2.1.3.4 Elgiloy - Beraloy A Wire Screen Processing Development. The transition to the two-metal screen from the all Beraloy A screen with regard to processing technique, was accomplished with a minimum of problems. Previous tests on stainless steel screen and Elgiloy samples had shown almost identical brazing characteristics and the Beraloy A techniques were fully compatible with the stainless steel. The calendering techniques were slightly modified since the difference in properties between the two materials shifted the proportion of wire reduction at the node area from 50-50 to about 90-10. Before switching to the two-metal screen, with Beraloy only at the nodes, reduction in total thickness could be from 0.018 to 0.011 inches. In the case of the two-metal screen, the as-woven thickness of 0.021 inches could be rolled or calendered to only 0.0135 - 0.014 inches without seriously crippling the Beraloy wire. Although the two-metal screen was woven from 0.009-inch diameter Elgiloy and 0.008-inch diameter Beraloy wires, the slightly different crimp attained in the Elgiloy warp caused the overall as-woven thickness to be 0.003 inches thicker than the all Beraloy screen woven of 0.009-inch wire in both directions.

Cleaning prior to plating posed an almost insoluble problem. Simultaneous cleaning of a copper-base alloy and a corrosion-resistant, cobalt-base alloy to attain a surface properly cleaned or activated for an adherent plating could not be done without affecting one or the other material. A compromise was attained by limiting cleaning to degreasing followed by immersion-cleaning in a hot, inhibited alkaline solution. (Oakite 165, 6 to 10 oz/gal at 180° F, a cleaner normally used for aluminum.) Subsequent silver-plating adhered well to the Beraloy but had a tendency to flake from the Elgiloy when it was abraded. No adverse results were ever attributed to the flaking.

No changes in the flux or the application procedures were required in the transition. Brazing procedures were only slightly modified to allow some additional furnace time to permit longer time for the flux to dissolve the highly refractive surface oxides on the Elgiloy. This was accomplished by adding a 2-1/2-inch extension to the top of the slot furnace.

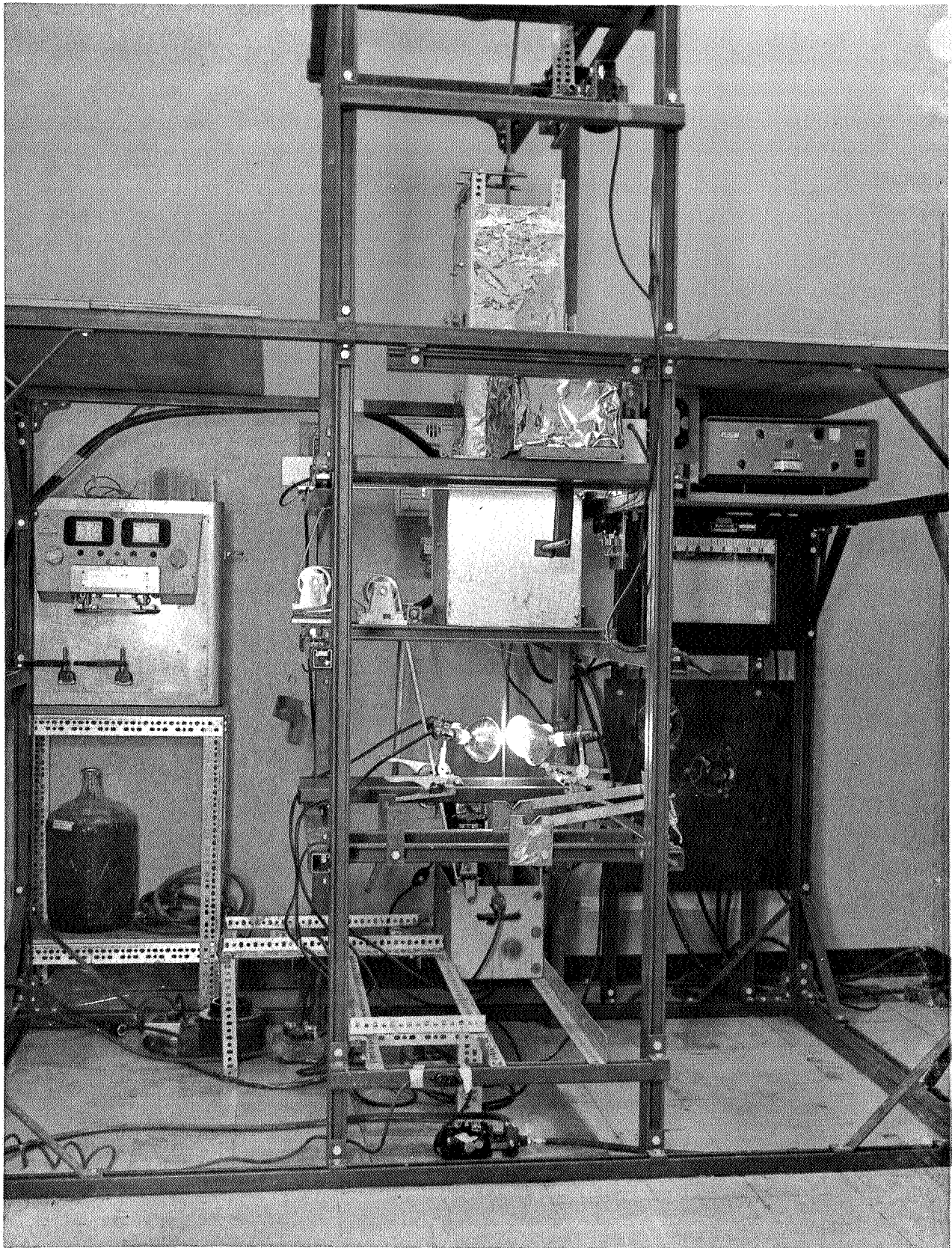


Figure 2. MOD I Continuous Screen Processing Equipment Shown In Flux/Braze Alloy Slurry Dipping Mode

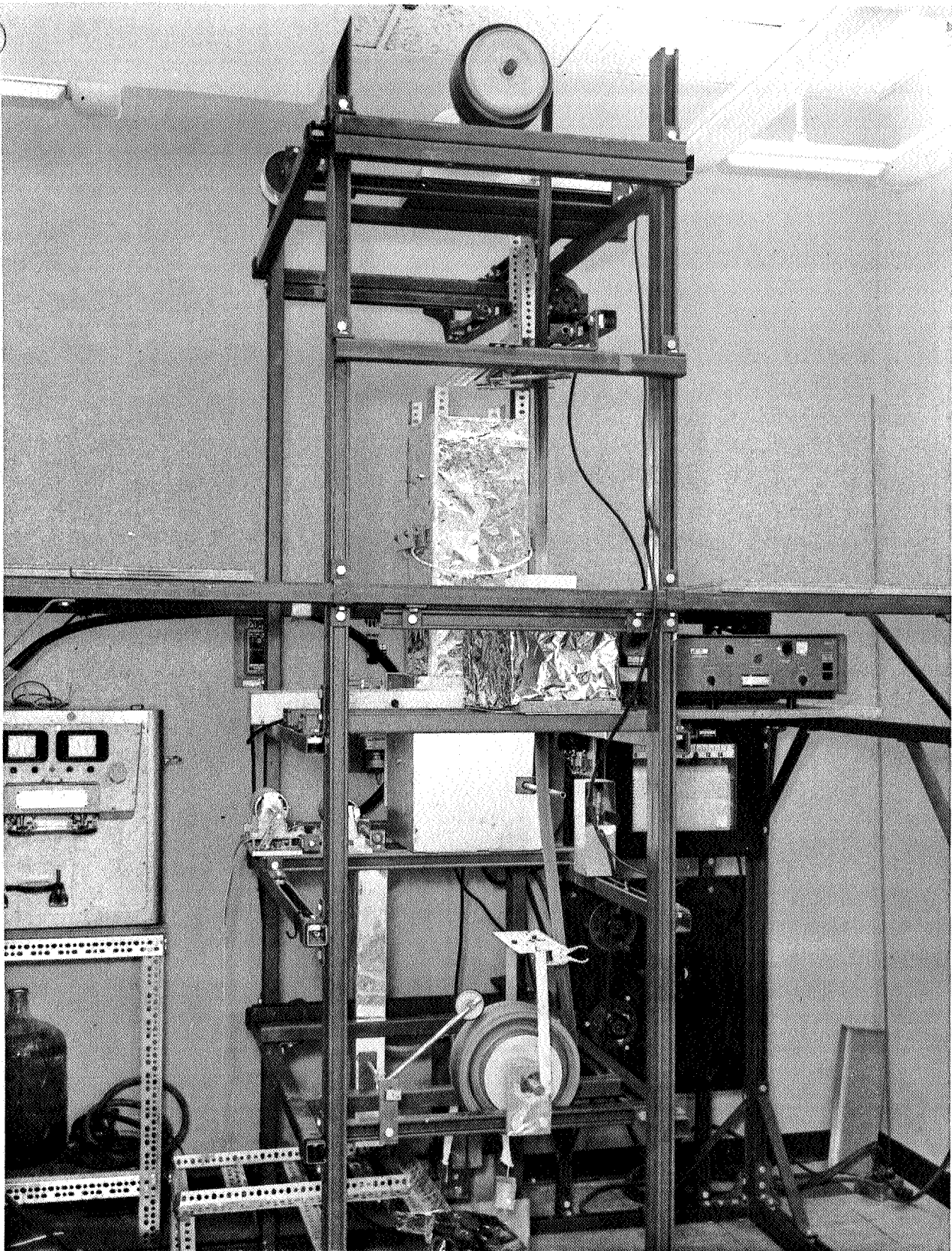


Figure 3. MOD I Continuous Screen Processing Equipment Shown In Brazing Mode

It was strongly suspected after brazing of the initial roll of Elgiloy screen that no heat-treat response had been obtained. This was confirmed by through-processing the brazed screen into boom shape. Upon flattening of the boom, the outer edge wires yielded. Subsequent investigation showed that the Elgiloy had been woven in an annealed condition. (The reason for annealed wire was found to be the result of the screen vendor ordering wire to a tensile and yield value rather than to a percent cold reduction.) Since the screen could not be rewoven without a delay of at least three months, it was decided to strive for a partial solution or an immediate fix, if one could be developed satisfactorily.

Investigation of the ductility of the screen in the as-brazed condition showed that it could be stretched up to 25 percent in length before random wire breakage caused catastrophic failure and complete cross-tearing of the screen. The first 2 percent of the stretch solely eliminated the longitudinal wire crimp. The loss of the longitudinal wire crimp by stretching caused an increase in the transverse wire crimp, giving the screen a total measured thickness of over 0.030 inches. Subsequent calendering was determined to be the only means to redistribute the crimp and to obtain a uniform thickness.

Stretched and recalendered screen was then put through a complete brazing cycle, including flux application, drying, and braze thermal cycle. These cycles were identical to the original rigidizing cycles, except for the complete elimination of powdered brazing alloy in the slurry. This reprocessed screen was found to have the expected physical properties. A completely satisfactory process was therefore found that not only salvaged the screen material but provided a straightening operation for the material. This, of course, resulted in an increase in total processing time of over 100 percent.

The stretching had the effect of changing the properties of the boom material. In addition to reducing the Elgiloy wire diameter from 0.0089 inches to 0.0082 inches, the 20 percent stretch reduced the mesh count of the shute wires from 14 to 12, 20 to 16 or 16.5, and 30 to 26, thus increasing the percent open area. Over 1000 feet of 4-inch wide screen were rigidized during this phase of the program; random breaks in the screen, causing the screen to part suddenly, were a source of unresolved problems.

Prior to using the equipment in an extended period of performance, a thorough overhaul and modification was undertaken to correct marginal design, and provide greater reliability and uniformity in performance. Figures 4 and 5 show the modified equipment in the flux application and brazing configurations, respectively. The major differences from the original versions are in the refinement of the equipment. Dismountable aluminum reels were instituted to prevent spillage of stored and rolled screen and to aid in uniformity of rewind. The screen-tension arrangement was changed from a pony-brake to a rubber pinch roll; tension on the brazing configuration was applied with an electric brake modified for this application. All bearings were

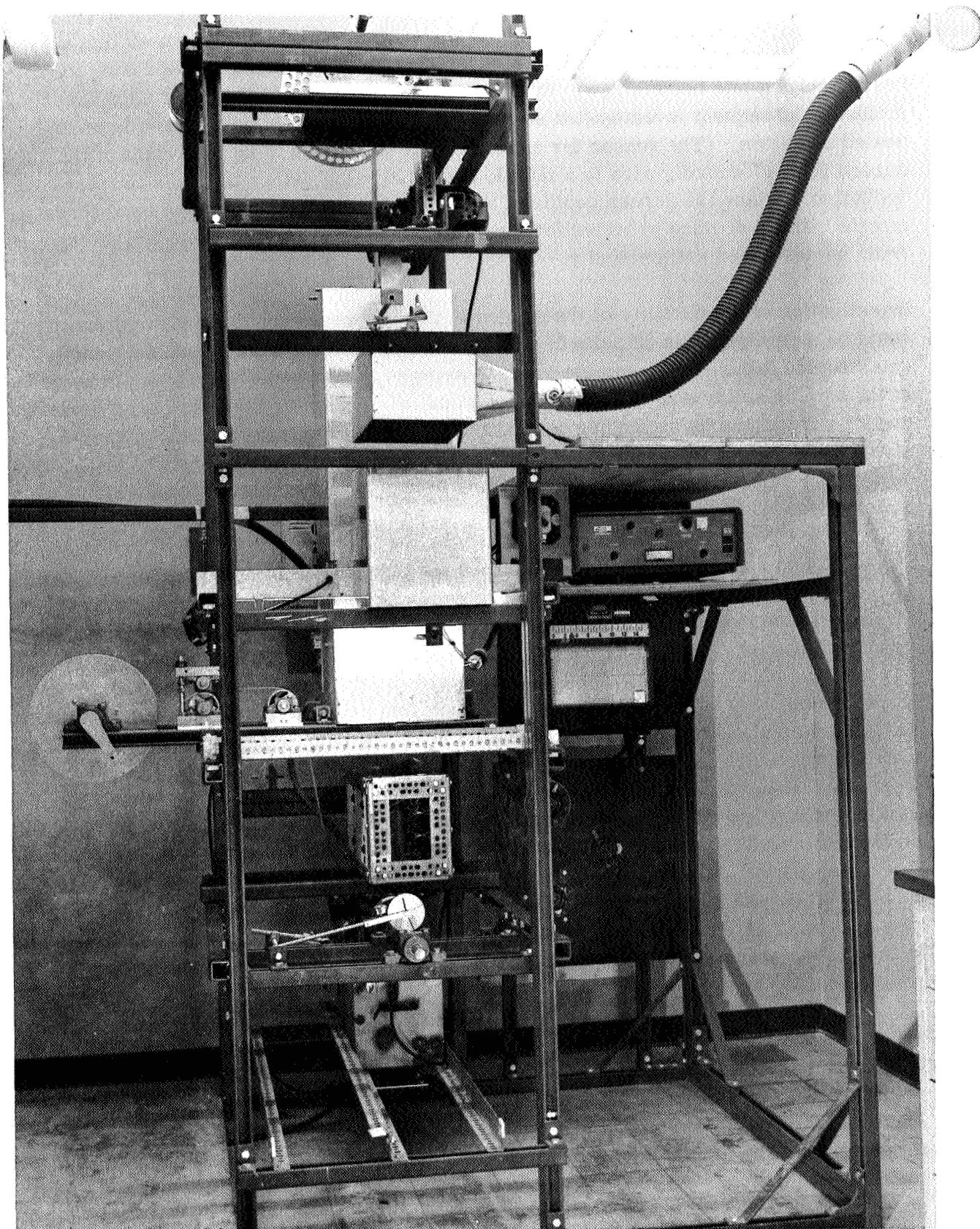


Figure 4. MOD II Continuous Screen Processing Equipment Shown In Flux/Braze Alloy Slurry Dipping Mode

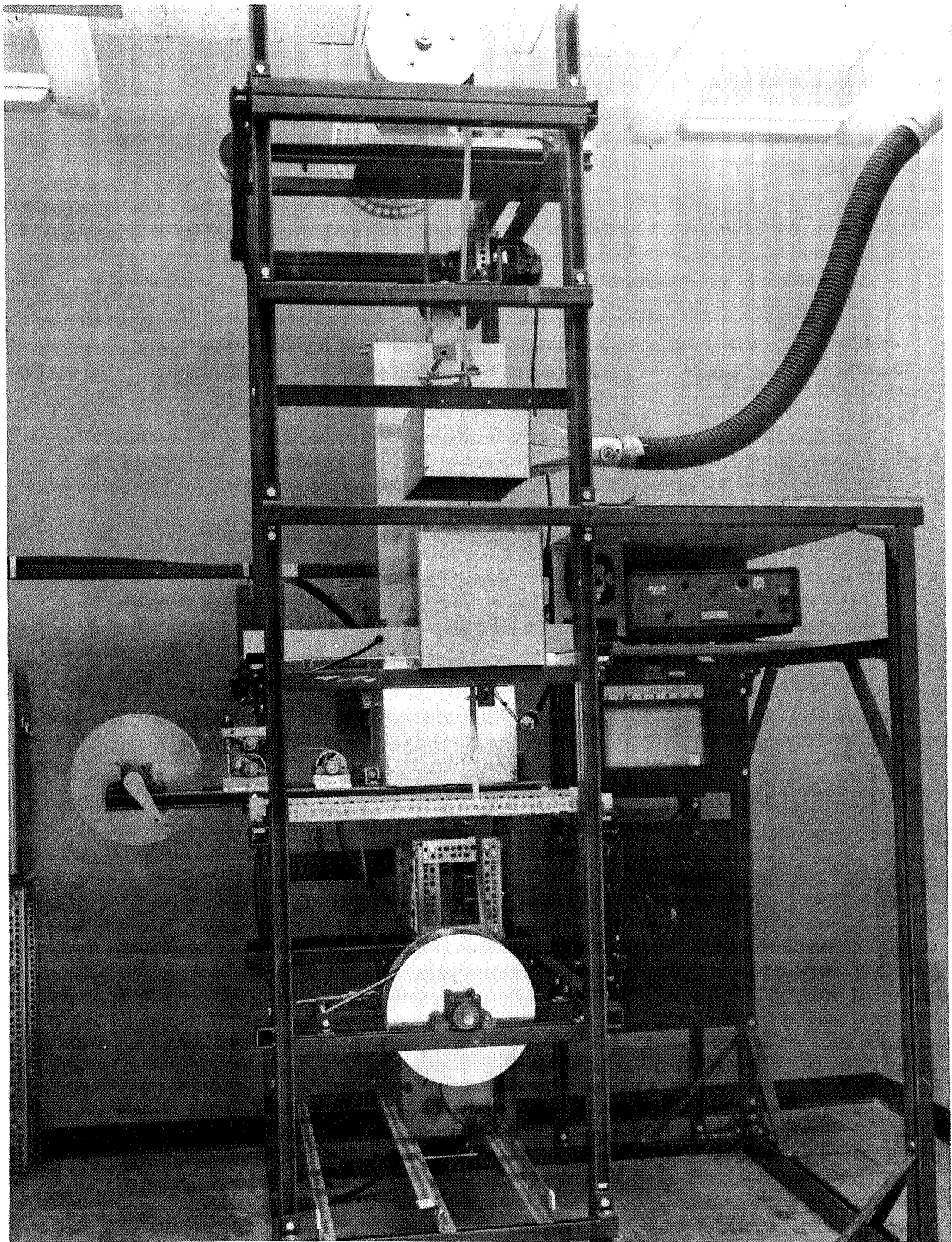


Figure 5. MOD II Continuous Screen Processing Equipment Shown In Brazing Mode

changed to bronze sleeve types, an infrared lamp bank was substituted for the individual reflector types previously used, the ovens and furnace were shrouded for greater uniformity, and a footage counter was added.

Contractually deliverable screen items were completely processed through the first braze cycle when it became apparent that overall brazing was exceedingly marginal. The cause of the problem was determined to be that of greatly changed flux-mixture properties. The flux had a nonuniform and highly irregular tendency to break down at the relatively low brazing temperatures and the short time cycle. This was found to be caused by the relatively short shelf life of the flux. Subsequent processing of additional screen through first braze, using a new batch of flux, was highly successful. Stretching of full rolls of screen (120 feet) was instituted during this final phase of the study. One additional problem appeared; the normally high ductility of the Elgiloy wires had decreased to nil, apparently at random, throughout the screen. One roll of processed screen was found to have Elgiloy wires with the nonductile characteristics only on the outer seven wires of one side of the normal 4-inch width. Reference to the processing records showed that this roll had been brazed with nonuniform tension throughout the length. In-process splicing had resulted in tension being concentrated on a single side. A subsequent test roll of screen was brazed with the normally-used tension forces applied to the first half of the roll and no tension used on the second half of the roll. The roll-half brazed under tension could not be stretched over 0.5 percent, while the remaining half, that was brazed in a no tension state, was stretched over 24 percent before failure was experienced. The mechanism of this phenomenon was not investigated due to time limitations. All subsequent Elgiloy, however, was processed by brazing without tension and without further incidents. Cold-work of the Elgiloy by stretching to 20 percent was accomplished on all deliverable items with only a minimum of random wire breaks. Processing of this stretched screen proceeded through modified flux application, braze thermal cycle, cleaning, and trimming without incident.

The entire screen rigidizing process, as developed, was found to be reasonably tolerant. There were, however, definite optimum temperatures, speeds, and flux compositions for each mesh size. Broadly stated, the three original mesh sizes selected for processing required three specific processing cycles. After stretching, the three new mesh sizes required three additional, different optimum cycles. The most critical aspects of the brazing process were those that determined the amount of braze alloy on the screen wires. This was a function of the percent of alloy in the flux mixture, the amount of flux that was put on the screen, and to some extent, the actual brazing conditions. The age of the flux, as explained earlier, was also extremely influential in this respect. Combinations of these factors were responsible for the excessive amount of braze alloy that was placed on the screen processed for delivery under the contract. The effect of this excessive amount of braze alloy coating the circumferential boom wires was to make these wires a damped spring. As a result, the screen would not immediately form a tube as required but took up to 48 hours to reach a stable diameter. The as-processed screen was stripped of excessive braze

alloy by controlled immersion in a room-temperature mixture of concentrated sulfuric and nitric acids in a ratio of 19:1. This treatment can only be considered as an intermediate fix. Future processing of screen would be more closely controlled since only a single size screen with new flux would be in process.

2.1.3.5 Calendering Operation. Wire screen is calendered by passing it between heavy rollers. This flattens the high points at the intersections of the wires and gives the material a smooth surface. While it is also known as rolling, the pressure, as used in this program, was much too light to consider it as such. The calendering of the Elgiloy - Beraloy screen was limited to reduction of total thickness of the screen from 20-21 mils as woven, to 13.5 mils as calendered. Since 90 percent of the actual thickness reduction and flattening at the nodes occurred in the Beraloy wire, the end thickness was limited to what could be termed a safe thickness of that wire at the node. The end thickness of 13.5 mils left a little over half of the original wire thickness. Subsequent brazing reinforced this area and consequently no deleterious results were incurred by the reduction in thickness.

Calendering was effective in increasing the percentage of brazed nodes in the screen from 80 to over 99. The reasons for this drastic change were 1) improvement of the contact area at the wire crossover from round - round to mating contour, and 2) reduction in the number of nodes that had no physical contact.

This operation was, and continues to be, a problem area in wire screen processing for long booms. The wire screen used in this application has a definite tendency to be sleazy or gauzy, limp, and difficult to handle. Screen with a high percentage of open area has crimp in the wires but not enough to truly lock each wire in place. During the calendering operation, the rolls tended to push the cross wires, rather than roll them. Several passes to achieve the desired reduction only increased the problem. Much greater uniformity was realized by a single pass through the mill to obtain the end thickness. Roll parallelism and rigidly-held or spaced rolls were of utmost importance. The effect of nonparallelism between the rolls was accumulative during the rolling of the 120-foot lengths. Since the wires are slightly pushed back when calendered, the side that received a slight bit more reduction had the wires pushed back a slight bit more thus accumulating a sweep-back. Straightness of the screen strip was not affected as it is when rolling solid sheet.

All calendering was done on a Fenn 6-inch, two-high rolling mill. A partial reduction in the occurrence of sweep-back was accomplished by operating the mill with the spacing between the rolls fixed by shims. These shim thicknesses were determined by trial and error. They were placed between the upper and lower bearing blocks, and then the roll screw-downs were tightened. In this manner the spacing between the rolls was fixed and became independent of the material being rolled.

Calendering of the brazed and stretched screen was much easier and could be accomplished with good precision. This operation on the stretched screen had the primary purpose of recrimping the longitudinal wires and again reducing the overall screen thickness to the desired level.

2.1.3.6 Beraloy A Heat Treatment. Determination of an optimum heat treatment for the Beraloy A was influenced by several considerations. It was realized that the effect of the brazing thermal cycle would be unknown and that the detailed published data on aging cycles could only be used as an approximate guide. The attainment of the highest yield strength was the dominant demand on the wire, since it would be the limiting factor in determining the minimum boom diameter for a single circumferential wire size. The effect of crimp in the circumferential wire was also unknown, as was the effect of residual brazing alloy overlay on the wire. Further consideration was given to the fact that the shortest heat treatment possible, consistent with high physical properties, would aid in the future design of a continuous heat treating furnace.

To initially evaluate the heat treatment response of the brazed screen, flat 6-inch specimens were cut from the rigidized material and heat-treated at 650°, 700°, 725°, and 750° F for 30, 60, 90, and 120 minutes at each temperature. Duplicate specimens were then subjected to a simple, three-point deflection test wherein deflection at a load and residual set after release of the load were determined over the entire usable measurement range. The data obtained were valuable only in revealing an unexpected lack of response compared to what should have been obtained. Analysis of the entire screen processing operation showed that a high-temperature flux-drying cycle was prematurely aging the alloy. This problem was resolved by the following modifications of procedures.

A screen was given a rigidizing cycle complete in all respects except for the lack of brazing alloy in the flux slurry. The longitudinal wires were then removed from the processed screen, straightened to remove the residual crimp, and then heat-treated in large coils under flux protection at 600°, 650°, 700°, 750°, and 800° F for 30, 60, 90, and 120 minutes. Individual wires were then tested on an Instron test machine and provided results as summarized in Table 4.

The results on single wires much more generally followed the published heat treatment guides of the producers. A total heat-treat cycle of 60 minutes at 650° F was judged to be the most satisfactory cycle, considering the prerequisites of strength, stability, and the need for a reasonable heat-treat cycle for continuous processing.

2.1.4 BOOM FORMING

2.1.4.1 Batch Process. Formation of a cylindrical tube of Beraloy brazed mesh was initially performed by rolling the mesh over a mandrel, inserting screen and mandrel into a stainless steel tube, and then removing the mandrel. The entire

Table 4. Beraloy A Physical Properties as Function of Aging Cycle
(Average of Two Specimens)

AGING CYCLE		ULTIMATE STRENGTH k (psi × 10 ³)	YIELD STRENGTH k (psi × 10 ³)		ELONGATION (%)
TEMPERATURE (° F)	TIME (min)		1% - 10 IN.	0.1% OFFSET	
600	30	134	62.5	101	10.0
	60	153	74.0	124	5.8
	90	155	70	123	3.8
	120	160	71	127	4.2
650	30	149	67	119	7.8
	60	155	71	129	3.4
	90	159	72	129	3.2
	120	159	82	137	2.7
700	30	142	69	111	3.1
	60	146	70	118	3.0
	90*	146	72	115	3.5
	120	143	79	118	2.8
750	30*	132	79	103	3.8
	60	128	67	108	4.0
	90	127	78	93	4.7
	120	125	75	93	4.3
800	30	118	72	86	4.9
	60	116	66	79	5.9
	90	114	67	76	6.2

*One sample broke out of 10-inch test section.

assembly was then heated in a conventional furnace for the complete heat treatment. Excellent protection was given to the screen by applying a thin wash coating of H & H B-1 flux prior to heating. Because of the tendency for the mesh tube to shrink and wind up due to the compressive stresses on the inside surfaces, the procedure was changed to perform 50 percent of the heat treatment freely within a tubular mandrel, cool to room temperature, remove the partially heat-treated tube from the fixture, and place it on an internal mandrel for the remainder of the aging cycle. Uniform and highly adequate sizing was accomplished in this manner. Length of the screen booms formed in this batch process was limited to the approximately 38-inch long screen sections brazed in the quasi-continuous rigidizing development phase.

2.1.4.2 Continuous Boom Forming. Development of the continuous boom forming equipment utilized the parameters generated in the formation of the batch forming process. Namely, 3/4-inch diameter boom, having a required heat treatment of 650° F for 60 minutes on two sizing mandrels. The heart of the continuous tube forming equipment was the furnace. An 84-inch long furnace was constructed having a heavy-wall, stainless steel tube indirectly heated by forced-convection air. The normal sag of the tube was corrected by adjustable hangers. A temperature profile of the tube, using instrumented screen while actually boom forming, showed a deviation of $\pm 5^\circ$ F over a 66-inch length with the characteristic, extremely sharp dropoff at either end.

The critical development portion of the equipment was the cold-forming nozzle. Requirements for forming screen differ markedly from those used for sheet, strip, or foil. The normal sliding action of strip over itself is replaced in screen by friction and interfering edge wires. Formation of a tapered tube-forming nozzle required that a portion of the nozzle be interspaced between the screen whenever it overlapped itself. Construction of a nozzle of the required shape and contour was finally accomplished by progressive formation of a slit, 1-1/4-inch OD tube into a tightly rolled 3/4-inch overlapping shape at one end while maintaining a large diameter at the opposite end. The large end was subsequently flattened and overlap spacing added at the small end. All attempts at formation of a stainless steel forming nozzle ended in failure; however, very successful nozzles were formed of 0.025-inch wall aluminum tubing.

The entrance nozzle of the equipment also contained an internal tubular mandrel for further shaping of the screen into a true diameter. The screen tube progressively proceeds from the forming nozzle into an external, tubular mandrel. The function of this is to restrain the screen in the desired shape until stress relieving and the initial winding up of the spring can occur during the first half of the heat treatment. In the middle of the furnace tube, the screen boom leaves the external mandrel and is slightly expanded over an internal mandrel for sizing during the last half of the aging cycle.

A controlled atmosphere was utilized throughout the hot zone by introduction of argon into the center of the furnace via the second mandrel axial restraint tube. An end view of the furnace is shown in Figure 6. This view shows the screen passing over an idler roll, through edge guides, and then into the forming nozzle. Note the axial tubes for argon and internal mandrel support.

Furnace construction provided sufficient room for the addition of a second tube. One tube is for heat treatment of boom sizes from 1/2 inch to 3/4 inch and the other covers the range from 5/8 inch through 1 inch.

Figure 7 is an overall view of the entire furnace assembly showing the long support trough on the exit end of the furnace. Boom lengths were limited by the unobstructed length of the laboratory, to 68 feet.

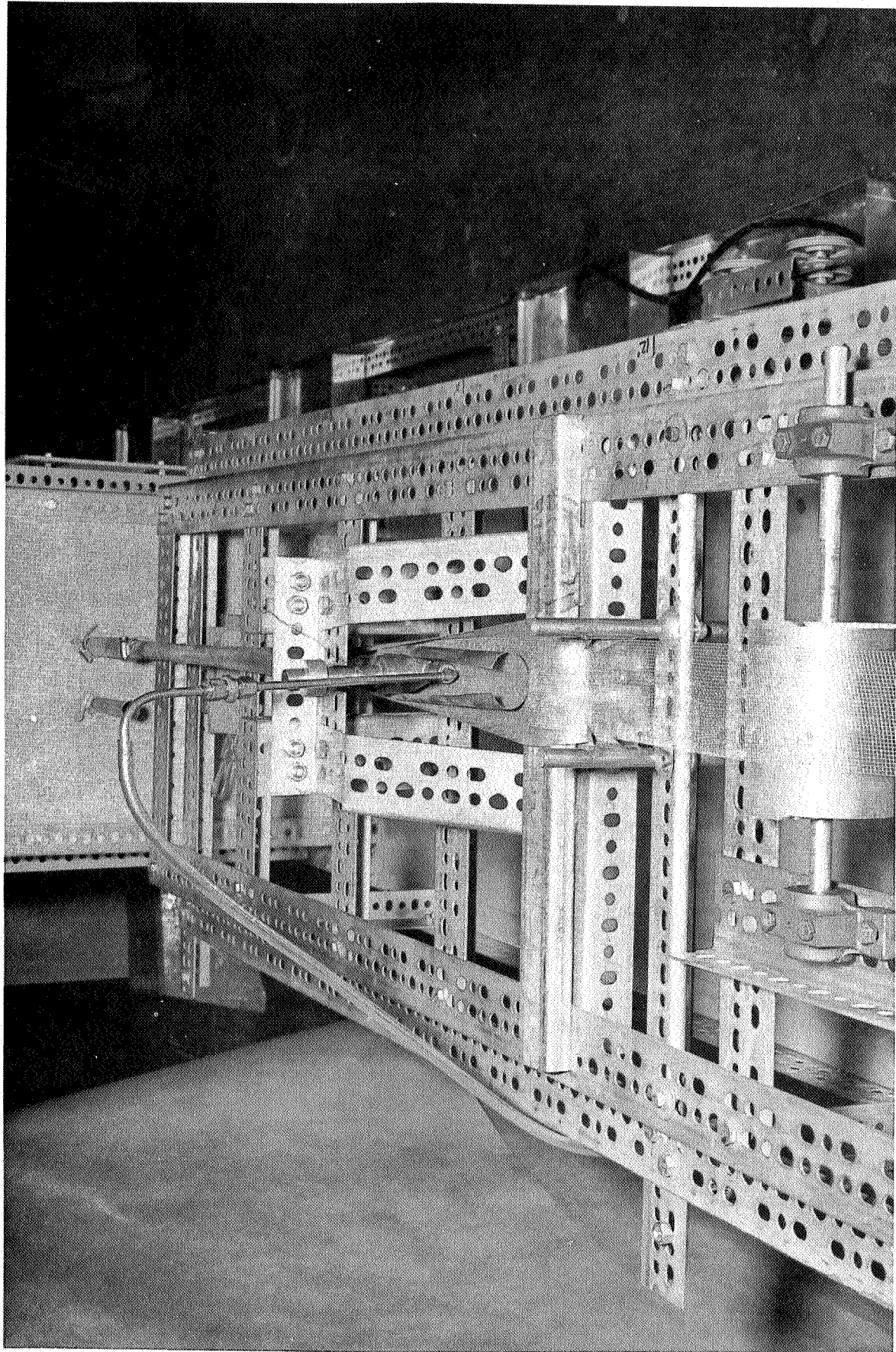


Figure 6. MOD I Continuous Tube Forming Furnace, End View, Showing Screen Cold Forming Nozzle

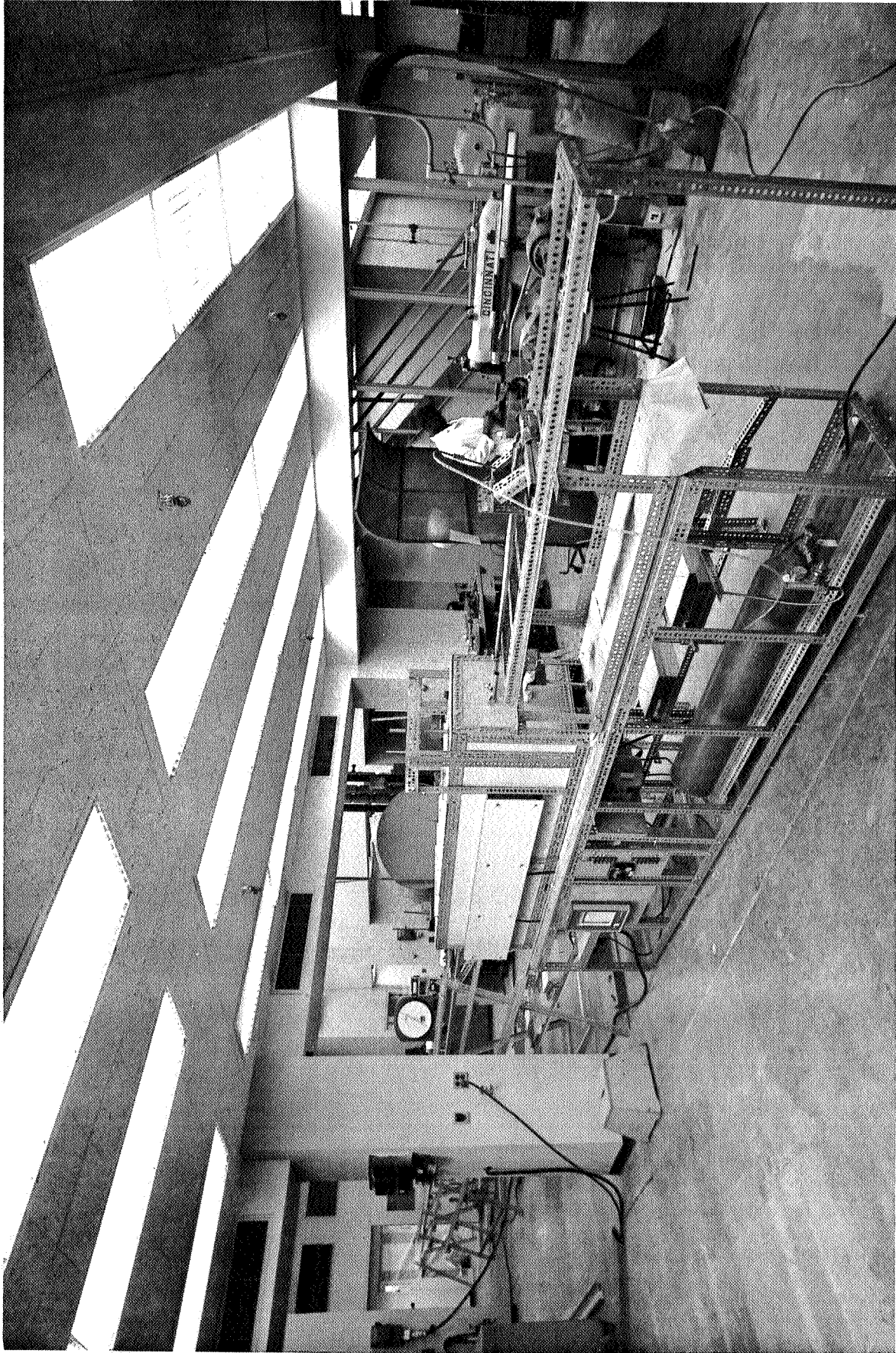


Figure 7. MOD I Continuous Tube Forming Equipment, Overall View

2.1.4.3 Continuous Boom Forming - Modifications for Rewind. Extensive modifications of the initial model of the boom former were made to eliminate its many drawbacks. The completed unit is shown in Figures 8 and 9. Figure 8, an overall view, shows a greatly shortened unit with an essentially unchanged front end. Figure 9 shows the major modifications at the exit end. Progressing from right to left, the screen, having left the forming furnace, proceeds into a high-velocity, air-water wash unit to remove molybdenum disulfide (MoS_2) solid lubricant from the screen. After passing through a low-temperature drying tube, the screen is slightly expanded over a support mandrel. A dual-pneumatic screen drive unit progressively clamps the screen in rubber jaws, moves screen and mandrel a given distance, releases the screen, and proceeds back to its starting position. A typical cycle of screen movement is 3.0 inches in 2 minutes and 43 seconds. The screen boom passes over a flattening mandrel, and then is backward rolled on a 7-inch reel hub. Hidden behind the 14-inch diameter reel sides is the reel drive motor and the required slip or friction clutch. The reel and drive unit is pivoted and counterbalanced to allow for roll diameter increase and for flattening forces at the end.

While initial trial runs of the entire continuous unit were being conducted, a stainless steel entrance forming nozzle was successfully fabricated. Use of this material reduced forming friction forces to such an extent that the MoS_2 solid lubricant could be eliminated from the process. As a result, the screen tube washer and dryer were never utilized.

The design of the tube or boom forming equipment has some inherent advantages with respect to straightness. The boom heat treatment is performed while the material is under constant tension. Adequate transition lengths are employed to eliminate outer wire yielding. The plane of the overlap seam can be changed from entrance to exit thus permitting the introduction of a well-controlled seam spiral, if desired.

Processing of three widely different screen configurations into the same size boom required three separate nozzle and mandrel sizes. Only one complete schedule for accurate boom sizing was fully developed during the program. This was for the optimum mesh size, 12 by 20. The identical schedule used for the 12 by 12 and 12 by 30 produced smaller and larger booms respectively. The 12 by 30 mesh size was produced in two configurations, 1) a straight 30-foot boom having an average diameter of 0.60 inches and 2) a rerolled configuration having an average diameter of 0.76 inches. This mesh size was outside of the envelope of practicability for forming as normally expected. The forces necessary to open or flatten the configuration were sufficient to firmly yield the outer-edge Elgiloy wires and produce a boom having a radius of curvature of 100 feet. Both configurations were supplied as delivery hardware for comparison purposes.

2.1.4.4 Metallography. Metallography was conducted primarily for examination of the braze joints to ensure joint integrity. The photomicrographs presented in the following series show longitudinal and transverse joints formed during the three major development areas of the program.

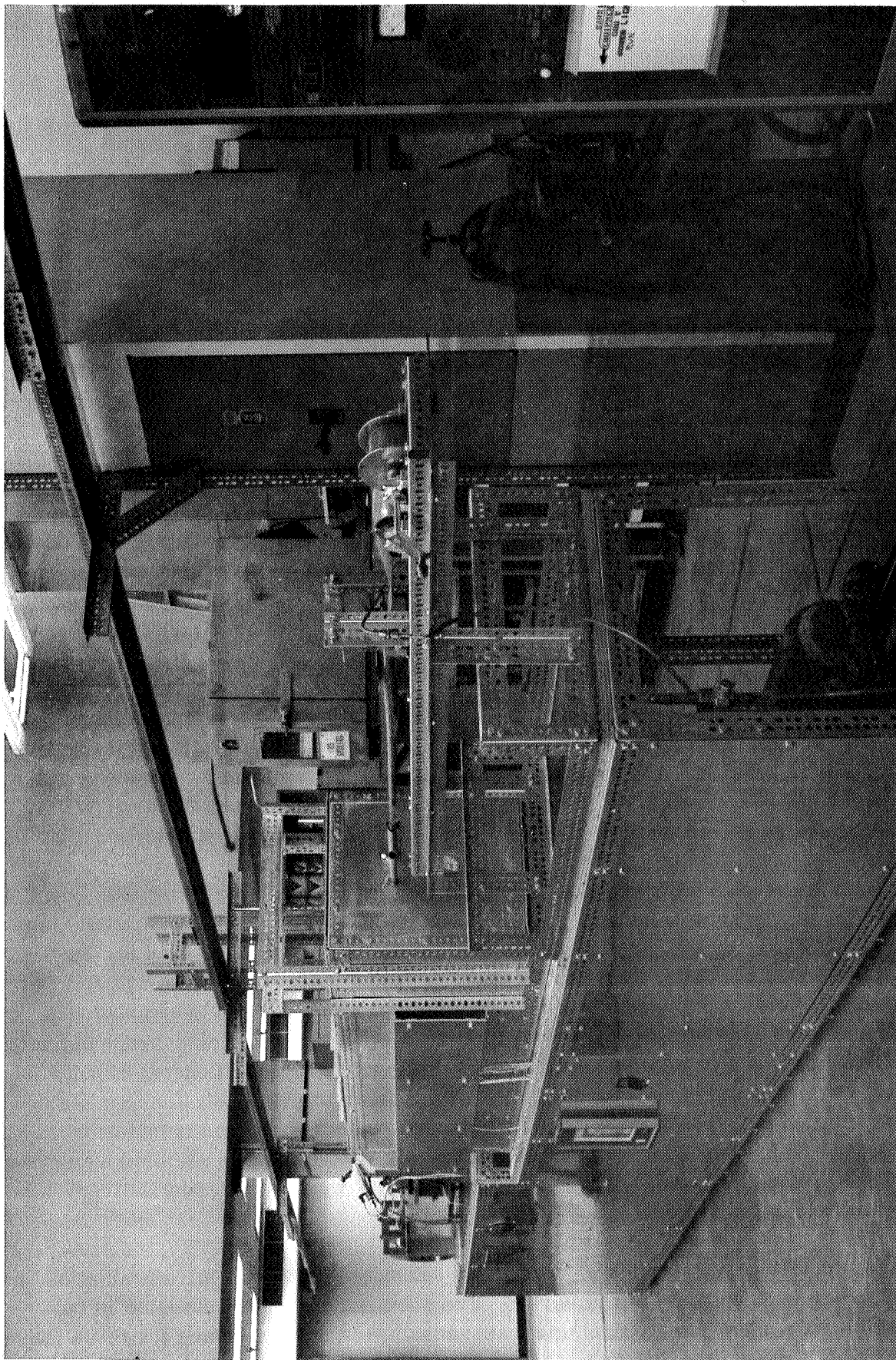


Figure 8. MOD II Continuous Tube Forming Equipment, Overall View

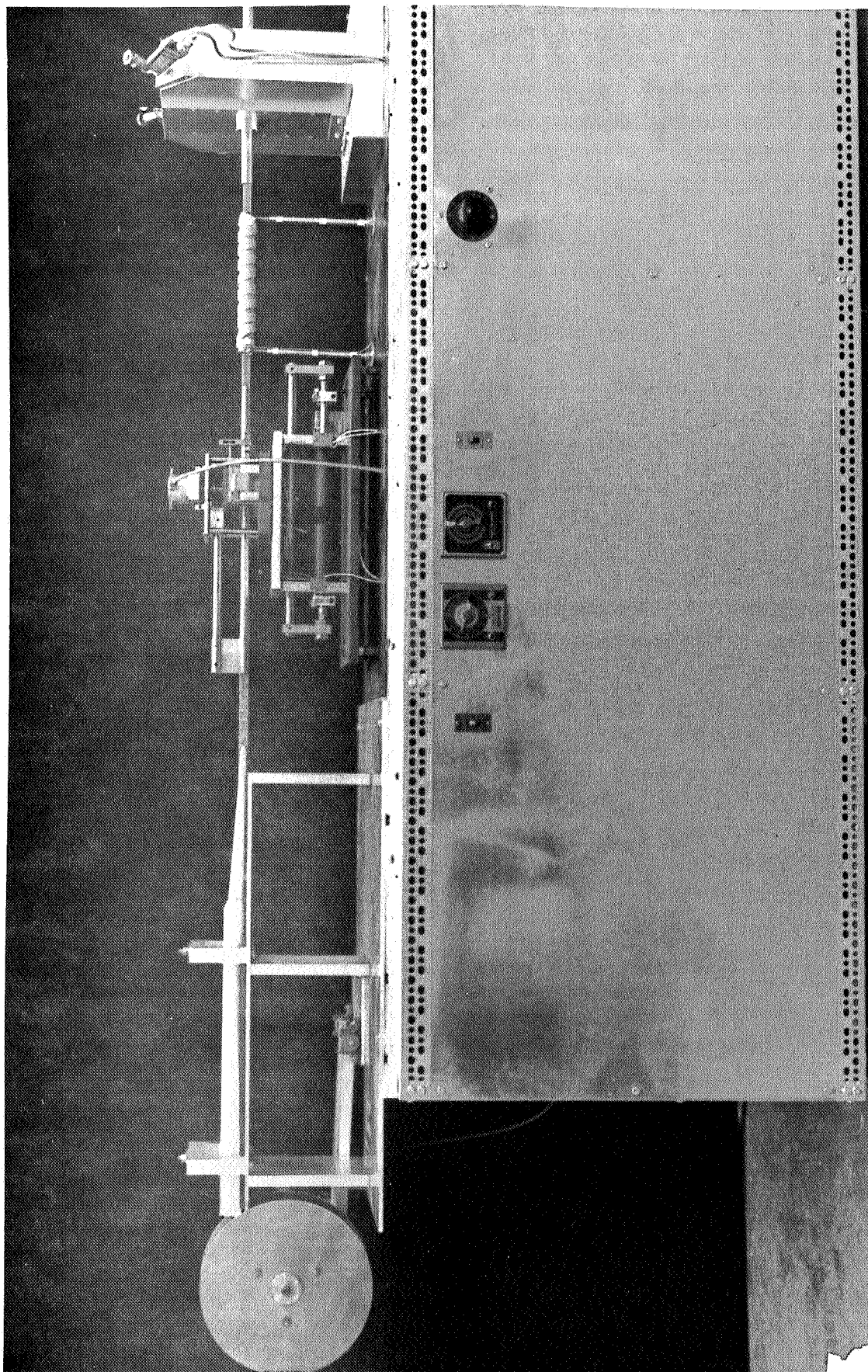


Figure 9. Transport Mechanism, Deforming Mandrel, and Take-Up Reel of Rewind Modification of Tube Forming Equipment

Figures 10 and 11 show transverse joint microstructures made on biaxial Beraloy A screen during the program phase prior to calendering, as evidenced by the round wires at the joint. The photomicrographs were taken to show the premature aging that was taking place as the result of excessively high temperature flux drying as discussed in Section 2.1.3.6. Figure 10 shows this premature precipitation in the as-brazed condition and Figure 11 shows the as-heat-treated structure. Note on both microstructures the good fillet of the silver braze alloy and the lack of any solution of the base material.

Figure 12 and 13 show longitudinal and transverse joints of biaxial Beraloy A in the as-brazed condition subsequent to introduction of all of the continuous processing improvements. Note the much larger contact areas for brazing as a result of calendering. Both figures also show evidence of excessive braze alloy, showing as an overlay on the wire at the bottom in each photograph. The premature aging of the Beraloy A is not evident in these figures.

Figures 14 and 15 are typical microstructures of the Elgiloy - Beraloy A screen selected for delivery. In both figures the unetched wire is the Elgiloy. The relative amounts of reduction of the wire cross sections can be clearly seen in these illustrations where the Beraloy A has taken the great majority. The change in the heat-treated microstructure of the Beraloy A as a result of combined calendering, stretching, and calendering with two thermal cycles into brazing temperatures is clearly evident in the high pressure point opposite the Elgiloy. The full cross-section in Figure 15 clearly shows the excessive grain size. This is, of course, local and did not prove to be deleterious to the overall structure. Both figures were taken subsequent to stripping of excessive braze alloy from the rigidized screen.

All photomicrographs were taken at 200X magnification. Etchant used was:

3 gm $(\text{NH}_4)_2\text{S}_2\text{O}_8$

100 ml H_2O

1 ml NH_4OH

Etchant was swabbed over the sample for 20 seconds.

2.1.4.5 Wire Screen Cutting and Trimming. Processing of rigidized screen into boom form can only be accomplished effectively when the screen is trimmed flush with a longitudinal wire. Wherever possible, the in-process screen edges were so trimmed. All screen trimming was conducted manually either with 8-inch scissors or with consumer-type electric scissors (Dritz or Pfaff). No attempt was made to mechanize this process because of the large number of variables.

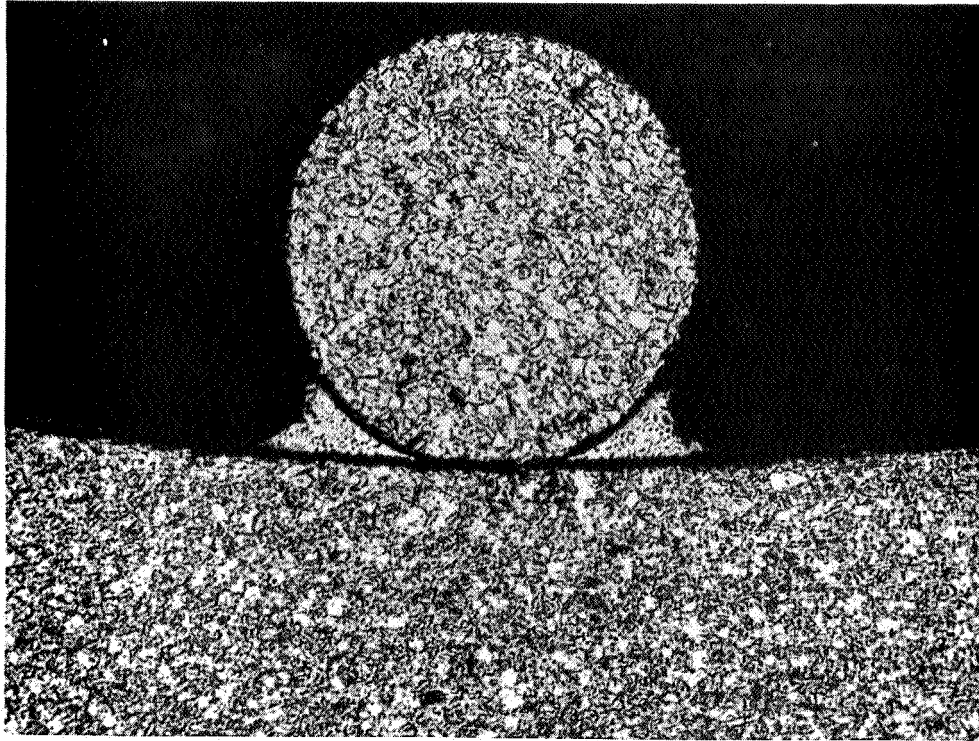


Figure 10. Biaxial Beraloy A Screen Joint As Brazed, Magnification 200X, Etch: See Text

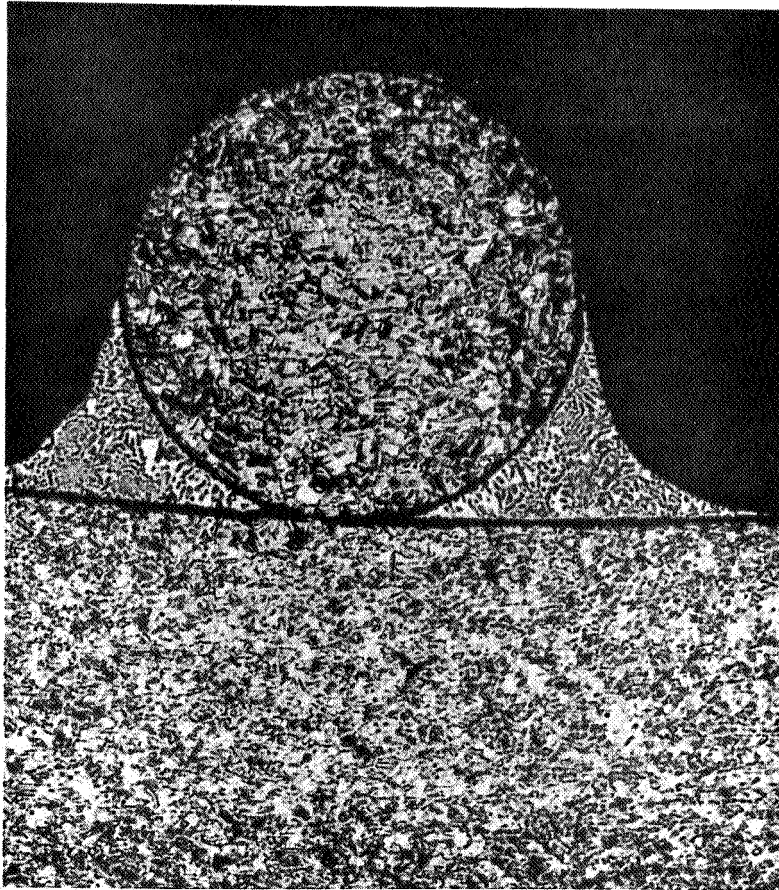


Figure 11. Biaxial Beraloy A Screen Joint As Brazed and Heat-Treated, Magnification 200X, Etch: See Text

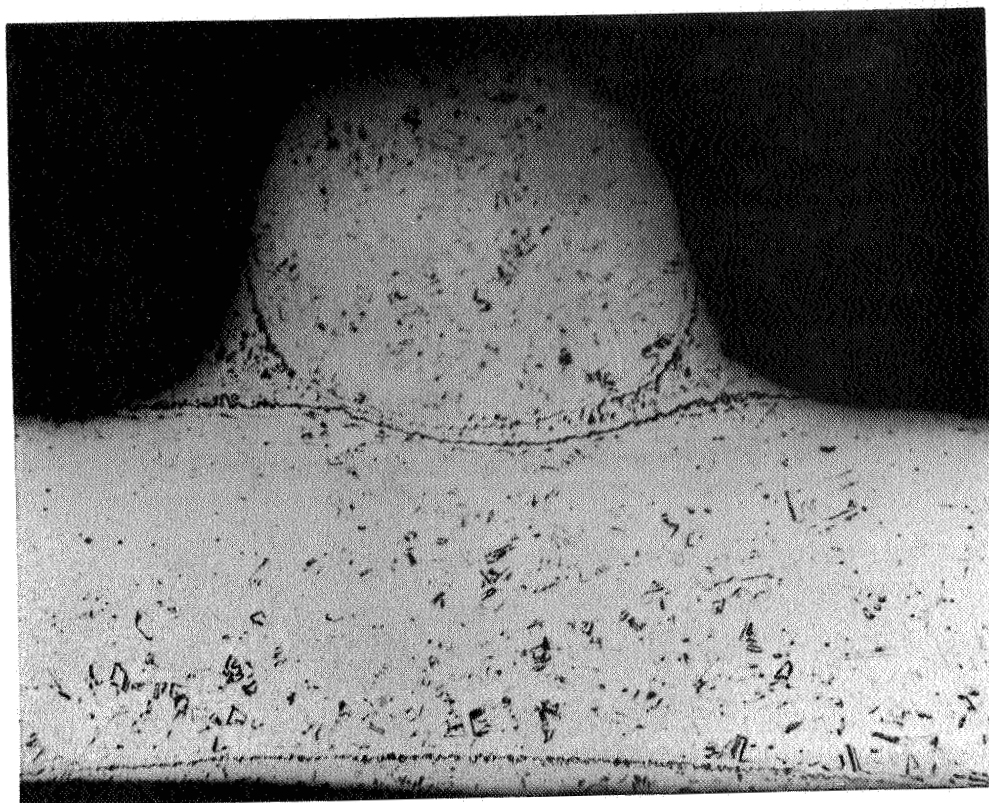


Figure 12. Biaxial Beraloy A (0.009 to 0.008 inch) Screen Joint As Brazed. Longitudinal Section Showing Circumferential Boom Wire In Cross-Section, Magnification 200X, Etch: See Text

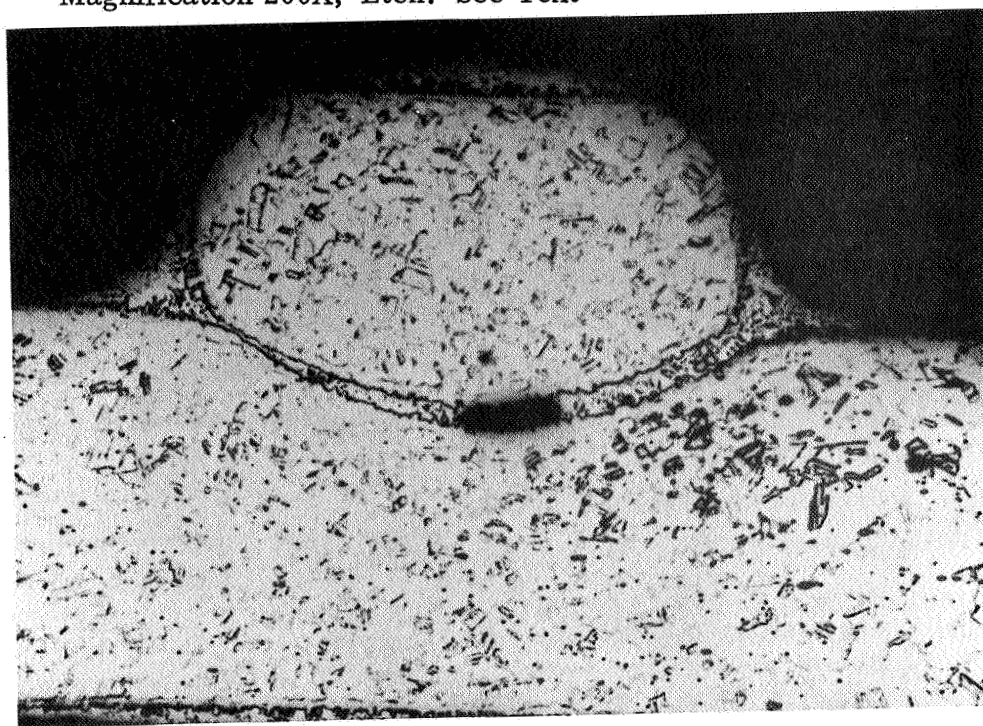


Figure 13. Biaxial Beraloy A (0.009 to 0.008 inch) Screen Joint As Brazed. Transverse Section Showing Longitudinal Boom Wire In Cross-Section, Magnification 200X, Etch: See Text

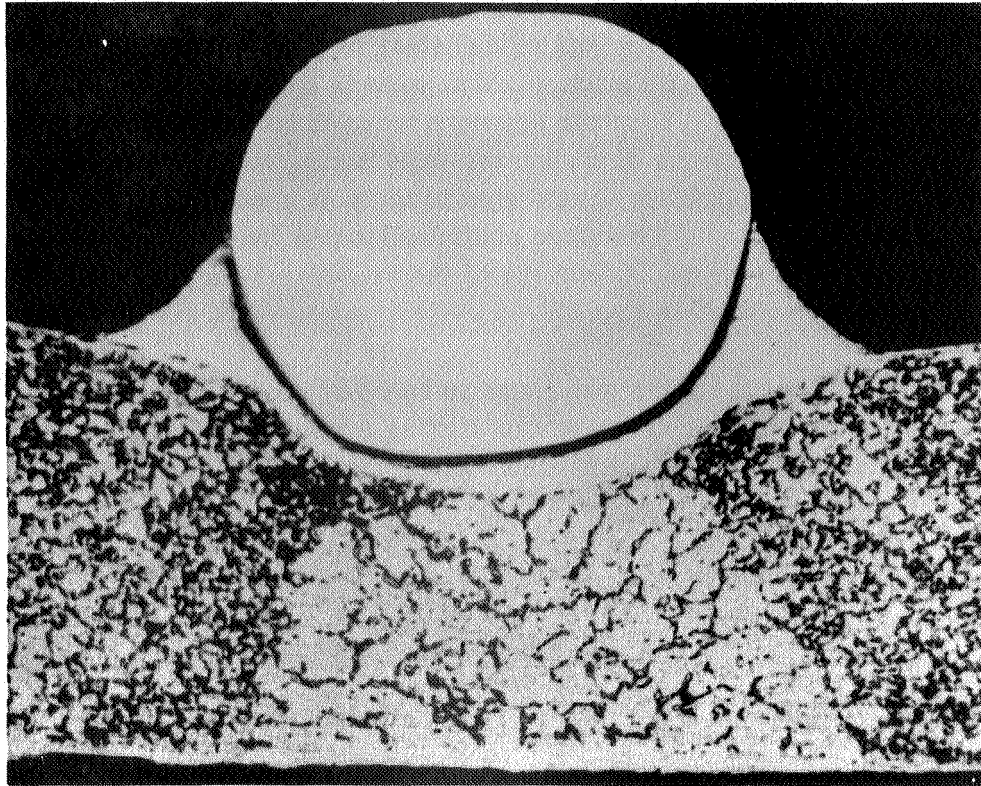


Figure 14. Elgiloy - Beraloy A Screen Boom Joint As Heat-Treated. Elgiloy in Circular Cross Section, Magnification 200X, Etch: See Text

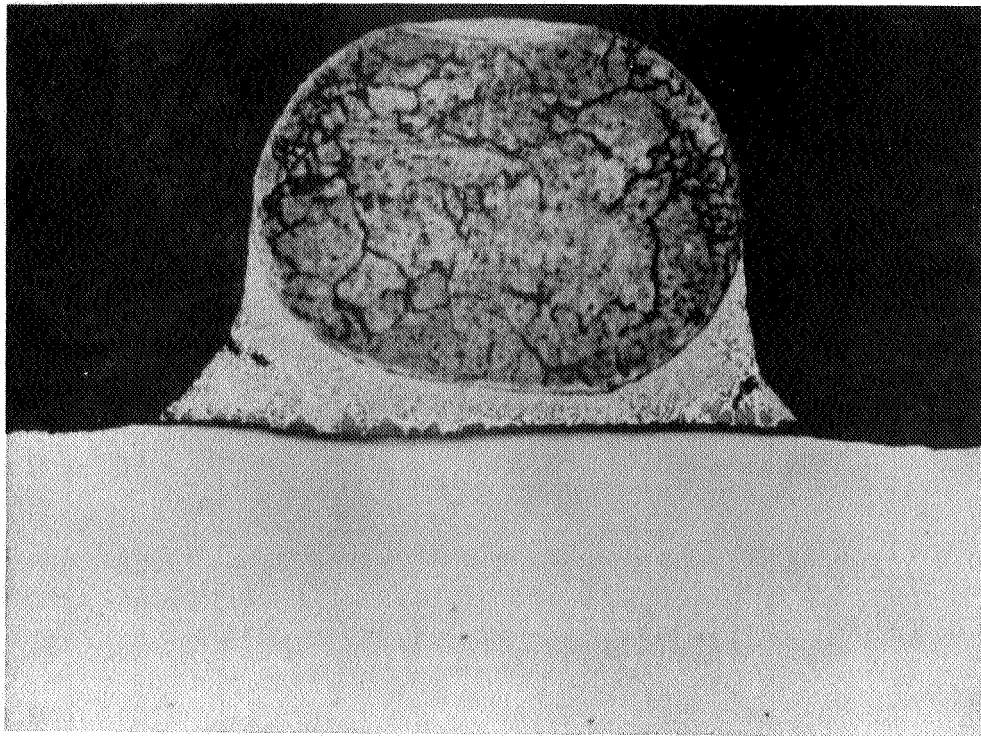


Figure 15. Elgiloy - Beraloy A Screen Boom Joint As Heat-Treated. Beraloy A in Circular Cross-Section, Magnification 200X, Etch: See Text

Trimming with electric scissors was established as the safest procedure. One of the hazards of trimming flush with a longitudinal wire is the possibility of accidental cutting or skiving of the wire. Electric scissors were found to be almost completely safe in this regard since they were of a vibrator-type having sufficient power to cut a 0.008-inch diameter copper beryllium wire in the soft condition but lacking in ability to cut the stronger Elgiloy. The blade configuration on these scissors was found to be of a self-guiding type. Manual trimming of the two-metal screen required one hour for both sides of a 120-foot roll.

Cutting of formed screen booms was found to be most readily accomplished by using needle-sharp embroidery scissors having cutting edges not over 1 inch in length. Circumferential cutting of the longitudinal wires can thus be performed without affecting the boom shape.

2.1.5 DELIVERED BOOMS

2.1.5.1 Physical Specifications. Physical specifications for the booms delivered to Goddard Space Flight Center are given in Table 5.

2.1.5.2 Certifications. Wire material certifications are reproduced in Figures 16 through 19.

Table 5. Physical Specifications of Delivered Booms,
Elgiloy - Beraloy A Wire Mesh

BOOM MESH	WIRE DIAMETER (in.)		OPEN AREA (%)		WEIGHT/ 100 FT. (lb)	REMARKS
	WARP	SHUTE	CALCULATED	MEASURED		
12 × 11.5	0.0082	0.0080	81.98	81.5	1.16	Run 312 on Reel
12 × 11.5	0.0082	0.0080	81.98	-	1.16	Run 318 on Reel
12 × 16.5	0.0082	0.0080	78.32	77.5	1.36	Run 319 on Reel
12 × 16.5	0.0082	0.0080	78.32	-	1.32	Run 317 on Deployer
12 × 26	0.0082	0.0080	71.56	71.0	1.54	Run 320
12 × 26	0.0082	0.0080	71.56	-	1.54	Run 322 on Reel

WILBUR B. DRIVER COMPANY

MELTERS AND MANUFACTURERS OF
PRECISION ALLOYS, IN WIRE, RIBBON AND STRIP
NEWARK 4, NEW JERSEY

W.S. Tyler Company
3615 Superior Avenue
Cleveland 14, Ohio

April 26, 1966

Our order 97681

Re: Your order 57907

Attention: Purchasing Agent

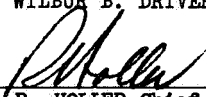
Gentlemen:

This is to certify that the 120.37 lbs. of .008, Beraloy A, $\frac{1}{2}$ Hard
shipped against your order
No. 57907 on March 24, 1966 is in conformance
with requirements as listed on your order and has the following
chemical analysis and physical properties:

PERCENTAGE OF					
Nickel	.04				
Chromium	< .005				
Carbon					
Manganese					
Silicon	.11				
Sulphur					
Phosphorus					
Molybdenum					
Wrought Iron Tin	.01				
Iron	.18				
Aluminum	.09				
Cobalt	.27				
Copper	8.1				
Beryllium	1.90				
Zinc	< .02				
Lead	< .002				
Melt Number	5095				

Physical Properties:

WILBUR B. DRIVER COMPANY


R. HOLLER-Chief Inspector

bdn

Figure 16. Alloy Certification, March 24, 1966 Shipment of Beraloy A

WILBUR B. DRIVER COMPANY

MELTERS AND MANUFACTURERS OF
PRECISION ALLOYS, IN WIRE, RIBBON AND STRIP

NEWARK 4, NEW JERSEY

W.S. Tyler Company
3615 Superior Avenue
Cleveland 14, Ohio

April 26, 1966

Our order 97681

Re: Your order 57907

Attention: Purchasing Agent

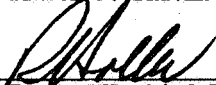
Gentlemen:

This is to certify that the 51.52 lbs. of .008, Beraloy A, & Hard
shipped against your order
No. 57907 on March 25, 1966 is in conformance
with requirements as listed on your order and has the following
chemical analysis and physical properties:

PERCENTAGE OF					
Nickel					
Chromium	.04				
Carbon	< .005				
Manganese					
Silicon	.11				
Sulphur					
Phosphorus					
Molybdenum	.01				
Molybdenum Tin					
Iron	.18				
Aluminum	.09				
Cobalt	.27				
Copper	Bal.				
Beryllium	1.90				
Zinc	< .02				
Lead	< .002				
Melt Number	5095				

Physical Properties:

WILBUR B. DRIVER COMPANY


R. HOLLER-Chief Inspector

bdn

Figure 17. Alloy Certification, March 25, 1966 Shipment of Beraloy A

WILBUR B. DRIVER COMPANY

MELTERS AND MANUFACTURERS OF
PRECISION ALLOYS, IN WIRE, RIBBON AND STRIP
NEWARK 4, NEW JERSEY

W.S. Tyler Company
3615 Superior Avenue
Cleveland 14, Ohio

April 26, 1966

Our order 97680

Re: Your order 57907

Attention: Purchasing Agent

Gentlemen:

This is to certify that the 53.77 lbs. of .009, Beraloy A, & Hard,
No. 57907 on March 31, 1966 shipped against your order
with requirements as listed on your order and has the following is in conformance
chemical analysis and physical properties:

PERCENTAGE OF					
Nickel	.04				
Chromium	< .005				
Carbon					
Manganese					
Silicon	.11				
Sulphur					
Phosphorus					
Molybdenum	.01				
Molybdenum Tin					
Iron	.18				
Aluminum	.09				
Cobalt	.27				
Copper	3.1				
Beryllium	1.82				
Zinc	< .02				
Lead	< .005				
Melt Number	5092				

Physical Properties:

WILBUR B. DRIVER COMPANY


R. HOLLER-Chief Inspector

hdm

Figure 18. Alloy Certification, March 31, 1966 Shipment of Beraloy A



ELGILOY

COMPANY

DIVISION OF AMERICAN GAGE & MACHINE COMPANY
853 DUNDEE AVE. ELGIN, ILLINOIS 60120

PHONE
AREA CODE 312
695-1900

March 23, 1966

The W. S. Tyler Company
Cleveland Plant
3615 Superior Avenue
Cleveland, Ohio 44114
Attn: Purchasing Department

Gentlemen:

We certify that the 62.84 lbs. .009" dia. wire,
of Elgiloy shipped against your Order #58036 today,
has the following chemical analysis and physical
properties:

Cobalt	-	40.0%
Chromium	-	20.0%
Nickel	-	15.0%
Molybdenum	-	7.0%
Manganese	-	2.0%
Carbon	-	0.15%
Beryllium	-	0.04%
Iron	-	Balance

This is to certify that the above shipment is in
conformance with the requirements, specifications
and/or drawings as listed on your order.

Very truly yours,

David G. Williams
Product Services Manager

DGW/jm

Witnessed:

DIVISIONS

SIZE CONTROL CO.
PRECISION GAGES

STANDARD TRANSFORMER CO.
POWER TRANSFORMERS

BATAVIA BODY CO.
REFRIGERATED TRUCK BODIES

WALSH PRESS & DIE CO.
PUNCH PRESSES

LABOUR PUMP CO.
CHEMICAL PUMPS

SIMPSON ELECTRIC CO.
ELECTRICAL INSTRUMENTS

Figure 19. Alloy Certification, Elgiloy

2.2 THERMAL ANALYSIS

A digital computer program was developed utilizing the isothermal node concept approach to the solution of a specific heat transfer problem. The problem is that of determining the temperature distribution around a screen-type tubular element exposed to solar radiation in deep space. Once the temperature gradient is obtained, the thermal deflection of the tube can be determined.

The details of the thermal mathematical model are presented in Appendix III. Details of the nodal division scheme and the methods used to obtain a solution are discussed. Variables include the tube diameter, solar absorptance, conductivity, the circumferential and longitudinal wire diameters, mesh sizes, and the absolute temperature level. In addition to a description of the input format, parametric results for a number of configurations are presented. Finally, a detailed listing of equations used and a program listing are presented.

Figure 20 presents the calculated temperature difference for the six Elgiloy - Beraloy wire mesh sizes at three absorptivities.

2.3 TESTING AND EVALUATION

2.3.1 SCREEN BOOM HANDLING CHARACTERISTICS. One of the major considerations in handling the wire mesh boom is the need for uniformity and mechanization during all flattening and forming operations. The screen configuration was found to be very sensitive to nonuniformity whenever either the flattening or forming operations were carried out. The problem fundamentally is that of preventing local yielding of the two edge wires of the screen strip during flattening or forming. The solution and preventive measures were sometimes extreme, but were based on having a completely uniform, mechanized method to open or close a boom.

Manual opening of any wire mesh boom was found to be an automatic and consistent means of destroying the uniformity of the boom material. The outer wires of a screen strip as they pass through the ploy or transition area are subjected to increased tensile forces, reaching a maximum at the flat configuration. Restraint of the tubular shape to keep the transition section straight maximizes the forces. Free formation of the boom from flat or vice versa minimizes the forces.

Development of the deployment mechanism, boom testing procedures, and fabrication methods was influenced almost solely by the need to prevent the local yielding of the outer wires. The deployment mechanism uses the completely free ploy section, the continuous forming furnace rewind uses an exceptionally long straight transition section to minimize forces, and the testing methods use a uniform combination of the two. Rolling of the screen boom onto a reel can only be accomplished backwards, i. e., with the outer surface of the boom on the inside of the reel. Rolled screen tension is highly important to prevent kinking of individual section of longitudinal wires. Loss

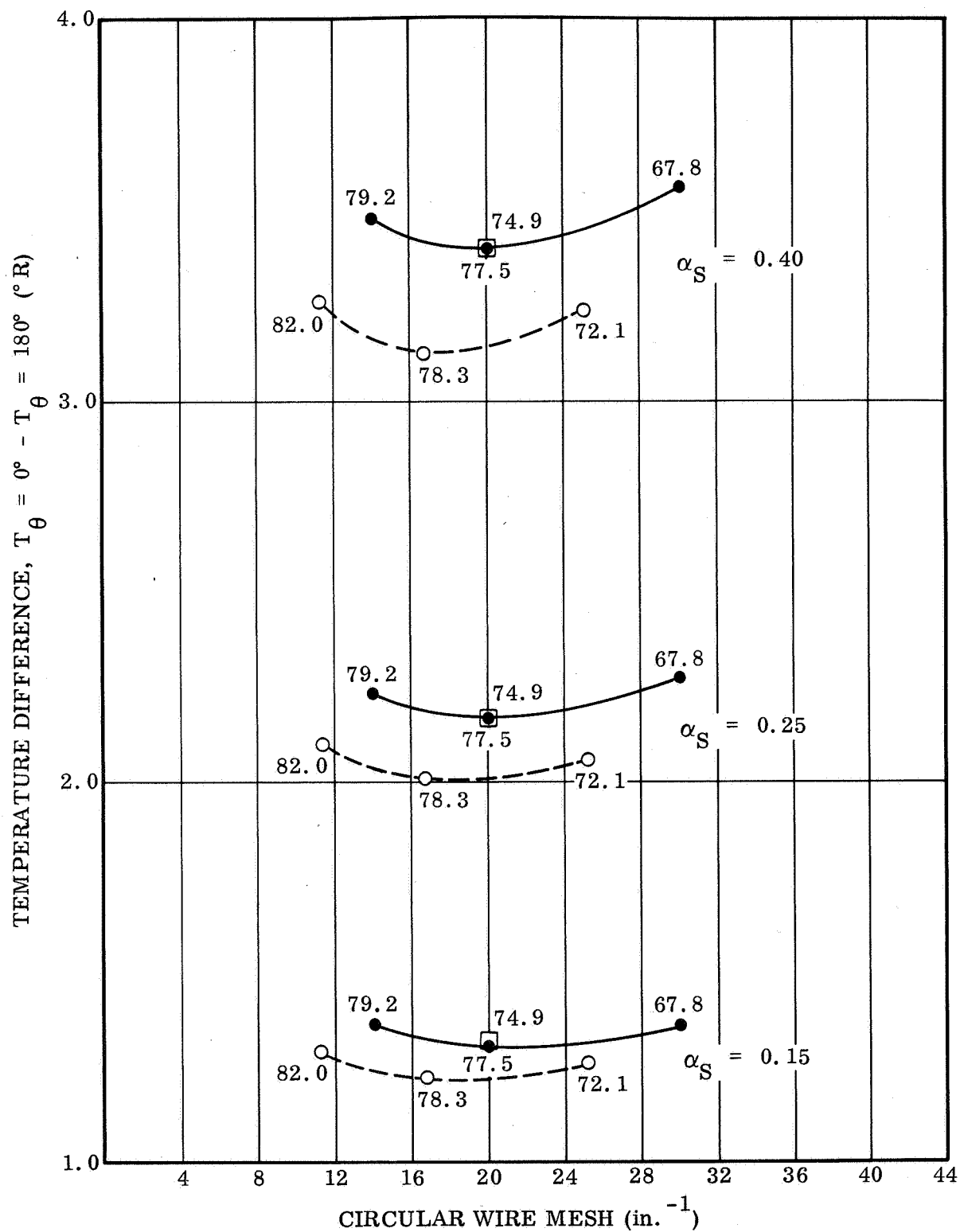


Figure 20. Temperature Difference vs. Circumferential Wire Mesh Size and Absorptivity for Elgiloy/Beryllium Copper Booms

of tension in a roll is not catastrophic as sometimes happens with foil, since there is considerable friction in the rolled state. Rolled screen booms retain a loose or a tight wind on a reel due to these high friction forces. Tightening of a loose wind, however, is not possible with the screen.

Removal of a section of screen boom from a spool or reel can be accomplished very readily by unrolling the screen uniformly under tension and allowing the screen to form the boom in a natural manner. As long as tension is maintained no change is ever found as a result of momentary stopping during the manual unrolling. Lack of tension at any time will probably cause kinking. A general rule that was employed successfully throughout the program was: to unroll a given length from a roll containing a longer length, unroll in one continuous motion while maintaining tension at all times; discard the first and last six inches of boom as probably being affected by cutting while in the flat condition.

2.3.2 BENDING STRENGTH

2.3.2.1 Test Method. Exploratory testing of wire mesh booms was conducted to determine a largely reproducible testing method and procedure. The requirement for a low-level torsional moment, simultaneously applied with a bending moment, was the major decision to utilize a special, four-point, constant-bending-moment test, in which the low-level torsional moment could be applied. A diagram of the basic concept is shown in Figure 21. Note that all of the forces, reaction, applied bending, and the applied torque, pass through the same point. Reduction of the concept to practice is illustrated in Figures 22, 23, and 24. Figure 22 shows details of the component parts of the screen sample, the balanced arms for torque application, and the bending load members. Note the recessed reaction points intersecting the two axes. Figure 23 shows the first model setup for measurement. The rigid base was used for screen specimens up to 40 inches in length and had fixed reaction points. Loads were applied by putting lead shot simultaneously into two weight pans hanging from the axial arms. Load vs. deflection relations were obtained using a cathetometer and a longitudinal wire reference point. A more refined version, shown in Figure 24, was used for all but the exploratory testing. In this, a movable reaction point was used to eliminate the effects of beam shortening as a result of deflection. Loads were applied uniformly using water from automatic burettes, and deflection was measured at the end of the axial arms. The latter change was made to eliminate the effect of twisting and its possible interpretation as deflection.

It should be noted that measured deflections are total deflections at the end of the axial loading rod and include the deflection or bending of the rod. Loading rod bending was found to be linear and well below the elastic limit of the material. Because of this, the rod deflection was included in the total deflection since its elimination would only change the slope of the curve.

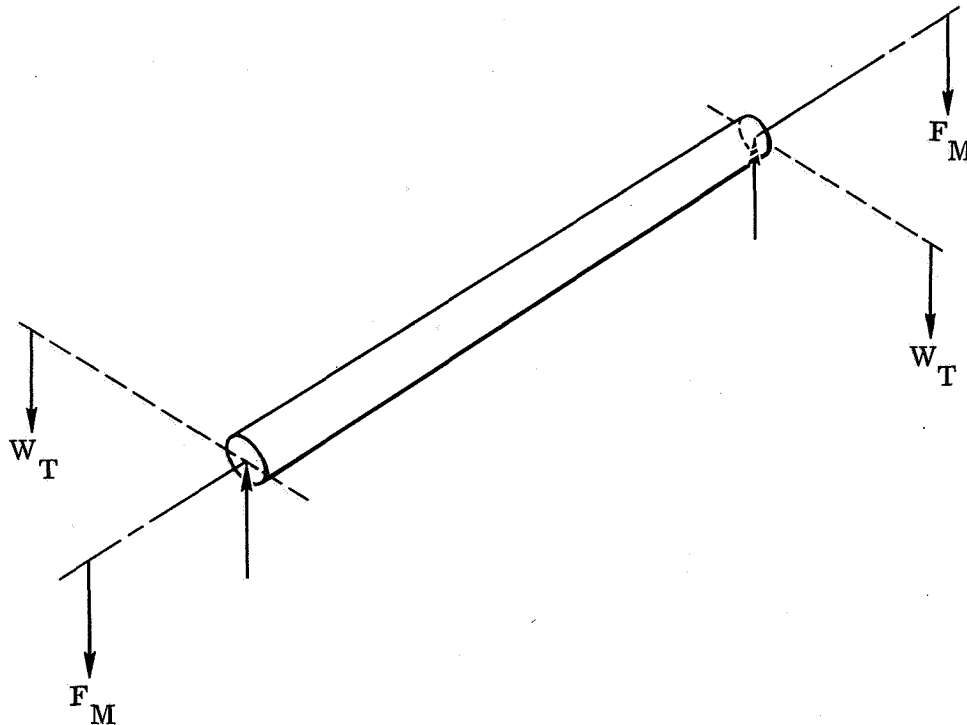


Figure 21. Constant Bending Moment Test With Simultaneously Applied Torsional Moment

The possible effect of end restraints was investigated as an adjunct to this testing phase. Since it was realized that this effect would be indicated by a change in the bending moment as a function of length, two 36-inch long booms of identical fabrication were tested as 1, 2, and 3-foot lengths. No difference in the failure load or mode was discernable. A second check was made on the 3-foot boom since it fortunately failed so as to yield a 1 and a 2-foot section for a second set of tests on the single boom. Again no differences were discernable.

The use of this method of mechanical testing for bending moment was judged to be superior to other methods since the entire test section was uniformly loaded. Failures or failure indications were taken as sudden and catastrophic collapse of longitudinal members in compression, as sudden and distinct failure in torsion, or through indications involving severe local buckling of an edge wire that would yield a permanent set in the boom. Most failures were sudden compression types.

2.3.2.2 Analysis of Test Results. The results of combined bending and torque testing are given in Tables 6 and 7. Table 6 summarizes the tests conducted on the bi-axial beryllium copper wire mesh screen and Table 7 summarizes those of the Elgiloy - Beraloy A screen booms. Two plots of bending moment versus boom diameter and bending moment versus circumferential mesh count, Figures 25 and 26, respectively,

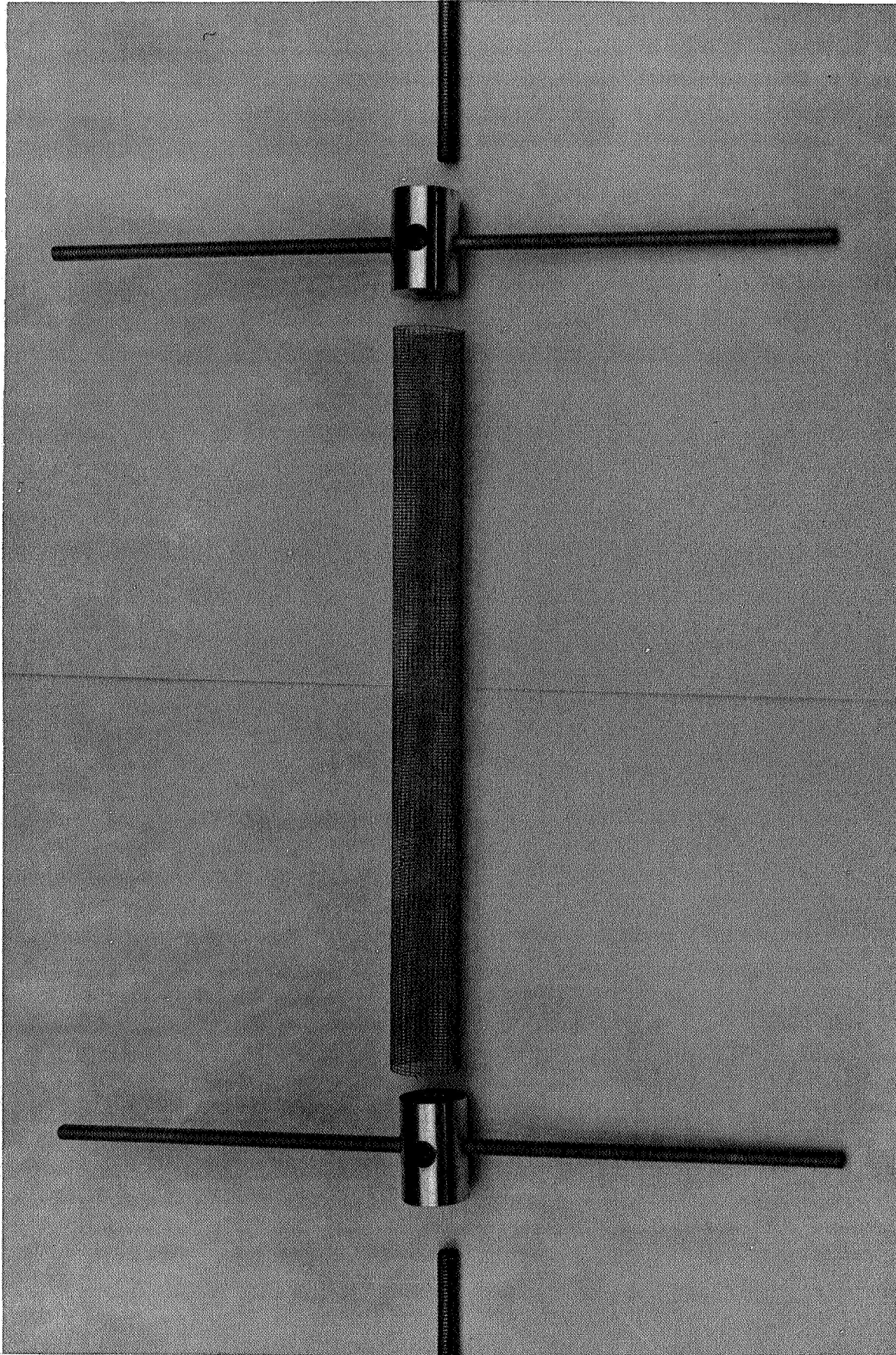


Figure 22. Component Parts of Test Sample

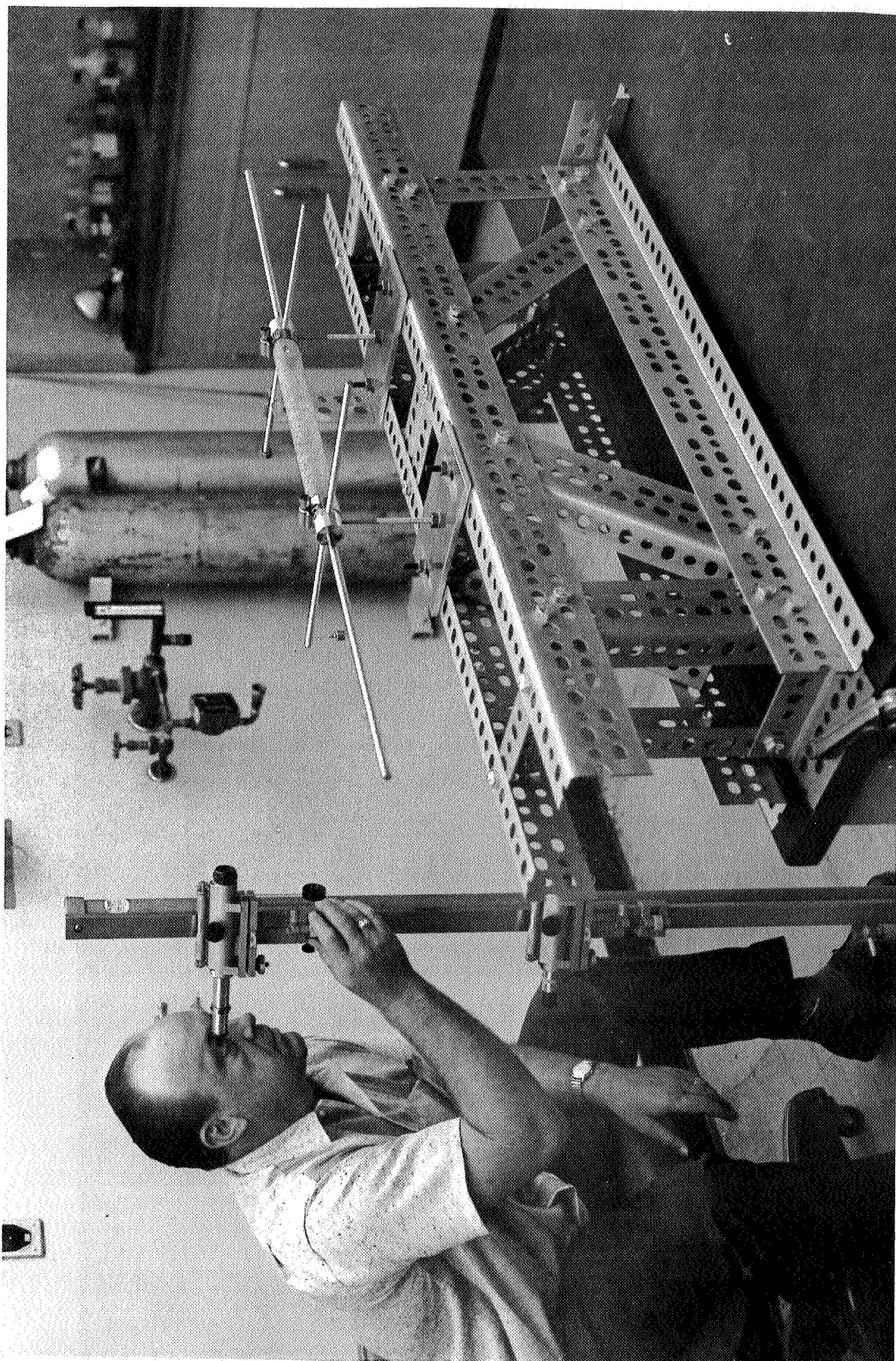


Figure 23. MOD I Combined Bending and Torsional Moment Test Apparatus

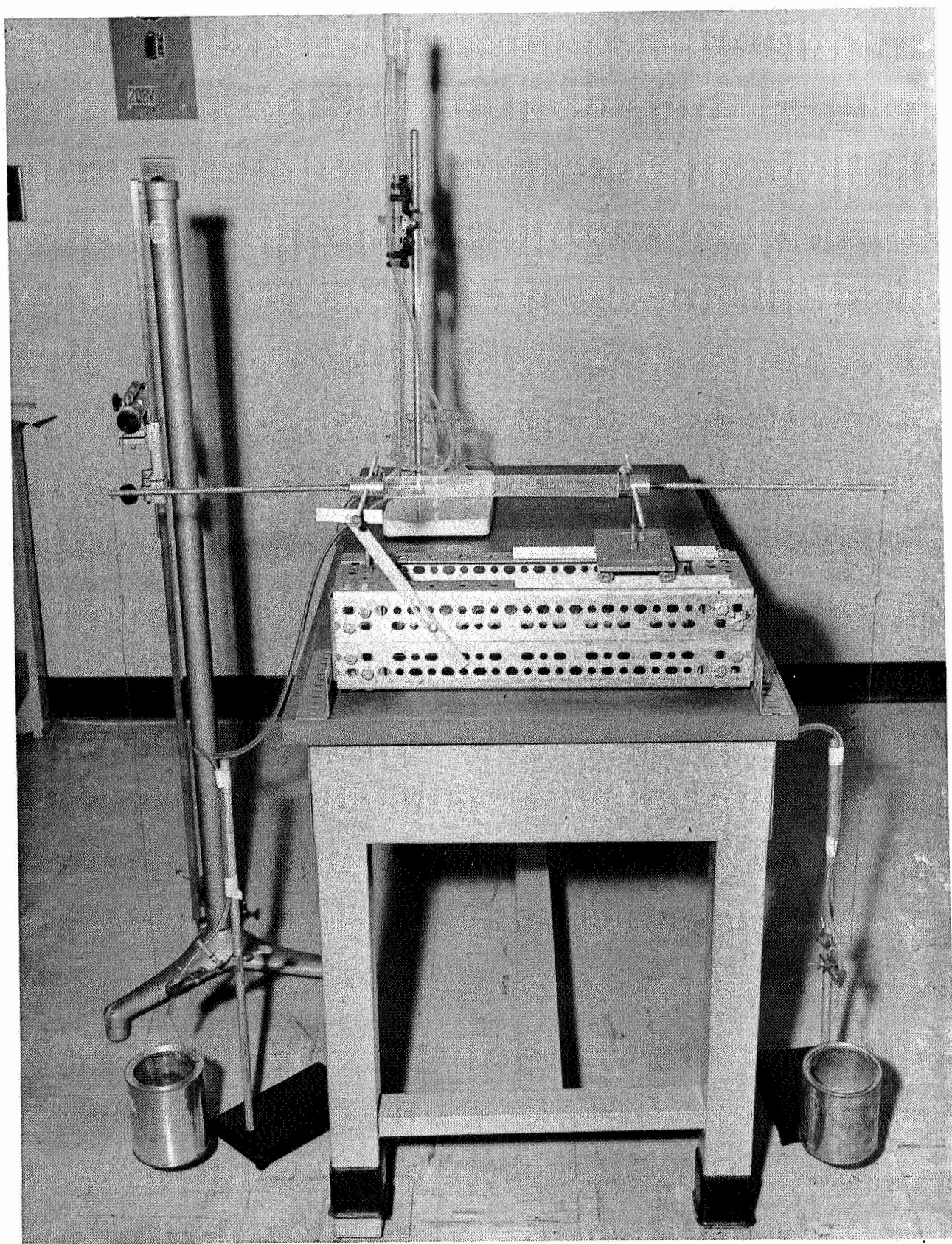


Figure 24. MOD II Combined Bending and Torsional Moment Test Apparatus

Table 6. Beraloy A Boom Strength, Average of Two Specimens

CONFIGURATION	DIAMETER (in.)	MESH OVERLAP	BENDING MOMENT (ft-lb) (with 0.005 ft-lb torque added)		
			SEAM POSITION		
			0°	90°	180°
12 × 20 × 0.009 × 0.009	1.0	1-2	1.66	1.52	1.36
12 × 20 × 0.009 × 0.009	0.75	1-2	1.36	1.08	1.02
12 × 20 × 0.009 × 0.009	0.50	1-2	0.86	0.84	0.62
12 × 16 × 0.009 × 0.009	1.0	1-2	1.49	1.20	0.93 ^T
12 × 16 × 0.009 × 0.009	0.75	1-2	1.04	0.96	0.87
12 × 12 × 0.009 × 0.009	0.75	1-2	0.89	0.84	0.86
12 × 14 × 0.009 × 0.008	0.68	4	0.99	0.98	0.84 ^T
12 × 20 × 0.009 × 0.008	0.75	2	1.05	0.76	0.82
12 × 20 × 0.009 × 0.008	0.70	4	1.54	1.17	0.87
12 × 20 × 0.009 × 0.008	0.60	8	1.20	1.24	1.20 ^T

0° - Seam in Tension

180° - Seam in Compression

T - Torque Failure

Table 7. Elgiloy - Beraloy A Boom Bending Strength

CONFIGURATION	DIAM- ETER (in.)	MESH OVER- LAP	BENDING MOMENT (with 0. 005 ft-lb torque added)			REMARKS
			SEAM POSITION			
			0°	90°	180°	
12 × 26 × 0. 0082 × 0. 0080	0. 62	2	1. 54	1. 20	0. 76 ^T	Run 320 DS
12 × 26 × 0. 0082 × 0. 0080	0. 62	1-2	1. 26	1. 18	0. 75 ^T	Average of 5 Runs Including Run 320
12 × 26 × 0. 0082 × 0. 0080	0. 62	8	1. 16	1. 36	1. 31	
12 × 16. 5 × 0. 0082 × 0. 0080	0. 76	~1	1. 08	0. 96	0. 78	
12 × 16. 5 × 0. 0082 × 0. 0080	0. 68	4	0. 79	0. 85	0. 68	Poor Braze
12 × 16. 5 × 0. 0082 × 0. 0080	0. 60	7	1. 04	1. 00	0. 86 ^T	Average of 5 Runs
12 × 11. 5 × 0. 0082 × 0. 0080	0. 60	8	0. 73	0. 77	0. 76	
12 × 11. 5 × 0. 0082 × 0. 0080	0. 70	2-3	0. 91	0. 74	0. 67	
12 × 11. 5 × 0. 0082 × 0. 0080	0. 73	2	0. 86	0. 78	0. 59	Run 318 DS
12 × 11. 5 × 0. 0082 × 0. 0080	0. 76	1	0. 84	0. 80	0. 71	

0° - Seam in Tension

180° - Seam in Compression

T - Torque Failure

DS - Delivered Screen Boom

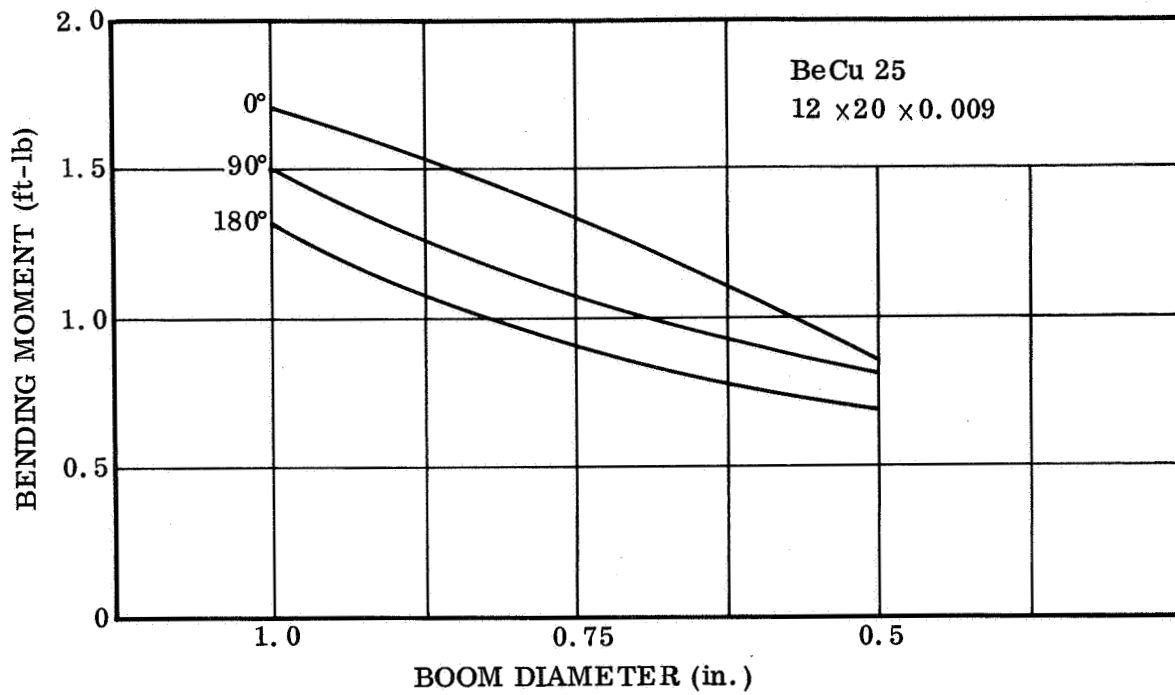


Figure 25. Bending Moment vs. Boom Diameter, 12 x 20 x 0.009 Beraloy A

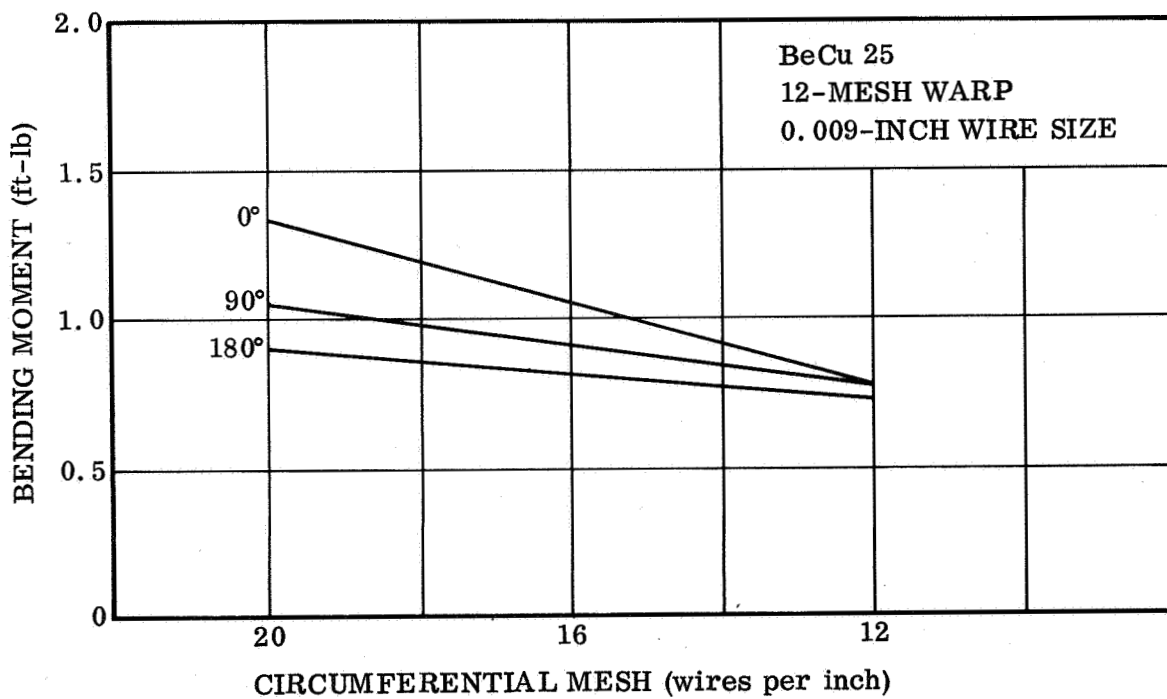


Figure 26. Bending Moment vs. Circumferential Mesh Count, Beraloy A, 12-Mesh Warp, 0.009-Inch Wire Size

were prepared from these tables. Full plots of bending moment versus deflection (three seam positions) for three of the delivered booms are given in Figures 27, 28, and 29, respectively.

Bending strength of the Elgiloy-Beraloy A screen booms did not attain the expected 1.0 ft-lb level, as shown in the illustrations and tables. This was due to the combined effect of having a smaller longitudinal wire diameter and a smaller circumferential wire mesh count as a result of the stretching operation. For example, the Elgiloy - Beraloy A wire mesh as ordered was 12 by 20 by 0.009 by 0.008. Subsequent to the stretching operation to impart cold work into the Elgiloy, the wire mesh became 12 by 16 by 0.0082 by 0.008. These 20 percent reductions in the wire and mesh sizes were the key factor in not attaining the expected bending moment level. A second factor that became evident during test was slight yielding of the outer two edge wires during processing and deployment. This had a definite effect on the ultimate bending level, since, where an outer wire had slightly yielded, a slight bulge or slight lengthening of this wire acted as failure starting point.

In all of the tests the 0 degree or seam-in-tension position was the strongest position, followed by the 90 degree and then the 180 degree or seam-in-compression position, with the singular exceptions of booms having large overlaps. There were some very definite relationships, as illustrated in Figures 25 and 26. These two figures also show the basic relationships upon which partially the selection of the Elgiloy - Beraloy A wire and mesh sizes were initially based. The singular cases, where overlaps of eight meshes were experienced, showed a much more uniform strength level or in fact a rising trend, as the seam position was rotated from 0 to 180 degrees. This was, of course, due to the stabilizing influence of the large double layer and the subsequent frictional forces of the overlapped screen.

Figures 27, 28, and 29 show typical moment vs. deflection curves. Only very slight variations in these curves were evident throughout the testing of screen. The effect of the 0.005 ft-lb of torque applied during bending moment testing was very small. Since this torque value was very low, as the screen boom deflected slightly during test, the one or two mesh overlap friction forces increased and were effective in nullifying the torque forces to a great extent. The effect of torque on initiating early failure of the booms was not apparent until 0.05 ft-lb of torque was applied. This is one full magnitude above that required.

2.3.3 BOOM STRAIGHTNESS TESTING

2.3.3.1 Test Method. Wire screen booms were tested for straightness using a simple water flotation method. A photograph of the 33-foot testing device is shown in Figure 30. The series of 14 by 18 by 3 inch aluminum trays are spaced 44 inches on centers and are interconnected by syphon tubes. The test boom was supported above the level water surface by two 3-inch-diameter by 2-inch-thick doughnuts of closed-cell

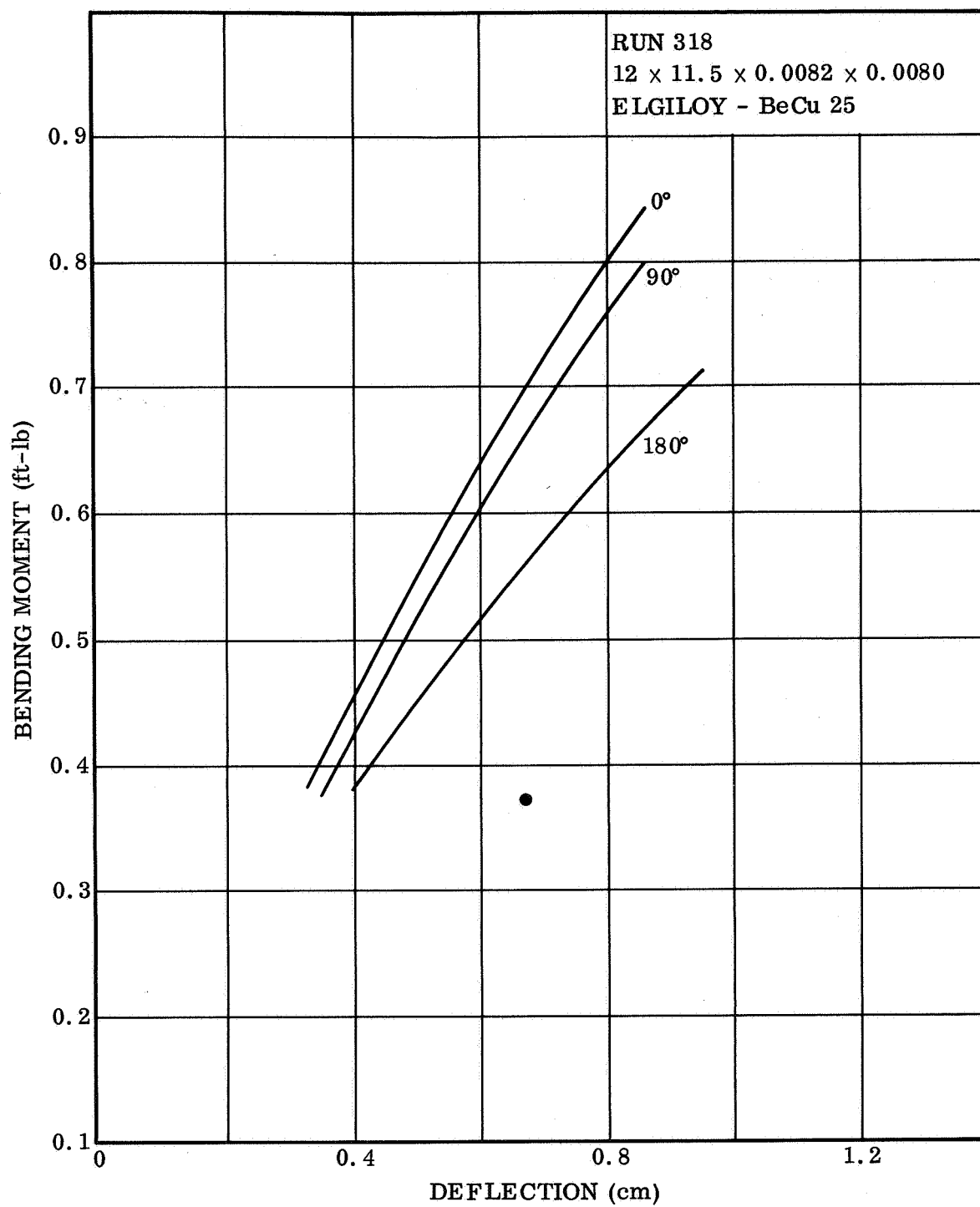


Figure 27. Bending Moment vs. Deflection for Three Seam Positions, Run 318

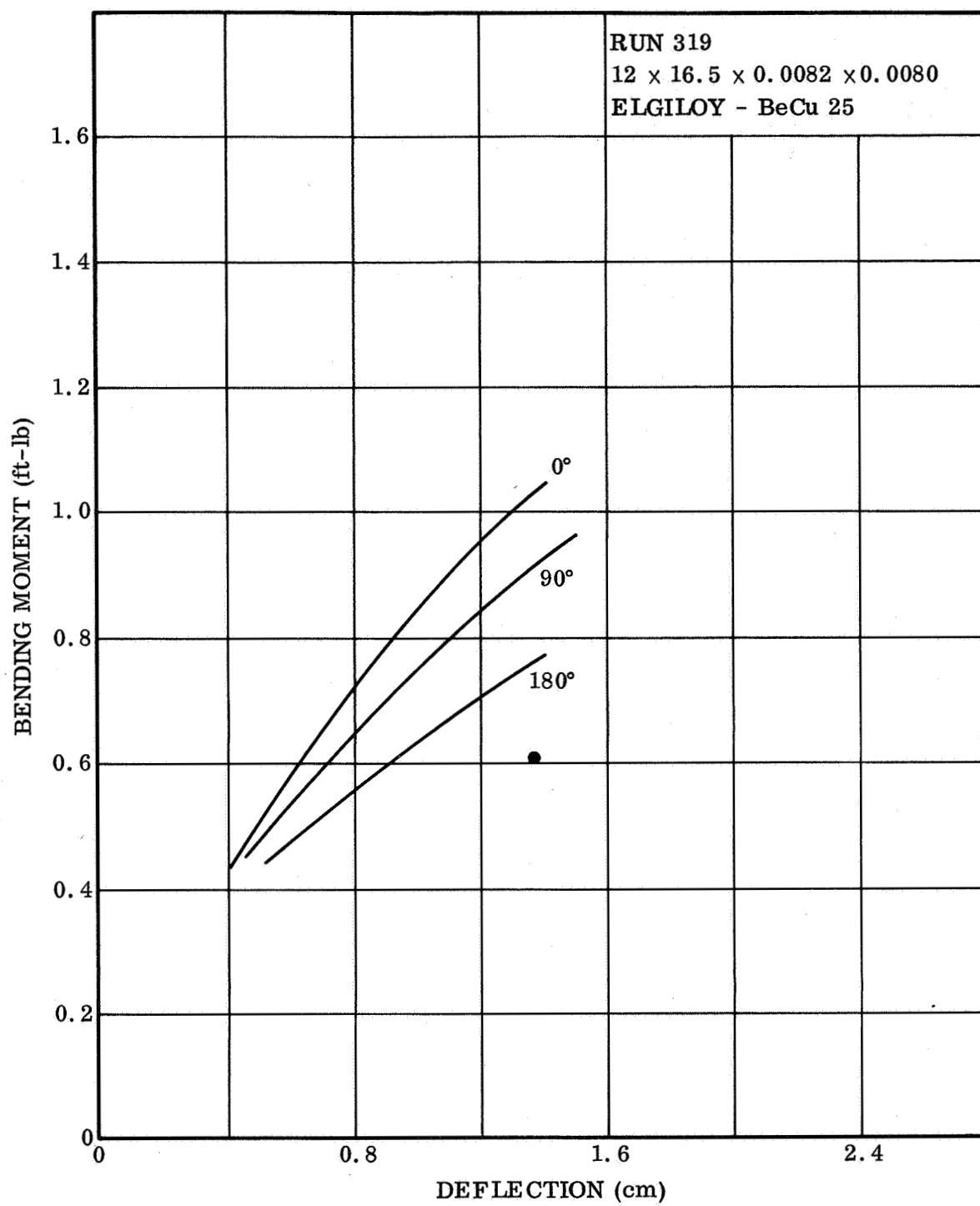


Figure 28. Bending Moment vs. Deflection for Three Seam Positions, Run 319

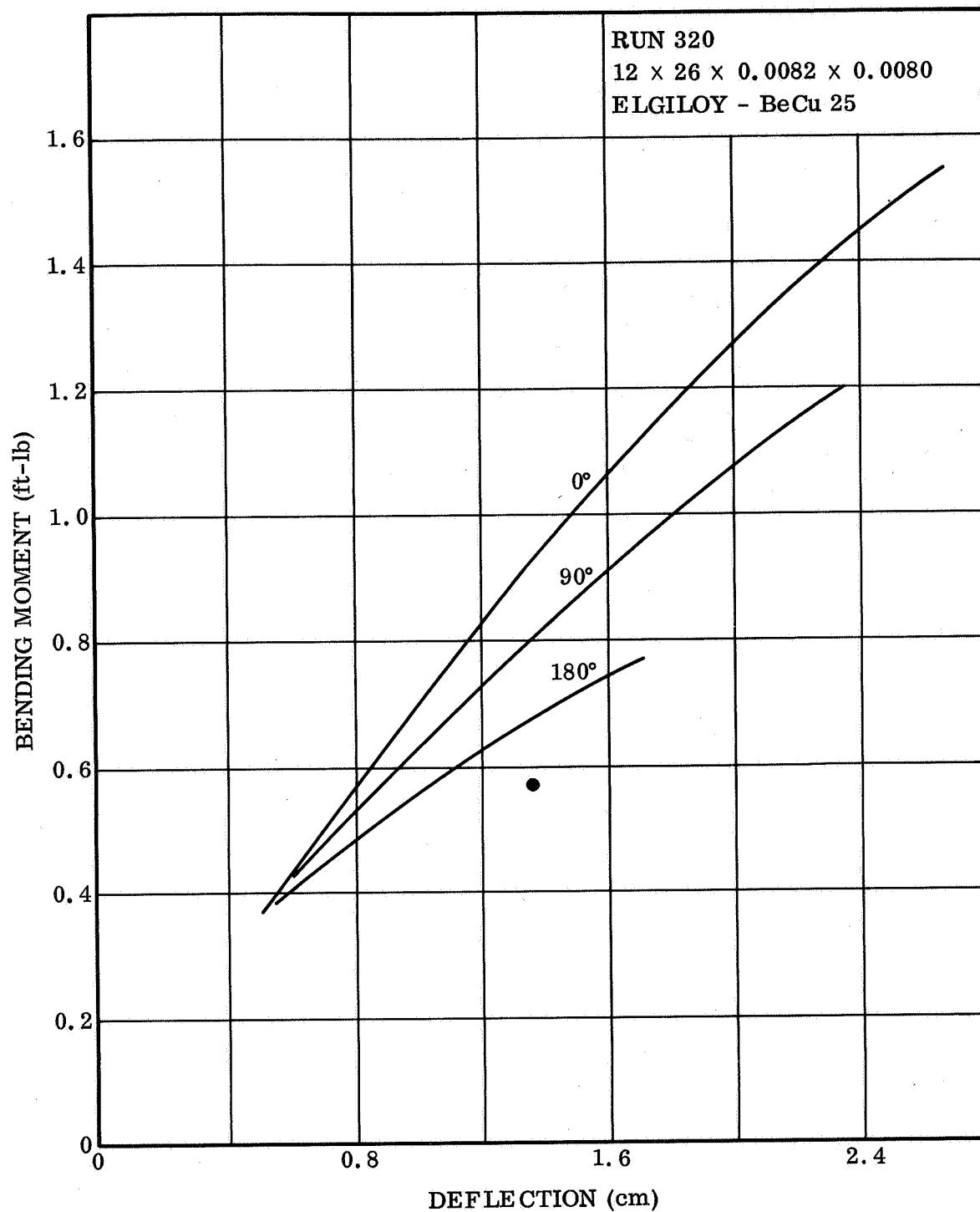


Figure 29. Bending Moment vs. Deflection for Three Seam Positions, Run 320

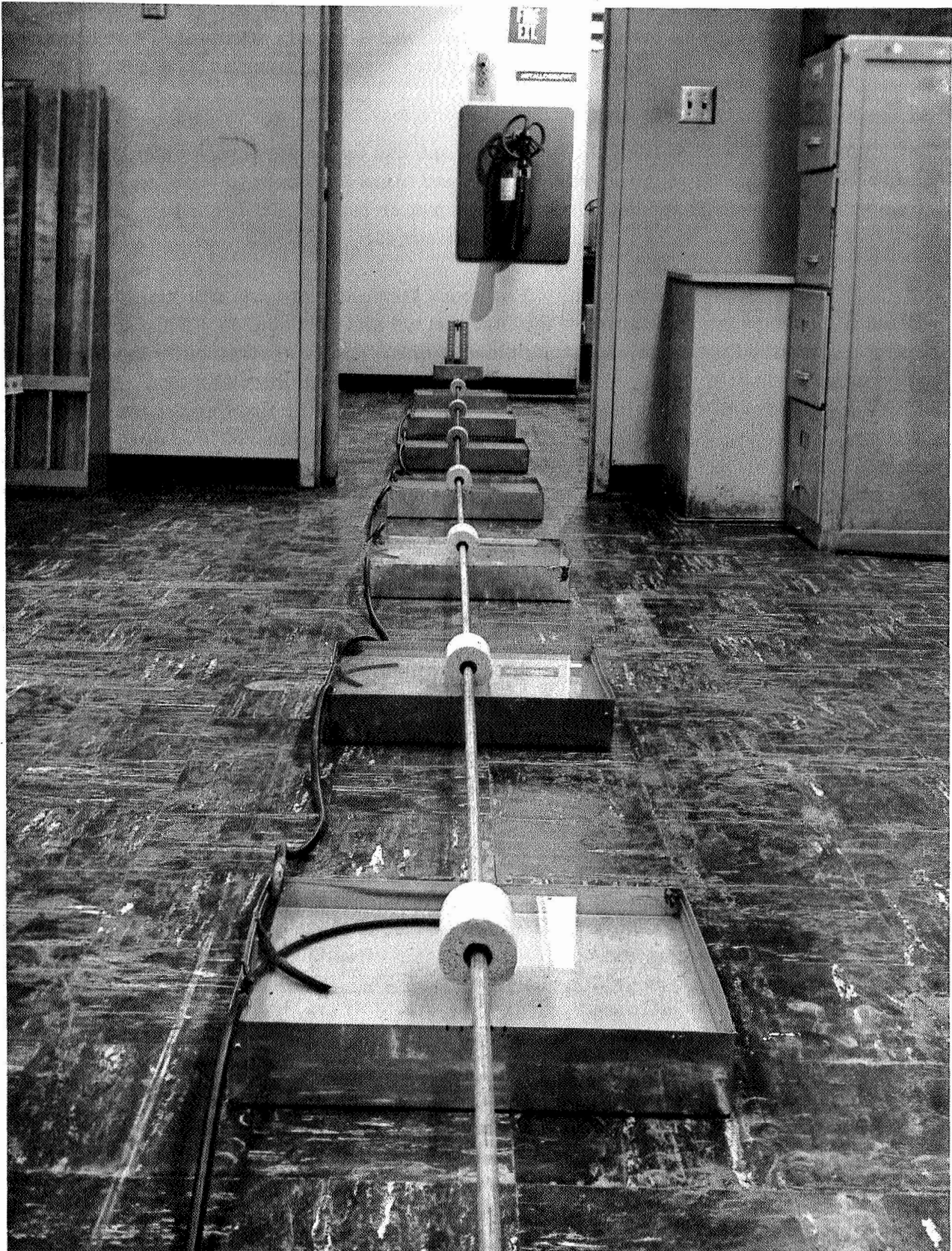


Figure 30. Boom Straightness Testing Via Water Flotation Method

polystyrene foam in each tray. The center hole was 1 inch in diameter. The boom was held at one end on an adjustable-height, axial support having an axis coincident with the calibrated pan centers.

Testing procedure was to float the boom, fix one end to the support, adjust the seam position on the support in the required plane and allow the boom to come to rest. Measurements were made of the deflection at each pan or station and recorded. Test results are given in graphical form in Figures 31 through 42.

2.3.3.2 Analysis of Test Results. The boom straightness tests are highly misleading without a thorough interpretation of the test method and procedures. This so-called zero-g test method is one in which one plane of the boom is restrained in the level, and the boom is permitted to attain its own equilibrium shape in the other two. By measuring the equilibrium deflections with the boom rotated to the four 90-degree axial positions, some measure of the actual straightness can be inferred. Although for practical purposes the system is considered friction-free, there are numerous forces and restraints imposed on the boom. Some of these are capillary attractions, flotation not axial, and change in the moment of inertia as an overlapping seam is changed from one quadrant to the next. During the testing of the wire mesh booms, the one most severe restraint was that of forcing a seam to be lined up in one plane. During the fabrication of the test booms an intentional spiral or seam twist was given to the boom. There was only one natural position for the boom during a test; all other positions were quite unlikely for the boom to take unless restrained unnaturally, the deviations are therefore unnatural. This is shown in some of the charts as natural or forced, respectively. Data for forced seam positions are presented only for the purpose of indicating the necessity for allowing the boom to reach its own equilibrium.

Although no test data can confirm the relationship between the slight waviness of a boom and the brazing procedures used, it was felt that one does exist. Natural variations in the straightness of the warp or longitudinal wire were noticed during the thermal cycles of brazing and heat treatment of the Elgiloy when tension was not used. Some curve could be seen in the approximate 6-foot length being processed and it could be exaggerated by applying nonuniform tension. Although this effect could be present in the booms tested, the thorough knowledge of additional processing variables involving the required or permitted tension forces in the Elgiloy direction will eliminate this assumed cause for waviness.

The major cause for nonstraightness of the Elgiloy-Beraloy A booms was from yielding of the two edge wires during the rewind after boom forming. This effect was from the same causes as that which lowered the bending strength, discussed in Section 2.3.2.2, namely, the effect of stretching and lowering the Elgiloy diameter and the circumferential wire mesh count. There is definite evidence of this yielding of the wires as seen in the comparison between Figures 31 through 33 (biaxial beryllium copper) and Figures 34 through 42, which plot the straightness of Elgiloy - beryllium copper alloy.

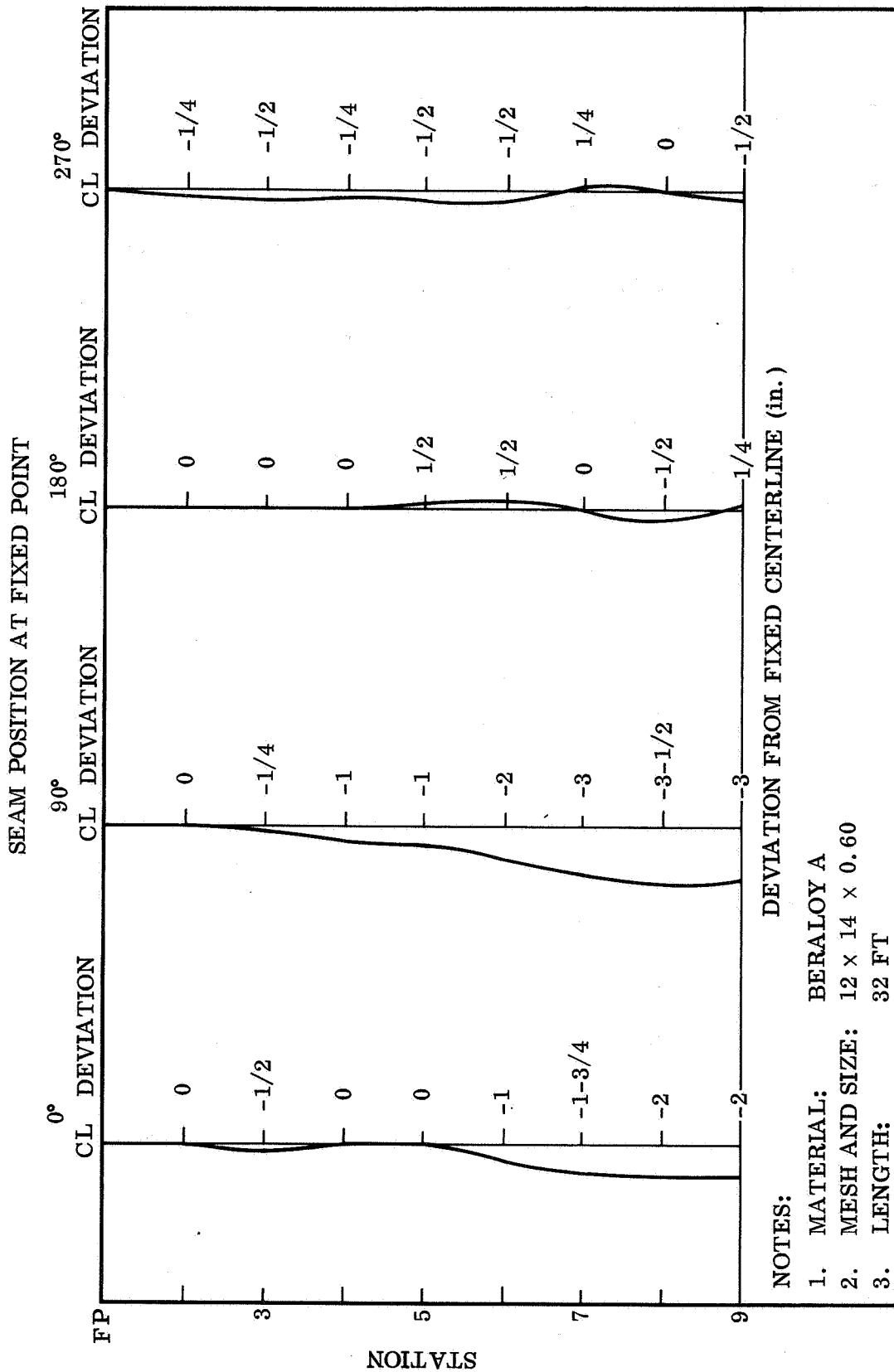


Figure 31. Boom Straightness, Biaxial Beryllium Copper, 12 x 14 Mesh, E-68

Figure 32. Boom Straightness, Biaxial Beryllium Copper, 12×14 Mesh

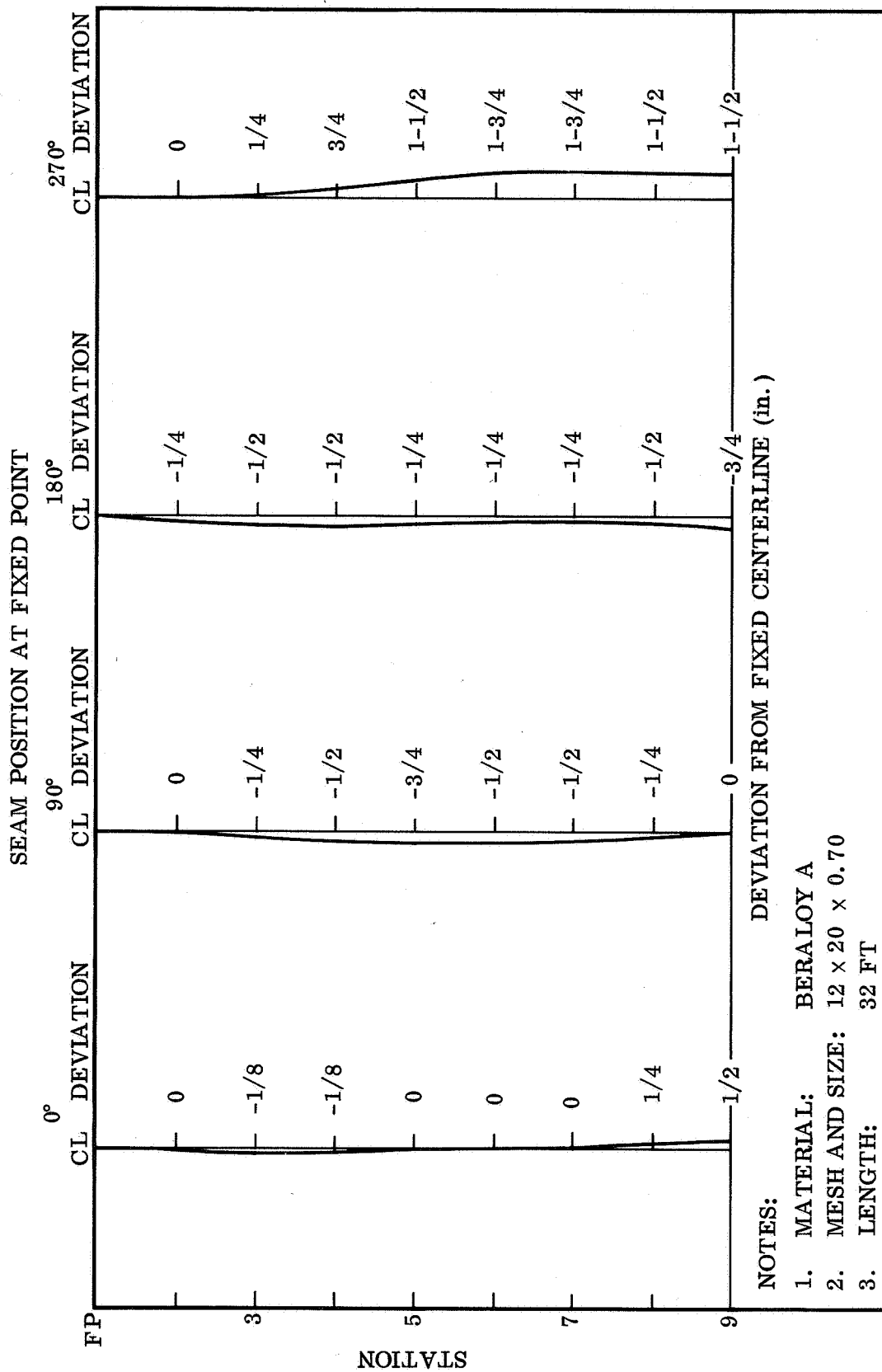


Figure 33. Boom Straightness, Biaxial Beryllium Copper, 12 x 20 Mesh, E-2

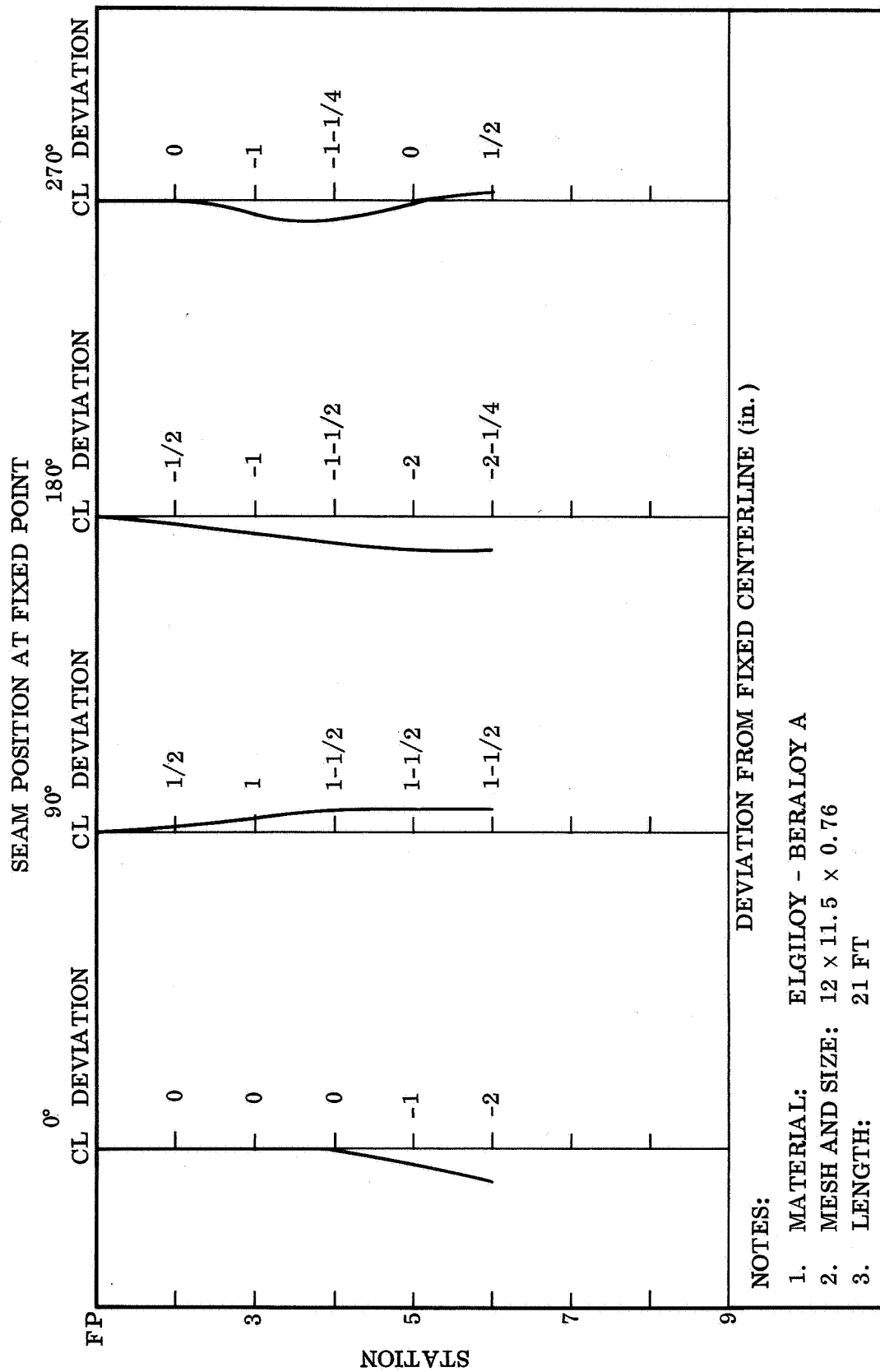


Figure 34. Boom Straightness, Elgiloy/Beryllium Copper, 12 x 11.5 Mesh, Run 318

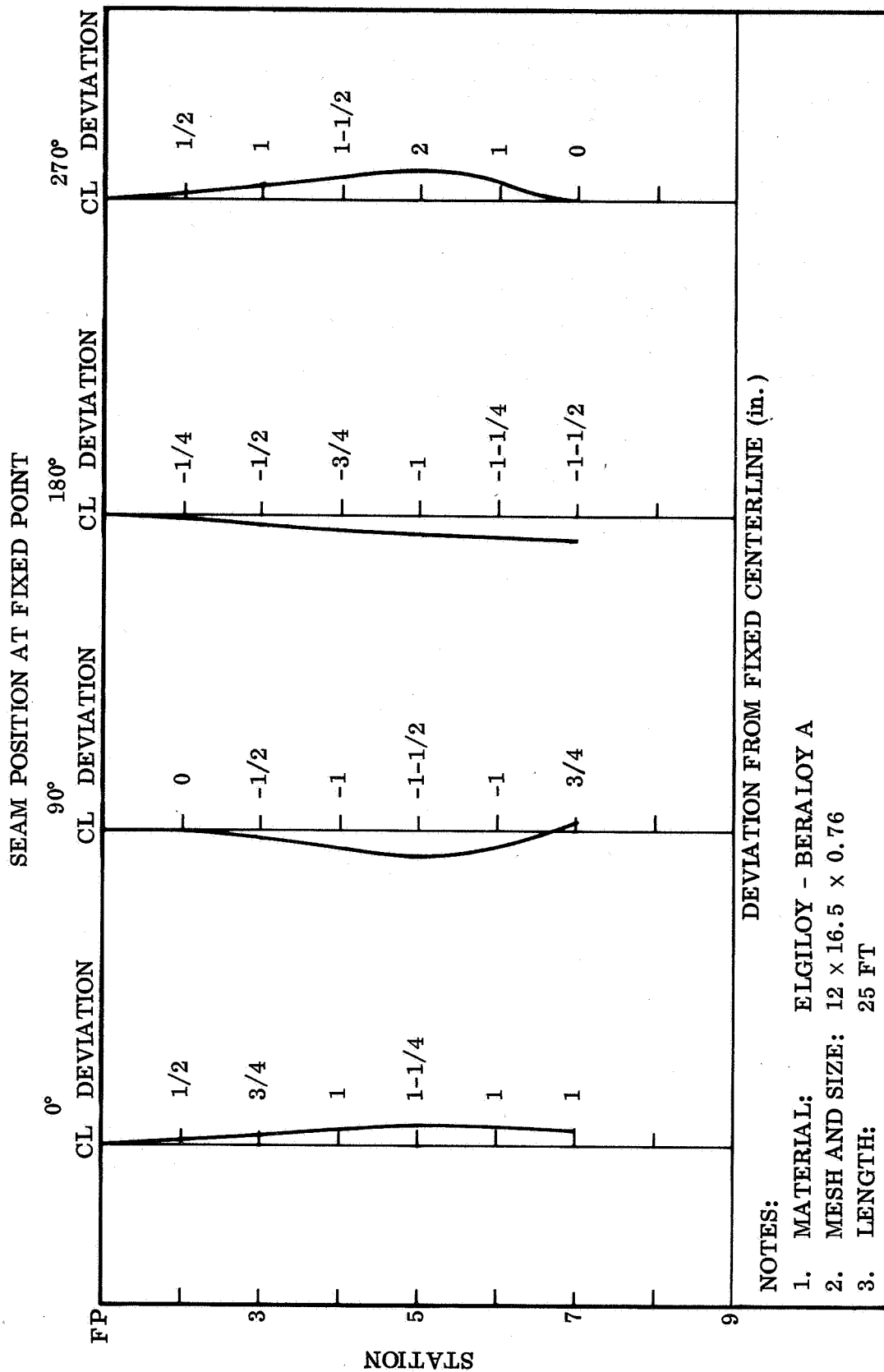


Figure 35. Boom Straightness, Elgiloy/Beryllium Copper, 12 x 16.5 Mesh, Run 319

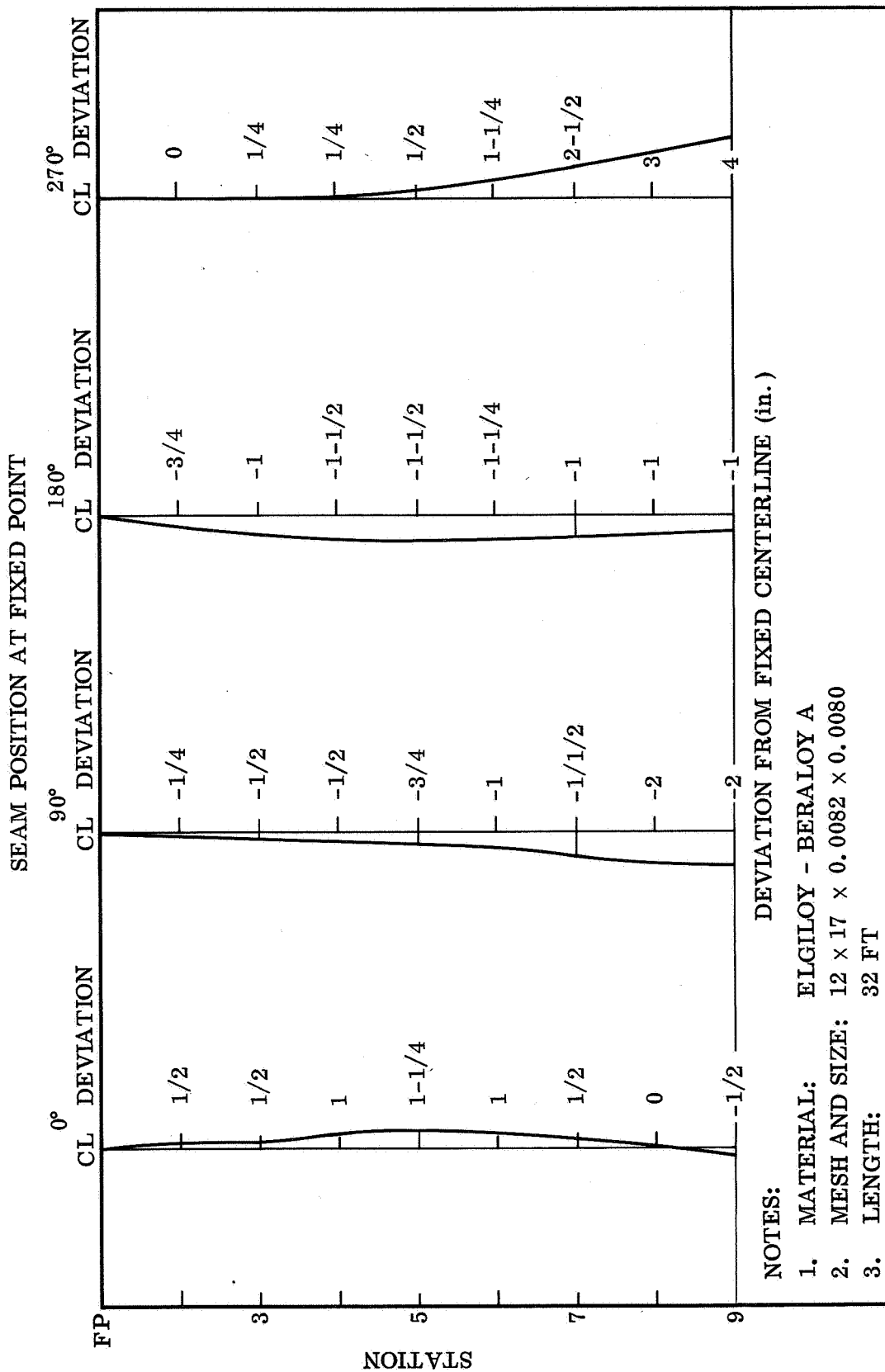


Figure 36. Boom Straightness, Elgiloy/Beryllium Copper, 12 × 17 Mesh

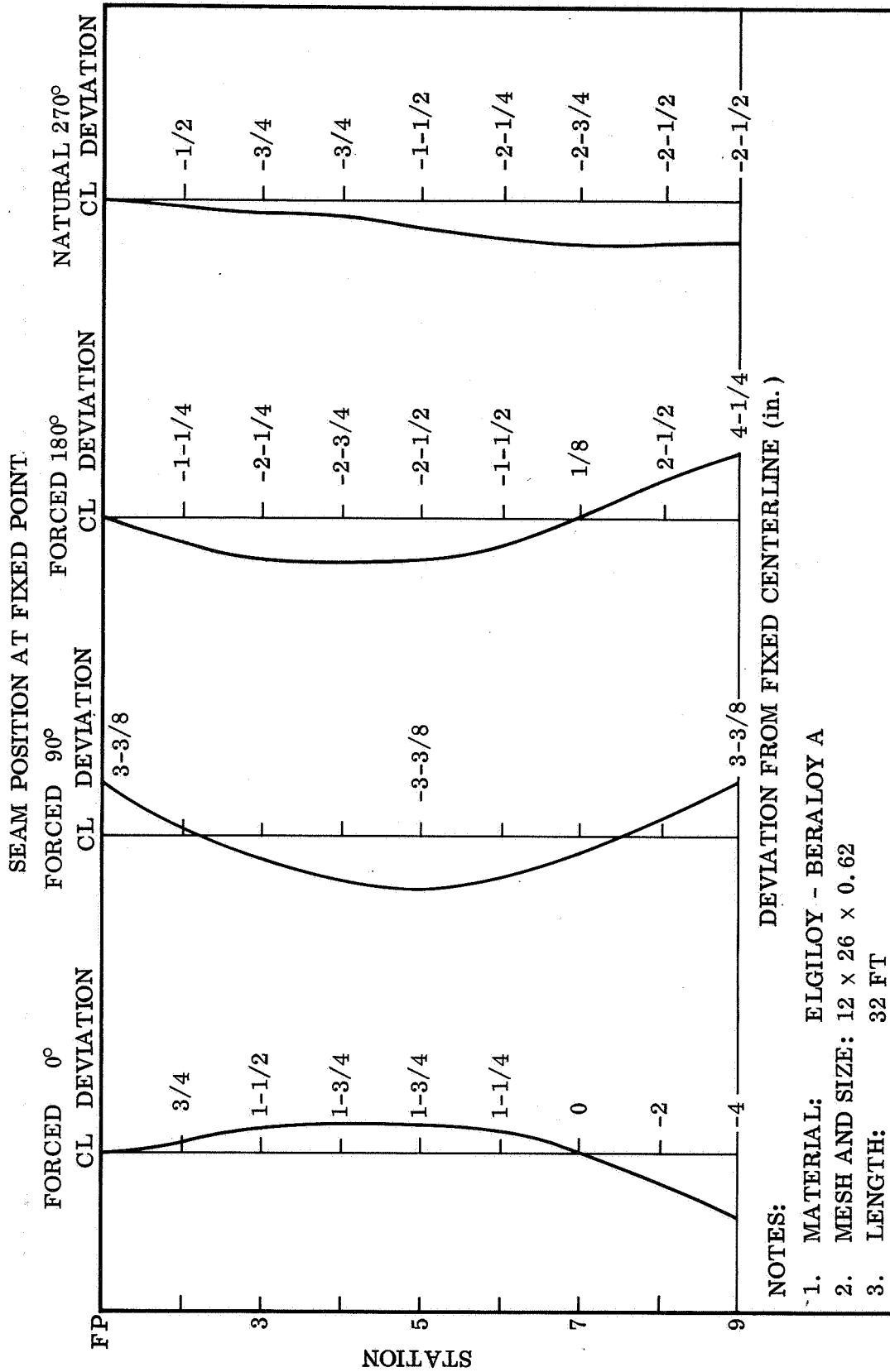


Figure 38. Boom Straightness, Elgiloy/Beryllium Copper, 12 x 26 Mesh, X-4

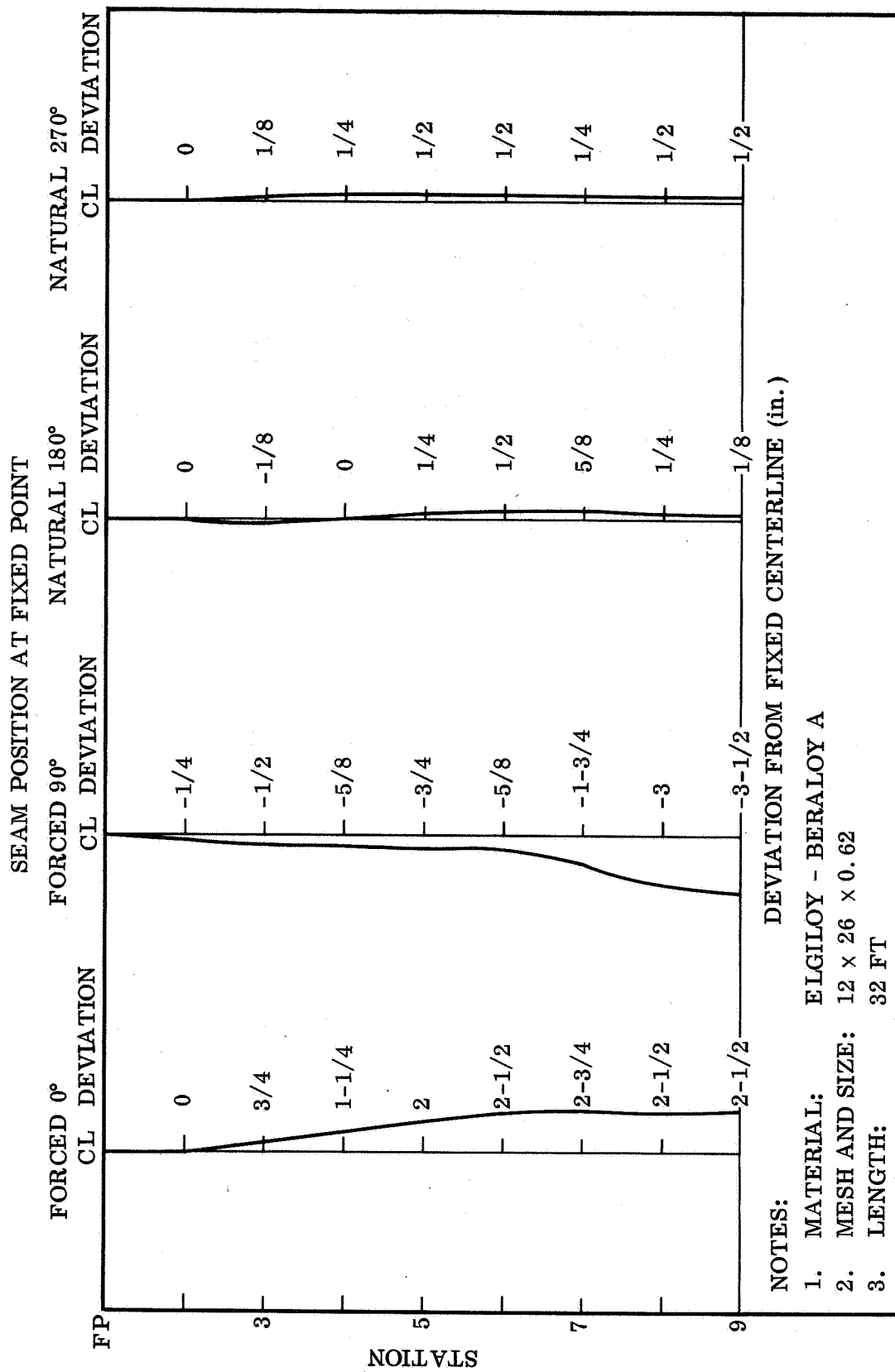


Figure 39. Boom Straightness, Elgiloy/Beryllium Copper, 12 x 26 Mesh, Run 320

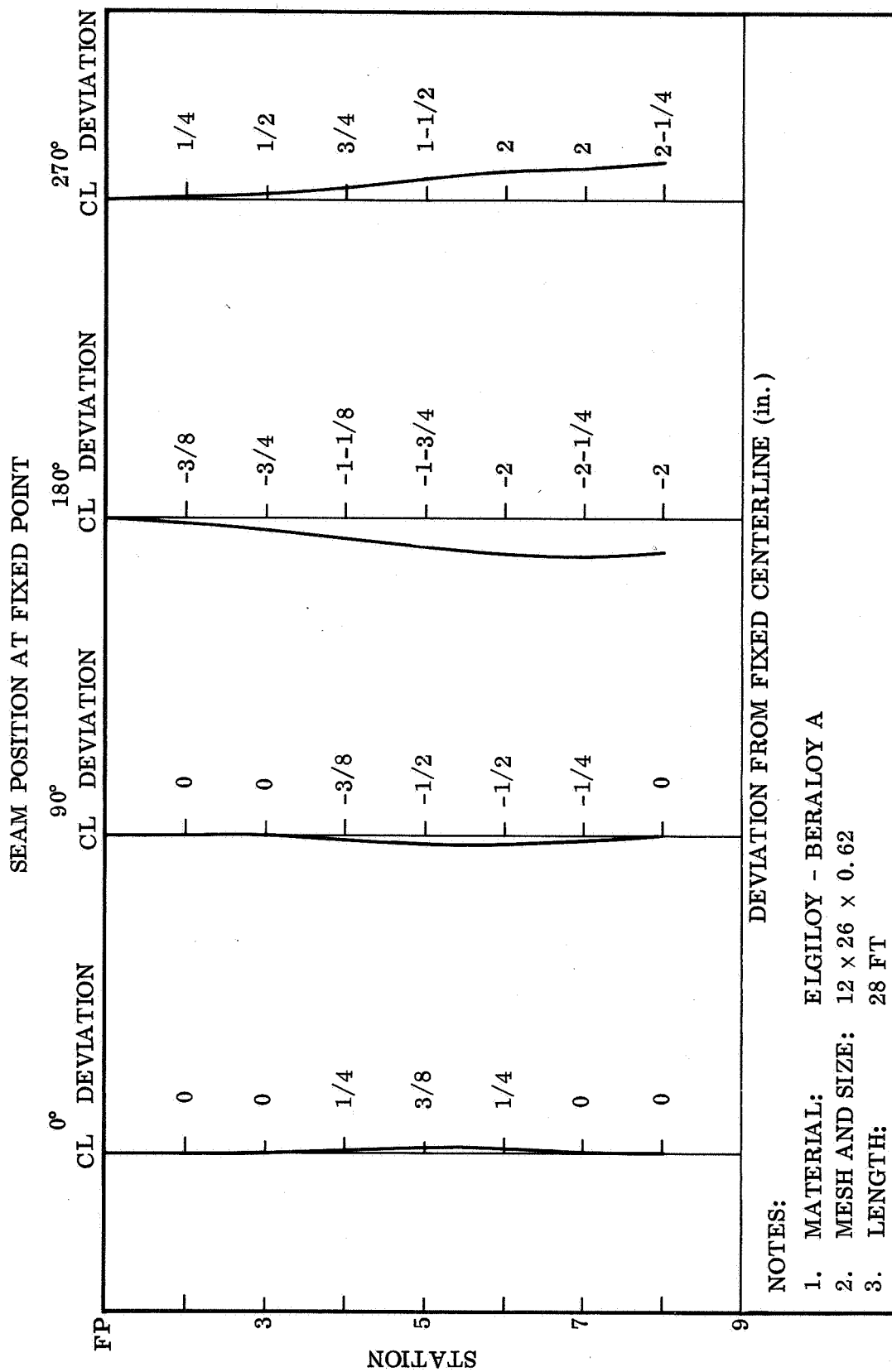


Figure 40. Boom Straightness, Elgiloy/Beryllium Copper, 12 x 26 Mesh, Run 320

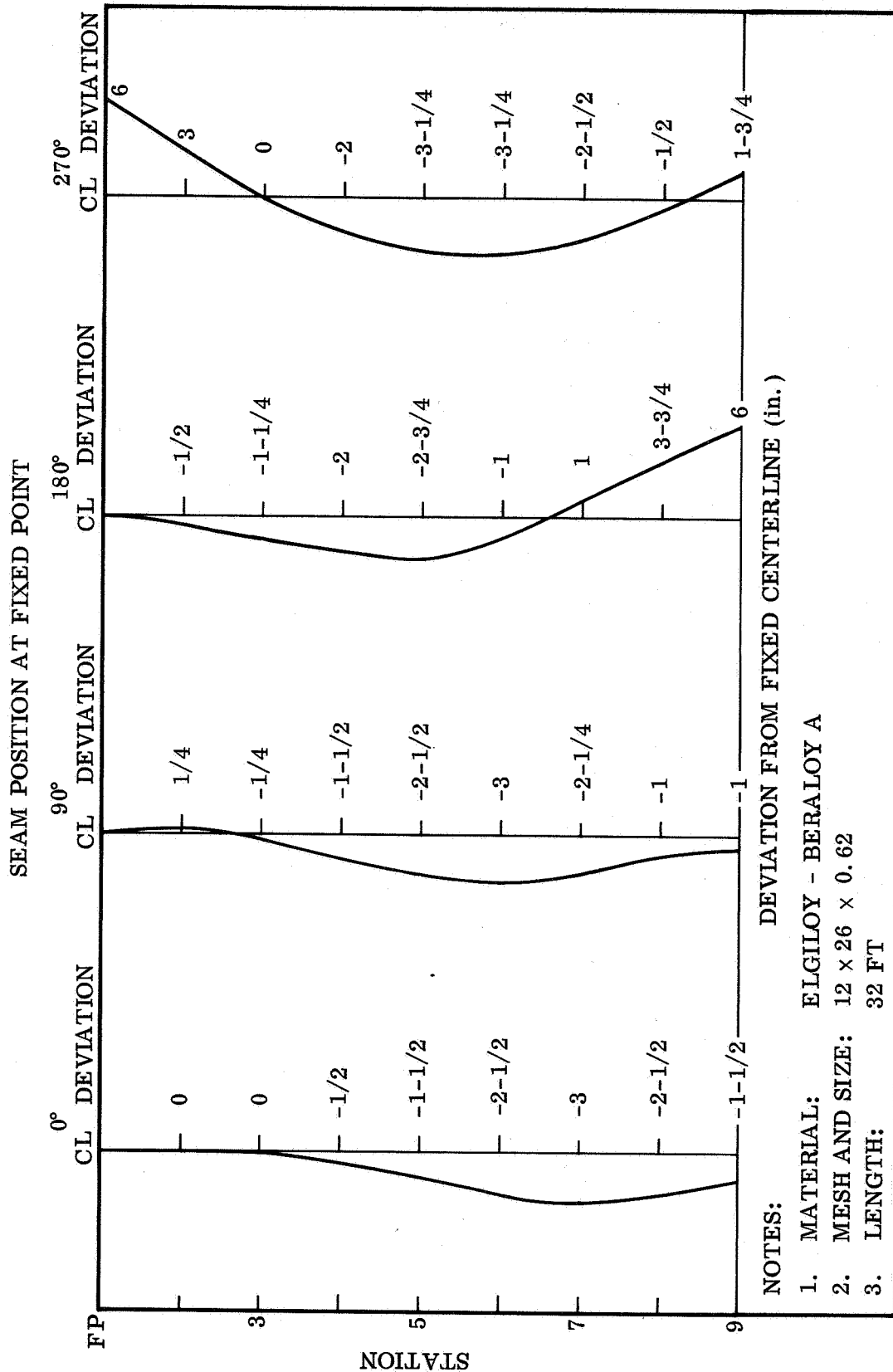


Figure 41. Boom Straightness, Elgiloy/Beryllium Copper, 12 x 26 Mesh, 1-66

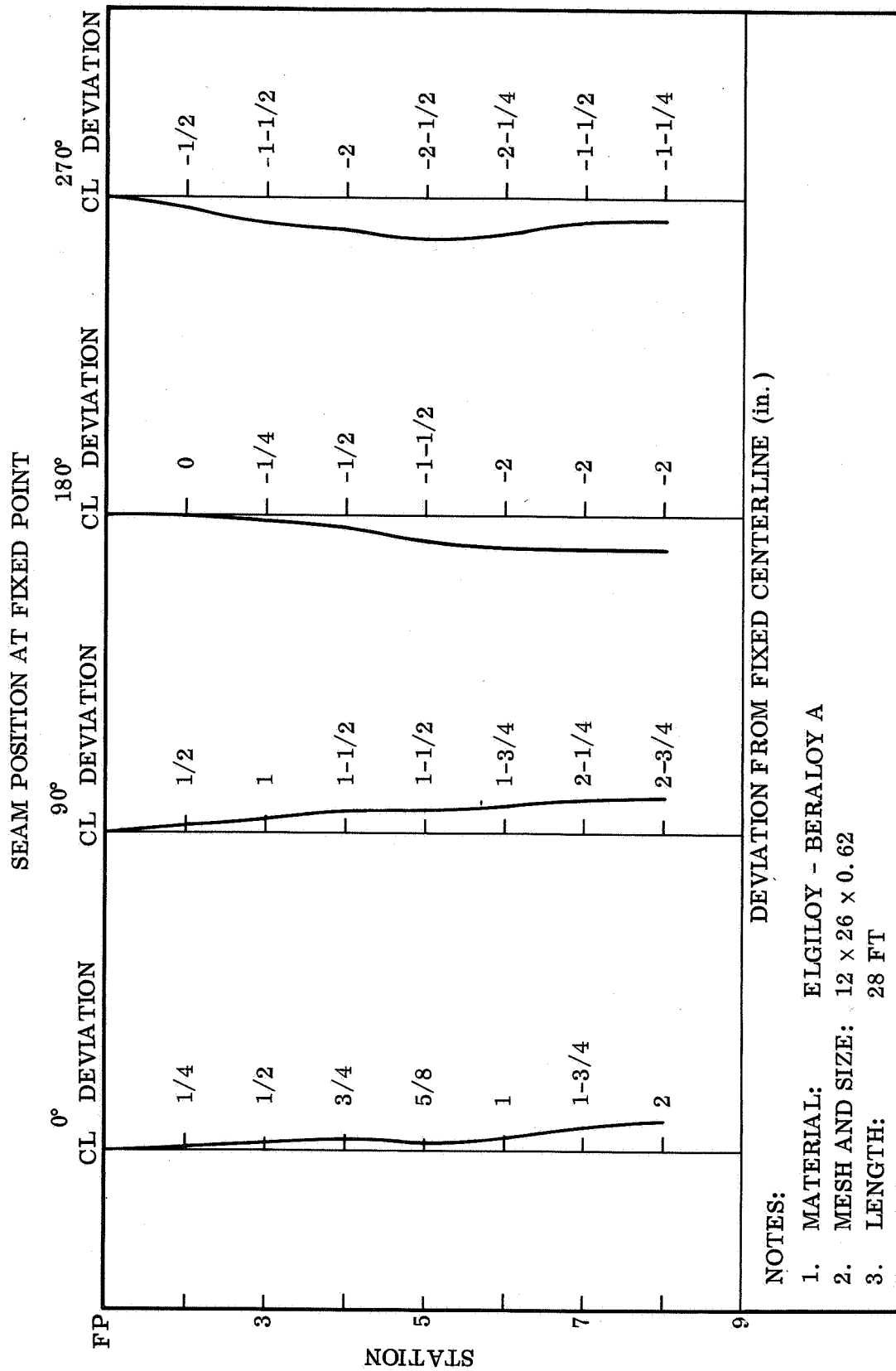


Figure 42. Boom Straightness, Elgiloy/Beryllium Copper, 12 x 26 Mesh, X-1

2.3.4 STORAGE AND FLEXURE TESTING. Storage and flexure testing as specified was not conducted because of unavailability of finished screen representing delivery quality until the end of the period of performance.

The problems of adequate handling of the wire mesh boom during the conduct of storage and flexure testing were not resolved until the deployment mechanism was adequately developed. As discussed in Section 2.3.1, screen boom handling characteristics are such as to preclude casual or nonmechanized flattening or reforming operations. Parameters for minimum equipment for conduct of the storage and flexure testing as specified are identical to those for the action and mechanism used in the deployer (discussed in Section 2.4). Such a mechanism, even if only in breadboard form, should have a replaceable reel or drum to enable testing of more than a single boom during any particular time period. It should permit fully mechanical handling of the wire mesh boom and preclude the almost certain damage that manual handling incurs.

Long-time storage tests were conducted on one section of 12 by 16.5 by 0.0082 by 0.0080 Elgiloy - Beraloy A screen boom. During a 7-month period stored in a laboratory atmosphere the boom, having a nominal 0.75-inch diameter, relaxed during storage to decrease the joint overlap from two meshes to one. This was approximately 4 percent. Single-flexure storage tests of up to two weeks duration indicate that a single square relaxation may be normal for that boom diameter and 0.0080-inch wire diameter.

2.3.5 THERMAL CYCLING

2.3.5.1 Test Method. The contract requirement for specimens, longer than 10 inches, representing the finished wire mesh to be cycled at least six times between +300° F and -300° F at a heating rate or cooling rate of at least 10° F per minute while undergoing repeated flattening once per minute was liberally interpreted. The thermal cycling test apparatus, shown in Figure 43, was constructed to complete the given test requirements in 6 minutes. Dimensions of the apparatus were made such that a 36-inch length of wire cloth boom could be cycled from -320° F to +300° F in one minute and be flattened once during that time. Spring tension applied in the endless belt arrangement permitted the flattening to occur with no discernable damage to the screen. Twelve-inch-long stainless steel tubes were utilized as heating and cooling chambers. The cooling chamber used liquid nitrogen, induced directly into the tube end, and the heating chamber used glass-insulated heating tape, wound throughout its length. Variac control and strip chart recording proved to be sufficient instrumentation. The very low thermal mass of the wire screen boom permitted the screen to be heated or cooled to the equilibrium temperature within the short exposure time. Following exposure, the screen was examined while in a flattened condition using a low-power lens. Physical testing was conducted on a Tineous Olsen, 60,000 lb testing machine on the 1200-lb range with the screen in tube form. Ultimate strength only was recorded.

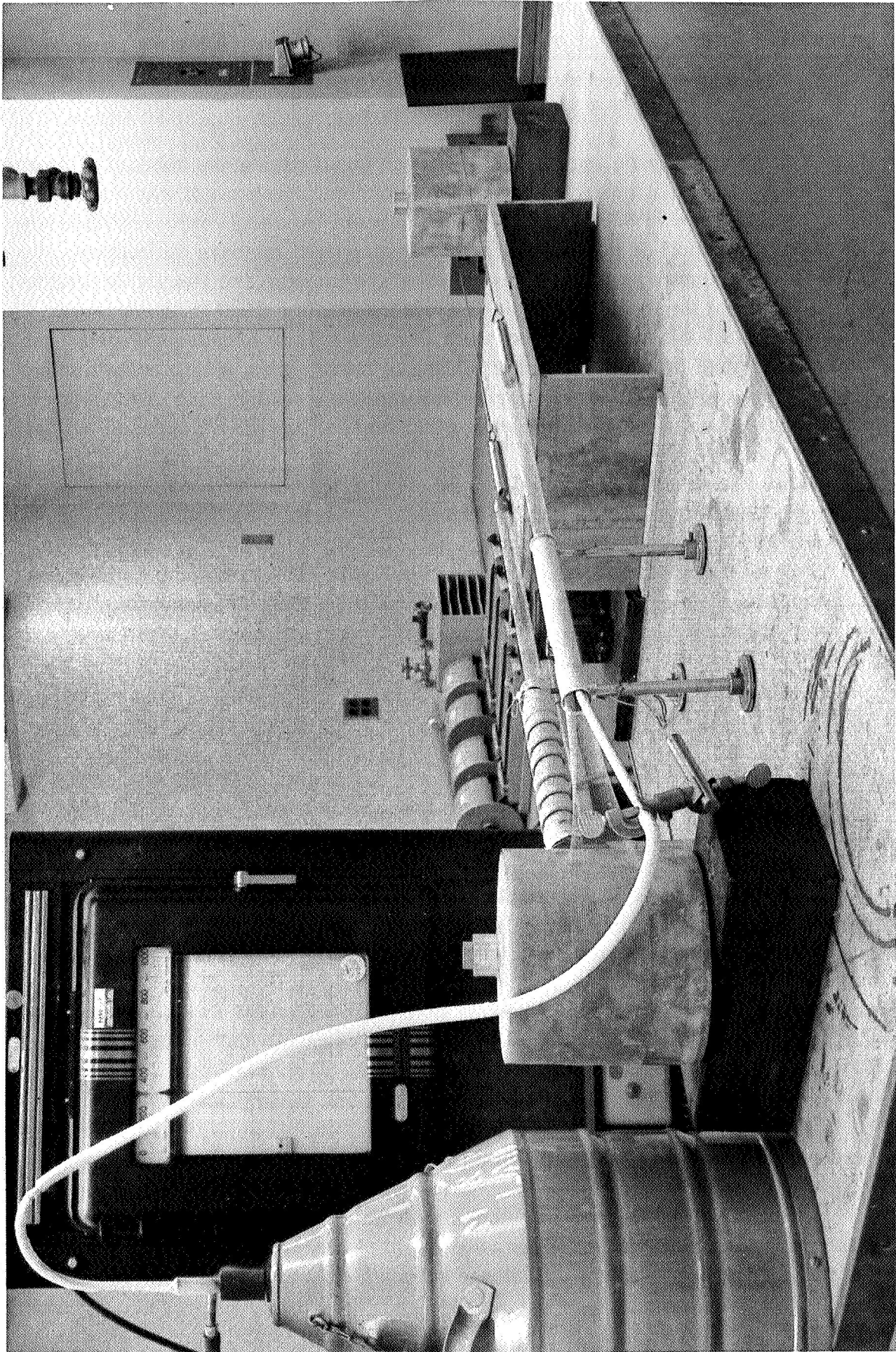


Figure 43. Thermal Cycling Test Apparatus

2.3.5.2 Thermal Cycling Test Results. Table 8 is a summary of the tests on three mesh sizes. Apparently joint integrity was not affected by the given thermal cycling test. Post-test analysis, however, shows that the tensile test on brazed wire mesh is completely insensitive to low levels of unbrazed or fractured joints. A section of wire screen of each mesh having an estimated minimum of 99% of the braze fillets removed by chemical stripping was found to have equal strength as the control samples which were completely brazed.

Table 8. Thermal Cycling Test Results

MESH SIZE AND TYPE	BREAKING STRENGTH		BRAZE JOINT INTEGRITY
	BEFORE TEST (lb)	AFTER TEST (lb)	
12 × 11.5 Elgiloy - BeCu 25	270	276	Intact
12 × 16.5 Elgiloy - BeCu 25	270	270	Intact
12 × 26 Elgiloy - BeCu 25	280	275	Intact

2.3.6 THERMAL DEFLECTION TESTING. These tests had two primary objectives. The first objective was to determine and compare the deflection characteristics of three types of screen booms when exposed to a simulated space environment. Deflections of a 30-inch boom sample were to be measured in a thermally-simulated space environment with one solar constant ($442 \text{ Btu/ft}^2\text{-hr}$) of simulated solar radiation directed toward one side of the boom.

The second objective was to measure the temperature gradient around the boom when exposed to the same environment. These data would then be used to evaluate a mathematical model of the complete boom.

2.3.6.1 Test Method. Six tests were performed of the following sample booms.

<u>Sample Description</u>	<u>Dimensions</u>	<u>Test Run No.</u>
12 × 12 × 0.009 Beraloy A	1 in. Dia. by 30 in. Lg	1 & 2
16 × 12 × 0.009 Beraloy A	1 in. Dia. by 30 in. Lg	3 & 4
12 × 16 × 0.009 Beraloy A	1 in. Dia. by 30 in. Lg	5 & 6

Two identical booms were exposed to the test environment simultaneously; one instrumented to record deflection, the other instrumented to record temperature.

Deflection was recorded photographically, using an electrically operated 35 mm camera with a 3X teleconverter on a 135 mm lens. The camera was mounted inside a protective pressure vessel, directly behind an optically flat window as shown in Figure 44. A sample boom was clamped directly over the outside of the window so that the camera viewed the inside of the boom. The boom was thermally insulated from the clamp with teflon. The camera was focused on the free end of the 30-inch boom. A thin glass plate, epoxied inside the camera at the focal plane, was scribed to serve as a reference frame when determining deflections. Camera and boom relationship is illustrated in Figure 45.

The second sample boom was similarly clamped beside the first. This boom was instrumented with 12 32-gage copper-constantan thermocouples. There were four thermocouples located 90 degrees apart at the boom center, and four more at each end 6 inches away from the center. The three orthogonal groups of thermocouples were clocked 30 degrees apart so that a thermocouple was located at each 30-degree increment around the boom. Thermocouple output voltages were recorded on punched paper tape.

The two booms were thermally shielded from each other and the mounting fixture by a black, liquid-nitrogen-chilled panel. The complete assembly was suspended inside a 56-inch diameter thermal-vacuum chamber. The chamber was lined with a black, liquid-nitrogen-chilled shroud. A xenon-arc solar simulator projected a 30-inch beam through a quartz window at one end of the chamber. Two views of the chamber and mounted test specimens are shown in Figures 46 and 47.

The three types of screen booms were tested in two orientations with respect to the direction of simulated solar radiation. Tests were performed with the longitudinal seam 180 and 90 degrees from the center of radiation impingement. All test runs were performed according to the following general procedure.

With the test assembly installed inside the chamber, the chamber pressure was reduced to less than $1 \text{ by } 10^{-5}$ torr and the chamber shroud and separator shroud chilled to -300° F with liquid nitrogen. These conditions were maintained throughout the test. The booms were allowed to cool by radiation to below -50° F . Simulated solar radiation at an intensity of one solar constant was then projected upon one side of the booms and photographs and thermocouple output recordings were made every ten seconds during radiation exposure. Radiation intensity was controlled to ± 2 percent. When boom temperatures stabilized, testing was terminated.

Reliable deflection measurements of the free ends of the screen booms were obtained for all runs and are shown in Figures 48 through 53. Deflections parallel (Y axis) and transverse (X axis) to the radiation beam are plotted against time, which is indicated in hundreds of seconds by the number over the plotted points.

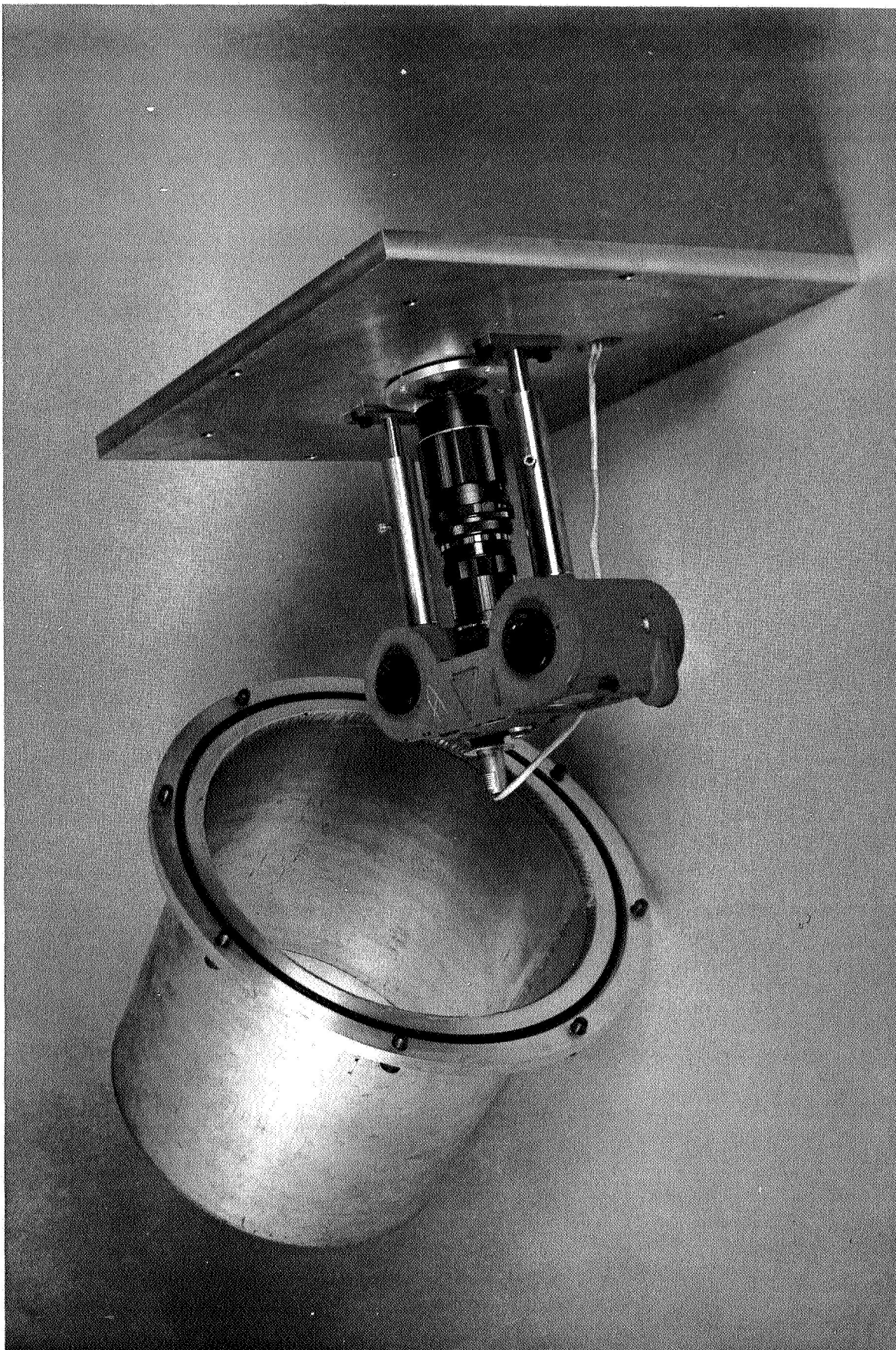


Figure 44. Deflection Recording Camera and Housing

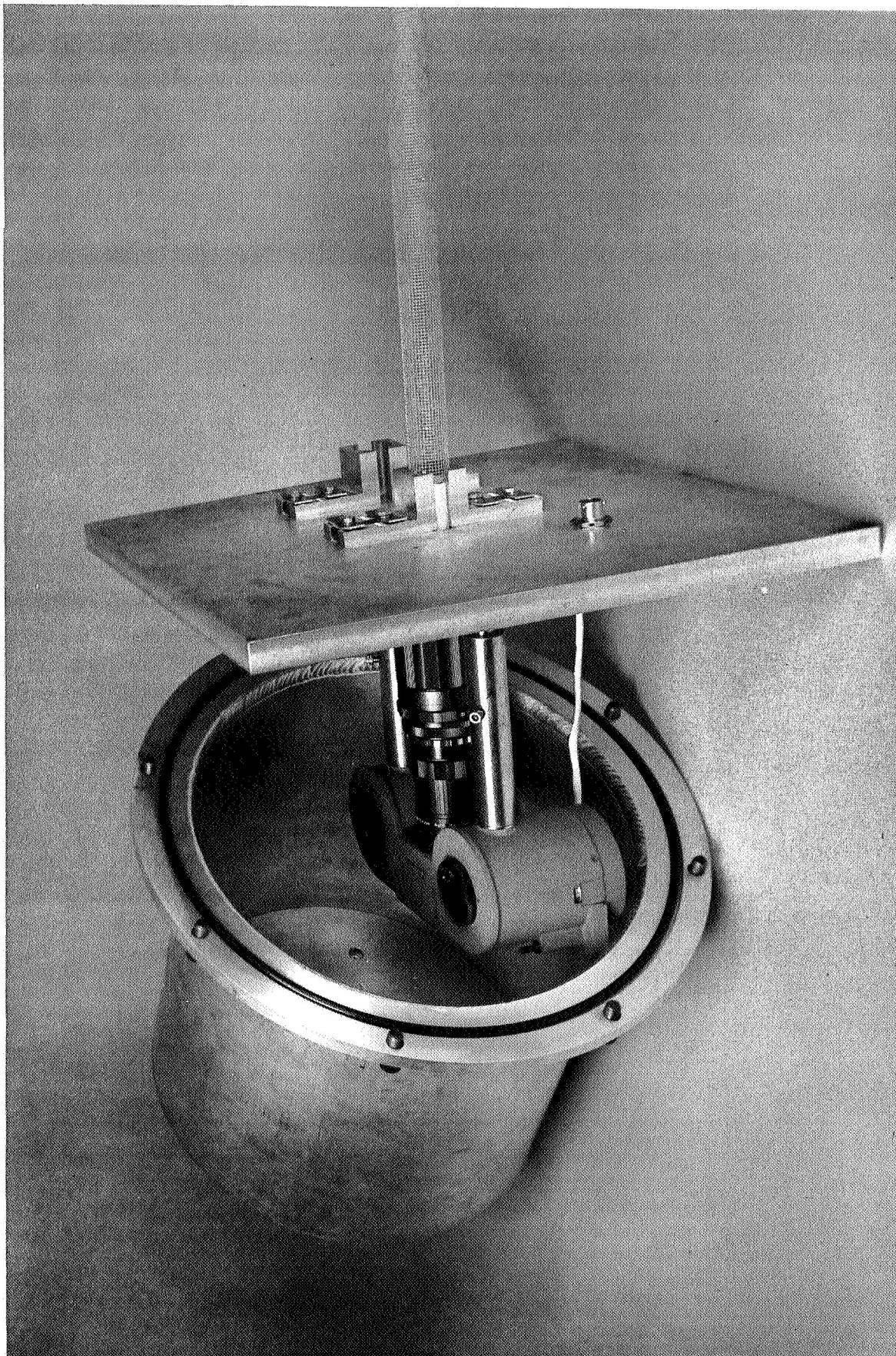


Figure 45. Camera Assembly with Sample Boom Mounted

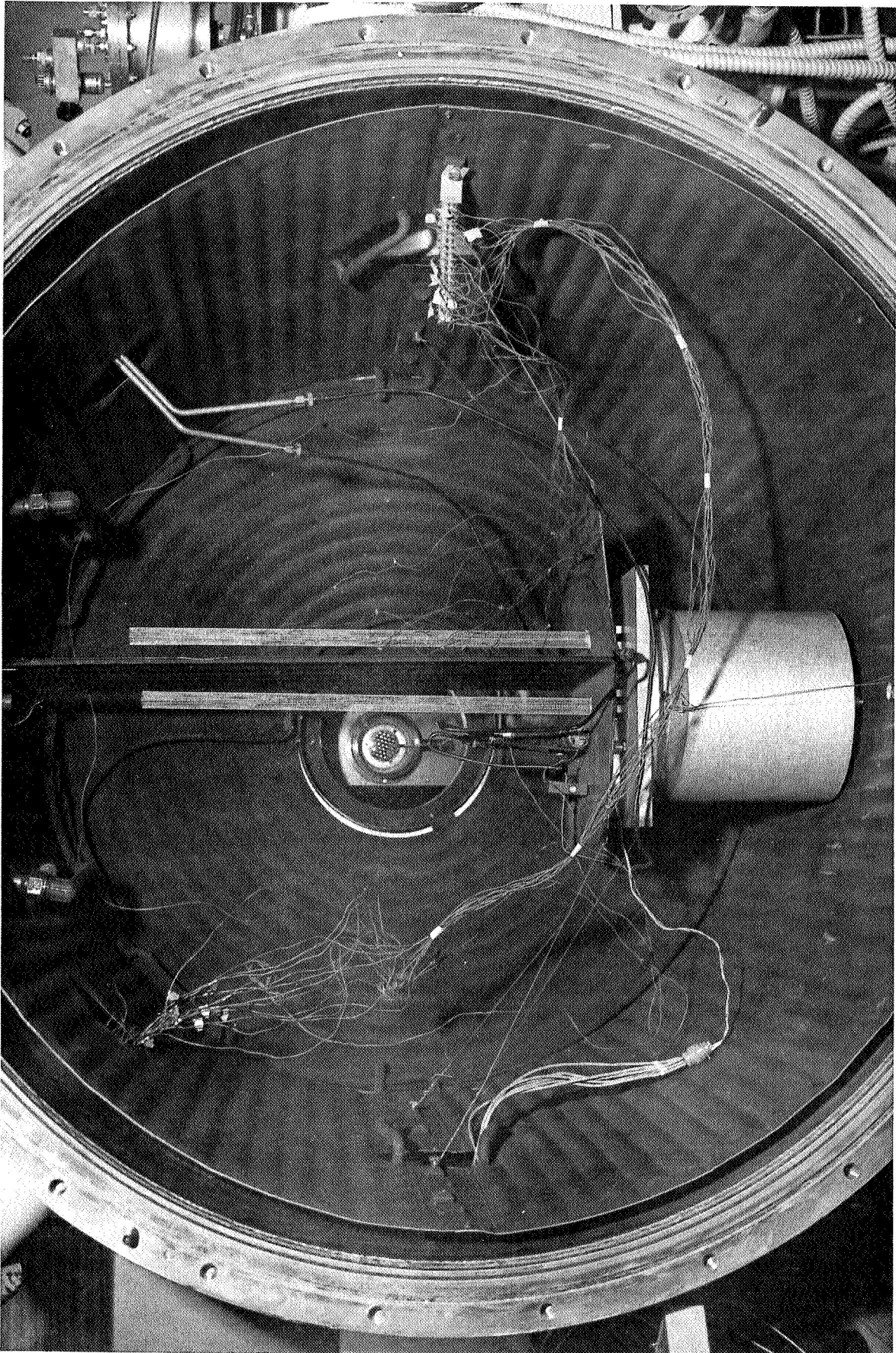


Figure 46. Boom Test Assembly in Thermal-Vacuum Chamber

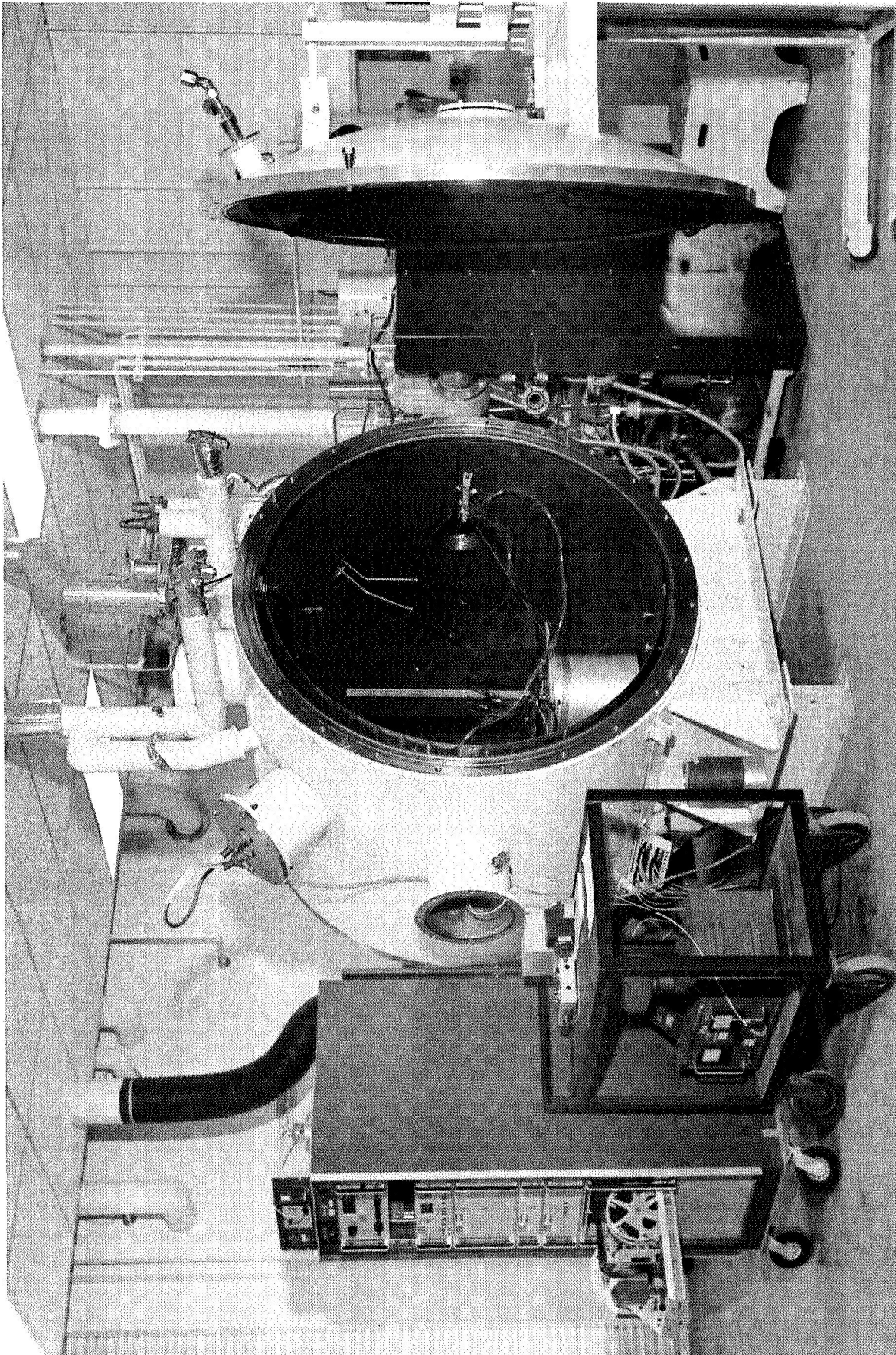


Figure 47. Complete Thermal-Vacuum Test Setup

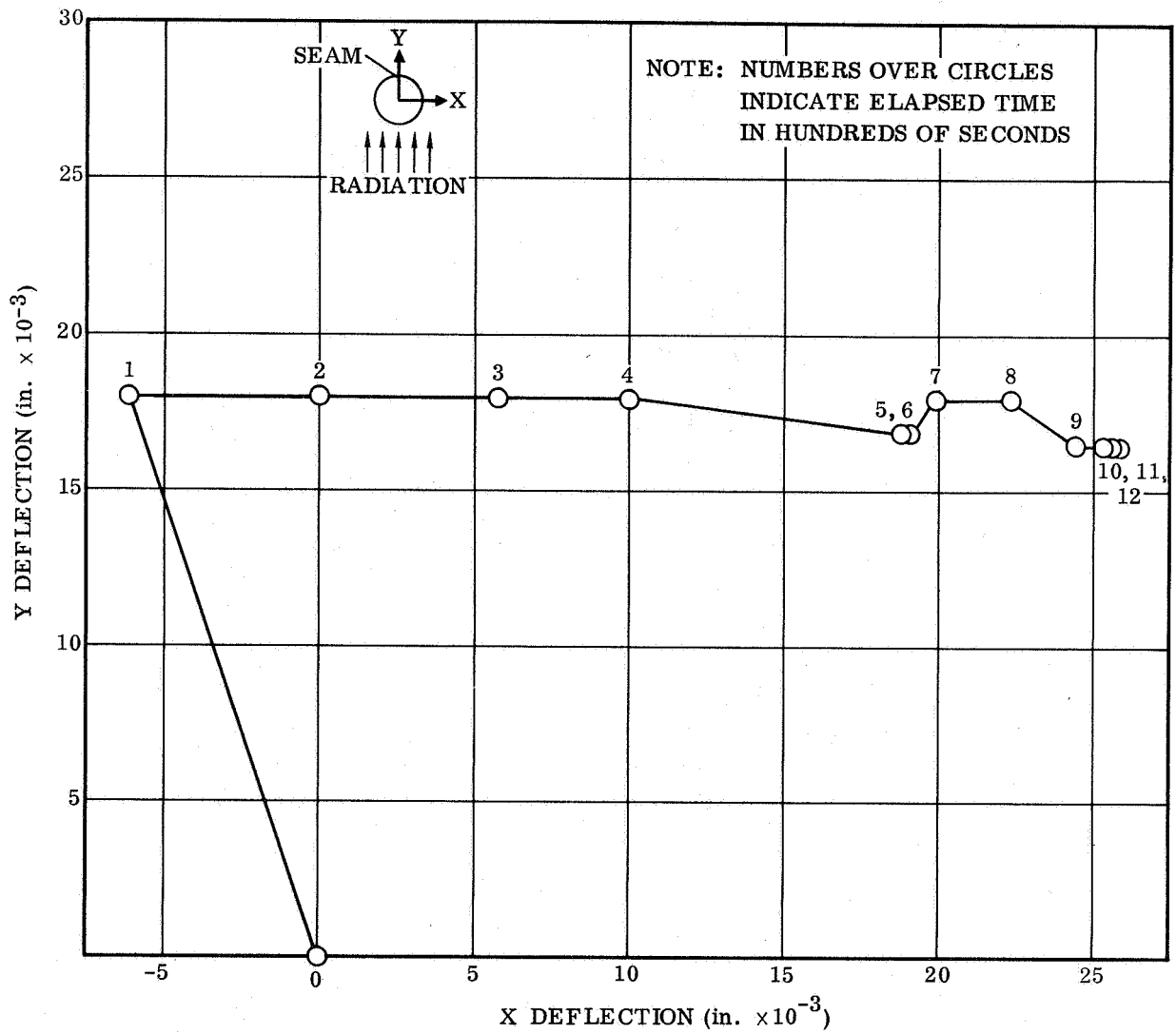


Figure 48. Thermal Deflection Test, Run 1

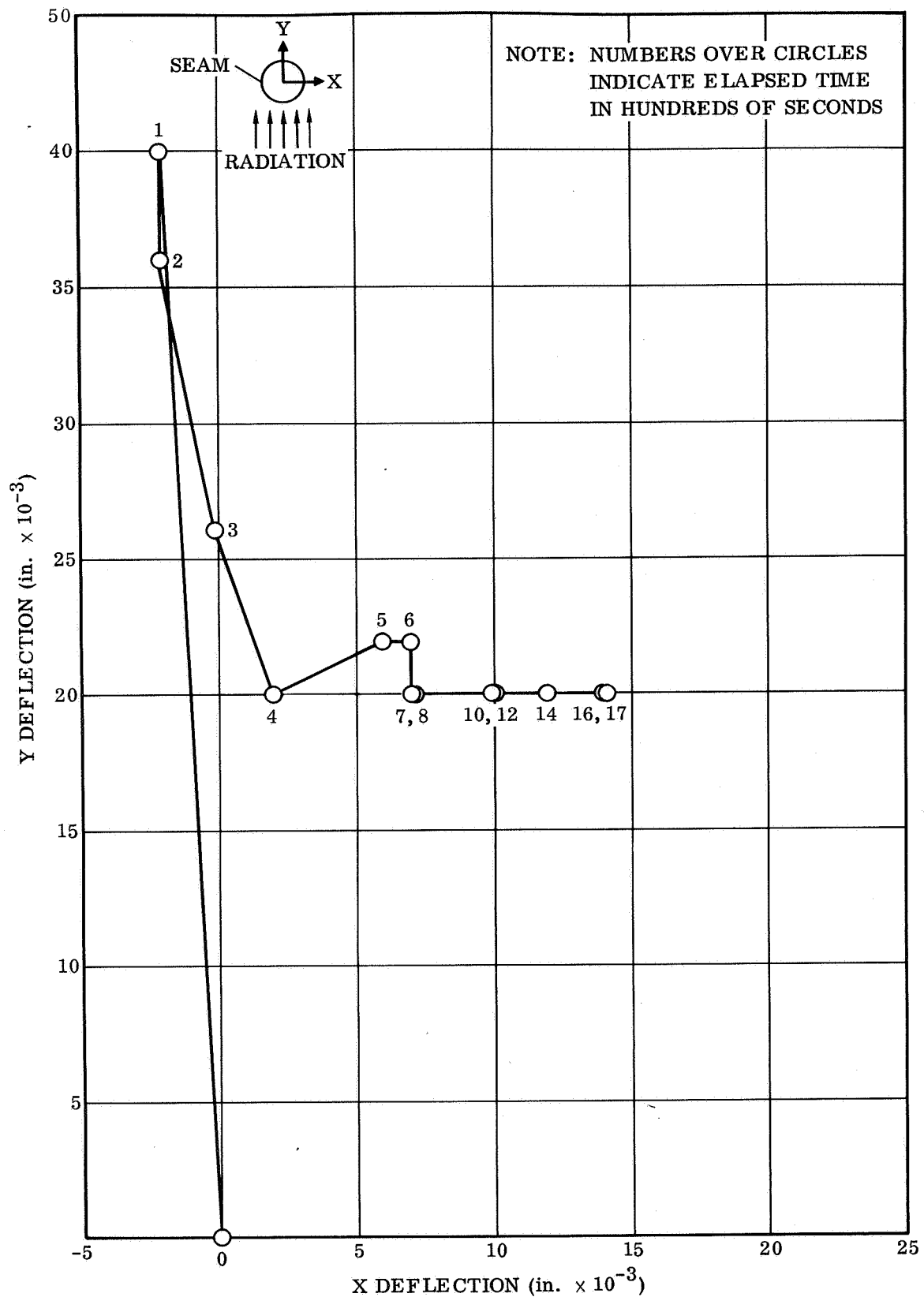


Figure 49. Thermal Deflection Test, Run 2

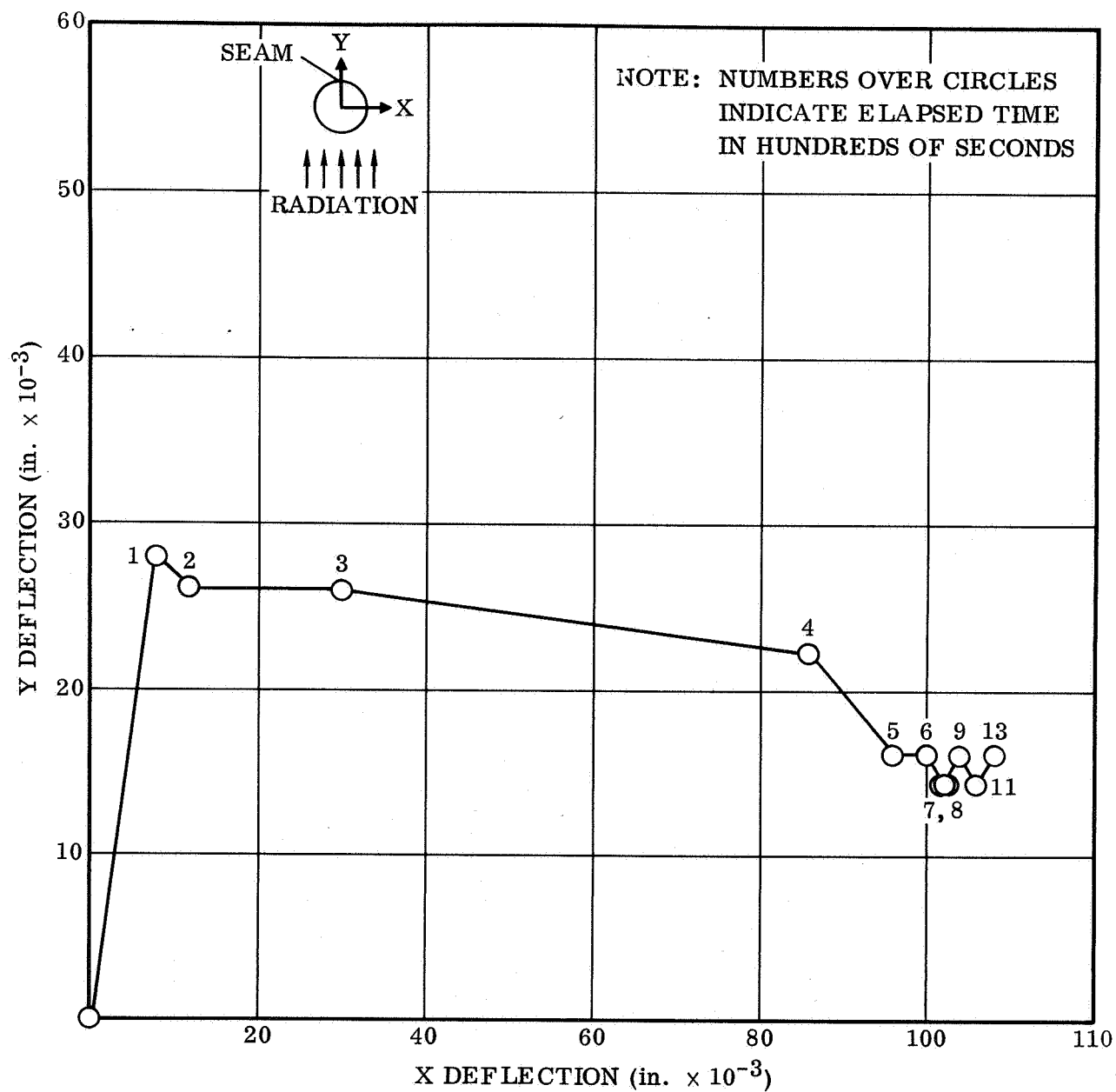


Figure 50. Thermal Deflection Test, Run 3

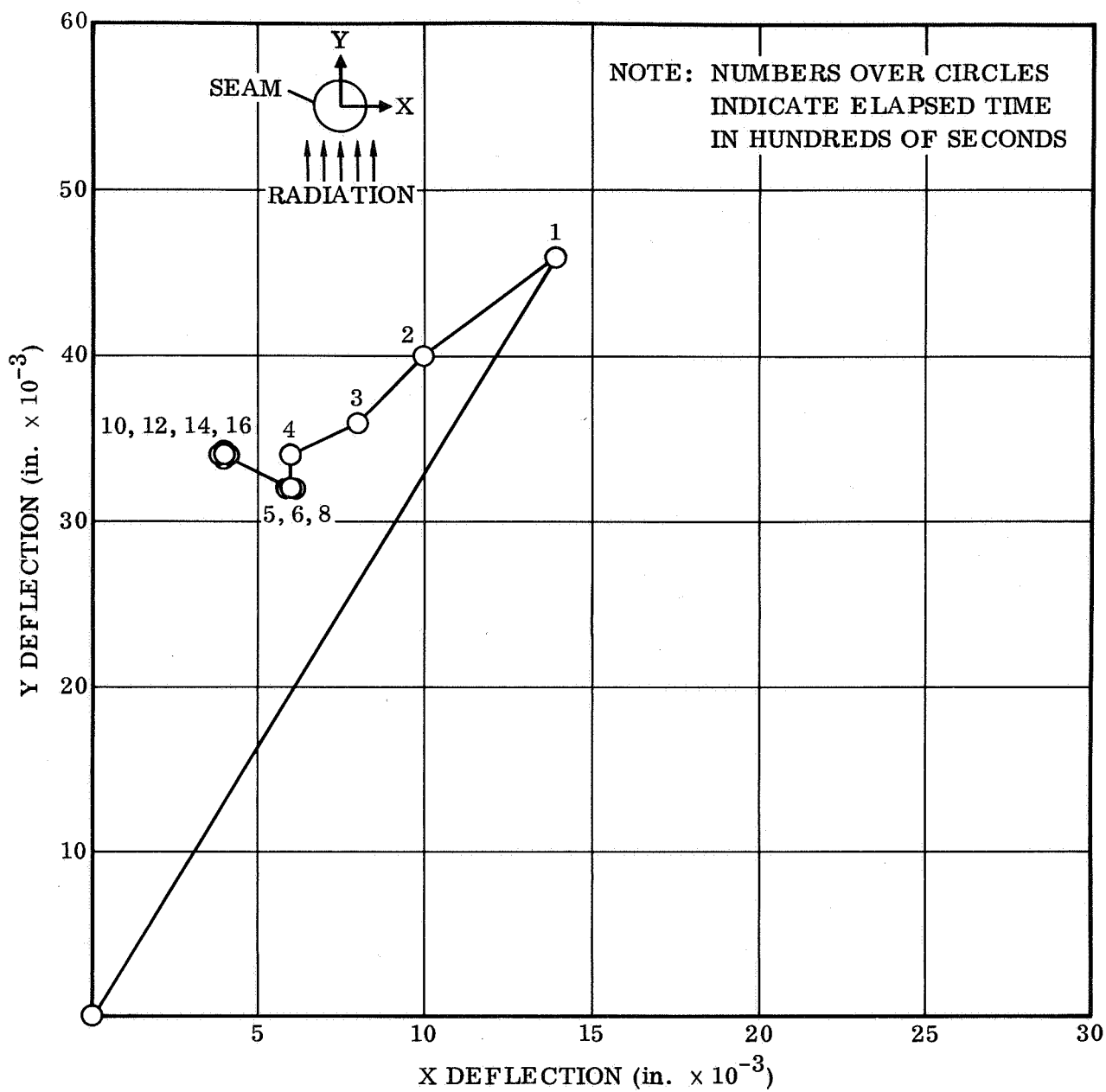


Figure 51. Thermal Deflection Test, Run 4

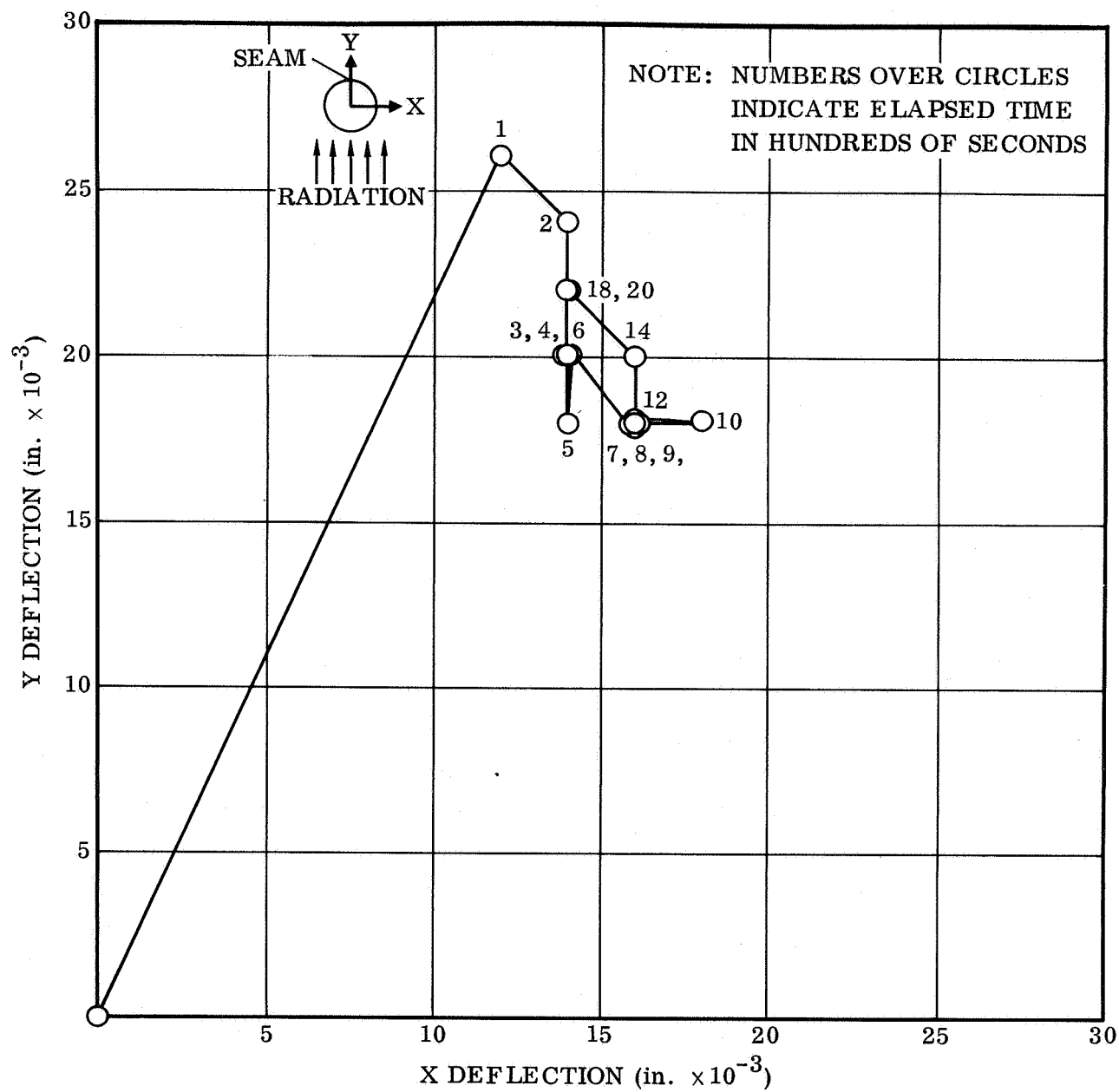


Figure 52. Thermal Deflection Test, Run 5

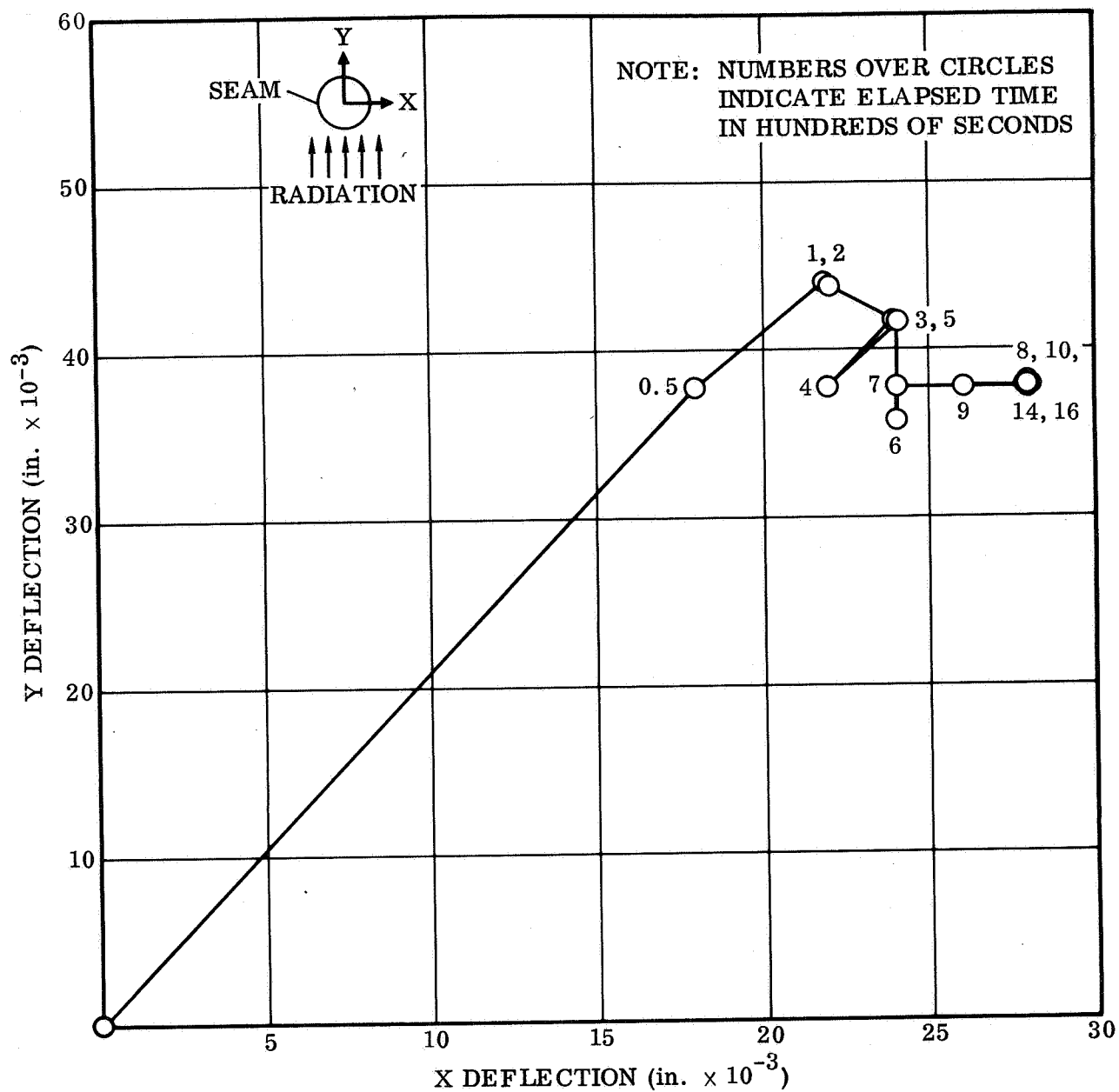


Figure 53. Thermal Deflection Test, Run 6

Deflection measurements were taken directly from the photographs, viewed through a 20 power microscope with a superimposed measuring grid. Accuracy was ± 0.001 inch. At time zero, the solar simulator was turned on and a photograph taken. The first frame was used as a base reference for all other frames taken during the run.

Temperature data were not as meaningful as deflection data. Dispersion in data resulted from the methods of attachment of thermocouples to the screen and (possibly) from longitudinal temperature gradients in the boom.

Temperature measurements were not usable from Runs 1 and 2. In these runs, thermocouple junctions were soft-soldered directly to the screen at an intersection of two boom wires. Heat into a junction was greatly affected by the size and adsorptance of the soldered joint, and comparison of temperature points on the boom could not be made.

The thermocouple junction was made along a single boom wire, between intersections, for Runs 3 through 6. This method resulted in a less bulky junction as the copper and constantan wires were positioned alongside a boom wire and tinned in place. The junction was along a longitudinal boom wire for Runs 3 and 4 and a circumferential boom wire for Runs 5 and 6. Temperature data were greatly improved using this method of mounting but still were too scattered for detailed analysis of the stabilized temperature gradient around the circumference of the boom. Temperature versus time data for four circumferential locations taken during Runs 5 and 6 are presented in Figures 54 and 55, respectively.

Figure 56 shows plots of deflections and temperature difference across the boom in the direction of deflection, versus time. These plots indicate the dependence of deflection on temperature gradient by the similarity in curve profiles.

It was difficult to obtain precise information from these data, however. Figure 57 shows plots of stabilized temperature versus angular location on the boom. The scatter is due to junction effects and end effects. Since each group of four thermocouples was located six inches apart on the boom, the longitudinal temperature gradient obscured the true angular temperature gradient. It is evident from these results that required temperature data accuracy (in this case $\pm 1^\circ \text{F}$) cannot be achieved using standard methods of attaching thermocouples to boom wires.

2.4 DEPLOYMENT MECHANISM FOR WIRE SCREEN BOOMS

A mechanism was designed and fabricated to deploy and retract wire screen booms without deleterious effect on the material. Design was undertaken using materials and techniques normally associated with satellite usage. The deployer, illustrated in Figures 58 through 62 is, with minor modification, the delivery item.

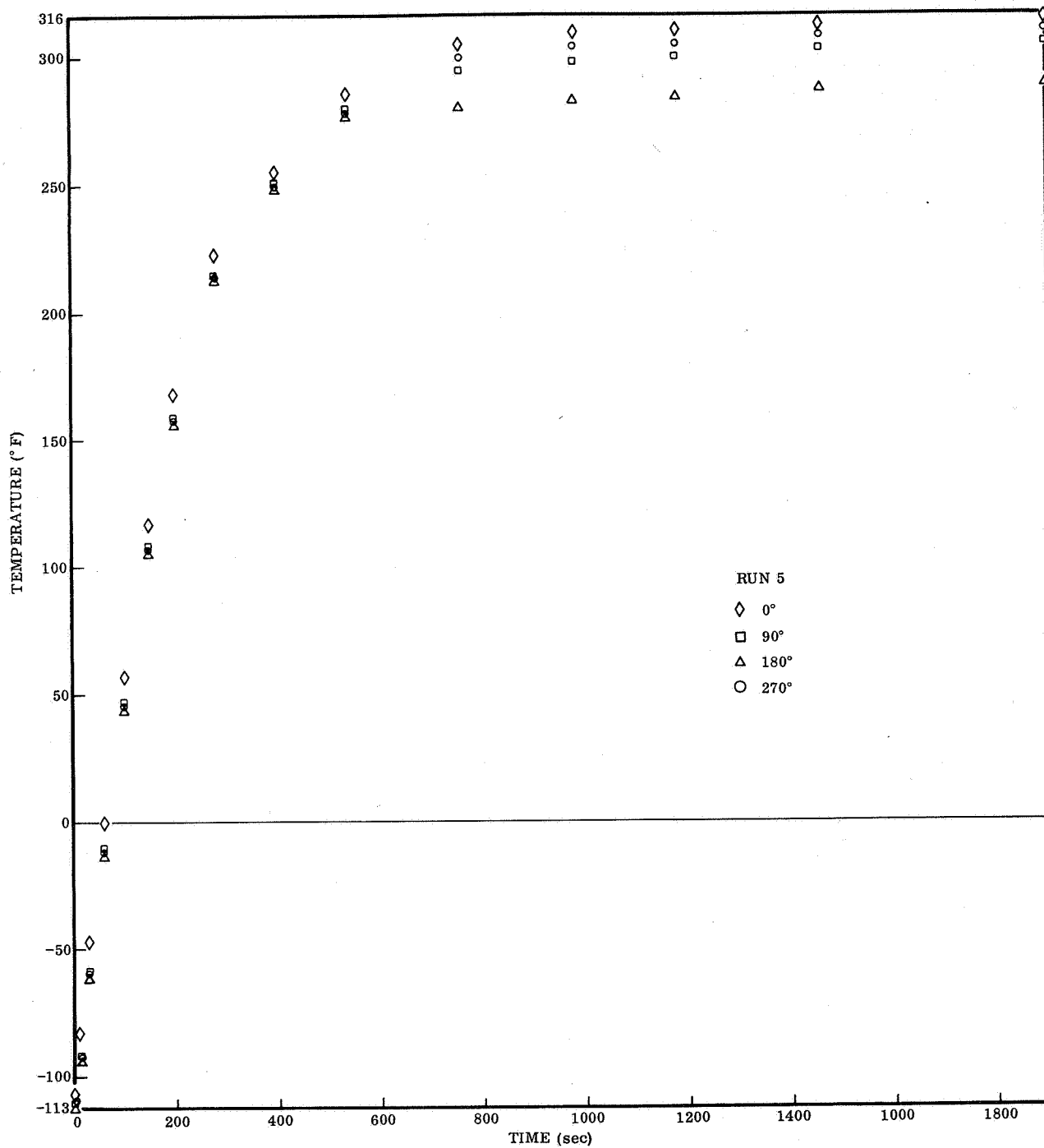


Figure 54. Temperature History, Run 5

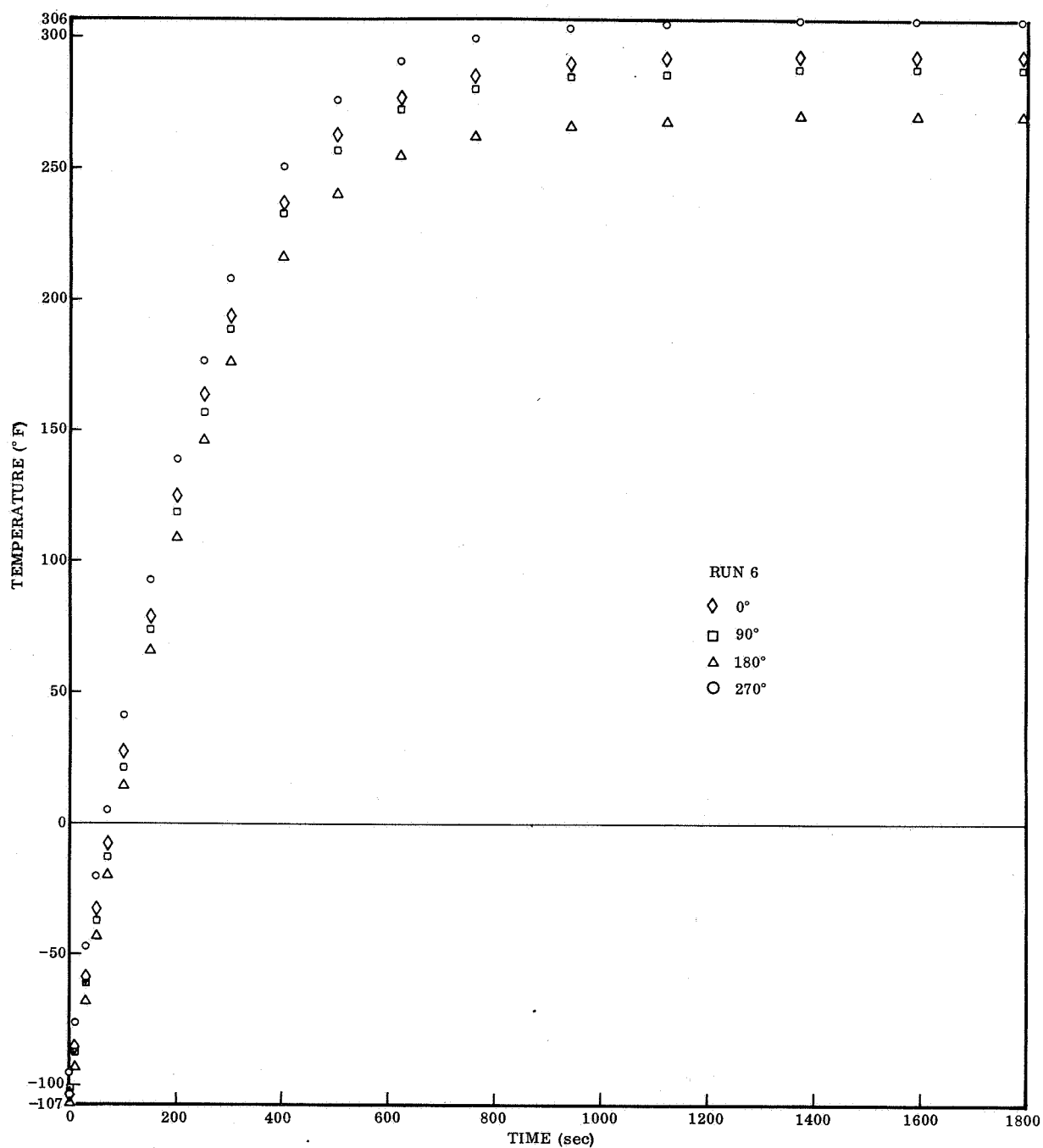


Figure 55. Temperature History, Run 6

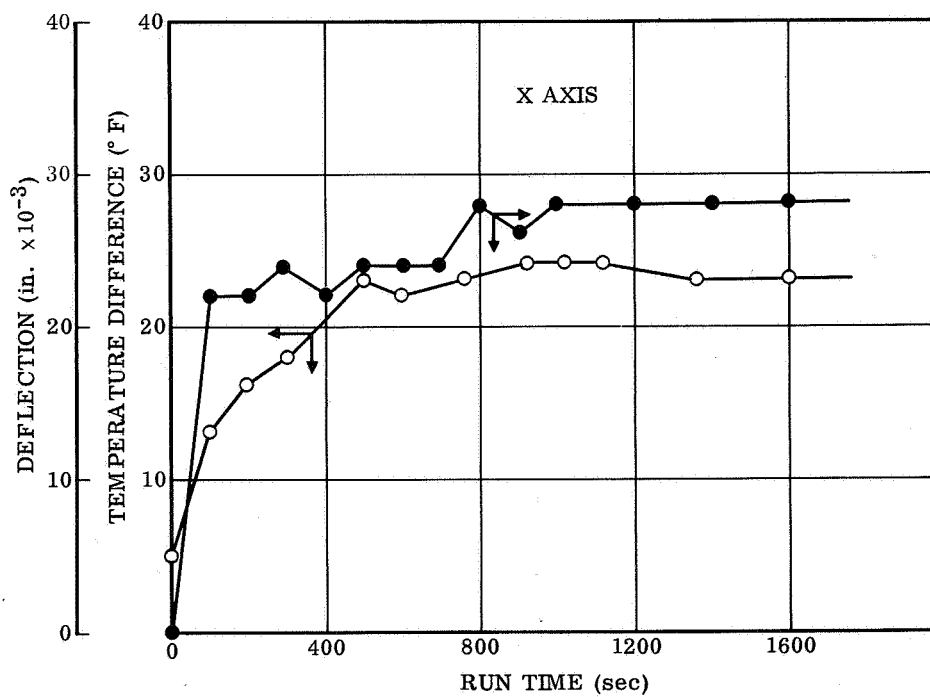
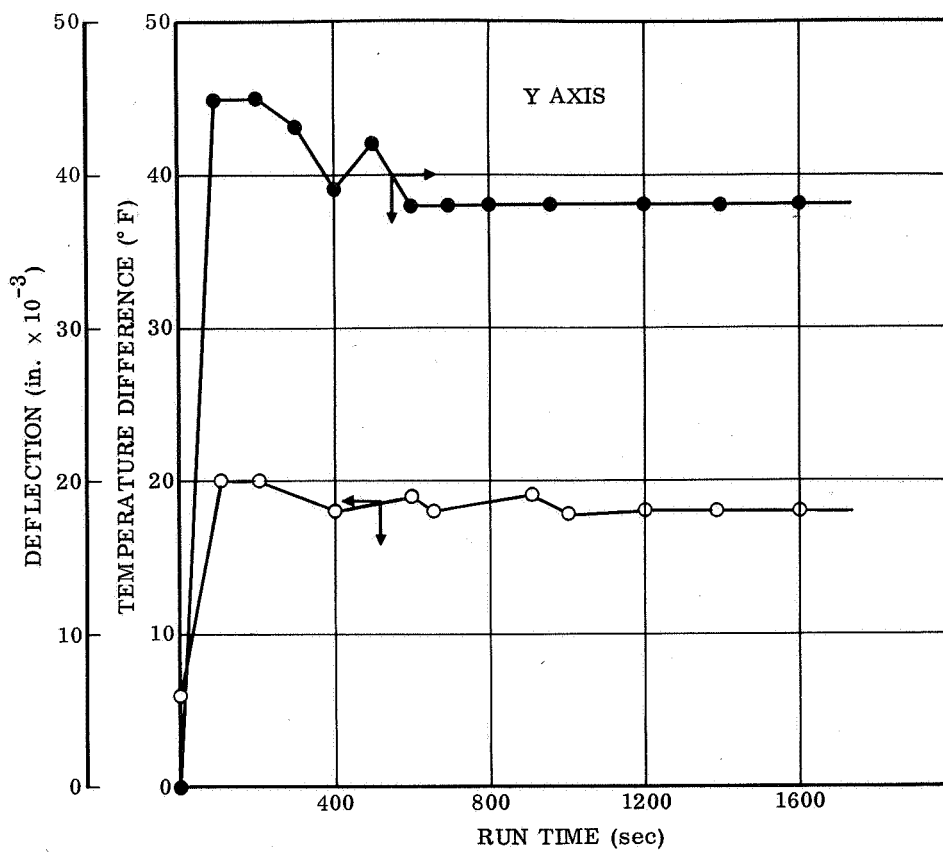


Figure 56. Temperature Difference and Deflection vs. Time, Run 6

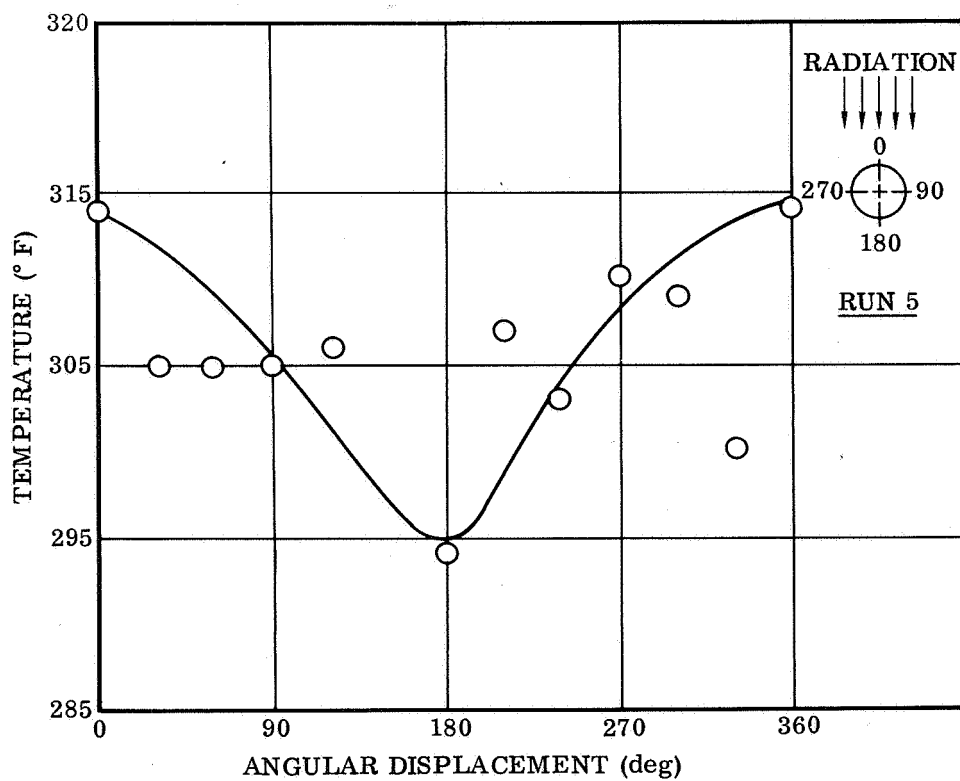
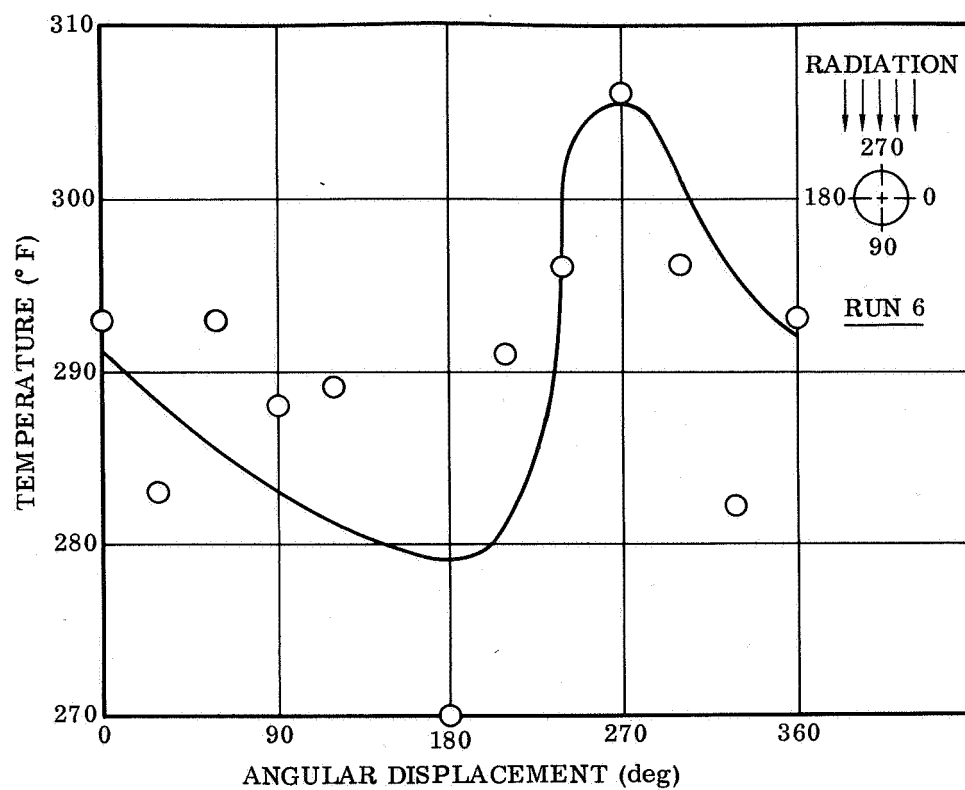


Figure 57. Stabilized Temperature vs. Angular Displacement

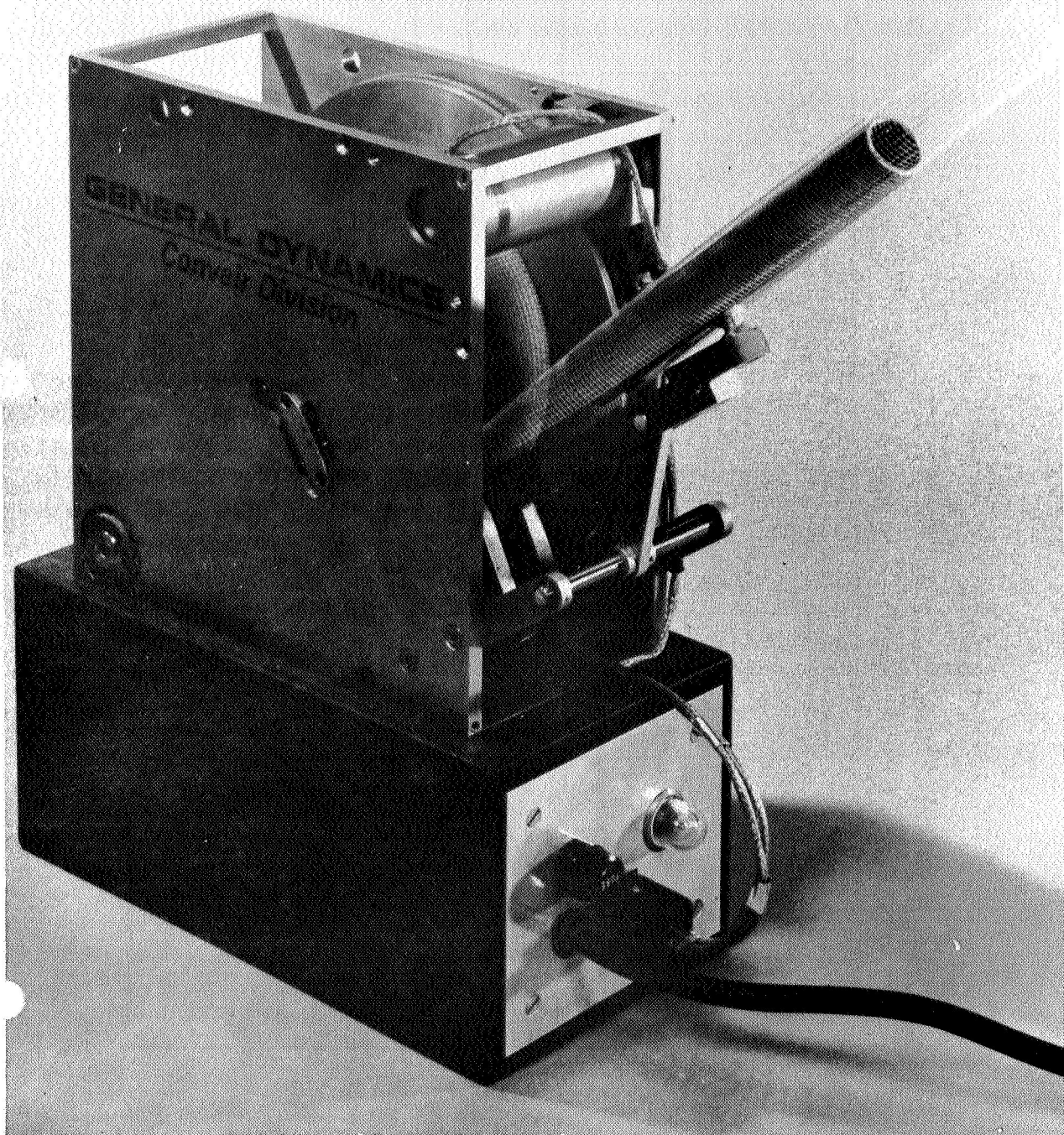


Figure 58. Deployment Mechanism with Partially Extended Screen Boom on DC Power Supply for Demonstration Purposes

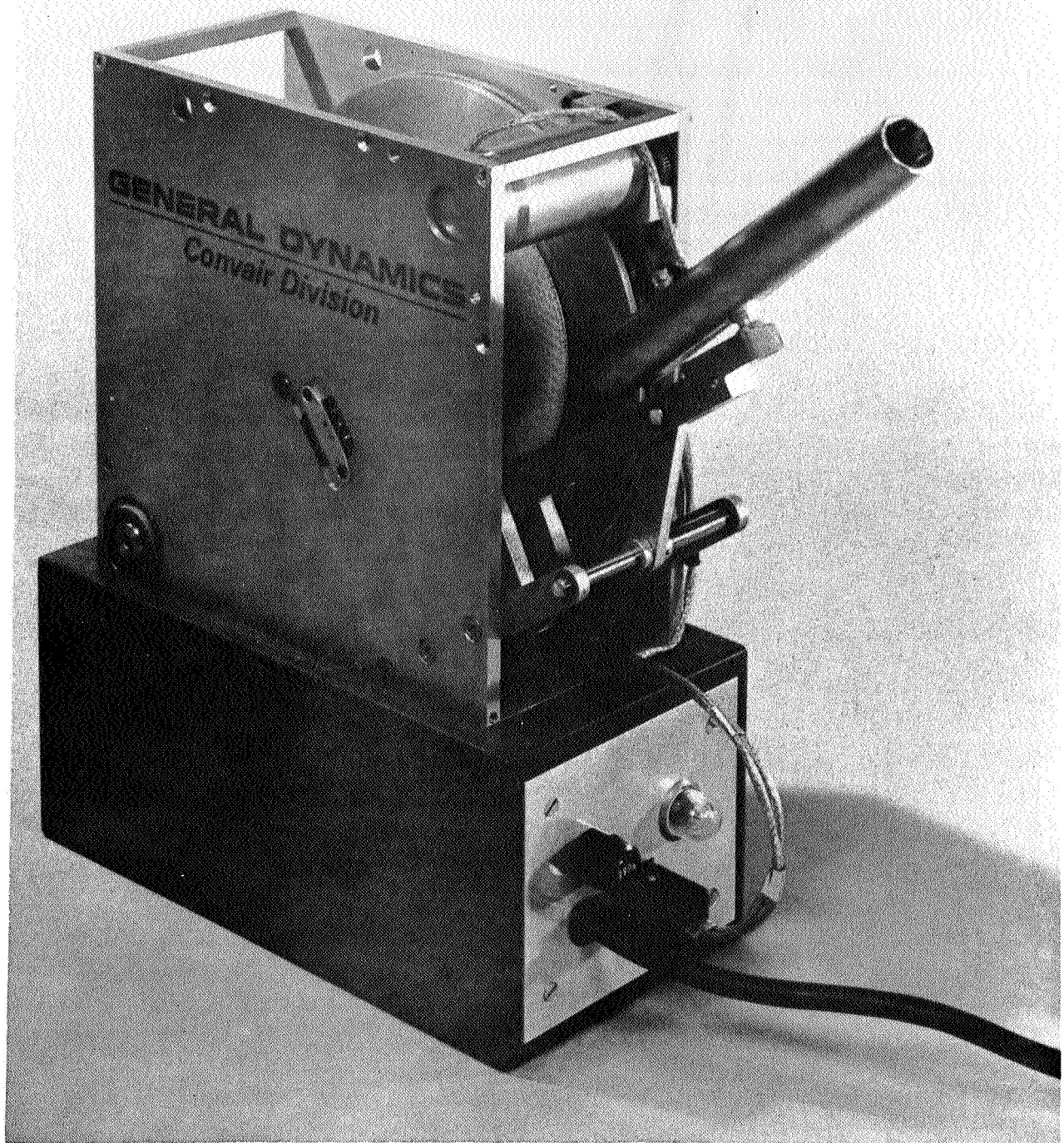


Figure 59. Deployment Mechanism with Screen Boom Fully Retracted to Show Details

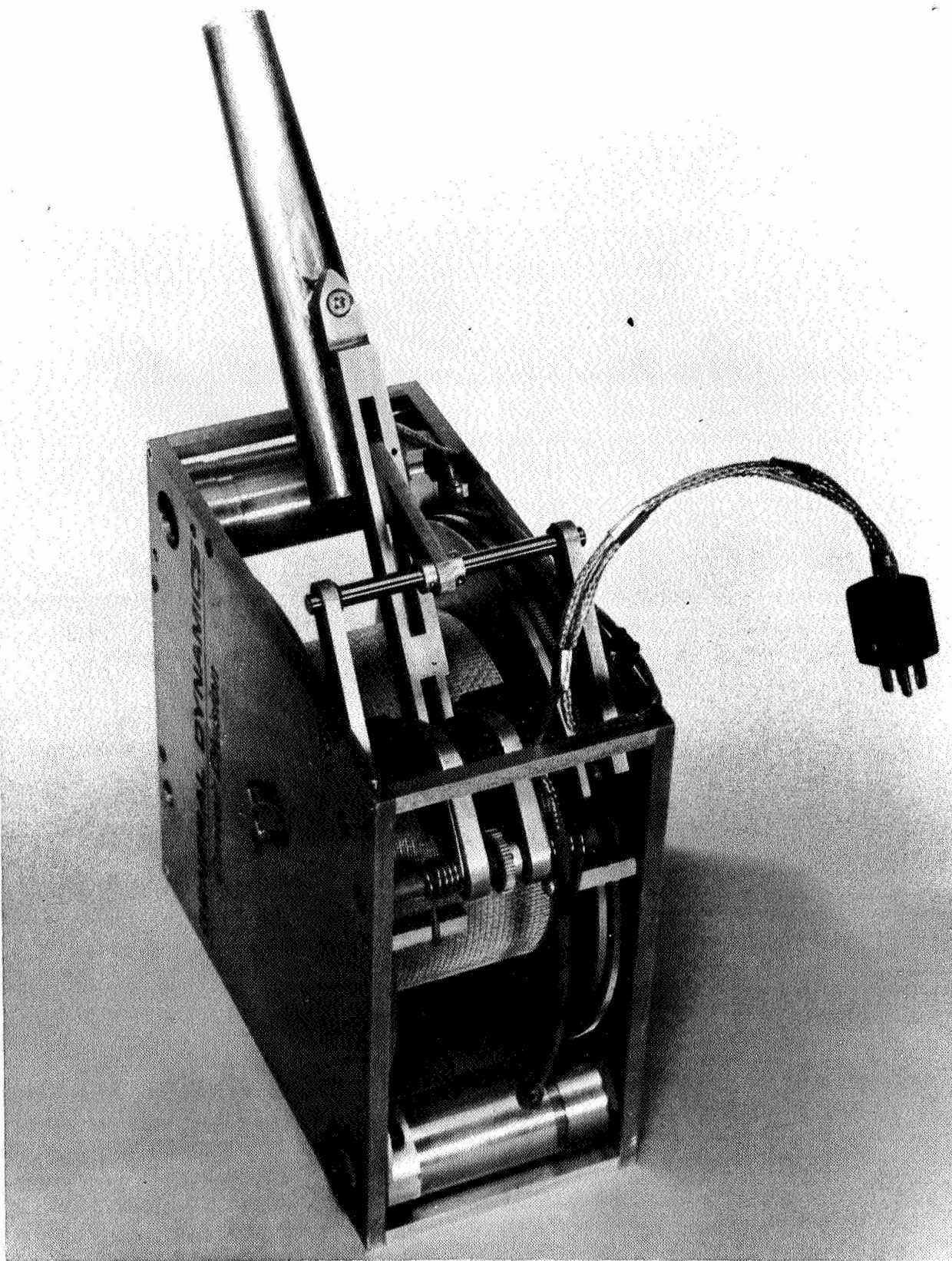


Figure 60. Deployment Mechanism, Oblique View, Showing Powered Roller, Drive and Guide

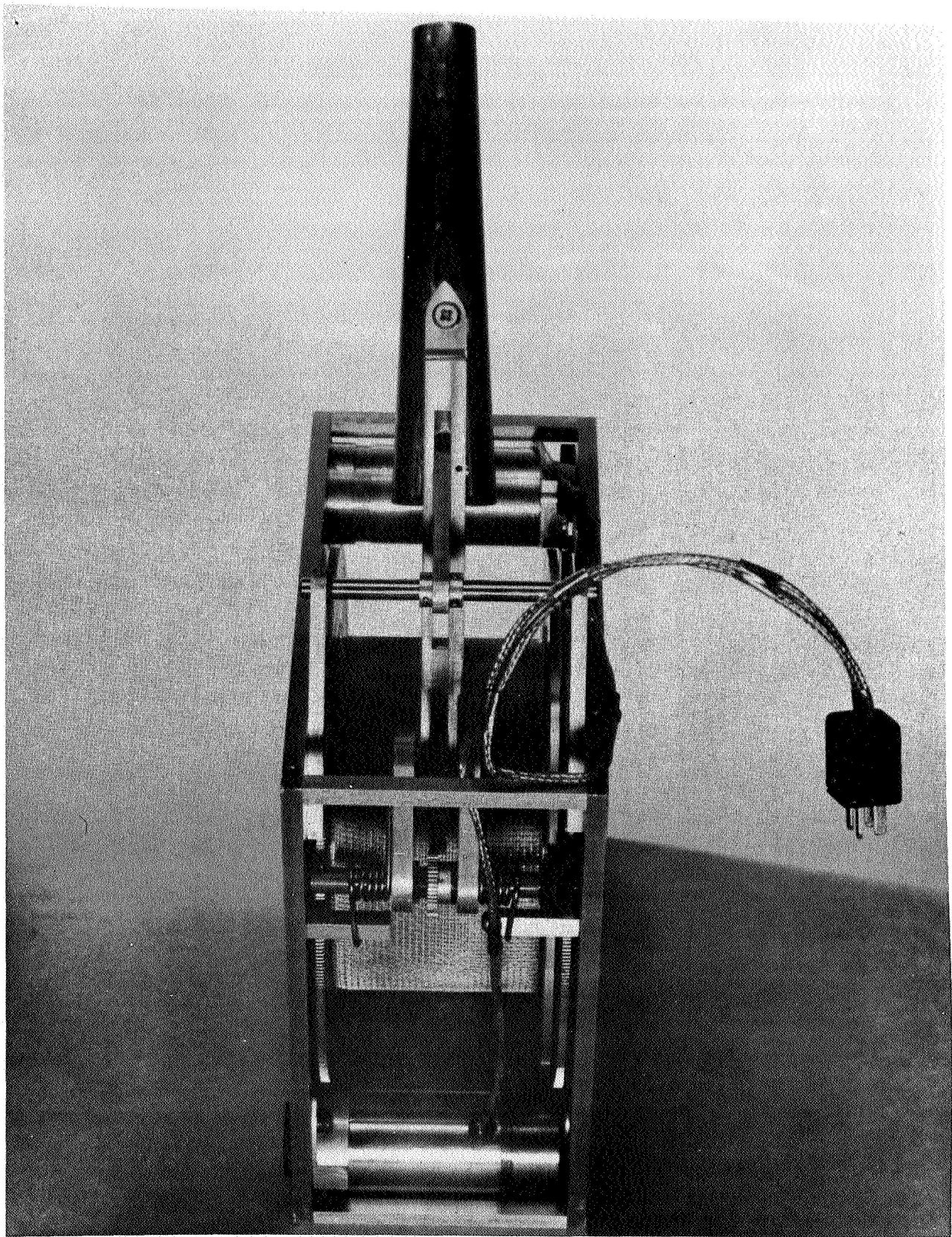


Figure 61. Deployment Mechanism, Bottom View, Showing Powered Roller, Drive, and Guide

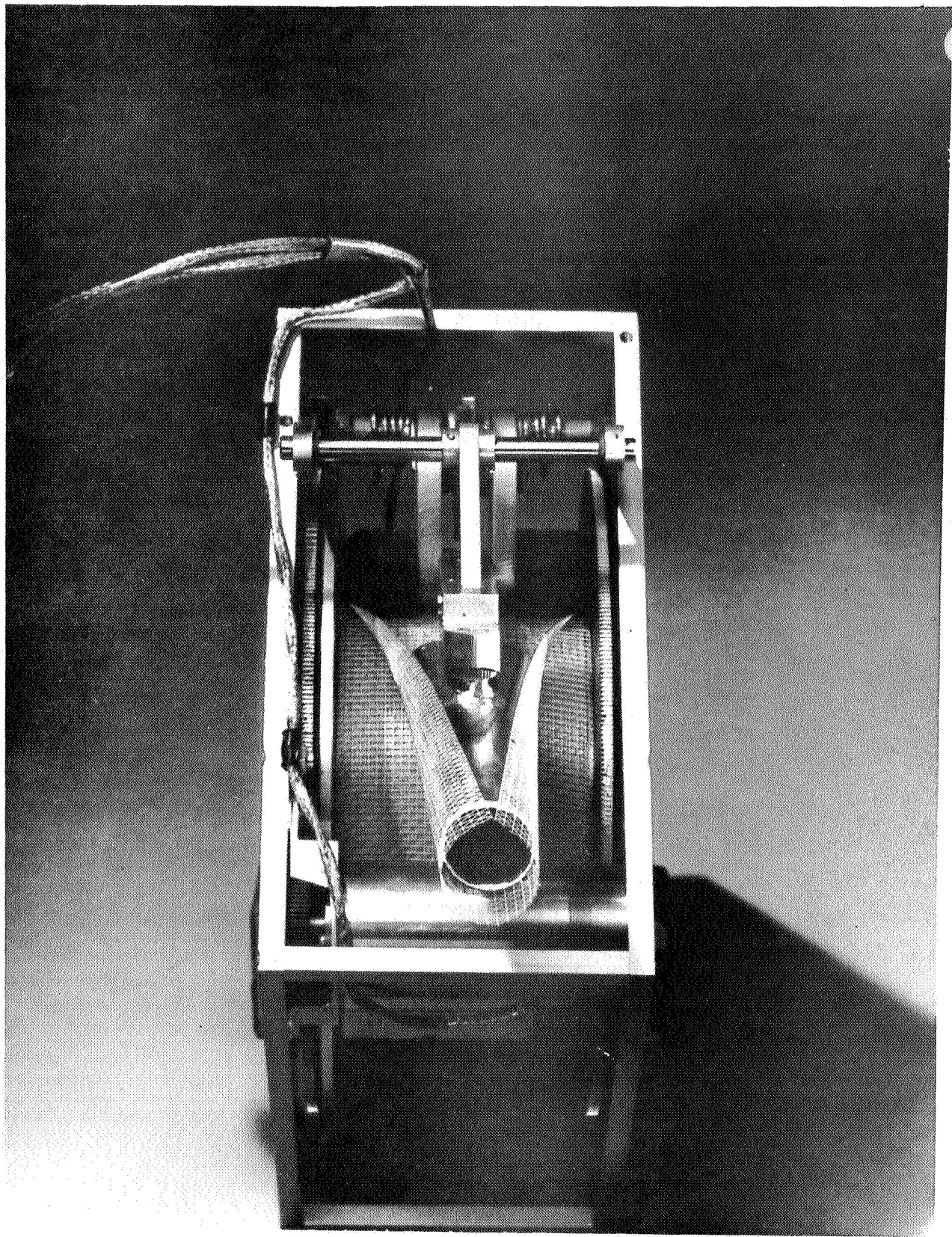


Figure 62. Deployment Mechanism, Boom End View, Showing Typical Screen Boom Ploy and Powered Contour Rollers

The most important feature of a deployer for wire screen booms is the necessity for ensuring that the screen will rewind on the spool tightly. Any inadvertent looseness will, without fail, damage the screen by kinking or yielding of the outermost edge wire. A two-motor system was chosen to provide the necessary assurance of a tight wind. During deployment, the screen boom is pulled from the drum or spool by driving the roller while the drum is restrained, through drag on a slip clutch, to keep the rolled screen under tension. For rewinding, both motors are employed; one drives the drum through the slip clutch and the second powers the rollers. During rewinding, the drum attempts to rewind the wire screen faster than permitted by the rollers. Thus, the screen is properly tensioned on the drum. Different motor speeds are compensated for by the slip clutch.

In Figures 58 and 59, the deployment mechanism is shown attached to a DC power supply (for demonstration purposes). The roller motor is at the upper right of the deployer and the drum motor with the slip clutch (showing), on the lower left. The boom guide is attached to the roller assembly and forms one element of a movable parallelogram. Constant angular deployment is provided by this arrangement.

Construction details of the powered roller and drive assembly are shown in the oblique view of the deployer in Figure 60 and the diagonal view in Figure 61. Power to the roller gear train is transmitted through the large idler gear on the right side of the drum. The typical, uniform ploy of the screen boom is illustrated in Figure 62. The contoured shape of the rollers ensures that the screen will rewind straight and not fold or pinch between roller and drum sidewall.

Other construction features, not entirely evident from the photographs, are:

- a. DC motors with attached spur geartrain are fully enclosed in sealed cans.
- b. All bearings are made of Delrin AF, a sintered Delrin - Teflon combination, providing the low coefficient of friction of Teflon with the stability of Delrin.
- c. An end-of-boom off switch (shown on the side in Figures 58 and 59) is activated by a spring-actuated arm extending through the hub on the last turn of the boom.
- d. Only nonmagnetic materials are used throughout.

Two modifications were made on the deployer just prior to delivery. These were 1) shortening of the boom guide and repositioning it so that it enclosed its support rather than being fastened to the top of it, and 2) housings were added to the spring reaction shaft to reduce friction.

Pertinent deployer characteristics are given in Table 9.

Table 9. Deployment Mechanism Characteristics

Weight (bare)	7.0 pounds
Dimensions (overall)	3.9 by 7.5 by 11.5 inches
Deployment speed	0.91 ft/sec
Rewind speed	1.08 ft/sec
Power at 27 vdc	
Deployment	20 watts
Rewind	17 watts
Screen boom capacity	140 feet

SECTION 3

CONCLUSIONS AND RECOMMENDATIONS

The Gravity Gradient Boom and Antenna Material Study program was successfully accomplished with the delivery of the three required wire screen booms in the three mesh sizes and of one deployment mechanism. The purpose of this section is to discuss the pertinent development areas and attempt an objective analysis of the entire wire screen boom concept.

3.1 WIRE CLOTH BOOM AND PROCESSING

The wire cloth or wire screen boom was developed from concept to practical hardware item during the conduct of the program. Continuous-processing methods were developed to take an unstable, as-woven wire cloth, rigidize it structurally, and form a deployable boom. The cloth was composed of two widely differing materials. Apparent noncompatibility in heat treatment was bypassed through processing techniques and a single, homogeneous composite material was developed.

One of the major problem areas that developed was the actual weaving of the cloth. Little, if any, wire screen has been woven of two dissimilar materials since biaxial properties are either desired in screen or the material is a secondary consideration. However, for the purpose of this program, the use of Elgiloy for low thermal expansion and Beraloy A for thermal conductivity was required. Weaving-technique development and wire problems imposed severe schedule problems, both for the vendor and the overall program. Weaving problems became minor with secondary choice of wire condition, i.e., the two-metal combination is highly weavable with both materials in an annealed condition.

Delivery of wire screen having Elgiloy in an annealed condition forced an unexpected development phase into the program. The problem of imparting cold work into the Elgiloy so that it would respond to heat treatment was resolved but with an approximate doubling of the total process requirements. Physical stretching of the rigidized wire screen was successful in imparting the required cold work necessary for attaining end properties, but it also changed the wire diameters, mesh sizes, and percent-open-areas. These effects are discussed below. Although the reasons for delivery of raw screen from the weaver with Elgiloy in the annealed condition were internal with the weaver, the problems of eventually weaving all-annealed material make it problematic that the Elgiloy could ever have been woven into useful screen with the desired 20 percent cold work prior to weaving.

The requirements for three widely differing mesh sizes for three different percent-open-area booms had a considerable impact on the overall program. The continuous brazing process that was developed required optimization for each mesh size and the

effect of screen stretching effectively doubled this requirement. The highest percent-open-area screen (82 percent from $12 \times 11.5 \times 0.0082 \times 0.0080$ mesh) is close to the upper limit of screen that could be processed by this particular process without a major change. There is no lower limit in open area with respect to rigidizing.

Mixing additives with the brazing flux to make a slurry was found to decrease the usable shelf life of the flux. Complete reprocessing of deliverable screen in the final configuration was required when contractual delays forced screen processing after usable shelf life of the flux had been greatly exceeded. The reprocessing, using fully active flux, increased the yield of the braze alloy in the slurry, and all deliverable screen was brazed with an excess of alloy. The excessive alloy overlay on the wires was removed with a chemical stripping operation.

Problems associated with the three screen meshes were most strongly felt in the boom forming operations. This was evident in the attainment of a uniform size for all three percent-open-area screens. A single procedure was finally used for all screens and a variable size accepted. The problem of sizing was accentuated by use of the 0.0080-inch-diameter wire size in the circumferential direction. Selection of this size was a compromise between thermal and strength requirements. On a 1-inch diameter boom, this wire would not yield on flattening of the boom. At the desired $3/4$ -inch boom diameter, however, some yielding occurred and sizing was accomplished by a combination of furnace mandrel parameters to overform, followed by allowing the circumferential wire to yield upon flattening, and then reform to the larger diameter. The first model of the boom forming equipment formed the boom undersize in a straight length. Screen boom handling characteristics, as they are, precluded anything but fully automated flattening and rewind. Subsequently, the Model II boom former was constructed with full provisions for rewind.

The entire wire cloth rigidizing process and boom forming procedure was successfully developed. The process of rigidizing was not a truly continuous process but was developed so that it could handle screen lengths limited only by the length of the woven material or by the physical size of the roll. The many variables which require control during the full process discourage continuous, end-to-end processing of raw screen to rigidized mesh. The boom forming equipment developed under the program, however, is truly continuous. Single lengths of flattened boom, rolled on a single roll, are limited only by the length of the screen material.

The further development of screen boom processing would normally be concerned with the equipment and control modifications required to increase the end-to-end uniformity of the processed material. The only major process modifications required are strand cleaning of the wire cloth prior to plating and continuous roll-to-roll stretching of the Elgiloy warp.

3.2 TESTING AND EVALUATION

Testing and evaluation was not considered a major portion of this study program and was conducted on a limited basis consistent with requirements. The bending moment tests were considered a primary requirement to all phases of the program since they constituted a design area upon which the screen parameters were based.

The testing and evaluation phase showed that the optimum boom configuration did not meet the specified bending moment requirement of 1.0 ft-lb. The primary reason was the change in wire diameter and mesh size as a result of imparting cold work into the Elgiloy by stretching. Change in mesh size from $12 \times 20 \times 0.009 \times 0.0080$ to $12 \times 16 \times 0.0082 \times 0.0080$ not only increased the circumferential wire mesh spacing by 20 percent but also decreased the longitudinal wire cross-sectional area by 20 percent. Consideration of biaxial copper beryllium boom strengths of the original $12 \times 20 \times 0.009 \times 0.008$ configuration with comparative strength (but higher modulus) Elgiloy, leaves no doubt that the originally conceived Elgiloy - Beraloy A boom would have met and probably exceeded the 1.0 ft-lb strength in the weakest direction.

The stretching operation was likewise instrumental in changing the percent-open-area requirements from 67.0 percent to 71.0 percent in the less than 67.5 percent range, from 74 percent to 77.5 percent in the 67.5 - 75 percent range, and from 78 percent to 81.5 percent in the above 75 percent open area range.

Straightness testing pointed out the marginal wire mesh design or screen parameters that evolved as a result of the stretching requirement. Straightness test comparison between equivalent biaxial copper beryllium booms and Elgiloy - Beraloy A booms shows definite yielding of the two Elgiloy edge wires during flattening operations; whereas this did not occur with the all-Beraloy A booms. The process, itself, is inherently one that will produce a straight boom, since all heat treatment in boom forming is performed under tension.

Storage and flexure testing was not conducted on the final boom configurations because of nonavailability of the configurations until program end. It has been pointed out that meaningful testing also required much more sophisticated screen handling equipment and could not be conducted by manual means. A modified deployment mechanism having interchangeable spools is the minimum acceptable equipment required for this type of test to obtain repeatable results.

Thermal deflection testing was entirely conducted on booms fabricated in batch-type operations prior to continuous processing equipment development. As indicated, the thermocouple instrumentation presented a major problem on the fine wire mesh. The tests, however, validated the very capable thermal analysis based on the mathematical model and digital computer program. A general conclusion drawn from the thermal deflection testing is that the absorptivity of the wire screen configuration is exceedingly high.

3.3 DEPLOYMENT MECHANISM

The engineering prototype model deployment mechanism for the wire cloth boom was considered to be an unqualified successful device. The design was conceived as a versatile deployer capable of handling a difficult material. The mechanism deployed and rewound screen booms in a tight roll mode at a uniform rate and at a constant deployment angle or direction.

The mechanism, in general, was designed for space application. Use of space-rated materials and mechanism design were used for the most part. Minor exceptions were Neoprene for the roller material and use of high-permeability fasteners in four places. Growth versions of this deployer would be modified to:

- a. Reduce weight 35 percent for the same capacity boom.
- b. Strengthen end support members.
- c. Ruggedize and shorten boom guide.
- d. Reduce oversize and eliminate superfluous parts.
- e. Eliminate fasteners where possible through use of aluminum dip brazing techniques.
- f. Provide interchangeable and replaceable reels or drums.

3.4 RECOMMENDATIONS FOR FUTURE WORK

The following recommendations are made for future studies and tests of the boom material and the deployer.

- a. Change wire mesh configuration to provide additional strength in the longitudinal wires to increase bending strength and eliminate outer wire yielding during processing.
- b. Investigate the absorptivity of the wire mesh configuration and methods of lowering the effective value.
- c. Investigate joining or repair techniques for wire cloth booms.
- d. Evaluate wire cloth boom and test deployer under space conditions.

SECTION 4

NEW TECHNOLOGY

The wire screen booms delivered were the direct result of two distinct developments. The first was the improvement of deployable booms by use of woven wire cloth rather than a solid strip of beryllium copper or steel tape, and the second was the development of a boom-forming process.

4.1 IMPROVED DEPLOYABLE BOOM

The use of woven wire cloth for a deployable boom was conceived on November 17, 1964 and disclosed on the following day. Following are the title, purpose, and description of the invention.

- a. Title of Invention. Improved Deployable Boom.
- b. Purpose of Invention. To reduce thermal distortion of deployable booms in the presence of solar heating in space.
- c. Concise But Complete Description of Structure and Operation. Currently available deployable booms consist of a strip of beryllium copper or steel which is pre-formed into a tube of circular cross-section with the tape edges overlapped to form a seam. For storage, the tube is opened along the seam and the strip flattened and coiled onto a spool (Reference: De Havilland Aircraft of Canada, "Stem" devices). The principal limitation of current tubes is produced by thermal bending when the tube is exposed to solar heating in space. The amount of bending is a function of the coefficient of thermal expansion of the material and the temperature difference between the sunlit and shaded sides of the tube. An ideal material would have a large thermal conduction coefficient (to minimize temperature differences) and a small coefficient of thermal expansion (to reduce bending at a given temperature difference). With ordinary materials having suitable spring characteristics, those that have small expansion have poor conduction and vice versa.

The subject invention consists of forming the tube material from a tape of woven wire cloth or screen in which the strands running lengthwise of the tape are drawn from a material having a low coefficient of expansion, such as invar, while the strands running across the tape (i.e., circumferentially when in the tubular condition) are drawn from a material having good thermal conductivity, for example, beryllium copper.

4.2 FORMING OF WIRE CLOTH BOOMS

The process for forming woven wire cloth into deployable booms was reported earlier in a New Technology Report, a copy of which is reprinted here.

GENERAL DYNAMICS

Convair Division

CONTRACT NAS 5-9597

NEW TECHNOLOGY REPORT

"Fabrication of Screen Tubing for Gravity Gradient Booms and Antennas"

A means of fabricating screen tubing utilizing Elgiloy in the longitudinal direction and Beryllium Copper Alloy 25 in the circumferential direction was required. Elgiloy was selected because of its expansivity and high strength, BECU₂₅ was chosen for its high thermal conductivity and strength. The screen fabricated by the process discussed in the following paragraphs is composed of the 0.008 diameter wire and is made into a 3/4 inch diameter tube. However, within reasonable limits, wire diameter, mesh size and tube diameter may be readily changed without affecting the fabrication process.

Because of the diverse nature of the metals employed, silver brazing was chosen as the best method of joining screen nodal points and effecting the rigidization required to handle shear loading. The fabrication process described below commences with four-inch wide flat screen woven of metal in the fully annealed state. This flat screen strip is maintained on storage reels.

Prior to the brazing procedure the strip of screen is calendered to obtain uniform screen thickness and maximum wire crossover contact area. Then in a continuous process, accomplished in a machine devised for the purpose, the strip of screen is:

Coated by a flash silver electroplate.

Washed and dried.

Dipped in a flux/braze slurry which applies a uniform overall coating.

Passed through a brazing oven at 1250° F.

After brazing and because Elgiloy does not respond to heat treatment unless it has been cold worked, the screen is stretched longitudinally to impart 18 to 20% cold work into each wire. It is then calendered again and returned to the machine where it is dipped into the flux/braze slurry and run through the 1250° F brazing oven. The screen, brazed at all crossover points, rigidized, and with the desired qualities imparted to the Elgiloy, is now ready to be trimmed and formed into tubing.

The screen width is trimmed from 4 inches to 2 1/2 inches and then in a continuous automated process, controlled by a specifically designed machine the screen is formed into tubular shape and precision heat treated at 650° F over interior and exterior mandrels. After the heat treatment the same machine flattens the screen and rolls it on storage reels.

Screen tubing up to 70 feet in length has been fabricated by the above process.

APPENDIX I

CONTRACT NAS5-9597 — WORK STATEMENT

SCHEDULEARTICLE I - STATEMENT OF WORK

The Contractor will conduct a 12 month extendable boom development program for Goddard Space Flight Center, National Aeronautics and Space Agency. The objective of the program is the production of rigidized, woven screen material having sufficient spring action to immediately and repeatedly form a tubular shape when freed of all restraint.

The program will consist of the following three phases:

1. The development of procedures for brazing or welding the nodes of woven screen material.
2. The generation and verification of a mathematical model to predict thermal deflection of uncoated screen materials.
3. A limited testing and evaluation program to verify the mechanical properties of the particular rigidized screens selected for delivery.

I. MATERIAL

- A. Concept - The woven mesh or screen will be composed of two dissimilar metallic wires or strips; the circumferential part of the screen being a copper-beryllium alloy similar to alloy 125 and with the longitudinal strand of the screen having a lower thermal expansion coefficient. Materials utilized will be compatible with their intended use in space and will be commercially available and presently in use. Chemical analyses from the manufacturer of each lot of wire will be supplied with each shipment of material.
- B. Mesh - A set of screens representing different mesh sizes and hole areas will be prepared for testing. One screen from each of the following three ranges will be selected:
 - 1) 40-60% open area
 - 2) 61-75% open area, and
 - 3) over 75% open area.
- C. Length - Specimen lengths of three, ten and forty-five feet will be delivered to GSFC as follows:

SCHEDULE

- 1) Two specimens of each of the above lengths in a mesh size determined to be the optimum configuration from analytical studies within nine months after initiation of the contract.
 - 2) Two specimens of each of the above lengths, in each of the other two mesh sizes, within eleven months after initiation of the contract.
- D. Configuration - The wire screen will receive heat treatments or forming operations such that the screen forms a tubular shape when released or deployed. The diameter of the tube will be less than two inches. A specific diameter based on strength and stiffness considerations shall be selected. A fabrication objective must be to maintain this diameter within a tolerance of $\pm 2\%$ over the total length; however, the maximum acceptable variation will be $\pm 4\%$.
- E. Wire Joining - Bonding of the wire contact points of the screen will be accomplished by brazing or welding. Joint integrity will be demonstrated by metallurgical and mechanical testing.
- F. Coatings - The wire screen will be clean and free of deleterious oxides and non-uniform discolorations. No platings or coatings will be applied to the screen.

II. TESTING

A limited amount of testing will be performed in order to determine certain boom properties. Delivered screen will meet the following specifications:

- A. Boom straightness for booms up to 45 feet length -
- 1) In a "zero-gravity" field with no sun, the best straight line drawn through the boom will not deviate from the required deployment direction by no more than 0.5 degrees.
 - 2) In a "zero-gravity" field with no sun, the actual boom center line will not deviate from the best straight line by more than 2 inches plus 0.1% of the length.
- B. Boom Stiffness - The boom material will not buckle or collapse upon the application of a one (1) ft-lb. bending moment during the simultaneous application of a torsional moment of not less than 0.005 ft-lb.

SCHEDULE

- C. Storage Volume - The undeployed boom and its deployment mechanism will be capable of being stored in a volume of 0.5 cu. ft. plus 0.002 cu. ft. per ft. of length. Configuration of the storage volume will be that of a rectangular parallelepiped or of a right circular cylinder of similar suitable volume having a maximum dimension of five (5) feet.
- D. Thermal deflection tests of 36-inch long specimens will be conducted only to provide data for use in verifying the mathematical model. Measure the deflection at a point 30 inches from the holding device.
- E. Storage and Flexure Testing - The integrity of the wire joints and the effect of storage will be determined by preliminary testing. A finished screen of more than three feet in length will be rolled, restrained and stored on a suitable drum for one week in a laboratory atmosphere; it will be released and re-rolled at least five times and then stored for an additional week. This weekly testing and storage will be conducted for a period of one month or more. Examination of the wire joints and determination of straightness of the tube will be carried out each week.
- F. Thermal Cycling - Specimens longer than 10 inches representing the finished wire mesh will be cycled at least six times between +300° F and -300° F at a heating rate or cooling rate of at least 10° F per minute while undergoing repeated flattening once per minute. The specimen will be examined for joint integrity and subsequently will be tested in tension to fracture at room temperature. Such tests will be applied to three specimens from each of the three selected mesh sizes.

III. DEPLOYMENT

One finished device capable of deploying a wire screen boom will be delivered to GSFC by the end of the contract period. The device will be manufactured from materials suitable for operation in a space environment and will be compatible with the electrical, magnetic, and mechanical requirements of a satellite system. The deployment rate of the boom will be $2 \pm 1/2$ feet per second. The device supplied will be capable of deploying the boom, such that when deployed in the vertical direction, the boom tip at 30 feet will not deviate by $\pm 1/2$ inch from the vertical. The mass of the device will not exceed 0.2 slug. The deployment device will have a low residual external dipole moment and will be capable of operating in a space environment without deteriorating and without contaminating the satellite.

APPENDIX II
WIRE SCREEN RIGIDIZING PROCESS
AND
CONTINUOUS BOOM FORMING

APPENDIX II

WIRE MESH SCREEN RIGIDIZING PROCESS AND CONTINUOUS BOOM FORMING

Wire screen rigidizing and subsequent tube forming was performed on the three basic mesh sizes (12 by 14, 12 by 20, and 12 by 30) in similar manner. The fundamental process for all mesh sizes was identical but the detail changes were sometimes extreme. A flow chart for the entire processing schedule is given in Figure II-1.

II.1 WIRE SCREEN PROCUREMENT

Wire screen was procured to Convair requirements. A single Elgiloy warp of 12 wires per inch was used for all mesh sizes. Beryllium-Copper Alloy 25 as the fill or shute was woven at 14, 20, and 30 wires per inch to furnish the specified basic mesh sizes. Ideally, wire mesh is woven with the wire in an annealed condition to obtain as great ductility as possible. The large difference between properties of the warp and shute wires required that the vendor extend his weaving technology to an extreme. The initial weaving attempts were made with two numbers hard (i.e., 1/2 hard) Alloy 25 in an effort to match the high tensile and yield values of the Elgiloy. A much increased ductility of Alloy 25 was found to be required, and subsequent efforts used fully annealed wire. The delivered screen was supplied in 120-foot rolls, 4 inches wide. These rolls were slit from a 48-inch wide woven roll. The crimp ratio of the mesh varied somewhat from mesh size to mesh size but in general averaged at 4 to 6 or 5 to 6. Occasional broken shute wires were observed but no broken warp wires were ever found. The screen, as delivered, was exceptionally clean and free of any oil, grease, or other contaminants normally observed in and on wire mesh. No cleaning operation was used prior to the next processing step.

II.2 WIRE SCREEN CALENDERING

As-received screen was respooled from the cardboard tube to an aluminum reel. Initial screen inspection occurred at this time. Calendering was performed on a 6-inch, two-high Fenn rolling mill. The screen was rolled to a total thickness of 13.5 to 14 mils from the original thickness of 21 mils. Approximately 90 percent of the reduction was taken in the soft BeCu 25 wire and the rest in the Elgiloy. The total reduction was taken in a single pass. Special techniques had to be developed for this calendering operation. These included precision shimming of the roll bearing-blocks to obtain a specified roll separation that was completely true from side to side on the roll. Very heavy, screw-down pressures were utilized to maintain the required separation and parallelism.

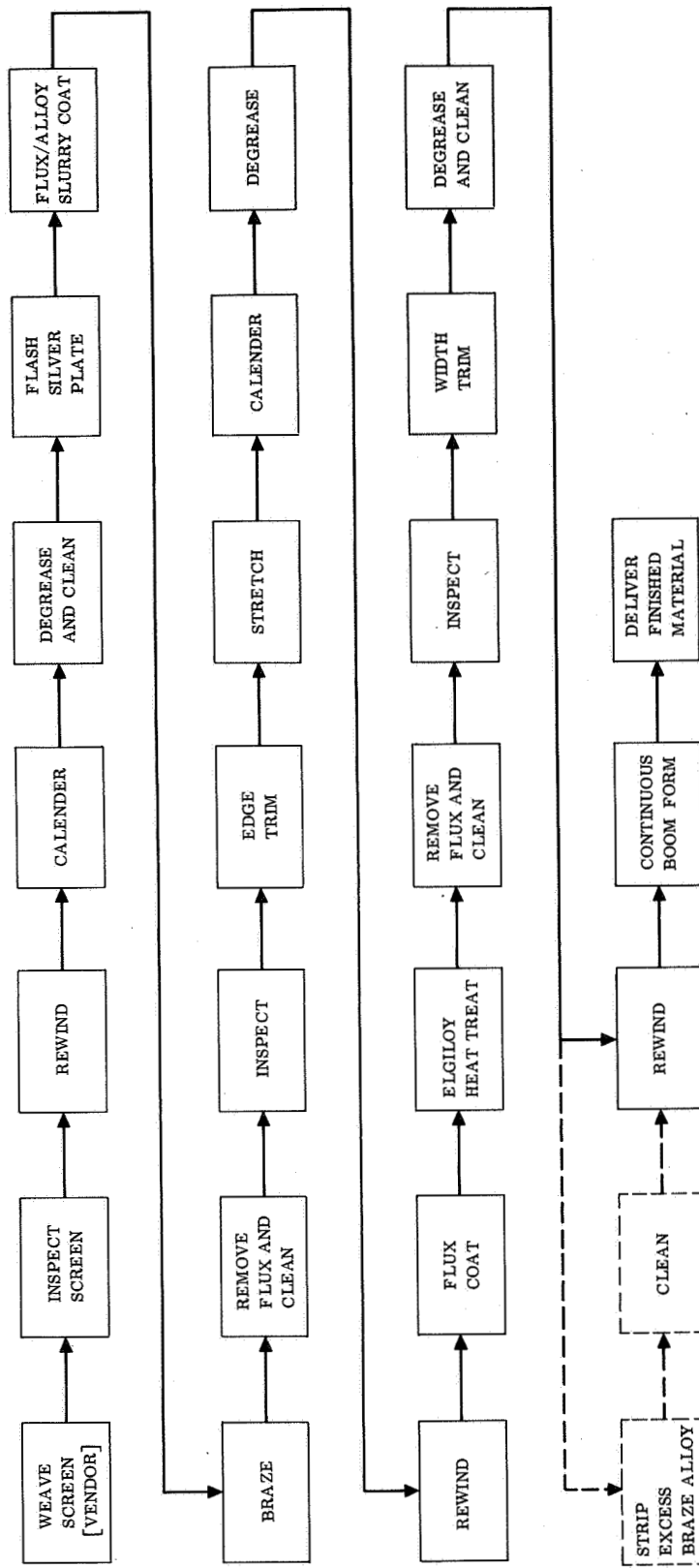


Figure II-1. Process Flow Chart, Wire Mesh Screen Boom

II.3 CLEANING

The wire screen, along with the required leaders, was rewound onto a special reel having multitudes of large perforations. The screen was initially degreased by immersion in a solvent, usually Freon TF. It was then given a 10-minute cleaning in Oakite 165 at 180° F. Solution concentration was 6 to 8 oz/gal. Thorough and repeated immersion rinsing in 140° F water completed the cycle.

II.4 SILVER PLATING

The undried screen was immediately loaded into a silver-plating line where it was plated, washed, tower-oven dried, and rewound on a continuous basis. Bath composition was:

Silver Cyanide	4.0 avdp oz/gal.
Potassium Cyanide	7.5 avdp oz/gal.
Potassium Carbonate	6.0 avdp oz/gal.

The bath was operated with a nominal 3.0 Troy oz/gal. metallic silver and 5.0 avdp oz/gal. free cyanide. An area of 56 inch² of screen (14-inch length, 4-inch width) was continuously in the bath, traveling at a speed of 36 inches per minute. Plating was conducted at 18 to 20 amp/ft² of actual wire surface area, at a bath temperature of 74° F. Plating voltage varied from 2 to 2.5 volts depending upon the screen mesh and the actual plating current.

II.5 FLUX-ALLOY SLURRY COATING

A uniform and complete coating of a modified flux and brazing alloy slurry was applied to the screen by continuous dipping at 2.25 ft/min. Tower-oven drying of the wet flux at progressively increasing temperature to 400° F allowed respooling to await subsequent operations. The slurry composition was:

Handy & Harman B-1 Flux	100 lb
Sodium Fluoride	15 lb
BAG-1a Braze Alloy, -400 mesh	2.78 lb avdp
Water	as required

II.6 BRAZING

The brazing cycle was nominally conducted at a continuous running speed of 2.4 ft/min. The vertical, slot-type furnace was operated at a wall temperature of 1630° F, thereby raising the coated screen temperature to a peak value of 1280° F.

II.7 POST-BRAZE CLEANING OPERATION

Postbrazing cleaning consisted of complete flux removal by bulk roll immersion in 140° F water. Thorough and complete immersion and spray rinses with 140° F water completed the cleaning. Roll drying was done in bulk in a forced-convection oven operated at 175° F.

II.8 EDGE TRIMMING

All screen was trimmed 1/6 inch on each side prior to stretching or cold working. This was two warp wires. Trimming was accomplished using consumer-type electric scissors.

II.9 ELGILOY STRETCHING OR COLD-WORK

Induction of cold work into the Elgiloy was accomplished by gross stretching of the screen in a longitudinal direction. A 22 percent stretch was imparted using a pneumatic powered chain hoist as a winch. Stretching was done at a rate of 1.5 percent per minute. A 2 percent stretch was required to remove normal warp wire crimp and the remaining 20 percent were effectively used to impart cold work into the Elgiloy.

II.10 CALENDERING SUBSEQUENT TO STRETCHING

Calendering, identical to the initial processing step was repeated to redistribute the crimp between the shute and warp wires. The final thickness was 13.5 to 14.0 mils.

II.11 CLEANING

An ultrasonic cleaning operation in Turco Caviclean No. 2 was performed on the calendered screen while in a bulk roll. Thorough immersion rinsing in hot water followed by flow-through rinsing and forced-convection drying completed the cleaning cycle. The screen was then respoled with the required leaders for the flux coating operation.

II.12 FLUX COATING

A second flux application, similar to the initial one, was given for protection during the succeeding step. No brazing alloy was used in the modified flux during this application.

II.13 SECOND BRAZE CYCLE

The screen was given a second complete braze cycle identical to the initial rigidizing cycle. Some additional joints are brazed during this thermal treatment, but the prime purpose is the development of desired properties in the Elgiloy.

II.14 POST BRAZE CLEANING OPERATION

Flux was removed as previously described.

II.15 INSPECTION

The screen was inspected and it was noted that it was covered with excessive brazing alloy.

II.16 EXCESS BRAZING ALLOY STRIPPING

Excess brazing alloy was stripped from the beryllium copper - Elgiloy screen by controlled immersion in a bath consisting of

Sulfuric acid, concentrated - 19 parts

Nitric acid, concentrated - 1 part

The time of immersion is dependent upon the quantity of alloy required to be stripped. A 40 to 50-second immersion at room temperature was found to be adequate. The stripping procedure is followed by a thorough cold-water rinse, ultrasonic cleaning to remove smut, and forced-air dry.

II.17 INSPECTION

The wire mesh screen is completely rigidized by brazing and the Elgiloy properties have been developed in the Elgiloy longitudinal wire at this point in the processing. Full evaluation of the screen is done visually to ascertain the overall condition, location of marginal braze areas, distorted mesh, and required trim-out areas.

II.18 TRIMMING

The screen was trimmed from approximately 3.65-inch width to the required width for tube forming. Both sides of the screen were trimmed with the previous inspection determining whether to trim equally or to favor one side or the other.

II.19 SPOOLING AND CLEANING

The trimmed screen was spooled on special narrow-width spools, ultrasonically cleaned in Turco Caviclean No. 2, washed, and dried as previously described.

II.20 BOOM FORMING

Boom forming was performed continuously on the automatic equipment developed and built for this purpose. Boom heat treatment for the Beryllium Copper Alloy 25 was 30 minutes at 650° F. This corresponded to a travel rate through the furnace of

66 inches per hour. Argon protective atmosphere was used throughout the cycle. Both 12×14 and 12×20 mesh screens were formed, flattened, and rewound in the required lengths. The 12×30 mesh screen was formed only. No post-heat-treatment cleaning was necessary.

APPENDIX III

**MATHEMATICAL MODEL AND DIGITAL COMPUTER PROGRAM FOR
SOLUTION OF TEMPERATURE DISTRIBUTION AROUND SCREEN
TYPE TUBULAR GRAVITY GRADIENT ELEMENTS**



TABLE OF CONTENTS

	Page
LIST OF ILLUSTRATIONS	ii
NOMENCLATURE	iv
SUMMARY	vii
INTRODUCTION	viii
1.0 MATHEMATICAL MODEL	1
1.1 GENERAL	1
1.2 HEAT BALANCE FOR A SEAMLESS TUBE	2
1.3 HEAT BALANCE WITH NO HEAT TRANSFER ACROSS THE SEAM	5
2.0 COMPUTER PROGRAM	8
2.1 GENERAL	8
2.2 DESCRIPTION OF INPUT	8
2.3 DESCRIPTION OF OUTPUT	11
3.0 RESULTS	13
3.1 GENERAL	13
3.2 PARAMETRIC RESULTS	13
3.3 ADDITIONAL RESULTS	16
3.3.1. SOLAR FLUX INCIDENT ANGLE	16
3.3.2 SEAM EFFECTS	18
3.3.3 BOOM DEFLECTION	19
4.0 CONCLUSIONS AND RECOMMENDATIONS	20
APPENDIX A. EQUATIONS	38
APPENDIX B. COMPUTER PROGRAM LISTING	52
REFERENCES	57 76

ILLUSTRATIONS

	Page
1. Temperature Distribution as a Function of Tube Diameter, K = 44 BTU/HR-FT-°R	21
2. Temperature Distribution as a Function of Absorptivity, K = 44 BTU/HR-FT-°R	22
3. Temperature Distribution as a Function of Conductivity	23
4. Temperature Distribution as a Function of Tube Diameter, K = 8 BTU/HR-FT-°R	24
5. Temperature Distribution as a Function of Absorptivity, K = 8 BTU/HR-FT-°R	25
6. Temperature Difference Vs. Circumferential Wire Mesh Size and Diameter for 0.5 Inch Tube Diameter	26
7. Temperature Difference Vs. Circumferential Wire Mesh Size and Diameter for 0.75 Inch Tube Diameter	27
8. Temperature Difference Vs. Circumferential Wire Mesh Size and Diameter for 1.0 Inch Tube Diameter	28
9. Temperature Difference Vs. Circumferential Wire Mesh Size and Longitudinal Wire Diameter for 0.75 Inch Tube Diameter	29
10. Temperature Difference Vs. Circumferential Wire Mesh Size and Longitudinal Wire Mesh Size for 0.75 Inch Tube Diameter	30
11. Temperature Distribution as a Function of Solar Flux Incident Angle	31



	Page
12. Temperature Difference Vs. Solar Flux Incident Angle	32
13. Temperature Vs. Solar Flux Incident Angle	33
14. Temperature Distribution for Tubes With No Heat Transfer Across the Seam	34
15. Temperature Distribution for Tubes With No Heat Transfer Across The Seam	35
16. Temperature Drop Across the Seam Vs. Seam Location	36
17. Comparison of Screen Tube and Thin Wall Tube Deflection	37

NOMENCLATURE

Apc	projected area of the circumferential wires of a node to solar flux	in^2
Apl	projected area of the longitudinal wires of a node to solar flux	in^2
At	approximate total wire surface area per unit length of tube	in^2
D	tube diameter	in
Dc	circumferential wire diameter	in
Dl	longitudinal wire diameter	in
e	coefficient of thermal expansion	$^{\circ}\text{R}^{-1}$
EA	effective radiation coefficient per unit length of tube to deep space	in^2
E _{eff}	effective emissivity based on the radiation coefficient EA and the approximate total wire surface area At	
l	element length	in
K	thermal conductivity of the circumferential wires	$\frac{\text{BTU}}{\text{HR-FT-}^{\circ}\text{R}}$
Mc	circumferential wire mesh size	$\frac{\text{wires}}{\text{in}}$
Ml	longitudinal wire mesh size	$\frac{\text{wires}}{\text{in}}$
N1, N2, N3 ...	total number of nodes assigned to sectors 1, 2, 3 ...	
Q	solar flux incident on nodal projected area	$\frac{\text{BTU}}{\text{HR-FT}^2}$
Q _s	solar constant	$\frac{\text{BTU}}{\text{HR-FT}^2}$

T	temperature	$^{\circ}\text{R}$
ΔT	temperature difference	$^{\circ}\text{R}$
Wt	approximate tube weight per foot of tube length	lbs
Y	tip deflection	in
α	absorptance	
σ	Stefan-Boltzman constant - $.1713 \times 10^{-8}$	$\frac{\text{BTU}}{\text{HR-FT}^2\text{-}^{\circ}\text{R}^4}$

ANGLES

γ angle between the plane which is tangent to the tube at a node and the plane defined by the tangent to a circumferential wire and the solar flux vector

$$0^{\circ} \leq \gamma \leq 90^{\circ}$$

$$\gamma = \sin^{-1} \left(\frac{\sin \Omega}{\sin \psi} \right) = \sin^{-1} \left(\frac{\sin \phi \cos \theta}{\sin (\cos^{-1} (\sin \phi \sin \theta))} \right)$$

θ angle measured around the periphery of the tube from the point on the tube which is closest to the sun

ϕ angle between the solar flux vector and the longitudinal axis of the tube

$$0^{\circ} < \phi \leq 90^{\circ}$$

ψ angle between the solar flux vector and the tangent to the circumferential wires

$$0^{\circ} \leq \psi \leq 90^{\circ}$$

$$\psi = \cos^{-1} (\sin \phi \sin \theta)$$

Ω angle the solar flux vector makes with the plane which is tangent to the tube at a node

$$0^\circ \leq \Omega \leq 90^\circ$$

$$\Omega = \sin^{-1} (\sin \phi \cos \theta)$$

CRITICAL ANGLES

Θ_{cc} minimum angle θ where no solar flux passes between circumferential wires

$$\Theta_{cc} = \cos^{-1} \left[\frac{Mc Dc \sin (\cos^{-1} (\sin \phi \sin \Theta_{cc}))}{\sin \phi} \right]$$

an iterative solution can be used to determine Θ_{cc} for given values of ϕ , Mc and Dc

Θ_{cl} minimum angle θ where no solar flux passes between longitudinal wires

$$\Theta_{cl} = \cos^{-1} \left[\frac{Dl}{D \sin \left(\frac{1}{D Ml} \right)} \right]$$

ϕ_c maximum angle ϕ where no solar flux passes through the illuminated side of the tube

$$\phi_c = \sin^{-1} (Mc Dc)$$

SUBSCRIPTS

eff effective

i ith node

N Nth node

ref reference

s solar

X, X+1 nodes next to tube seam

1, 2, etc. node 1, 2, etc.



SUMMARY

The Convair Division of General Dynamics Corporation has developed a digital computer program utilizing the isothermal node concept approach to the solution of a specific heat transfer problem. The problem is that of determining the temperature distribution around a screen type tubular element exposed to solar radiation in deep space. Once the temperature gradient is obtained, the thermal deflection of the tube can be determined.

The details of the thermal mathematical model are discussed such as the nodal division scheme and the methods used to obtain a solution. Variables include the tube diameter, solar absorptance, conductivity, the circumferential and longitudinal wire diameters, mesh sizes, and the absolute temperature level.

In addition to a description of the input format, parametric results for a number of configurations are presented.

Finally, a detailed listing of equations used and a program listing are presented in Appendices A and B respectively.

This report is published as part of the documentation required under Contract NAS5-9597.

INTRODUCTION

The purpose of this report is to document the mathematical equations and formulas required to calculate the temperature distribution around tubular elements constructed of wire screen material which are subjected to solar heating in space. Because of the complex geometry of the screen tube configuration, certain simplifying assumptions are made. One of these is that it is assumed that there is no radiation heat transfer across the interior of the tube between elements of the tube. The error introduced by this assumption should be negligible since the magnitude of the temperature differences between elements of the tube is small and the percent open area of the woven screen is large.

The method used in obtaining the temperature gradient is the isothermal node concept. Equations are developed which describe the solar heat absorbed, the heat transfer paths, and the heat radiated to deep space for each isothermal node. The steady state temperature gradient around the periphery of the tube is then found for any arbitrary temperature level and screen material properties.

The wire screen used to make the tubes is initially rolled in order to increase the wire contact area at the intersections. The wire intersections are then brazed together in order to improve the mechanical properties of the screen. Brazing the intersections also increases the conductive path between the circumferential and longitudinal wires. The screen is then formed into a circular cross-sectioned tube with little overlap but with some physical contact at the seam. The mathematical model developed can be used to calculate the temperature gradient for a seamless tube, or a tube



which has no heat transfer across the seam. The latter, of course, will be the worst case since even a small amount of physical contact at the seam will tend to decrease the temperature gradient.

1.0/MATHEMATICAL MODEL

1.1 GENERAL

The temperature profile around the periphery of a screen tube configuration can be determined by dividing the tube into a number of assumed isothermal nodes and equating the heat absorbed to the heat rejected for each node.

The temperature gradient along the length of the tube is assumed to be zero, thus all calculations are based on a one inch unit length of tube unless otherwise stated. This assumption is valid as long as the heat source remains constant over long lengths of the tube.

Difficulties arise in defining the division of nodes since the orientation of the tube with respect to the sun determines the illuminated areas of the tube and the shadowing which occurs between wires.

It was found that orientations with respect to the sun could be used to define the following four cases.

Case 1. The incident solar flux is normal to the longitudinal axis of the tube. $\Phi = \frac{\pi}{2}$

Case 2. The solar flux is at an incident angle such that the angle around the periphery of the tube from the sun side to where the longitudinal wires start shadowing each other is less than the angle where the circumferential wires start shadowing each other. $\frac{\pi}{2} > \Phi > \Phi_c$ and $\Theta_{cl} < \Theta_{cc}$

Case 3. The reverse of Case 2. regarding the critical shadowing angles. $\frac{\pi}{2} > \Phi > \Phi_c$ and $\Theta_{cc} < \Theta_{cl}$

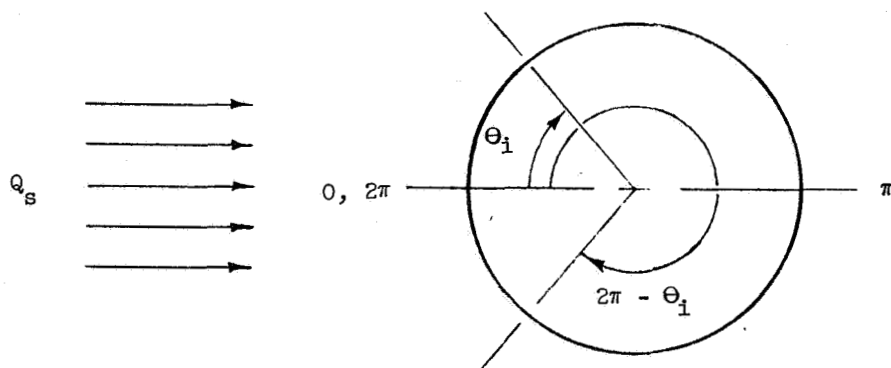
Case 4. The solar flux is at an incident angle such that no solar flux passes through the illuminated side of the tube.

$$0 < \phi < \phi_c$$

The four cases listed above are used in developing the nodal division schemes. The equations used in defining the heat absorbed and the heat transferred via conduction and radiation for each node are presented in Appendix A. These equations are used below in developing the heat balance equations.

1.2 HEAT BALANCE FOR A SEAMLESS TUBE

For a seamless tubular configuration, the temperature distribution will be symmetric with respect to the points on the tube which are closest to and farthest from the sun as indicated in the following figure. At $\Theta = 0$, and $\Theta = \pi$, the temperature gradient will be zero.



$$T_{\Theta_1} = T_{2\pi - \Theta_1}$$

The temperature distribution around the tube can then be found by considering only half the tube.

For N number of nodes between $\Theta = 0$ and $\Theta = \pi$ inclusive, the following set of equations can be used.

$$.5 \frac{Q_1}{144} \alpha_s (Apc+Apl)_1 = .5 \frac{\Delta \Theta_1}{2\pi} EA \frac{\sigma}{144} T_1^4 + \frac{K Dc^2 Mc \pi}{12D (\Delta \Theta_1 + \Delta \Theta_2)} (T_1 - T_2)$$

$$\begin{aligned} \frac{Q_i}{144} \alpha_s (Apc+Apl)_i &= \frac{\Delta \Theta_i}{2\pi} EA \frac{\sigma}{144} T_i^4 + \frac{K Dc^2 Mc \pi}{12D (\Delta \Theta_{i-1} + \Delta \Theta_i)} (T_i - T_{i-1}) \\ &+ \frac{K Dc^2 Mc \pi}{12D (\Delta \Theta_i + \Delta \Theta_{i+1})} (T_i - T_{i+1}) \end{aligned}$$

where i goes from 2 to N-1

$$\begin{aligned} .5 \frac{Q_N}{144} \alpha_s (Apc+Apl)_N &= .5 \frac{\Delta \Theta_N}{2\pi} EA \frac{\sigma}{144} T_N^4 \\ &+ \frac{K Dc^2 Mc \pi}{12D (\Delta \Theta_{N-1} + \Delta \Theta_N)} (T_N - T_{N-1}) \end{aligned} \quad (1)$$

For the above set of N equations, the absorption and radiation terms for node #1 ($\Theta = 0$) and node #N ($\Theta = \pi$) are adjusted by a factor of .5 since only half the tube is used.

In order to find the temperature level as well as the temperature distribution, a detailed knowledge of the overall radiation factor of the

screen tube for deep space is required. It was found in this study that the temperature gradient around the periphery of the tube is not a very strong function of the absolute temperature of the tube for a given solar absorptivity. Thus, the above equations are solved by assuming a reference temperature (T_{ref}) for node N, and proceeding as follows.

First, an initial estimate of EA is determined by assuming that the tube radiates to deep space at an average temperature T_{ref} .

$$EA = \frac{144 \sum Q_{(absorbed)}}{\sigma (T_{ref})^4} \quad (2)$$

$$\begin{aligned} \text{where } \sum Q_{(absorbed)} = & 2 \left(.5 \frac{Q_1}{144} \alpha_s (Apc+Apl)_1 + \sum_{i=2}^{N-1} \frac{Q_i}{144} \alpha_s (Apc+Apl)_i \right. \\ & \left. + .5 \frac{Q_N}{144} \alpha_s (Apc+Apl)_N \right) \end{aligned} \quad (3)$$

Now, starting with the equation for node #N, and setting $T_N = T_{ref}$, the temperature for each node can be obtained. In order to have a correct solution, the following equation must be satisfied.

$$\sum Q_{(absorbed)} = \sum Q_{(radiated)} \quad (4)$$

where $\sum Q_{(absorbed)}$ is defined above, and

$$\begin{aligned} \sum Q_{(radiated)} = & 2 \left(.5 \frac{\Delta \Theta_1}{2\pi} EA \frac{\sigma}{144} T_1^4 + \sum_{i=2}^{N-1} \frac{\Delta \Theta_i}{2\pi} EA \frac{\sigma}{144} T_i^4 \right. \\ & \left. + .5 \frac{\Delta \Theta_N}{2\pi} EA \frac{\sigma}{144} T_N^4 \right) \end{aligned} \quad (5)$$

A rapid convergence method is used to find the value of EA which yields a temperature distribution T_i , where i goes from 1 to N , which satisfies equation (4) above.

The EA term calculated for the case where the solar flux is normal to the longitudinal axis of the tube ($\Phi = \frac{\pi}{2}$) can be used to find the temperature level and the temperature distribution for cases where $\Phi < \frac{\pi}{2}$. Here, T_N is adjusted until the temperature distribution T_i , where i goes from 1 to N , satisfies equation (4) above.

1.3 HEAT BALANCE WITH NO HEAT TRANSFER ACROSS THE SEAM

The temperature distribution around the periphery of a tubular screen type configuration involving a seam is dependent on the heat transfer paths across the seam. The heat transferred at the seam depends upon the physical contact between wires at the seam, and the radiation interchange between wires at the seam. These heat transfer paths are difficult if not impossible to define analytically. The best case would be where there is enough physical contact such that there is no change in the temperature distribution compared to the seamless case. The worst possible case would be where there is no heat transfer across the seam. Although this case is not realistic, it defines the limit or the worst temperature distribution imaginable.

For the seamless tube case it was found (see Figures 1, 2, and 3) that the temperature distributions showed zero temperature gradients at $\Theta = 0^\circ$, $\Theta \cong 115^\circ$, $\Theta = 180^\circ$, and $\cong 245^\circ$. Since a zero temperature gradient means no heat transfer, if the seam is located at these positions, the temperature distribution will be identical to the no seam case. For other seam locations,

the temperature distribution will not be symmetrical, and the following equations are used. The total number of nodes around the periphery of the tube is set equal to $2N-2$ for convenience.

$$\frac{Q_1}{144} \alpha_s (A_{pc} + A_{pl})_1 = \frac{\Delta \Theta_1}{2\pi} EA \frac{\sigma}{144} T_1^4 + \frac{K Dc^2 Mc \pi}{12D (\Delta \Theta_1 + \Delta \Theta_2)} (T_1 - T_2) \\ + \frac{K Dc^2 Mc \pi}{12D (\Delta \Theta_1 + \Delta \Theta_{2N-2})} (T_1 - T_{2N-2})$$

$$\frac{Q_i}{144} \alpha_s (A_{pc} + A_{pl})_i = \frac{\Delta \Theta_i}{2\pi} EA \frac{\sigma}{144} T_i^4 + \frac{K Dc^2 Mc \pi}{12D (\Delta \Theta_i + \Delta \Theta_{i+1})} (T_i - T_{i+1}) \\ + \frac{K Dc^2 Mc \pi}{12D (\Delta \Theta_i + \Delta \Theta_{i-1})} (T_i - T_{i-1})$$

where i goes from 2 to $2N-3$

$$\frac{Q_{2N-2}}{144} \alpha_s (A_{pc} + A_{pl})_{2N-2} = \frac{\Delta \Theta_{2N-2}}{2\pi} EA \frac{\sigma}{144} T_{2N-2}^4 \\ + \frac{K Dc^2 Mc \pi}{12D (\Delta \Theta_{2N-2} + \Delta \Theta_1)} (T_{2N-2} - T_1) \\ + \frac{K Dc^2 Mc \pi}{12D (\Delta \Theta_{2N-2} + \Delta \Theta_{2N-3})} (T_{2N-2} - T_{2N-3}) \quad (6)$$

With the seam located between arbitrary nodes x and $x+1$, all the conduction terms involving temperature differences $(T_x - T_{x+1})$ and $(T_{x+1} - T_x)$

are set equal to zero.

An iterative method is used to solve the above set of equations. First an EA term is found based on a T_{ref} and a solution for the no seam case where the solar flux is normal to the longitudinal axis of the tube. This EA term is then used with the above equations to find the temperature distribution with the seam between nodes x and $x+1$. The iteration is started by assuming a value of T_x and solving for T_i where i goes from 1 to $2N-2$. A solution is obtained when T_i satisfies the following equation.

$$\sum Q_{(absorbed)} = \sum Q_{(radiated)} \quad (7)$$

$$\text{where } \sum Q_{(absorbed)} = \sum_{i=1}^{2N-2} \frac{Q_i}{144} \alpha_s (A_{pc} + A_{pl})_i \quad (8)$$

$$\text{and } \sum Q_{(radiated)} = \sum_{i=1}^{2N-2} \frac{\Delta \Theta_i}{2\pi} EA \frac{\sigma}{144} T_i^4 \quad (9)$$

The temperature distribution obtained using the above equations will represent the worst case since no matter how bad the seam is, there will undoubtedly be some heat transfer paths across the seam and thus the temperature difference across the seam will be less than predicted.



2.0/COMPUTER PROGRAM

2.1 GENERAL

This computer program was developed to solve a specific heat transfer problem; that of determining the temperature distribution around the periphery of a screen type tubular element exposed to the sun.

The amount of input required to run a problem is kept to a minimum by using the computer to calculate all the nodal parameters such as the heat absorbed and the heat transfer paths. The printed output includes not only the temperature distribution but also the nodal parameters.

A detailed description of the program input and output is presented below.

2.2 DESCRIPTION OF INPUT

The following is a list of the input variables with their definitions. They are presented in order of input to the program.

- | | |
|-----|--|
| N1 | The total number of nodes assigned to Sector (1). |
| N2 | The total number of nodes assigned to Sector (2). |
| N3 | The total number of nodes assigned to Sector (3). For Cases 1 and 4 (see Appendix A) the program will reset $N2 = N2 + N3$. |
| PHI | Angle in degrees between the solar flux and the longitudinal axis of the tube. $0^{\circ} < \text{PHI} \leq 90^{\circ}$ |
| THB | Angle in degrees between the point on the tube closest to the sun and the location of the seam. $0^{\circ} < \text{THB} < 180^{\circ}$.
Omission of a value for THB yields a solution for a seamless tube. |

D Diameter of the tube in inches.

DC Diameter of the circumferential wires in inches.

DL Diameter of the longitudinal wires in inches.

AMC Circumferential wire mesh size in wires per inch.

AML Longitudinal wire mesh size in wires per inch.

QS Solar constant in $\frac{\text{BTU}}{\text{HR-FT}^2}$

ALFE Solar absorptivity of external surfaces of the wire screen tube.

ALFI Solar absorptivity of internal surfaces of the wire screen tube. The present program does not use this variable. Changes to the program to include different external and internal thermal coatings can be made in the future without changing the input format.

AKC Thermal conductivity of the circumferential wires in $\frac{\text{BTU}}{\text{HR-FT-}^\circ\text{R}}$

TREFL Reference temperature level. Omission of this variable for any set of data following the first run will force a solution based on the radiation coefficient to deep space used or calculated in the previous run.

DEN Density of the wire screen material in LBS/FT^3 . This variable should only be used where the circumferential and longitudinal wires are of the same material.

The formats applicable for input, card columns, and a typical example are presented below. The input data for one run requires a total of three cards.

First Card	Format	Card Columns	Example
N1	I2	1 - 2	12
N2	I2	3 - 4	04
N3	I2	5 - 6	04
PHI	E13.7	7 - 19	90.
THB	E13.7	20 - 32	120.

Second Card

D	E13.7	1 - 13	.75
DC	E13.7	14 - 26	.008
DL	E13.7	27 - 39	.0128
AMC	E13.7	40 - 52	16.
AML	E13.7	53 - 65	12.

Third Card

QS	E13.7	1 - 13	450.
ALFE	E13.7	14 - 26	.4
ALFI	E13.7	27 - 39	.4
AKC	E13.7	40 - 52	44.
TREFL	E13.7	53 - 65	500.
DEN	F7.3	66 - 72	500.

There is no limit to the number of problems which may be set up for one computer run.

2.3 DESCRIPTION OF OUTPUT

The program output for a typical problem is presented in Appendix B. Output symbols which are not explained in Section 2.2 above are presented below in the order of their appearance on the output list.

THCL	Angle Θ_{cl} in degrees	
THCC	Angle Θ_{cc} in degrees	
N	Node number	
TH	Node central angle Θ in degrees	
APC	Nodal projected area of circumferential wires to the solar flux	in^2
APL	Nodal projected area of longitudinal wires to the solar flux	in^2
AFLEFC	Effective absorptivity of circumferential wires to the solar flux	
ALFEFL	Effective absorptivity of longitudinal wires to the solar flux	
QF	Solar flux incident on nodal projected areas	$\frac{\text{BTU}}{\text{HR-FT}^2}$
AKCC (N to N+1)	Conduction coefficient between nodes N and N+1	
T	Node temperature in $^{\circ}\text{R}$	
T(N) - T(NN)	Difference in temperature between node N and the node at $\text{TH} = 180^{\circ}$	
EAEFF	Effective radiation coefficient for a one inch length of the tube to deep space in square inches	

AEFF Exposed wire surface area for a one inch length
 of tube in square inches

EEFF Effective wire surface emissivity calculated by
 dividing EAEFF by AEFF

The first four printed lines of output are the problem input variables.
The following set of 8 columns of output are nodal quantities including
the central angle, projected areas, effective absorptivities, incident
solar flux, and the conduction coefficients. The next set of 4 columns
of output data include the temperature distribution, and the temperature
difference between each node and the node whose central angle θ is 180° .
Thus the temperature difference between the points on the tube closest to
the sun and farthest from the sun can be obtained from the data print out
for node #1. Additional printed output is self explanatory.

3.0/RESULTS

3.1 GENERAL

The use of a screen type tubular element in gravity gradient stabilization systems can lead to significant gains in system pointing accuracies. The pointing accuracy is dependent, to a large extent, on the thermal deflection of the rod like elements. In the past, tubular elements of thin sheet metal have been used. For this type of configuration, the temperature gradient is primarily a function of the heat absorbed on the illuminated side of the tube and the conductive heat transfer path around the periphery of the tube. For a screen type configuration, a portion of the solar flux will pass through the illuminated side of the tube and will be absorbed by the shade side of the tube. Here, the temperature gradient depends on the difference in the heat absorbed between the sun side and the shade side of the tube and the conductive path around the periphery of the tube.

3.2 PARAMETRIC RESULTS

Parametric results for a number of variables have been obtained and are included in this report. The majority of the results are based on a solar constant of 450 BTU/HR-FT^2 , and a beryllium copper material with a solar absorptivity of .4, and a conduction coefficient of $44 \text{ BTU/HR-FT-}^{\circ}\text{R}$. A reference temperature of 500°R was used in most cases.

Figure 1 shows the large effect that the tube diameter has on the temperature difference across the tube as well as the typical temperature distribution around a seamless tube. The temperature difference between the sun and shade sides of the tube is approximately proportional to the

square of the tube diameter. Figure 1 also shows that at $\theta = 0^\circ$, $\theta \cong 120^\circ$, and $\theta = 180^\circ$, the temperature gradient ($\frac{dT}{d\theta}$) is zero. Thus, since there is no heat transfer where the temperature gradient is zero, a tube involving a seam would have the same temperature distribution provided the seam is located at a point where the temperature gradient for a seamless tube is zero.

Figure 2 presents the effect that the solar absorptivity has on the temperature difference across the tube. For this case, the temperature difference between the sun and shade sides of the tube is approximately proportional to the absorptivity.

The temperature distributions presented in Figure 3 show the effect the thermal conductivity of the wire material has on temperature difference between the sun and shade sides of the tube. Here, the temperature difference is approximately inversely proportional to thermal conductivity.

The results shown in Figures 1, 2, and 3 and the conclusions drawn above are only approximate in that they only apply to configurations which have small temperature differences between the sun and shade sides. Figures 4 and 5 are similar to Figures 1 and 2 with the exception that a smaller thermal conductivity is used. A comparison of the two sets of figures shows that the variables do not effect the temperature differences of Figures 4 and 5 as much as that of Figures 1 and 2. For example, Figure 2 shows a temperature difference at $\alpha_s = .6$ of about 2.8 times the temperature difference at $\alpha_s = .2$, where as Figure 5 shows that it is only 2.15 times as large. The influencing factor here is the heat radiated from the tube to deep space. For very low temperature differences, the heat radiated

to deep space is fairly evenly distributed around the periphery of the tube. For large temperature differences, a significantly greater portion of the heat radiated to deep space occurs on the hot side of the tube. Thus the amount of heat to be conducted around the tube to the cold side decreases which tends to decrease the temperature gradient. In other words, for larger and larger temperature differences radiation to deep space becomes a dominating factor which reduces the effects of other variables such as the solar absorptivity and the tube diameter.

Figures 6, 7, and 8 present the effects of the circumferential wire diameter and the circumferential wire mesh size on the temperature differences for .5 inch, .75 inch, and 1.0 inch tubes. The following conclusions can be made.

1. In general, the smallest diameter tube yields the smallest temperature difference.
2. The temperature difference decreases as the circumferential wire diameter increases at a fixed circumferential wire mesh size.
3. The temperature difference decreases, reaches a minimum, and then starts to increase as the circumferential wire mesh size increases at a fixed circumferential wire diameter. For all cases presented in Figures 6, 7, and 8, the minimum temperature difference occurred at a percent open area of between about 60 to 70%. A trade off between percent open area and the circumferential conduction cross sectional area is evident here. Increasing the circumferential wire mesh size decreases the former while increasing the latter.



Figures 9 and 10 show the effects of varying the longitudinal wire diameter and the longitudinal wire mesh size. Reducing either parameter, while maintaining a fixed circumferential wire diameter and mesh size, increases the percent open area which reduces the temperature difference between the sun and shade sides of the tube.

3.3 ADDITIONAL RESULTS

The results discussed above are parametric in nature and were obtained with the incident solar flux normal to the longitudinal axis of the tube. In addition, it was assumed that the location of the seam was such that the temperature distribution was identical to that for a seamless tube. The results discussed in the following sections were obtained using a typical configuration. These results are presented in order to show additional characteristics of the wire screen type tubular configuration.

3.3.1 SOLAR FLUX INCIDENT ANGLE. A typical configuration was used to show the effect the incident solar flux angle has on the temperature distribution around the tube. The results are based on an assumed reference temperature of 500°R for the case where the solar flux is normal to the longitudinal axis of the tube. That is, at $\phi = 90^{\circ}$, the temperature of the point on the periphery of the tube farthest from the sun, ($\theta = 180^{\circ}$) is 500°R . For solar flux incident angles less than 90° , the deep space radiation coefficient for the 90° case is used. Thus, the results for incident angles less than $\phi = 90^{\circ}$ yield not only the temperature difference across the tube, but also the absolute temperature of the tube relative to the $\phi = 90^{\circ}$ case. These results are presented in Figures 11, 12, and 13, and discussed below.

Temperature distributions for several incident solar flux angles are presented in Figure 11. As angle ϕ initially decreases, the amount of energy absorbed on the shade side of the tube decreases more rapidly than that absorbed on the illuminated side resulting in an increase in the temperature difference across the tube. For this configuration, as ϕ decreases to about 7° to 8° , no solar flux passes through the illuminated side of the tube, and the temperature difference across the tube reaches a peak. At lower angles, the temperature distribution is similar to a tube with no open area. The temperature difference across the tube decreases rapidly with angle and reaches zero, of course, when the solar flux is parallel to the longitudinal axis of the tube. The solar flux incident angle at which the peak temperature difference occurs is a function of the circumferential wire size and spacing.

The temperature difference across the tube as a function of solar flux incident angle is presented in Figure 12. The peak temperature difference at about 7° to 8° is clearly shown.

The temperature of the tube as a function of solar flux incident angle is plotted in Figure 13. These data as mentioned above, are based on a deep space radiation coefficient for the tube which yields a 500°R shade side temperature when the solar flux is normal to the longitudinal axis of the tube. A thin walled tube would have a temperature versus angle relationship as shown by the dotted line. For the thin walled tube case, the temperature is proportional to $(\sin \phi)^{\frac{1}{4}}$ as shown in Reference 1. The screen tube temperature is higher since although the projected area of the longitudinal wires is proportional to $\sin \phi$, that of the circumferential wires is not except for very low incident angles.

3.3.2 SEAM EFFECTS. As mentioned previously, the heat transfer paths across the seam of a screen type tubular configuration are difficult if not impossible to define analytically. The limiting cases, however, should be as follows.

Case 1. Heat transfer paths identical to continuous screen material.

Case 2. No heat transfer paths across the seam.

The first case, of course, is the "no seam" case, and the results presented above are applicable.

The second case is the worst case imaginable. The configuration used in Section 3.3.1 was used here to show the effect of a "no heat transfer" seam on the temperature distribution around the periphery of the tube. The results are shown in Figures 14 and 15 and discussed below.

Figure 14 shows the temperature distributions for seam locations at $\theta = 0, 17^\circ, 39^\circ, 74^\circ, \sim 119^\circ$, and 180° . Temperature distributions for seam locations at $\theta = 80^\circ, 90^\circ, 100^\circ, 113^\circ, 127^\circ$, and 141° , are presented in Figure 15. For this configuration, location of the seam at about 119° yields a temperature distribution which is identical to that of a seamless tube. The maximum temperature difference across the seam occurs at seam locations where the temperature gradient ($\frac{dT}{d\theta}$) for the seamless tube case is maximum. This occurs at an angle of about 70° to 80° as shown in Figure 16.

These results show that the location of the seam could have significant effect on the temperature distribution provided there is no transfer of heat across the seam. No matter how poor the seam is, however, there will be some heat transfer across the seam and the temperature difference will

not be as severe as that shown. In order to reduce the adverse effects of the seam on the deflection of screen type booms, the booms should be manufactured such that the seam is spiralled along the length of the tube when deployed.

3.3.3 BOOM DEFLECTION. The temperature difference between the hot and cold sides of the screen type tubular boom element will cause the element to bend away from the heat source. For small temperature gradients or for short elements, the tip deflection can be approximated by the following expression:

$$Y = \frac{e l^2 \Delta T}{2D}$$

This expression can also be used for long tube lengths provided a step by step calculation is used along the length of the tube. This was done using the .75 inch diameter configuration and data of Figure 12 and is presented in Figure 17. In addition, this figure shows the deflection for the 0.5 inch diameter thin walled tube of Reference 1. The wire screen type configuration shows a significant reduction in tip deflection compared to the thin walled tube case. Even greater reductions in tip deflection can be obtained by using a 0.5 inch diameter screen type tube. Current studies at Convair, however, indicate that smaller diameter tubes do not have the mechanical properties required.



4.0/CONCLUSIONS AND RECOMMENDATIONS

This report presents the thermodynamic analysis of the screen tube configuration exposed to solar heating in space. The results show that the thermal deflection of long screen type booms is significantly less when compared to current state of the art thin walled tubes.

Further decreases in boom deflection can be realized by varying the thermal radiation properties of the internal and external surfaces of the tube. The proper choice of thermal coatings should yield no temperature difference between the sun side and the dark side of the tube. It is recommended that additional work be accomplished in this area in order to further reduce the thermal deflection of booms exposed to solar heating in space.

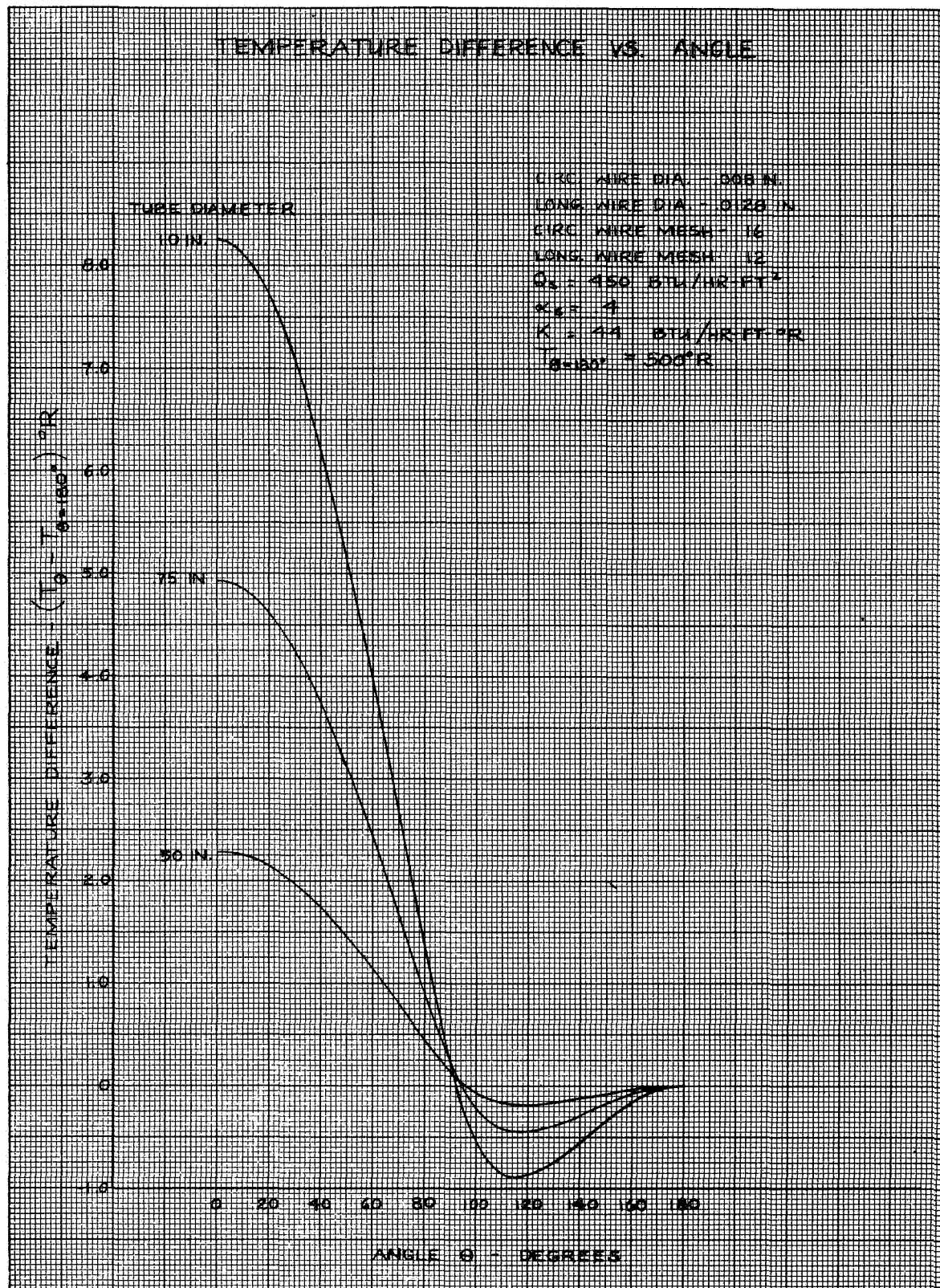


Figure 1

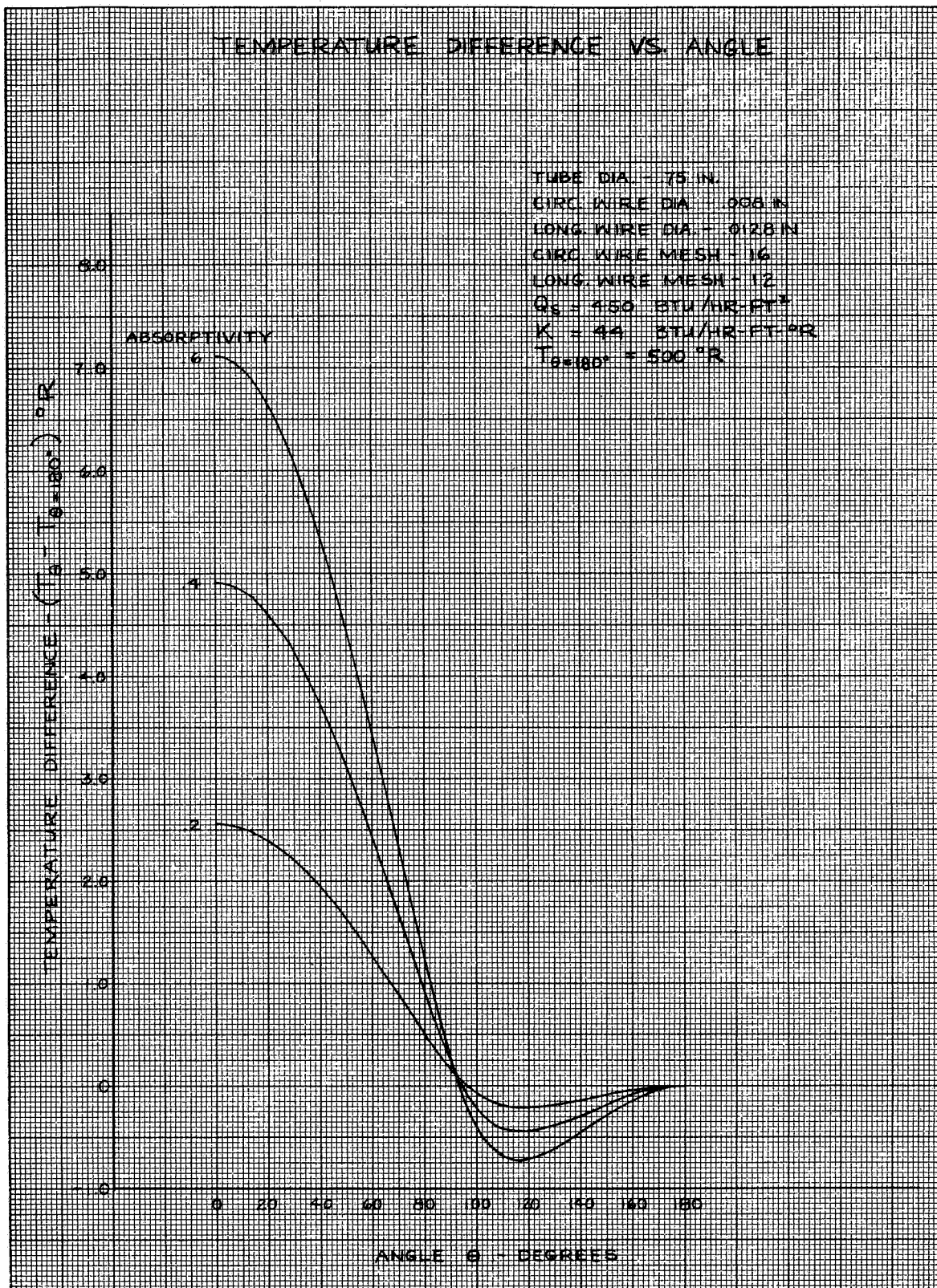


Figure 2

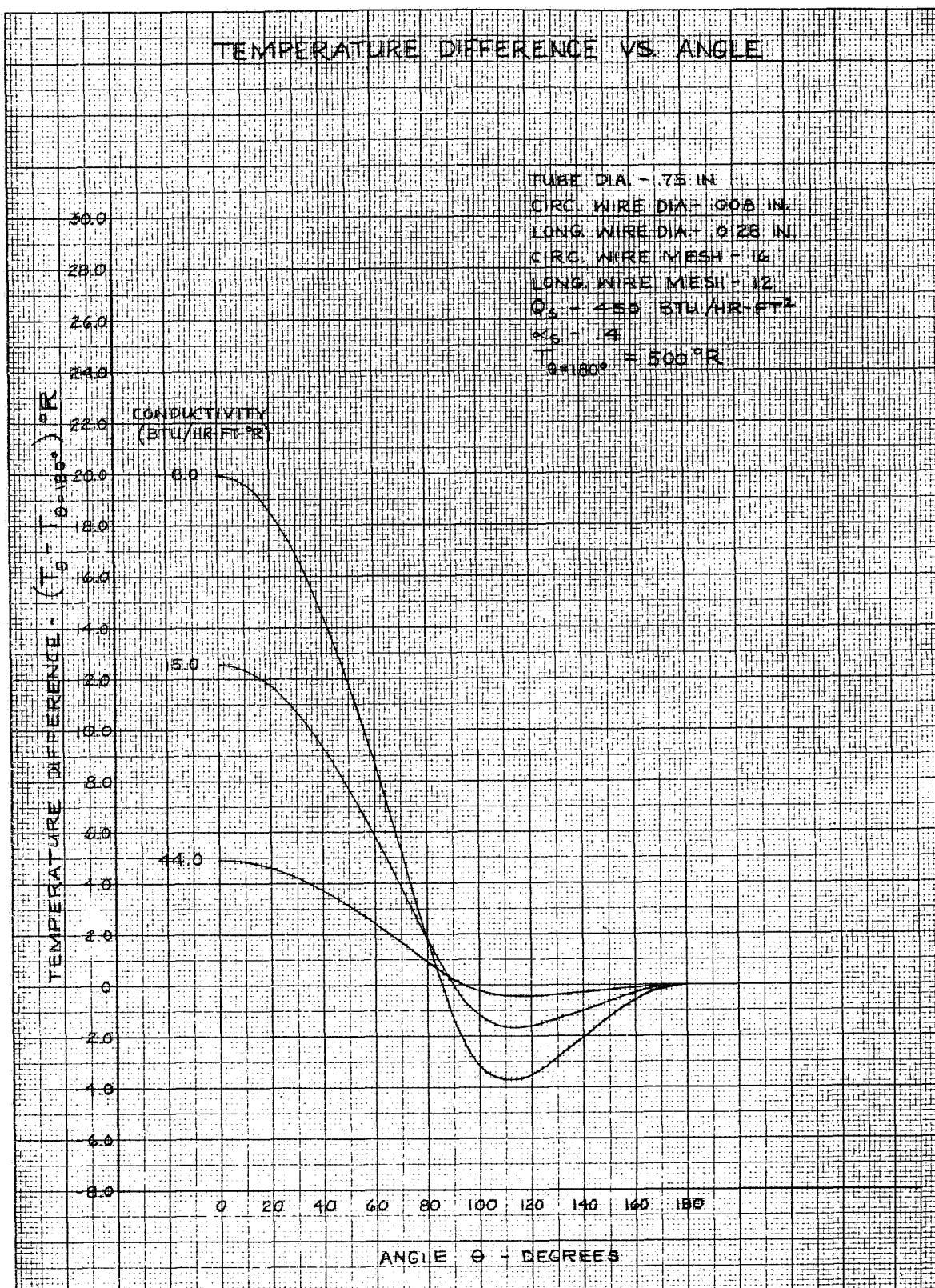


Figure 3

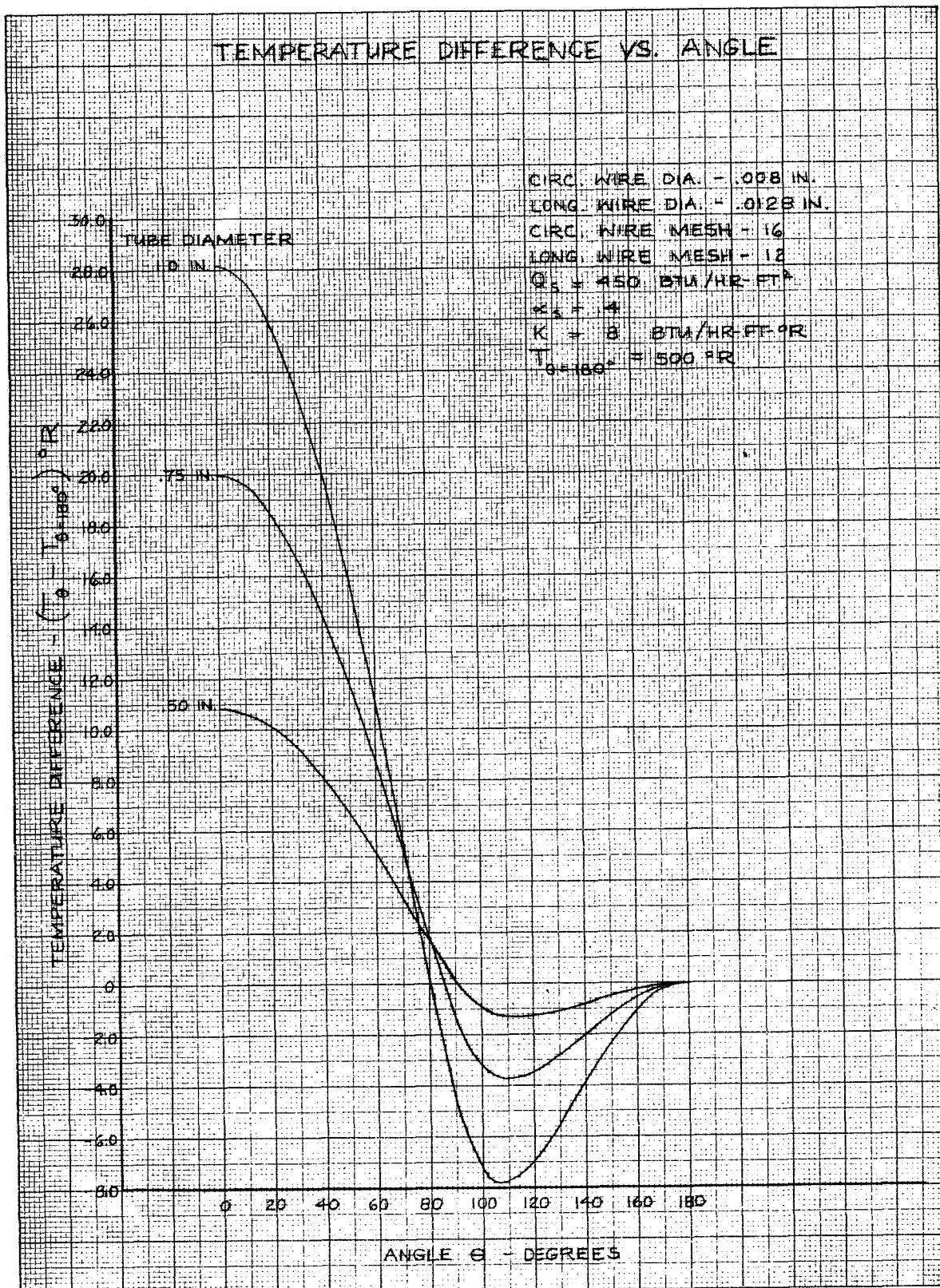


Figure 4

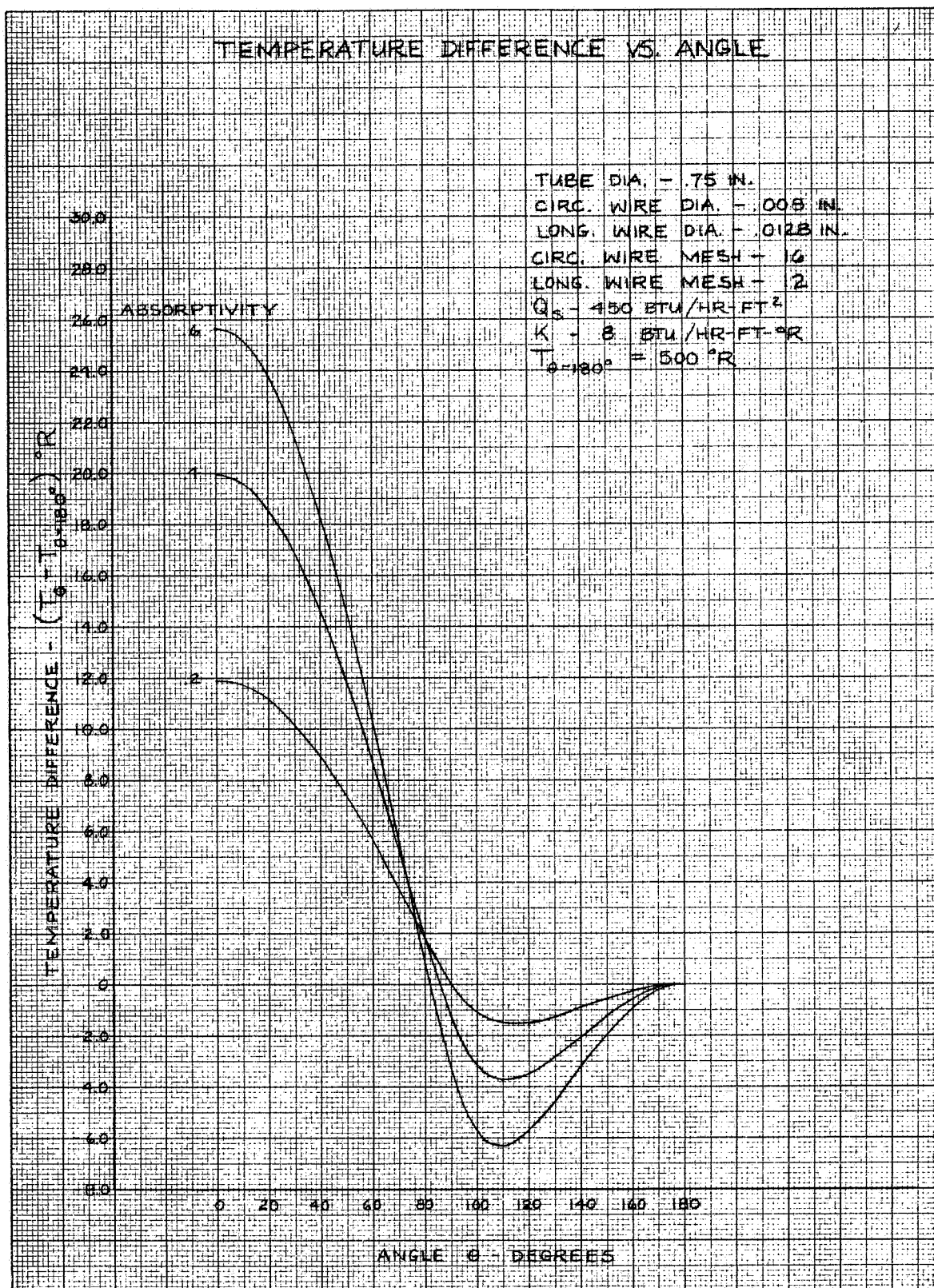


Figure 5

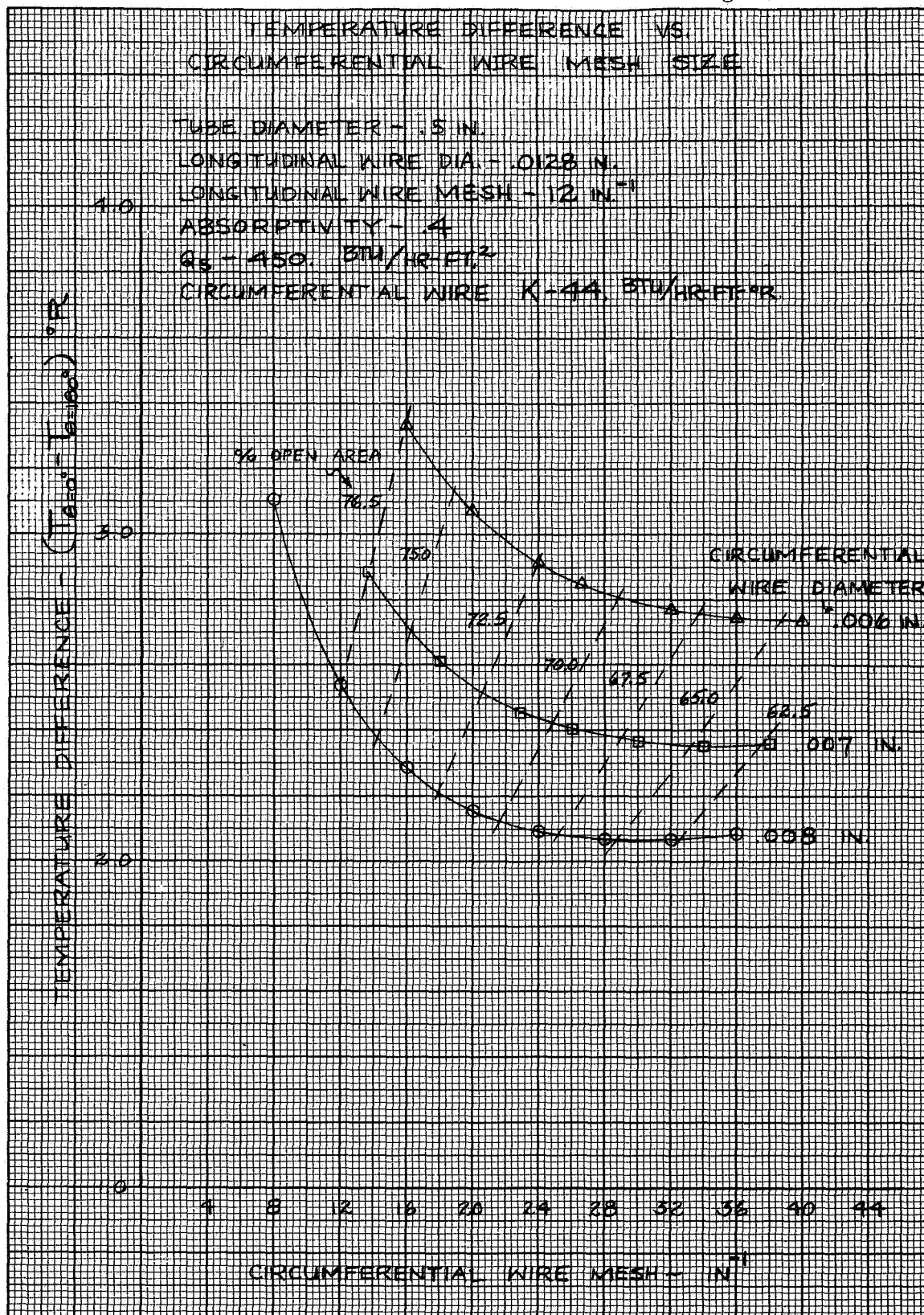


Figure 2

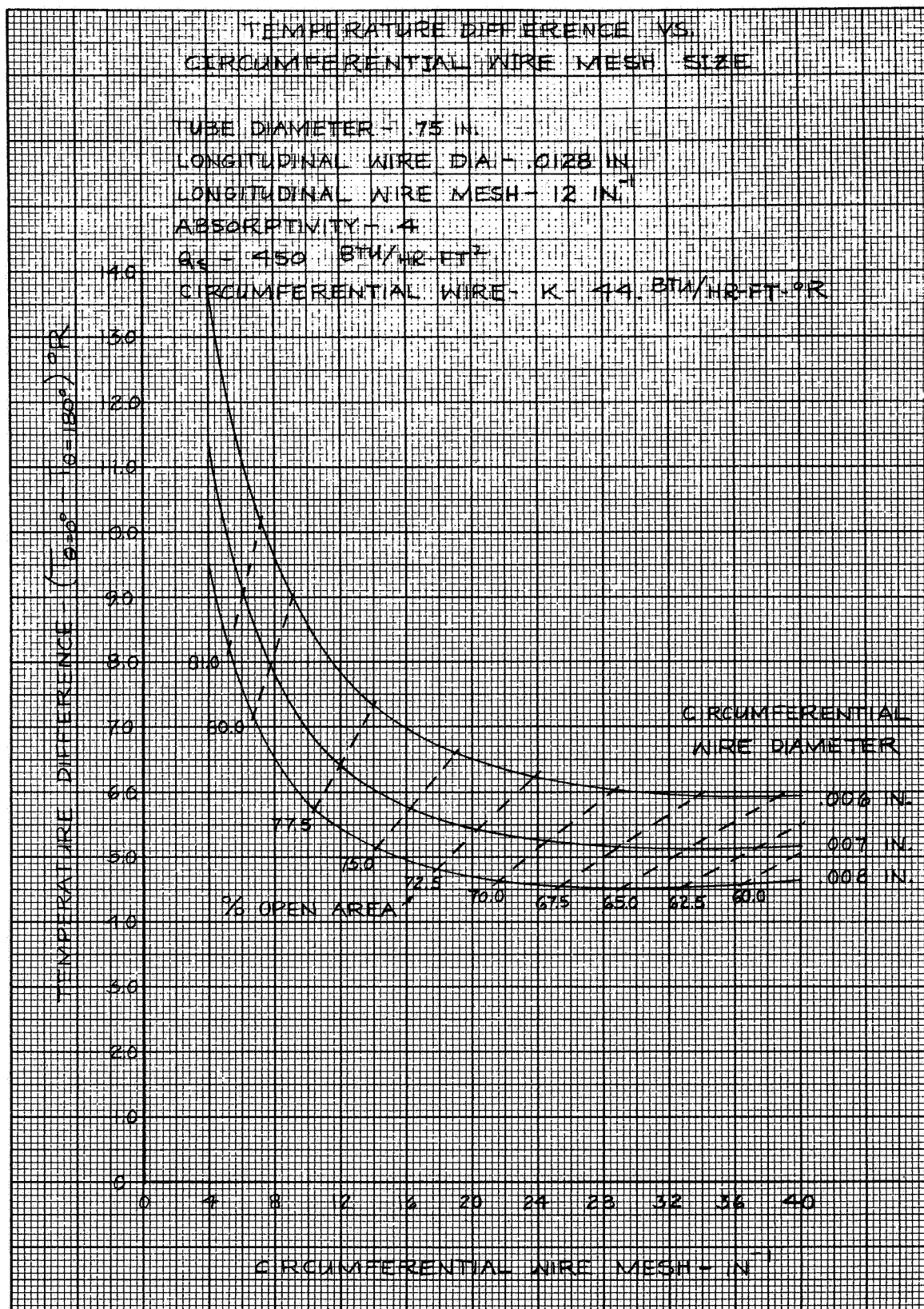


Figure 7

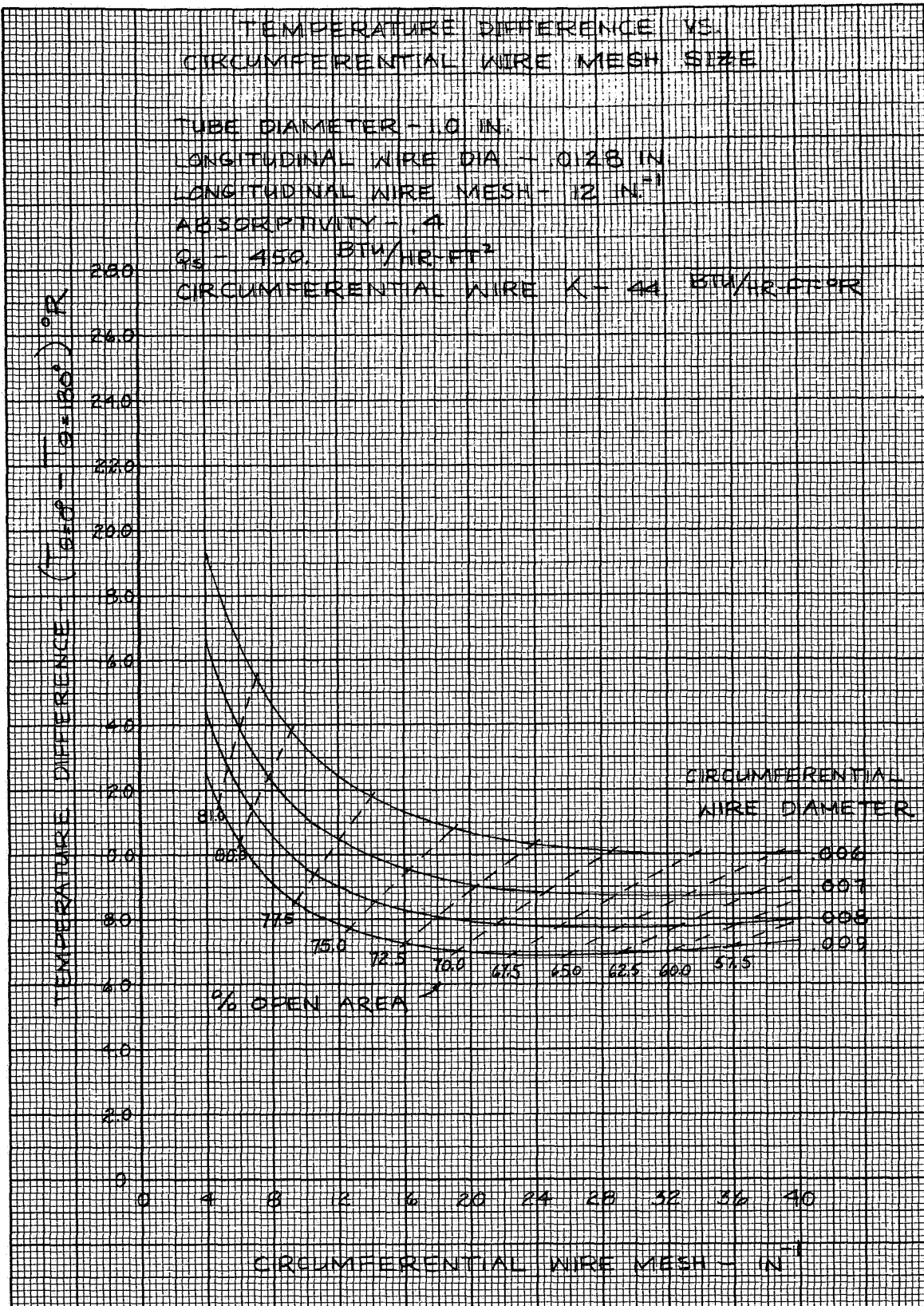


Figure 8

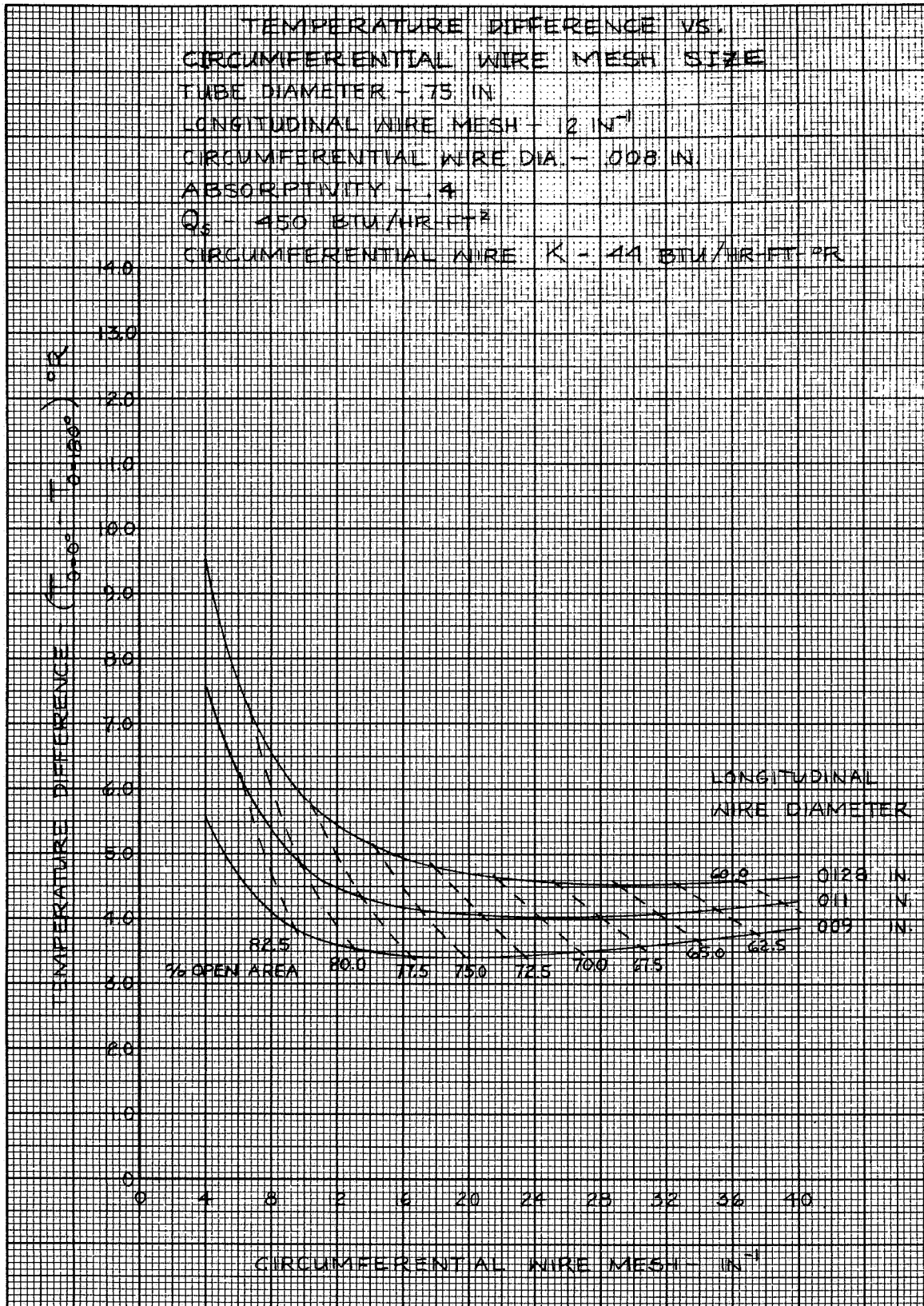


Figure 9

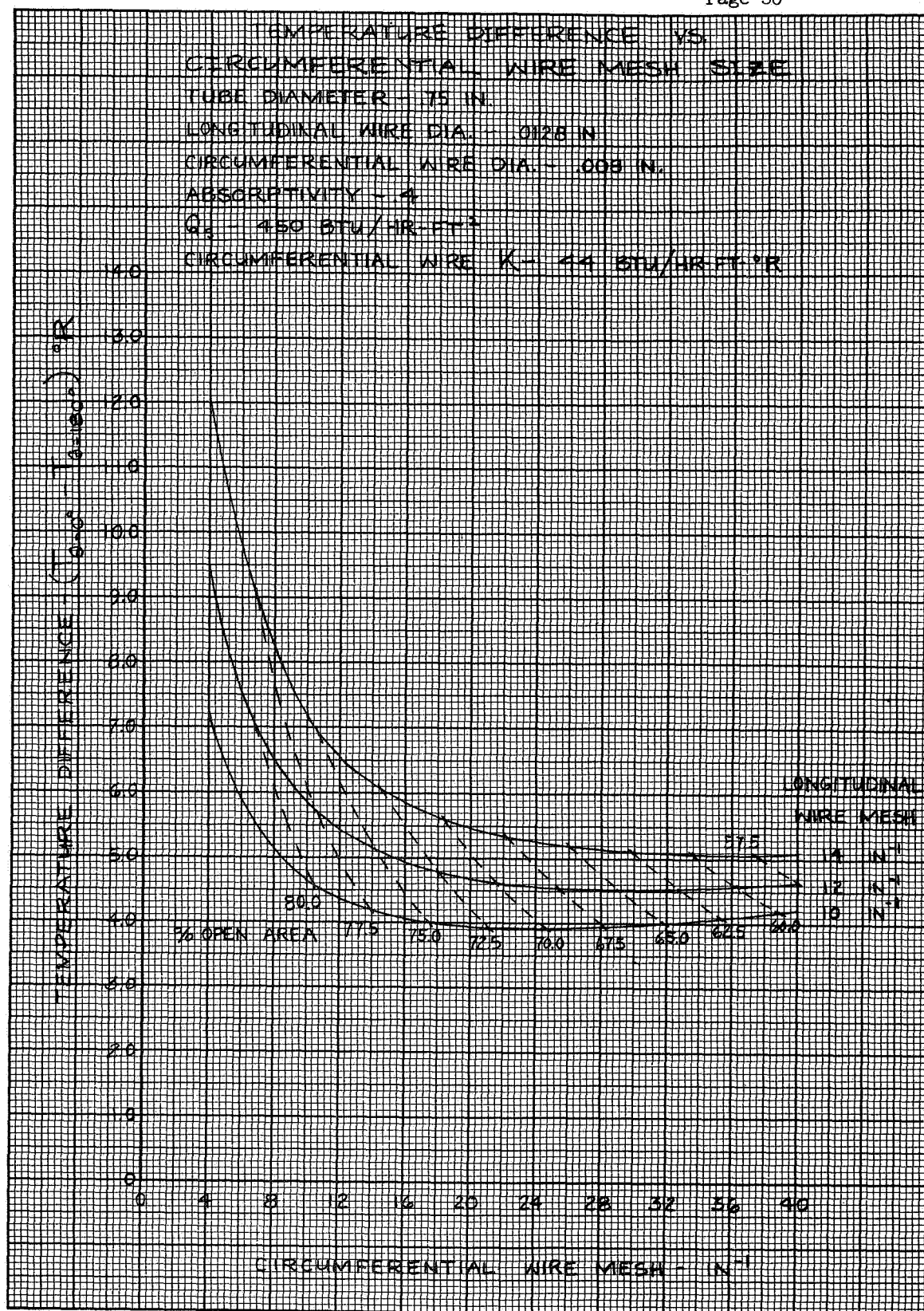


Figure 10

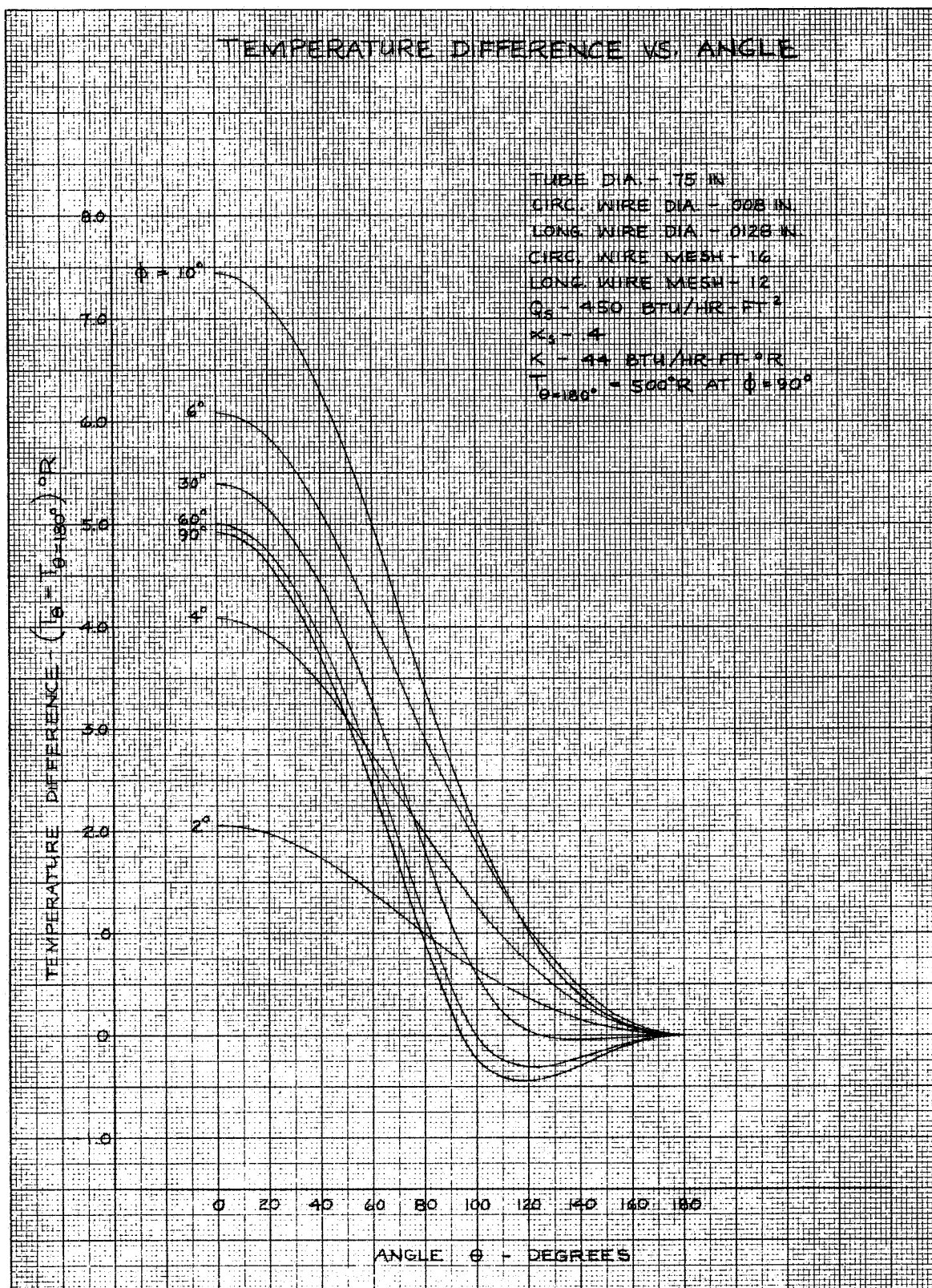


Figure 11

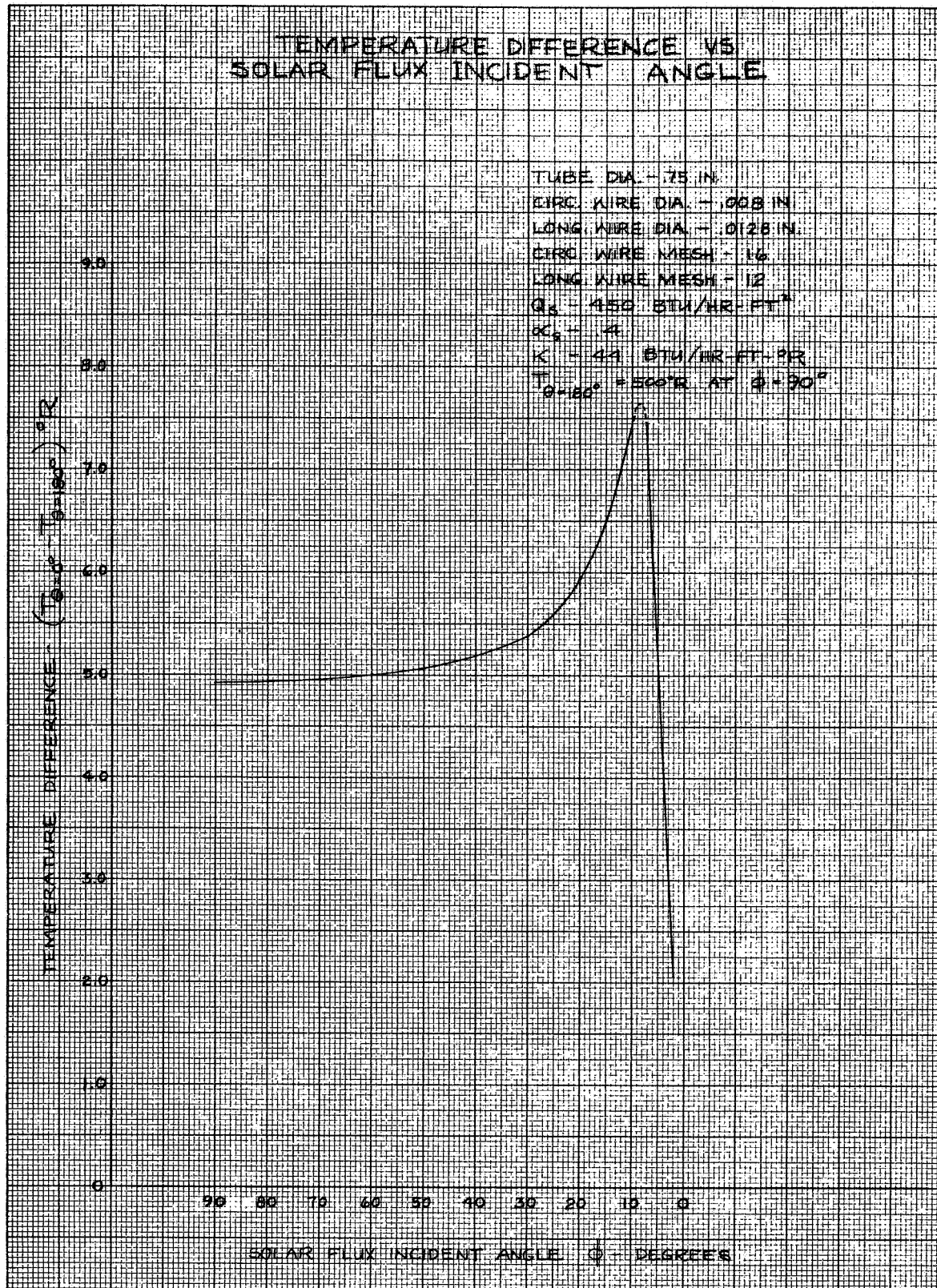


Figure 12

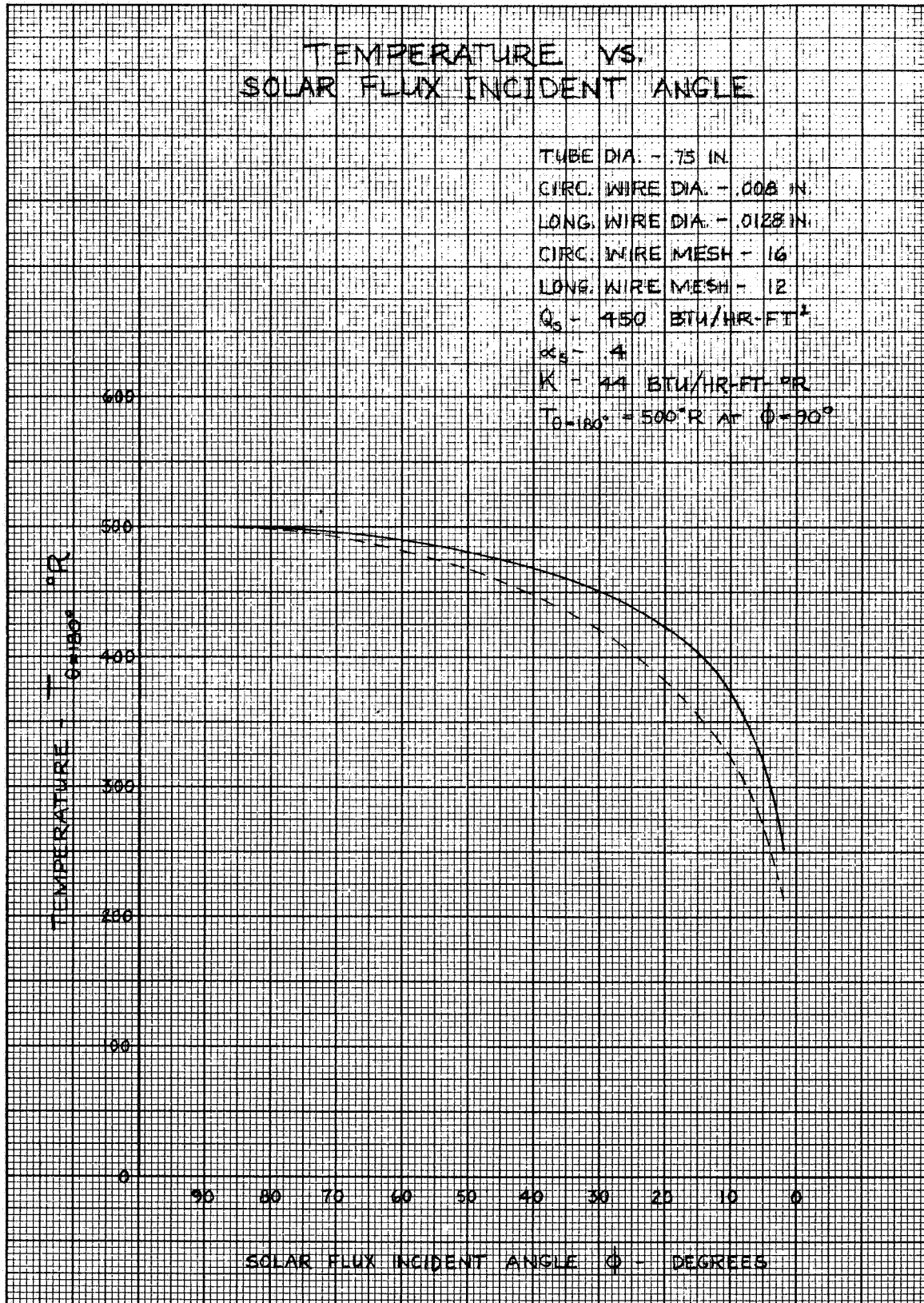


Figure 13

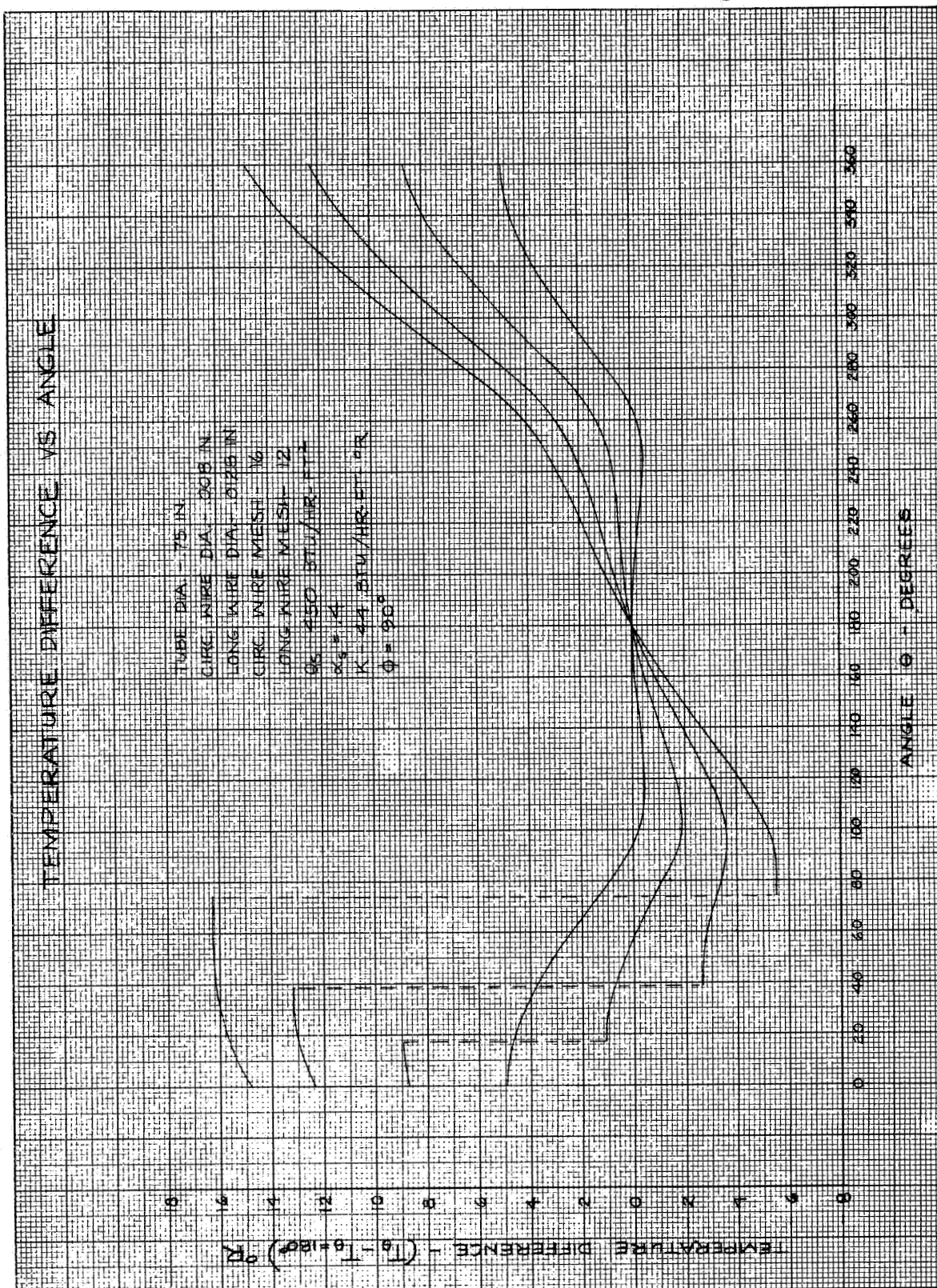


Figure 14

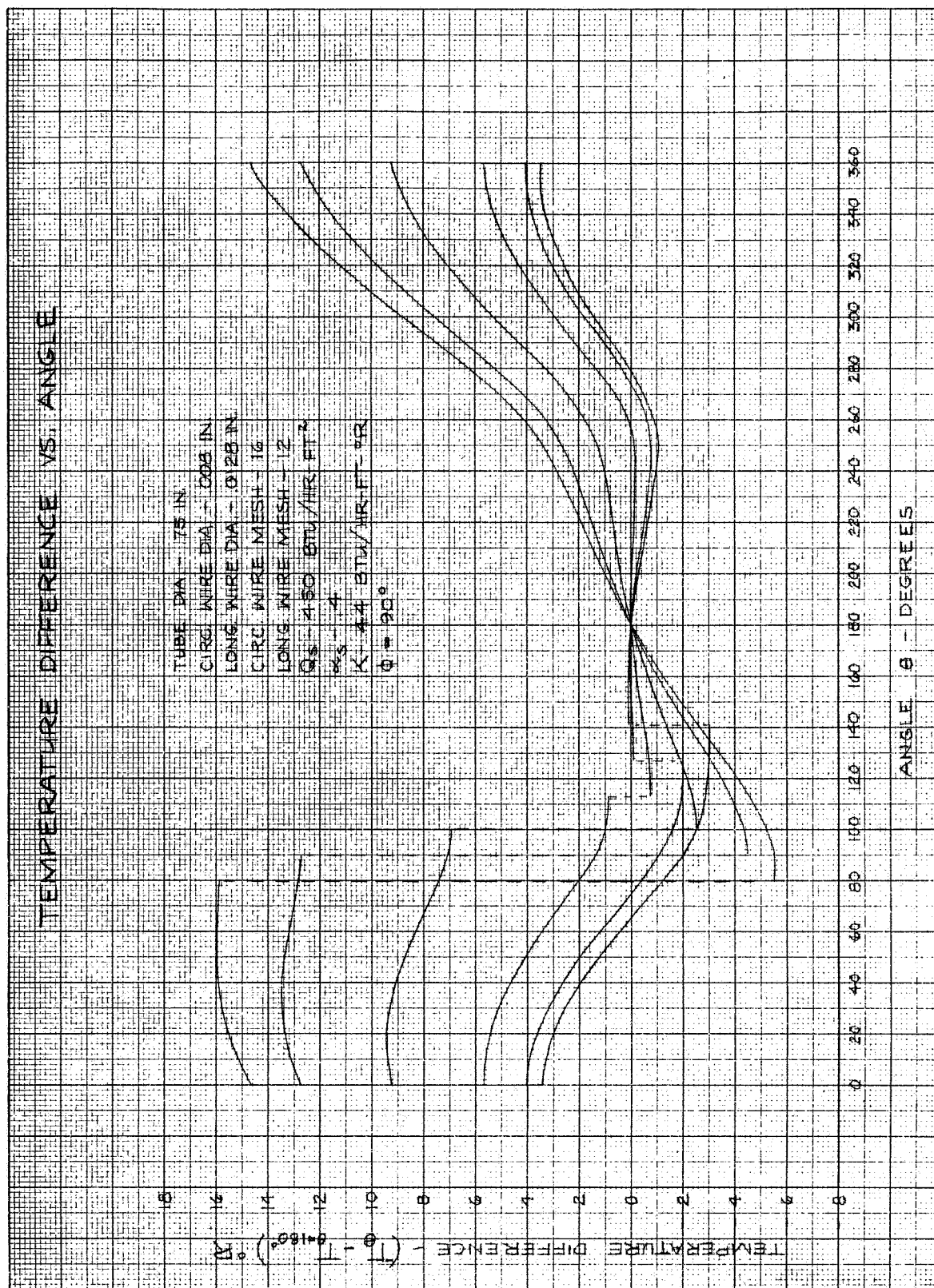


Figure 15

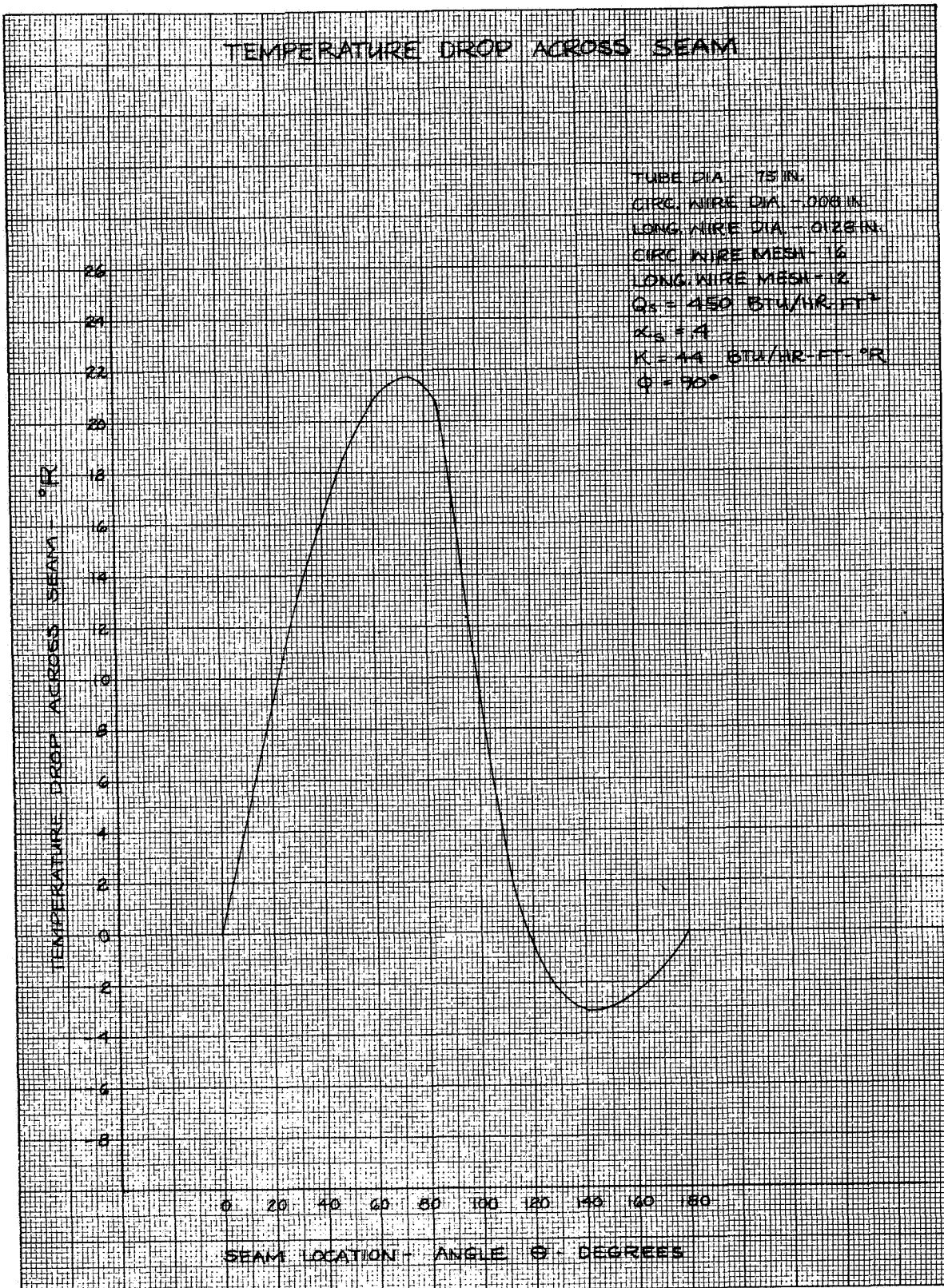


Figure 16

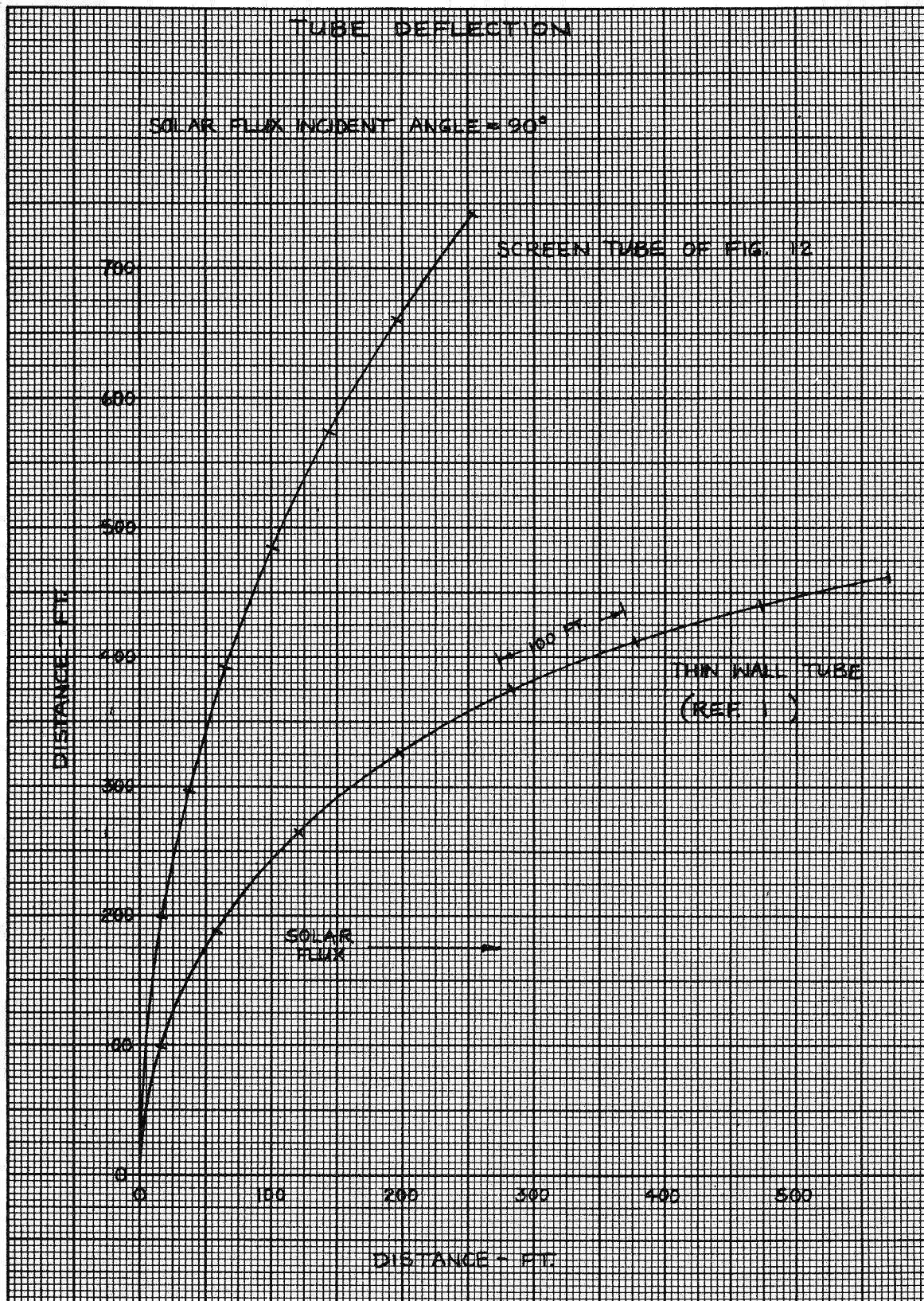


Figure 17

APPENDIX A

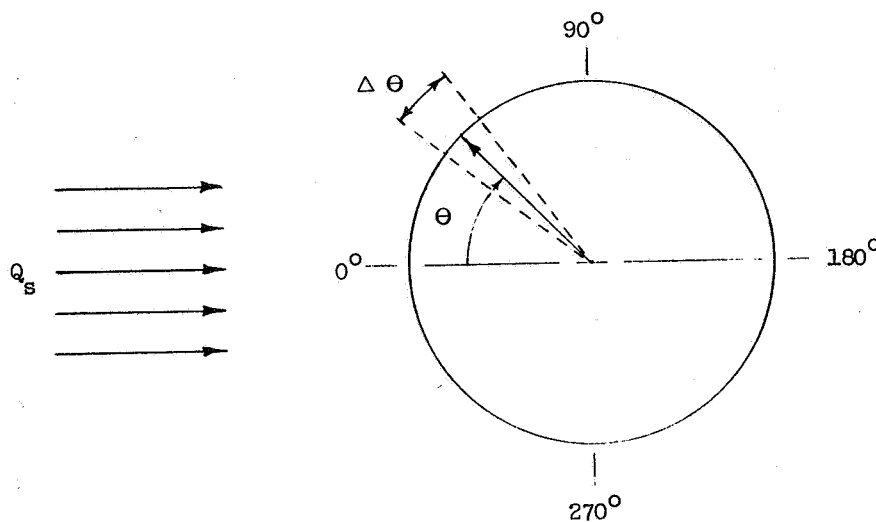
A.1 INTRODUCTION

Equations used for determining the division of nodes for the screen type tube configuration are presented below. Four cases are considered based on the orientation of the tube with respect to the sun and the shadowing which occurs between the longitudinal wires and between the circumferential wires.

A.2 NODAL DIVISION, PROJECTED AREAS, AND INCIDENT HEAT FLUX

The following equations are used in defining the nodal division schemes, the projected area of each node with respect to the solar flux, and the value of the incident solar flux. On the illuminated side of the tube the incident solar flux is equal to one solar constant ($450 \frac{\text{BTU}}{\text{HR-FT}^2}$), whereas inside the tube, the average value of the incident solar flux is dependent on the open area, and the shadowing between wires.

For all cases presented below, a node is defined by an angle $\Delta \theta$, and its position around the periphery of the tube is defined by its central angle θ measured from the sun side of the tube as illustrated in the following figure. Node #1 is located at $\theta = 0^\circ$ and node N at $\theta = 180^\circ$.



Equations describing nodal parameters are presented for $0 \leq \theta \leq 180^\circ$ and the values obtained can be used for $360^\circ \geq \theta \geq 180^\circ$. The total number of nodes around the periphery of the tube is equal to $2N-2$.



CASE 1

$$\Phi = \frac{\pi}{2}$$

Sector (1)

$$\Delta \Theta = \frac{\Theta_{c1}}{N1-.5}$$

$$\Theta = 0, \Delta \Theta, 2 \Delta \Theta, \dots, (N1-1) \Delta \Theta$$

$$A_{pc} = D M_c D_c \left(\cos \Theta \sin \frac{\Delta \Theta}{2} - .25 \Delta \Theta M1 D1 \right)$$

$$A_{pl} = .5 D \Delta \Theta M1 D1 (1-.5 M_c D_c)$$

$$Q = Q_s$$

Sector (2)

$$\Delta \Theta = \frac{\frac{\pi}{2} - \Theta_{c1}}{N2}$$

$$\Theta = \Theta_{c1} + \frac{\Delta \Theta}{2}, \Theta_{c1} + 3 \frac{\Delta \Theta}{2}, \dots, \Theta_{c1} + (2N2-1) \frac{\Delta \Theta}{2}$$

$$A_{pc} = .5 D M_c D_c \cos \Theta \sin \frac{\Delta \Theta}{2}$$

$$A_{pl} = D \cos \Theta \sin \frac{\Delta \Theta}{2} (1-.5 M_c D_c)$$

$$Q = Q_s$$

Sector (3)

$$\Delta \Theta = \frac{\frac{\pi}{2} - \Theta_{c1}}{N3} \quad \text{where } N3 = N2$$

$$\Theta = \frac{\pi}{2} + \frac{\Delta \Theta}{2}, \frac{\pi}{2} + 3 \frac{\Delta \Theta}{2}, \dots, \frac{\pi}{2} + (2N3-1) \frac{\Delta \Theta}{2}$$

$$A_{pc} = -.5 D M_c D_c \cos \Theta \sin \frac{\Delta \Theta}{2}$$

$$A_{pl} = -D \cos \Theta \sin \frac{\Delta \Theta}{2} (1. - .5 M_c D_c)$$

$$Q = 0.$$

Sector (4)

$$\Delta \Theta = \frac{\Theta c1}{N4-.5} \quad \text{where } N4 = N1$$

$$\Theta = \pi - \Theta c1 + \frac{\Delta \Theta}{2}, \pi - \Theta c1 + 3 \frac{\Delta \Theta}{2}, \dots, \pi - \Theta c1 + (2N4-1) \frac{\Delta \Theta}{2}$$

$$A_{pc} = - D M_c D_c \left(\cos \Theta \sin \frac{\Delta \Theta}{2} + .25 \Delta \Theta M_l D_l \right)$$

$$A_{pl} = .5 D \Delta \Theta M_l D_l (1. - .5 M_c D_c)$$

$$Q = Q_s \left(1. + \frac{A_{pc} + A_{pl}}{D \cos \Theta \sin \frac{\Delta \Theta}{2}} \right)$$

For CASE 1, the total number of nodes for $\Theta = 0 \rightarrow \pi$ is

$$N = N1 + N2 + N3 + N4 = 2 (N1 + N2)$$

CASE 2

$$\Phi_c < \Phi < \frac{\pi}{2}; \Theta c1 < \Theta cc$$

Sector (1)

$$\Delta \Theta = \frac{\Theta c1}{N1-.5}$$

at $\Theta = 0$

$$A_{pc} = D M_c D_c \left(\sin \frac{\Delta \Theta}{2} - .25 \Delta \Theta M_l D_l \right)$$

$$A_{pl} = .5 D \Delta \Theta M_l D_l (\sin \Phi - .5 M_c D_c)$$

$$Q = Q_s$$

and at

$$\Theta = \Delta \Theta, 2 \Delta \Theta, \dots, (N1-1) \Delta \Theta$$

$$A_{pc} = .5 D \Delta \Theta M_c D_c \left(\sin \psi - \frac{.5 M_l D_l \sin \left(\beta + \frac{\pi}{2} - \phi \right)}{\sqrt{\sin^2 \beta + \cos^2 \beta \cos^2 \Theta}} \right)$$

$$A_{pl} = .5 D \Delta \Theta M_l D_l \left(\sin \phi - \frac{.5 M_l D_l \sin \left(\beta + \frac{\pi}{2} - \phi \right)}{\sqrt{\sin^2 \beta + \cos^2 \beta \cos^2 \Theta}} \right)$$

where

$$\beta = \tan^{-1} \left(\frac{\cos^2 \Theta}{\tan \left(\frac{\pi}{2} - \phi \right)} \right)$$

$$Q = Q_s$$

Sector (2)

$$\Delta \Theta = \frac{\Theta_{cc} - \Theta_{cl}}{N2}$$

$$\Theta = \Theta_{cl} + \frac{\Delta \Theta}{2}, \Theta_{cl} + 3 \frac{\Delta \Theta}{2}, \dots, \Theta_{cl} + (2N2-1) \frac{\Delta \Theta}{2}$$

$$A_{pc} = .25 D \Delta \Theta M_c D_c \sin \psi$$

$$A_{pl} = .5 D \left(2 \cos \Theta \sin \frac{\Delta \Theta}{2} \sin \phi - .5 \Delta \Theta M_c D_c \sin \psi \right)$$

$$Q = Q_s$$

Sector (3)

$$\Delta \Theta = \frac{\frac{\pi}{2} - \Theta_{cc}}{N3}$$

$$\Theta = \Theta_{cc} + \frac{\Delta \Theta}{2}, \Theta_{cc} + 3 \frac{\Delta \Theta}{2}, \dots, \Theta_{cc} + (2N3-1) \frac{\Delta \Theta}{2}$$

$$A_{pc} = .5 D \cos \Theta \sin \frac{\Delta \Theta}{2} \sin \Phi$$

$$A_{pl} = .5 D \cos \Theta \sin \frac{\Delta \Theta}{2} \sin \Phi$$

$$Q = Q_s$$

Sector (4)

$$\Delta \Theta = \frac{\frac{\pi}{2} - \Theta_{cc}}{N4} \quad \text{where } N4 = N3$$

$$\Theta = \frac{\pi}{2} + \frac{\Delta \Theta}{2}, \frac{\pi}{2} + 3 \frac{\Delta \Theta}{2}, \dots, \frac{\pi}{2} + (2N4-1) \frac{\Delta \Theta}{2}$$

$$A_{pc} = -.5 D \cos \Theta \sin \frac{\Delta \Theta}{2} \sin \Phi$$

$$A_{pl} = -.5 D \cos \Theta \sin \frac{\Delta \Theta}{2} \sin \Phi$$

$$Q = 0.$$

Sector (5)

$$\Delta \Theta = \frac{\Theta_{cc} - \Theta_{cl}}{N5} \quad \text{where } N5 = N2$$

$$\Theta = \pi - \Theta_{cl} + \frac{\Delta \Theta}{2}, \pi - \Theta_{cl} + 3 \frac{\Delta \Theta}{2}, \dots, \pi - \Theta_{cl} + (2N5-1) \frac{\Delta \Theta}{2}$$

$$A_{pc} = .25 D \Delta \Theta M_c D_c \sin \psi$$

$$A_{pl} = .5 D (2 \cos \Theta \sin \frac{\Delta \Theta}{2} \sin \Phi + .5 \Delta \Theta M_c D_c \sin \psi)$$

$$Q = 0$$

Sector (6)

$$\Delta \Theta = \frac{\Theta c_1}{N_6 - .5} \quad \text{where } N_6 = N_1$$

at

$$\Theta = \pi - \Theta c_1 + \frac{\Delta \Theta}{2}, \pi - \Theta c_1 + 3 \frac{\Delta \Theta}{2}, \dots, \pi - \Theta c_1 + (2N_6 - 3) \frac{\Delta \Theta}{2}$$

$$A_{pc} = .5 D \Delta \Theta M_c D_c \left(\sin \psi - \frac{.5 M_l D_l \sin (\beta + \frac{\pi}{2} - \Phi)}{\sqrt{\sin^2 \beta + \cos^2 \beta \cos^2 \Theta}} \right)$$

$$A_{pl} = .5 D \Delta \Theta M_l D_l \left(\sin \Phi - \frac{.5 M_c D_c \sin (\beta + \frac{\pi}{2} - \Phi)}{\sqrt{\sin^2 \beta + \cos^2 \beta \cos^2 \Theta}} \right)$$

where

$$\beta = \tan^{-1} \left(\frac{\cos^2 \Theta}{\tan (\frac{\pi}{2} - \Phi)} \right)$$

$$Q = Q_s \left(1. + \frac{A_{pc} + A_{pl}}{D \cos \Theta \sin \frac{\Delta \Theta}{2} \sin \Phi} \right)$$

and at $\Theta = \pi$

$$A_{pc} = D M_c D_c \left(\sin \frac{\Delta \Theta}{2} - .25 \Delta \Theta M_l D_l \right)$$

$$A_{p1} = .5 D \Delta \Theta M1 D1 (\sin \Phi - .5 M_c D_c)$$

$$Q = Q_s \left(1. - \frac{A_{pc} + A_{p1}}{.5 D \sin \frac{\Delta \Theta}{2} \sin \Phi} \right)$$

For CASE 2, the total number of nodes for $\Theta = 0 \rightarrow \pi$ is

$$N = N1 + N2 + N3 + N4 + N5 + N6 = 2 (N1 + N2 + N3)$$

CASE 3

$$\Phi_c < \Phi < \frac{\pi}{2}, \Theta_{cc} < \Theta_{cl}$$

Sector (1)

$$\Delta \Theta = \frac{\Theta_{cc}}{N1 - .5}$$

at

$$\Theta = 0^\circ$$

A_{pc} = Same as Sector (1) of CASE 2

A_{p1} = Same as Sector (1) of CASE 2

Q = Same as Sector (1) of CASE 2

at

$$\Theta = \Delta \Theta, 2 \Delta \Theta, \dots, (N1-1) \Delta \Theta$$

A_{pc} = Same as Sector (1) of CASE 2

A_{p1} = Same as Sector (1) of CASE 2

Q = Same as Sector (1) of CASE 2

Sector (2)

$$\Delta \Theta = \frac{\Theta_{cl} - \Theta_{cc}}{N2}$$

$$\theta = \theta_{cc} + \frac{\Delta \theta}{2}, \theta_{cc} + 3 \frac{\Delta \theta}{2}, \dots, \theta_{cc} + (2N_2 - 1) \frac{\Delta \theta}{2}$$

$$A_{pc} = .5 D \sin \phi \left(2 \cos \theta \sin \frac{\Delta \theta}{2} - .5 \Delta \theta M_1 D_1 \right)$$

$$A_{pl} = .25 D \Delta \theta M_1 D_1 \sin \phi$$

$$Q = Q_s$$

Sector (3)

$$\Delta \theta = \frac{\frac{\pi}{2} - \theta_{cl}}{N_3}$$

$$\theta = \theta_{cl} + \frac{\Delta \theta}{2}, \theta_{cl} + 3 \frac{\Delta \theta}{2}, \dots, \theta_{cl} + (2N_3 - 1) \frac{\Delta \theta}{2}$$

$$A_{pc} = .5 D \cos \theta \sin \frac{\Delta \theta}{2} \sin \phi$$

$$A_{pl} = .5 D \cos \theta \sin \frac{\Delta \theta}{2} \sin \phi$$

$$Q = Q_s$$

Sector (4)

$$\Delta \theta = \frac{\frac{\pi}{2} - \theta_{cl}}{N_4} \quad \text{where } N_4 = N_3$$

$$\theta = \frac{\pi}{2} + \frac{\Delta \theta}{2}, \frac{\pi}{2} + 3 \frac{\Delta \theta}{2}, \dots, \frac{\pi}{2} + (2N_4 - 1) \frac{\Delta \theta}{2}$$

$$A_{pc} = -.5D \cos \Theta \sin \frac{\Delta \Theta}{2} \sin \Phi$$

$$A_{pl} = -.5 D \cos \Theta \sin \frac{\Delta \Theta}{2} \sin \Phi$$

$$Q = 0.$$

Sector (5)

$$\Delta \Theta = \frac{\Theta_{cl} - \Theta_{cc}}{N5} \quad \text{where } N5 = N2$$

$$\Theta = \pi - \Theta_{cl} + \frac{\Delta \Theta}{2}, \pi - \Theta_{cl} + 3 \frac{\Delta \Theta}{2}, \dots, \pi - \Theta_{cl} + (2N5-1) \frac{\Delta \Theta}{2}$$

$$A_{pc} = -.5 D \sin \Phi (2 \cos \Theta \sin \frac{\Delta \Theta}{2} + .5 \Delta \Theta M1 D1)$$

$$A_{pl} = .25 D \Delta \Theta M1 D1 \sin \Phi$$

$$Q = 0.$$

Sector (6)

$$\Delta \Theta = \frac{\Theta_{cc}}{N6 - .5} \quad \text{where } N6 = N1$$

at

$$\Theta = \pi - \Theta_{cc} + \frac{\Delta \Theta}{2}, \pi - \Theta_{cc} + 3 \frac{\Delta \Theta}{2}, \dots, \pi - \Theta_{cc} + (2N6-3) \frac{\Delta \Theta}{2}$$

A_{pc} = Same as Sector (6) of CASE 2

A_{pl} = Same as Sector (6) of CASE 2

Q = Same as Sector (6) of CASE 2

at

$$\Theta = \pi$$

Apc = Same as Sector (6) of CASE 2

Apl = Same as Sector (6) of CASE 2

Q = Same as Sector (6) of CASE 2

For CASE 3, the total number of nodes for $\Theta = 0 \rightarrow \pi$ is

$$N = N1 + N2 + N3 + N4 + N5 + N6 = 2 (N1 + N2 + N3)$$

CASE 4

$$\Phi \leq \Phi_c$$

Sector (1)

$$\Delta \Theta = \frac{\Theta_{c1}}{N1 - .5}$$

$$\Theta = 0, \Delta \Theta, 2 \Delta \Theta, \dots, (N1-1) \Delta \Theta$$

$$Apc = D \sin \Phi \left(\cos \Theta \sin \frac{\Delta \Theta}{2} - .25 \Delta \Theta M1 D1 \right)$$

$$Apl = .25 D \Delta \Theta M1 D1 \sin \Phi$$

$$Q = Q_s$$

Sector (2)

$$\Delta \Theta = \frac{\frac{\pi}{2} - \Theta_{c1}}{N2}$$

$$\theta = \theta_{c1} + \frac{\Delta \theta}{2}, \theta_{c1} + 3 \frac{\Delta \theta}{2}, \dots, \theta_{c1} + (2N2-1) \frac{\Delta \theta}{2}$$

$$A_{pc} = .5 D \cos \theta \sin \frac{\Delta \theta}{2} \sin \phi$$

$$A_{pl} = .5 D \cos \theta \sin \frac{\Delta \theta}{2} \sin \phi$$

$$Q = Q_s$$

Sector (3)

$$\Delta \theta = \frac{\frac{\pi}{2} - \theta_{c1}}{N3} \quad \text{where } N3 = N2$$

$$\theta = \frac{\pi}{2} + \frac{\Delta \theta}{2}, \frac{\pi}{2} + 3 \frac{\Delta \theta}{2}, \dots, \frac{\pi}{2} + (2N3 - 1) \frac{\Delta \theta}{2}$$

$$A_{pc} = -.5 D \cos \theta \sin \frac{\Delta \theta}{2} \sin \phi$$

$$A_{pl} = -.5 D \cos \theta \sin \frac{\Delta \theta}{2} \sin \phi$$

$$Q = 0.$$

Sector (4)

$$\Delta \theta = \frac{\theta_{c1}}{N4} \quad \text{where } N4 = N1$$

$$\theta = \pi - \theta_{c1} + \frac{\Delta \theta}{2}, \pi - \theta_{c1} + 3 \frac{\Delta \theta}{2}, \dots, \pi - \theta_{c1} + (2N4-1) \frac{\Delta \theta}{2}$$

$$A_{pc} = -D \sin \Phi \left(\cos \Theta \sin \frac{\Delta \Theta}{2} + .25 \Delta \Theta M_1 D_1 \right)$$

$$A_{pl} = .25 D \Delta \Theta M_1 D_1 \sin \Phi$$

$$Q = 0.$$

For CASE 4, the total number of nodes for $\Theta = 0 \rightarrow \pi$ is

$$N = N_1 + N_2 + N_3 + N_4 = 2 (N_1 + N_2)$$

The heat absorbed by node i is obtained as follows:

$$Q_{(\text{absorbed})_i} = \frac{Q_i}{144} \alpha_s (A_{pc} + A_{pl})_i$$

A.3 INTERNODAL CONDUCTION TERMS

Heat is transferred around the periphery of the tube via conduction along the circumferential wires. The heat transferred via conduction from node i to node i+1 is defined as follows.

$$Q_{\text{conduction}_{i \rightarrow i+1}} = \frac{K \pi D c^2 M_c}{12 D (\Delta \Theta_i + \Delta \Theta_{i+1})} (T_i - T_{i+1})$$

A.4 RADIATION TERMS

Heat is transferred via radiation between nodes and via radiation to deep space. The former has been neglected in this analysis since the temperature gradient around the periphery of the tube is small, and the radiosity network between nodes is very complex due to the geometry of the wire screen configuration.

The heat transferred to deep space via radiation for node i is calculated as follows.

$$Q_{\text{radiated } i} = \frac{\Delta \theta_i}{2 \pi} EA \frac{\sigma}{144} T_i^4$$

A.5 MISCELLANEOUS

Several equations have been included in the program as follows.

1. Approximate total wire surface area per unit length of tube in square inches.

$$A_t = \pi^2 D (D_c M_c + D_l M_l - D_c D_l M_c M_l)$$

2. Effective emissivity

$$E_{\text{eff}} = \frac{EA}{A_t}$$

3. Percent open area of the screen

$$\% \text{ open area} = (1. - D_c M_c - D_l M_l + D_c D_l M_c M_l) \times 100.$$

4. Approximate tube weight in pounds per foot of tube length.

$$W_t = \frac{.25 D \pi^2}{144} (D_c^2 M_c + D_l^2 M_l) \times \rho$$



GENERAL DYNAMICS
Convair Division

GD/C-DDB66-005
Page 52

APPENDIX B

```

*      LIST8
*      FORTRAN
C      METHOD FOR CALCULATING THE TEMPERATURE GRADIENT AROUND THE
C      PERIFERY OF A TUBULAR SCREEN TYPE GRAVITY GRADIENT
C      STABILIZATION ELEMENT FOR PHI=0 TO 90 DEGREES.      G.A. HOWELL
      DIMENSION N(3),DTH(3),TH(40),APC(40),APL(40),ALFEFC(40),ALFEFL(40)
      1,QF(40),AKCC(40),QA(40),QR(78),T(78),ANDTH(40)
      COMMON NN,N1,N2,N3,THCL,THCC,TH,APC,APL,ALFEFC,ALFEFL,QF,
      1QS,D,DC,DL,AMC,AML,AKC,ALFE,ALFI,A1,A2,A3,AKCC,QA,GAT,T,
      1ANDTH,EAEFR,AEFR,EEFR
99  RIT 5,2000,N1,N2,N3,PHI,THB
      RIT 5,2001,D,DC,DL,AMC,AML
      RIT 5,2001,QS,ALFE,ALFI,AKC,TREFL,DEN
      PI=3.1415927
      RAD=57.295780
      AOPEN=(1.-DC*AMC-DL*AML+DC*DL*AMC*AML)*100.
      WT=.25*D*PI**2*(DC**2*AMC+DL**2*AML)/144.*DEN
      PHIA=PHI
      WOT 6,2010,N1,N2,N3
      WOT 6,2011,D,DC,DL,AMC,AML
      WOT 6,2011,QS,ALFE,ALFI,AKC,TREFL,DEN
      WOT 6,2012,PHIA
      PHI=PHI/RAD
      THCL=ACOSF(DL/(D*SINF(1./(D*AML))))
      K=1
      IF (PHIA-90.)41,40,41
40  N3=N2+N3
      N2=0
      GO TO 60
41  PHIC=ASINF(AMC*DC)
      K=4
      IF (PHI-PHIC)40,40,42
42  GAMC=ASINF(AMC*DC)
C      CALCULATE THCC
      GAMR=ASINF(SINF(PHI)*COSF(THCL)/
      1(SINF(ACOSF(SINF(PHI)*SINF(THCL)))))
      IF (GAMC-GAMR)444,43,44
43  THCC=THCL
      N3=N2+N3
      N2=0
      K=2
      GO TO 60
44  THCR=.9*THCL
      GO TO 445
444 THCR=.5*(THCL+PI/2.)
445 THR1=THCL
      6  GAMR1=GAMR
      GAMR=ASINF(SINF(PHI)*COSF(THCR)/
      1(SINF(ACOSF(SINF(PHI)*SINF(THCR)))))
      E=GAMR-GAMC
      IF (ABS(E)-.001)5,5,3
      3  THCC=THR1+(THCR-THR1)*(GAMC-GAMR1)/(GAMR-GAMR1)
      IF (THCC-PI/2.)7,8,8
      8  THCC=1.555
      IF (THCC-THCR)7,9,7
      9  WOT 6,3000
      GO TO 99

```



```

7   THR1=THCR
    THCR=THCC
    GO TO 6
5   THCC=THCR
    IF (THCL-THCC)45,43,46
45  K=2
    GO TO 60
46  K=3
    N3=N2+N3
    IF (THCL-THCC-.31)47,47,48
47  N1=N1-N2
    GO TO 60
48  AN1=N1
    DTHA=THCL/AN1
    AN2=(THCL-THCC)/DTHA
    N2=AN2
    N1=N1-N2
    IF (N1-2)49,60,60
49  N2=N1+N2-2
    N1=2
    GO TO 60
60  N(1)=N1
    N(2)=N2
    N(3)=N3
    AN1=N1
    AN2=N2
    AN3=N3
    NN=2*(N1+N2+N3)
    NNN=NN+1
    TH(1)=0.
    TH(NN)=PI
    COSPHI=COSF(PHI)
    SINPHI=SINF(PHI)
    A1=D*AMC*DC
    A2=.25*AML*DL
    A3=.5*AMC*DC
    GO TO (61,64,65,61),K
61  DTH(1)=THCL/(AN1-.5)
    DTH(3)=(.5*PI-THCL)/AN3
    TH(N1+1)=THCL+.5*DTH(3)
    L=2
    M=N1
    DO 62 J=L,M
62  TH(J)=TH(J-1)+DTH(1)
    L=N1+2
    M=N1+N3
    DO 63 J=L,M
63  TH(J)=TH(J-1)+DTH(3)
    GO TO (69,69,99,69),K
64  IF (THCC-THCL)99,61,644
644 DTH(1)=THCL/(AN1-.5)
    DTH(2)=(THCC-THCL)/AN2
    DTH(3)=(.5*PI-THCC)/AN3
    TH(N1+1)=THCL+.5*DTH(2)
    L=(N1+N2+1)
    TH(L)=THCC+.5*DTH(3)
    GO TO 66

```

```

65 DTH(1)=THCC/(AN1-.5)
   DTH(2)=(THCL-THCC)/AN2
   DTH(3)=(.5*PI-THCL)/AN3
   TH(N1+1)=THCC+.5*DTH(2)
   L=(N1+N2+1)
   TH(L)=THCL+.5*DTH(3)
   GO TO 66
66 L=2
   M=N1
   DO 67 I=1,3
   DO 68 J=L,M
68 TH(J)=TH(J-1)+DTH(I)
   L=L+N(I)
67 M=M+N(I+1)
69 M=NN/2
   DO 699 J=1,M
   L=NNN-J
699 TH(L)=PI-TH(J)
   THCLA=THCL*RAD
   WOT 6,2013,THCLA
   GO TO (72,71,71,73),K
71 THCCA=THCC*RAD
   GO TO 74
73 THCCA=0.
74 WOT 6,2014,THCCA
72 GO TO (100,200,200,400),K
100 APC(1)=.5*A1*(SINF(.5*DTH(1))-DTH(1)*A2)
   APL(1)=D*DTH(1)*A2*(1.-A3)
   QF(1)=QS
   QF(NN)=QS*(1.-(APC(1)+APL(1))/(.5*D*SINF(.5*DTH(1))))
   DO 110 J=2,N1
   APC(J)=A1*(COSF(TH(J))*SINF(.5*DTH(1))-DTH(1)*A2)
   APL(J)=2.*A2*D*DTH(1)*(1.-A3)
   QF(J)=QS
   L=NNN-J
110 QF(L)=QS*(1.-(APC(J)+APL(J))/(D*COSF(TH(J))*SINF(.5*DTH(1))))
   L=N1+1
   M=N1+N3
   DO 111 J=L,M
   APC(J)=A3*D*COSF(TH(J))*SINF(.5*DTH(3))
   APL(J)=APC(J)*(1.-A3)/A3
   QF(J)=QS
   I=NNN-J
111 QF(I)=0.
   GO TO 500
200 APC(1)=.5*A1*(SINF(.5*DTH(1))-DTH(1)*A2)
   APL(1)=D*DTH(1)*A2*(SINPHI-A3)
   QF(1)=QS
   QF(NN)=QS*(1.-(APC(1)+APL(1))/(.5*D*SINF(.5*DTH(1))*SINPHI))
   DO 210 J=2,N1
   A4=ATANF(COSF(TH(J))*2/TANF(PI*.5-PHI))
   A5=(SINF(A4)**2+COSF(A4)**2*COSF(TH(J))*2)**.5
   SINPSI=SINF(ACOSF(SINPHI*SINF(TH(J))))
   APC(J)=.5*A1*DTH(1)*(SINPSI-2.*A2*SINF(A4+PI*.5-PHI)/A5)
   APL(J)=2.*A2*D*DTH(1)*(SINPHI-A3*SINF(A4+PI*.5-PHI)/A5)
   QF(J)=QS
   L=NNN-J

```

```

210 QF(L)=QS*(1.-(APC(J)+APL(J))/(D*COSF(TH(J))*SINF(.5*DTH(1))
1*SINPHI))
IF (K-3)208,309,208
208 L=N1+1
IF (THCC-THCL)2089,2088,2089
2088 M=N1+N3
GO TO 206
2089 M=N1+N2
DO 211 J=L,M
SINPSI=SINF(ACOSF(SINPHI*SINF(TH(J))))
APC(J)=.25*A1*DTH(2)*SINPSI
APL(J)=.5*D*(2.*COSF(TH(J))*SINF(.5*DTH(2))*SINPHI-A3*DTH(2)*
1SINPSI)
QF(J)=QS
I=NNN-J
211 QF(I)=0.
207 L=L+N2
M=M+N3
206 DO 212 J=L,M
APC(J)=.5*D*COSF(TH(J))*SINF(.5*DTH(3))*SINPHI
APL(J)=APC(J)
QF(J)=QS
I=NNN-J
212 QF(I)=0.
GO TO 500
309 L=N1+1
M=N1+N2
308 DO 310 J=L,M
APC(J)=.5*D*SINPHI*(2.*COSF(TH(J))*SINF(.5*DTH(2))-2.*A2*DTH(2))
APL(J)=D*A2*DTH(2)*SINPHI
QF(J)=QS
I=NNN-J
310 QF(I)=0.
IF (K-4)311,410,311
311 GO TO 207
400 APC(1)=D*SINPHI*(.5*SINF(.5*DTH(1))-.125*DTH(1)*AML*DL)
APL(1)=A2*D*.5*DTH(1)*SINPHI
QF(1)=QS
QF(NN)=0.
DTH(2)=DTH(1)
L=2
M=N1
GO TO 308
410 L=N1+1
M=N1+N2
GO TO 206
500 M=NN/2
DO 501 J=1,M
L=NNN-J
APC(L)=APC(J)
501 APL(L)=APL(J)
DO 502 J=1,NN
ALFFFC(J)=ALFF
502 ALFEFL(J)=ALFE
QAT=0.
DO 510 J=1,NN
QA(J)=QF(J)*(APC(J)*ALFFFC(J)+APL(J)*ALFEFL(J))/144.

```

```

510 QAT=QAT+QA(J)
   ANDTH(1)=.5*DTH(1)
   L=2
   M=N1
   DO 1010 J=L,M
1010 ANDTH(J)=DTH(1)
   GO TO (1013,1011,1011,1013),K
1011 IF (THCC-THCL)1017,1013,1017
1017 L=M+1
   M=M+N2
   DO 1012 J=L,M
1012 ANDTH(J)=DTH(2)
1013 L=M+1
   M=M+N3
   DO 1014 J=L,M
1014 ANDTH(J)=DTH(3)
   M=NN/2
   DO 1015 J=1,M
   L=NNN-J
1015 ANDTH(L)=ANDTH(J)
   AKCC(1)=AKC/12.*DC**2*AMC*PI/(D*(2.*ANDTH(1)+ANDTH(2)))
   M=NN-2
   DO 1016 J=2,M
1016 AKCC(J)=AKC/12.*DC**2*AMC*PI/(D*(ANDTH(J)+ANDTH(J+1)))
   AKCC(NN-1)=AKC/12.*DC**2*AMC*PI/(D*(ANDTH(NN-1)+2.*ANDTH(NN)))
   IF (THB)1019,1019,1018
1018 WOT 6,2018,THB
1019 WOT 6,1000
   IF (THB)1099,1099,4000
1099 DO 70 J=1,NN
   ATH=TH(J)*RAD
   70 WOT 6,1001,J,ATH,APC(J),APL(J),ALFEFC(J),ALFEFL(J),
   IQF(J),AKCC(J)
   T(NN)=TREFFL
   LFLAG=1
   IF (TREFFL)99,2099,75
   75 EAEFR=2.*QAT/(.1713/144.*((TREFFL/100.))**4))
   GO TO 76
2099 T(NN)=((2.*QAT)/(.1713/144.*EAEFR))**.25*100.
   LFLAG=2
   76 MFLAG=0
   NFLAG=0
1025 QR(NN)=EAEFR*ANDTH(NN)/(2.*PI)*.1713/144.*((T(NN)/100.))**4)
   T(NN-1)=T(NN)+(QR(NN)-QA(NN))/AKCC(NN-1)
   L=NN-1
   DO 1020 J=2,L
   M=NN-J
   QR(M+1)=EAEFR*ANDTH(M+1)/(2.*PI)*.1713/144.*((T(M+1)/100.))**4)
1020 T(M)=T(M+1)+(QR(M+1)-QA(M+1))/AKCC(M)+AKCC(M+1)*(T(M+1)-T(M+2))/
   1AKCC(M)
   QR(1)=EAEFR*ANDTH(1)/(2.*PI)*.1713/144.*((T(1)/100.))**4)
   QRT=0.
   DO 1021 J=1,NN
1021 QRT=QRT+QR(J)
   E=(QAT-QRT)/QAT
   IF (ABS(E)-.00001)106,1028,1028
1028 GO TO (1026,3001),LFLAG

```

```

1026 IF (MFLAG)1022,1022,1023
1022 EAEFRN=(1.0+.05*E/ABS(E))*EAEFR
      MFLAG=1
      GO TO 1024
1023 EAEFRN=EAEFR1-(QRT1-QAT)*(EAEFR1-EAEFR)/(QRT1-QRT)
1024 EAEFR1=EAEFR
      EAEFR=EAEFRN
1029 QRT1=QRT
      NFLAG=NFLAG+1
      GO TO 1025
3001 IF (MFLAG)3002,3002,3003
3002 TNNN=(1.0+.02*E/ABS(E))*T(NN)
      MFLAG=1
      GO TO 3004
3003 TNNN=TNN1-(QRT1-QAT)*(TNN1-T(NN))/(QRT1-QRT)
3004 TNN1=T(NN)
      T(NN)=TNNN
      GO TO 1029
106 WOT 6,1002
      AEFR=PI**2*D*(DC*AMC+DL*AML-DC*DL*AMC*AML)
      EEFR=EAEFR/AEFR
      DO 51 J=1,NN
      ADT=T(J)-T(NN)
      ATH=TH(J)*RAD
51 WOT 6,1001,J,ATH,T(J),ADT
      IF (THB)5003,5003,5001
5003 WOT 6,2015,EAEFR
      WOT 6,2016,AEFR
      WOT 6,2017,EEFR
      WOT 6,2019,AOPEN
      WOT 6,2020,WT
      WOT 6,1003,NFLAG
      GO TO 99
4000 NT=2*NN-2
      AKCC(NN)=AKCC(NN-1)
      THB=THB/RAD
      DO 4001 J=1,NN
      IF (THB-TH(J))4002,4001,4001
4001 CONTINUE
4002 NB=J-1
      AKCCH=AKCC(NB)
      AKCC(NB)=0.
      APC(1)=2.*APC(1)
      APL(1)=2.*APL(1)
      APC(NN)=APC(1)
      APL(NN)=APL(1)
      DO 4003 J=1,NN
      ATH=TH(J)*RAD
4003 WOT 6,1001,J,ATH,APC(J),APL(J),ALFEFC(J),ALFEFL(J),
10F(J),AKCC(J)
      AKCC(NB)=AKCCH
      L=NN+1
      DO 4004 I=L,NT
      J=NT+2-I
      ATH=(2.*PI-TH(J))*RAD
4004 WOT 6,1001,I,ATH,APC(J),APL(J),ALFEFC(J),ALFEFL(J),
10F(J),AKCC(J-1)

```

```

T(NB) = ((2.*QAT)/(0.1713/144.*EAEFR))**.25*100.
NFLAG=0
MFLAG=0
400A QR(NB) = EAEFR*ANDTH(NB)/(2.*PI)*.1713/144.*((T(NB)/100.))**4)
T(NB-1) = T(NB) + (QR(NB) - QA(NB))/AKCC(NB-1)
L = NB-1
DO 4005 J=2,L
M = NB-J
QR(M+1) = EAEFR*ANDTH(M+1)/(2.*PI)*.1713/144.*((T(M+1)/100.))**4)
4005 T(M) = T(M+1) + (QR(M+1) - QA(M+1))/AKCC(M) + AKCC(M+1)*(T(M+1) - T(M+2))/
1AKCC(M)
QR(1) = EAEFR*ANDTH(1)/PI*.1713/144.*((T(1)/100.))**4)
T(NT) = T(1) + (QR(1) - 2.*QA(1))/AKCC(1) + AKCC(1)*(T(1) - T(2))/AKCC(1)
QR(NT) = EAEFR*ANDTH(2)/(2.*PI)*.1713/144.*((T(NT)/100.))**4)
T(NT-1) = T(NT) + (QR(NT) - QA(2))/AKCC(2) + AKCC(1)*(T(NT) - T(1))/AKCC(2)
L = NN-2
DO 4006 J=2,L
M = NT-J
QR(M+1) = EAEFR*ANDTH(J+1)/(2.*PI)*.1713/144.*((T(M+1)/100.))**4)
4006 T(M) = T(M+1) + (QR(M+1) - QA(J+1))/AKCC(J+1) + AKCC(J)*(T(M+1) - T(M+2))/
1AKCC(J+1)
QR(NN) = EAEFR*ANDTH(NN)/PI*.1713/144.*((T(NN)/100.))**4)
T(NN-1) = T(NN) + (QR(NN) - 2.*QA(NN))/AKCC(NN-1) + AKCC(NN-1)*(T(NN) -
1T(NN+1))/AKCC(NN-1)
L = NN-NB-1
DO 4007 J=2,L
M = NN-J
QR(M+1) = EAEFR*ANDTH(M+1)/(2.*PI)*.1713/144.*((T(M+1)/100.))**4)
4007 T(M) = T(M+1) + (QR(M+1) - QA(M+1))/AKCC(M) + AKCC(M+1)*(T(M+1) - T(M+2))/
1AKCC(M)
QR(NB+1) = EAEFR*ANDTH(NB+1)/(2.*PI)*.1713/144.*((T(NB+1)/100.))**4)
QRT=0.
DO 4020 J=1,NT
4020 QRT = QRT + QR(J)
E = (2.*QAT - QRT)/(2.*QAT)
IF (ABSF(E) - .00001) 106, 4021, 4021
4021 IF (MFLAG) 4022, 4022, 4023
4022 TNNB = (1.0 + .02*E/ABSF(E))*T(NB)
MFLAG=1
GO TO 4024
4023 TNNB = TNNB - (QRT1 - 2.*QAT)*(TNNB - T(NB))/(QRT1 - QRT)
4024 TNNB = T(NB)
T(NB) = TNNB
QRT1 = QRT
NFLAG = NFLAG + 1
GO TO 4008
5001 L = NN+1
DO 5002 I=L,NT
J = NT+2-I
ADT = T(I) - T(NN)
ATH = (2.*PI - TH(J))*RAD
5002 WQT 6,1001,I,ATH,T(I),ADT
GO TO 5003
1000 FORMAT (//2H N,12X,2HTH,11X,3HAPC,10X,3HAPL,10X,6HALFEFC,7X,
16HALFEFL,7X,2HQF,11X,15HAKCC (N TO N+1)//)
1001 FORMAT (1H 12,11X,7(F11.6,2X))
1002 FORMAT (2H1N,12X,2HTH,11X,1HT,12X,10HT(N) - T(NN),3X//)

```

1003 FORMAT (///1H I4)
2000 FORMAT (3I2,2F13.7)
2001 FORMAT (5E13.7,F7.3)
2010 FORMAT (1H15(I2,4X))
2011 FORMAT (1H 7(F11.6,2X))
2012 FORMAT (//7H PHI= ,F11.6)
2013 FORMAT (7H THCL= ,F11.6)
2014 FORMAT (7H THCC= ,F11.6)
2015 FORMAT (//8H EAEFF= ,F11.6)
2016 FORMAT (8H AEFF= ,F11.6)
2017 FORMAT (8H CEFF= ,F11.6)
2018 FORMAT (7H THB= ,F11.6)
2019 FORMAT (21H PERCENT OPEN AREA = ,F11.6)
2020 FORMAT (27H WEIGHT IN LBS. PER FOOT = ,F11.6)
3000 FORMAT (21HNO SOLUTION FOR THCC)
END

N	TH	APC	APL	ALFEFC	ALFEFL	UF	AKCC (N TO N+1)
12	0.750000	0.008000	0.012800	16.000000	12.000000	-0.	
4	0.400000	0.400000	0.400000	44.000000	500.000000		
PHI=	90.000000						
THCL=	81.140036						
1	0.	0.002727	0.003320	0.400000	0.400000	450.000000	0.063853
2	7.056177	0.005409	0.006640	0.400000	0.400000	450.000000	0.063853
3	14.112354	0.005275	0.006640	0.400000	0.400000	450.000000	0.063853
4	21.168531	0.005055	0.006640	0.400000	0.400000	450.000000	0.063853
5	28.224708	0.004751	0.006640	0.400000	0.400000	450.000000	0.063853
6	35.280885	0.004369	0.006640	0.400000	0.400000	450.000000	0.063853
7	42.337062	0.003913	0.006640	0.400000	0.400000	450.000000	0.063853
8	49.393239	0.003391	0.006640	0.400000	0.400000	450.000000	0.063853
9	56.449417	0.002811	0.006640	0.400000	0.400000	450.000000	0.063853
10	63.505594	0.002161	0.006640	0.400000	0.400000	450.000000	0.063853
11	70.561770	0.001512	0.006640	0.400000	0.400000	450.000000	0.063853
12	77.617948	0.000813	0.006640	0.400000	0.400000	450.000000	0.110392
13	81.699409	0.000067	0.00979	0.400000	0.400000	450.000000	0.407104
14	82.806154	0.000058	0.000849	0.400000	0.400000	450.000000	0.407104
15	83.912899	0.000049	0.000719	0.400000	0.400000	450.000000	0.407104
16	85.019645	0.000040	0.000583	0.400000	0.400000	450.000000	0.407104
17	86.126390	0.000031	0.000458	0.400000	0.400000	450.000000	0.407104
18	87.233134	0.000022	0.000327	0.400000	0.400000	450.000000	0.407104
19	88.339880	0.000013	0.000196	0.400000	0.400000	450.000000	0.407104
20	89.446625	0.000004	0.000065	0.400000	0.400000	450.000000	0.407104
21	90.553376	0.000004	0.000065	0.400000	0.400000	0.	0.407104
22	91.660122	0.000013	0.000196	0.400000	0.400000	0.	0.407104
23	92.766867	0.000022	0.000327	0.400000	0.400000	0.	0.407104
24	93.873611	0.000031	0.000458	0.400000	0.400000	0.	0.407104
25	94.980357	0.000040	0.000589	0.400000	0.400000	0.	0.407104
26	96.087102	0.000049	0.000719	0.400000	0.400000	0.	0.407104
27	97.193847	0.000058	0.000849	0.400000	0.400000	0.	0.407104
28	98.300592	0.000067	0.000979	0.400000	0.400000	0.	0.110392
29	102.382053	0.000813	0.006640	0.400000	0.400000	111.138413	0.063853
30	109.438231	0.001512	0.006640	0.400000	0.400000	211.172588	0.063853
31	116.494407	0.002811	0.006640	0.400000	0.400000	257.207568	0.063853
32	123.550585	0.004369	0.006640	0.400000	0.400000	283.274441	0.063853
33	130.606760	0.006640	0.006640	0.400000	0.400000	299.737377	0.063853
34	137.662939	0.00913	0.006640	0.400000	0.400000	310.810303	0.063853
35	144.719114	0.012393	0.006640	0.400000	0.400000	318.519676	0.063853
36	151.775293	0.015725	0.006640	0.400000	0.400000	323.950592	0.063853
37	158.831469	0.019055	0.006640	0.400000	0.400000	327.725143	0.063853
38	165.887648	0.022385	0.006640	0.400000	0.400000	330.212394	0.063853
39	172.943823	0.025715	0.006640	0.400000	0.400000	331.628986	0.063853
40	180.000002	0.029045	0.003320	0.400000	0.400000	332.087256	0.

N	TH	T	T(N)-T(NN)
1	0.	504.922764	4.922764
2	7.056177	504.883961	4.883961
3	14.112354	504.767193	4.767193
4	21.168531	504.574928	4.574928
5	28.224708	504.311241	4.311241
6	35.280885	503.981750	3.981750
7	42.337062	503.593536	3.593536
8	49.393239	503.155037	3.155037
9	56.449417	502.675922	2.675922
10	63.505594	502.160958	2.160958
11	70.561770	501.639839	1.639839
12	77.617948	501.107021	1.107021
13	84.674125	500.560791	0.560791
14	91.730302	500.000000	0.000000
15	98.786479	500.407646	0.407646
16	105.842656	500.815292	0.815292
17	112.898833	501.222938	1.222938
18	119.955010	501.630584	1.630584
19	127.011187	502.038230	2.038230
20	134.067364	502.445876	2.445876
21	141.123541	502.853522	2.853522
22	148.179718	503.261168	3.261168
23	155.235895	503.668814	3.668814
24	162.292072	504.076460	4.076460
25	169.348249	504.484106	4.484106
26	176.404426	504.891752	4.891752
27	183.460603	505.299398	5.299398
28	190.516780	505.707044	5.707044
29	197.572957	506.114690	6.114690
30	204.629134	506.522336	6.522336
31	211.685311	506.929982	6.929982
32	218.741488	507.337628	7.337628
33	225.797665	507.745274	7.745274
34	232.853842	508.152920	8.152920
35	239.910019	508.560566	8.560566
36	246.966196	508.968212	8.968212
37	254.022373	509.375858	9.375858
38	261.078550	509.783504	9.783504
39	268.134727	510.191150	10.191150
40	275.190904	510.598796	10.598796

EAEFF= 0.665506
AEFF= 1.938927
EEFF= 0.343234
PERCENT OPEN AREA = 73.806079
WEIGHT IN LBS. PER FOOT = -0.

N	TH	APC	APL	ALFEFC	ALFEFL	QF	AKCC (N TO N+1)
12	0.750000	0.008000	0.012800	12.000000	-0.	-0.	
4	0.400000	0.400000	0.400000	44.000000			
450.000000							
PHI=	90.000000						
THCL=	81.146036						
THB=	120.000000						
1	0.	0.005454	0.006640	0.400000	0.400000	450.000000	0.063853
2	7.056177	0.005409	0.006640	0.400000	0.400000	450.000000	0.063853
3	14.112354	0.005275	0.006640	0.400000	0.400000	450.000000	0.063853
4	21.168531	0.005055	0.006640	0.400000	0.400000	450.000000	0.063853
5	28.224708	0.004751	0.006640	0.400000	0.400000	450.000000	0.063853
6	35.280885	0.004369	0.006640	0.400000	0.400000	450.000000	0.063853
7	42.337062	0.003913	0.006640	0.400000	0.400000	450.000000	0.063853
8	49.393239	0.003391	0.006640	0.400000	0.400000	450.000000	0.063853
9	56.449417	0.002811	0.006640	0.400000	0.400000	450.000000	0.063853
10	63.505594	0.002181	0.006640	0.400000	0.400000	450.000000	0.063853
11	70.561770	0.001512	0.006640	0.400000	0.400000	450.000000	0.063853
12	77.617948	0.000813	0.006640	0.400000	0.400000	450.000000	0.110392
13	81.699409	0.000067	0.000979	0.400000	0.400000	450.000000	0.407104
14	82.806154	0.000058	0.000849	0.400000	0.400000	450.000000	0.407104
15	83.912899	0.000049	0.000719	0.400000	0.400000	450.000000	0.407104
16	85.019645	0.000040	0.000581	0.400000	0.400000	450.000000	0.407104
17	86.126390	0.000031	0.000456	0.400000	0.400000	450.000000	0.407104
18	87.233134	0.000022	0.000327	0.400000	0.400000	450.000000	0.407104
19	88.339880	0.000013	0.000196	0.400000	0.400000	450.000000	0.407104
20	89.446625	0.000004	0.000065	0.400000	0.400000	450.000000	0.407104
21	90.553376	0.000004	0.000065	0.400000	0.400000	0.	0.407104
22	91.660122	0.000013	0.000196	0.400000	0.400000	0.	0.407104
23	92.766867	0.000022	0.000327	0.400000	0.400000	0.	0.407104
24	93.873611	0.000031	0.000458	0.400000	0.400000	0.	0.407104
25	94.980357	0.000040	0.000581	0.400000	0.400000	0.	0.407104
26	96.087102	0.000049	0.000719	0.400000	0.400000	0.	0.407104
27	97.193847	0.000058	0.000849	0.400000	0.400000	0.	0.407104
28	98.300592	0.000067	0.000979	0.400000	0.400000	0.	0.110392
29	102.382053	0.000813	0.006640	0.400000	0.400000	111.138413	0.063853
30	109.438231	0.001512	0.006640	0.400000	0.400000	211.172588	0.063853
31	116.494407	0.002181	0.006640	0.400000	0.400000	237.207586	0.063853
32	123.550585	0.002811	0.006640	0.400000	0.400000	283.274441	0.063853
33	130.606760	0.003391	0.006640	0.400000	0.400000	299.737377	0.063853
34	137.662939	0.003913	0.006640	0.400000	0.400000	310.810303	0.063853
35	144.719114	0.004369	0.006640	0.400000	0.400000	318.519476	0.063853
36	151.775293	0.004751	0.006640	0.400000	0.400000	323.950592	0.063853
37	158.831469	0.005055	0.006640	0.400000	0.400000	327.725143	0.063853
38	165.887648	0.005275	0.006640	0.400000	0.400000	330.212399	0.063853
39	172.943823	0.005454	0.006640	0.400000	0.400000	331.628986	0.063853
40	180.000002	0.005549	0.006640	0.400000	0.400000	332.089256	0.063853
41	187.056179	0.005609	0.006640	0.400000	0.400000	331.628986	0.063853
42	194.112356	0.005675	0.006640	0.400000	0.400000	330.212399	0.063853
43	201.168533	0.005675	0.006640	0.400000	0.400000	327.725143	0.063853
44	208.224710	0.004751	0.006640	0.400000	0.400000	323.950592	0.063853
45	215.280888	0.004369	0.006640	0.400000	0.400000	318.519476	0.063853
46	222.337065	0.003913	0.006640	0.400000	0.400000	310.810303	0.063853
47	229.393242	0.003391	0.006640	0.400000	0.400000	299.737377	0.063853

GENERAL DYNAMICS
Convair Division

GD/C-DDB66-005
Page 64

48	236.449417	0.002811	0.006640	0.400000	0.400000	283.274441	0.063853
49	243.505594	0.002181	0.006640	0.400000	0.400000	257.207588	0.063853
50	250.561771	0.001512	0.006640	0.400000	0.400000	211.172588	0.063853
51	257.617947	0.000813	0.006640	0.400000	0.400000	111.138413	0.110392
52	261.699406	0.000067	0.000979	0.400000	0.400000	0.	0.407104
53	262.806152	0.000056	0.000849	0.400000	0.400000	0.	0.407104
54	263.912899	0.000049	0.000719	0.400000	0.400000	0.	0.407104
55	265.019646	0.000040	0.000583	0.400000	0.400000	0.	0.407104
56	266.126389	0.000031	0.000458	0.400000	0.400000	0.	0.407104
57	267.233135	0.000022	0.000327	0.400000	0.400000	0.	0.407104
58	268.339878	0.000013	0.000196	0.400000	0.400000	0.	0.407104
59	269.446625	0.000004	0.000065	0.400000	0.400000	0.	0.407104
60	270.553375	0.000004	0.000065	0.400000	0.400000	450.000000	0.407104
61	271.660122	0.000013	0.000196	0.400000	0.400000	450.000000	0.407104
62	272.766865	0.000022	0.000327	0.400000	0.400000	450.000000	0.407104
63	273.873611	0.000031	0.000458	0.400000	0.400000	450.000000	0.407104
64	274.980354	0.000040	0.000583	0.400000	0.400000	450.000000	0.407104
65	276.087101	0.000049	0.000719	0.400000	0.400000	450.000000	0.407104
66	277.193844	0.000058	0.000849	0.400000	0.400000	450.000000	0.407104
67	278.300591	0.000067	0.000979	0.400000	0.400000	450.000000	0.110392
68	282.382053	0.000813	0.006640	0.400000	0.400000	450.000000	0.063853
69	289.438229	0.001512	0.006640	0.400000	0.400000	450.000000	0.063853
70	296.494408	0.002181	0.006640	0.400000	0.400000	450.000000	0.063853
71	303.550587	0.002811	0.006640	0.400000	0.400000	450.000000	0.063853
72	310.606762	0.003391	0.006640	0.400000	0.400000	450.000000	0.063853
73	317.662937	0.003913	0.006640	0.400000	0.400000	450.000000	0.063853
74	324.719116	0.004369	0.006640	0.400000	0.400000	450.000000	0.063853
75	331.775295	0.004751	0.006640	0.400000	0.400000	450.000000	0.063853
76	338.831470	0.005055	0.006640	0.400000	0.400000	450.000000	0.063853
77	345.887646	0.005275	0.006640	0.400000	0.400000	450.000000	0.063853
78	352.943821	0.005409	0.006640	0.400000	0.400000	450.000000	0.063853

N	TH	T	T(N)-T(NN)
1	0.	504.854092	4.698093
2	7.056177	504.805473	4.649475
3	14.112354	504.678791	4.522793
4	21.168531	504.476501	4.320503
5	28.224708	504.202667	4.046669
6	35.280885	503.862892	3.706894
7	42.337062	503.464245	3.308247
8	49.393239	503.015152	2.859154
9	56.449417	502.525272	2.369274
10	63.505594	502.005356	1.849358
11	70.561770	501.467087	1.311083
12	77.617948	500.922909	0.766911
13	84.674126	500.378731	0.222739
14	91.730303	500.834553	0.372566
15	98.786480	500.290375	0.289833
16	105.842657	500.746197	0.208485
17	112.898834	500.202019	0.128948
18	119.955011	500.657841	0.051647
19	127.011188	500.113663	-0.022991
20	134.067365	500.569485	-0.094540
21	141.123542	500.025307	-0.162571
22	148.179719	499.481129	-0.228771
23	155.235896	498.936951	-0.287445
24	162.292073	498.392773	-0.344292
25	169.348250	497.848595	-0.397411
26	176.404427	497.304417	-0.446808
27	183.460604	496.760239	-0.492481
28	190.516781	496.216061	-0.534435
29	197.572958	495.671883	-0.675426
30	204.629135	495.127705	-0.803963
31	211.685312	494.583527	-0.856293
32	218.741489	494.039349	-0.347481
33	225.797666	493.495171	-0.311382
34	232.853843	492.950993	-0.254383
35	239.910020	492.406815	-0.188305
36	246.966197	491.862637	-0.122917
37	254.022374	491.318459	-0.066135
38	261.078551	490.774281	-0.024094
39	268.134728	490.230103	-0.001171
40	275.190905	489.685925	0.
41	282.247082	489.141747	-0.021469
42	289.303259	488.597569	-0.064716
43	296.359436	488.053391	-0.127136
44	303.415613	487.509213	-0.204372
45	310.471790	486.965035	-0.290318
46	317.527967	486.420857	-0.377083
47	324.584144	485.876679	-0.454922
48	331.640321	485.332501	-0.512039
49	338.696498	484.788323	-0.534172
50	345.752675	484.244145	-0.503582
51	352.808852	483.699967	-0.396420
52	359.865029	483.155789	-0.267593
53	366.921206	482.611611	-0.228928
54	373.977383	482.067433	-0.186531
55	381.033560	481.523255	-0.140400
56	388.089737	480.979077	-0.090534
57	395.145914	480.434899	-0.036930
58	402.202091	479.890721	0.020412

59	269.446625	500.217492	0.081493
60	270.553375	500.302315	0.146317
61	271.660122	500.370667	0.214664
62	272.766865	500.442120	0.286121
63	273.873611	500.516247	0.360249
64	274.980354	500.592621	0.436623
65	276.087101	500.670818	0.514820
66	277.193844	500.750412	0.594414
67	278.300591	500.830978	0.674980
68	282.382053	501.130116	0.974117
69	289.438229	501.654636	1.498638
70	296.494408	502.173481	2.017483
71	303.550587	502.674183	2.518185
72	310.606762	503.145035	2.989037
73	317.662937	503.575264	3.419266
74	324.719116	503.955189	3.799191
75	331.775295	504.276360	4.120361
76	338.831470	504.531685	4.375687
77	345.887646	504.715538	4.559540
78	352.943821	504.823833	4.667835

EAEFF= 0.665506
AEFF= 1.938927
EEFF= 0.343234
PERCENT OPEN AREA = 73.806079
WEIGHT IN LBS. PER FOOT = -0.

4

REFERENCES

1. Temperature Gradients and Profile Changes in Long Tubular Elements due to Incident Radiation. A. Kemper, K. Farrell, and J. MacNaughton, The DeHavilland Aircraft of Canada Limited Report DHC-SP-TN 164, December 1962.